The impact of climate change on bushfire weather condition and fuel load

Author:
Clarke, Hamish

Publication Date:
2015

DOI:
https://doi.org/10.26190/unsworks/18187

The impact of climate change on bushfire weather conditions and fuel load

Hamish Clarke

A thesis in fulfilment of the requirements for the degree of Doctor of Philosophy

Climate Change Research Centre
School of Biological, Earth and Environmental Sciences
Faculty of Science
University of NSW

February 2015

ORIGINALITY STATEMENT

‘I hereby declare that this submission is my own work and to the best of my knowledge it contains no materials previously published or written by another person, or substantial proportions of material which have been accepted for the award of any other degree or diploma at UNSW or any other educational institution, except where due acknowledgement is made in the thesis. Any contribution made to the research by others, with whom I have worked at UNSW or elsewhere, is explicitly acknowledged in the thesis. I also declare that the intellectual content of this thesis is the product of my own work, except to the extent that assistance from others in the project's design and conception or in style, presentation and linguistic expression is acknowledged.’

Signed………………………………………………..

Date…………………………………………………..

COPYRIGHT STATEMENT

AUTHENTICITY STATEMENT

ABSTRACT

Despite considerable environmental and social impacts of bushfire, there are no high resolution, spatially continuous projections of bushfire risk across Australia under climate change which take into account the interplay between rising carbon dioxide levels and vegetation growth. This thesis aims to address this gap. First, observations are analysed for the presence of trends in fire weather conditions across Australia. Significant increases in average (90^{th} percentile) fire weather were observed at 16 (24) of 38 stations across Australia, with none recording a significant decrease. Second, future fire weather is projected in eastern Australia using skill-selected global climate models. Global climate models project strong increases in fire weather conditions in the southeast, including a lengthened fire season, but little change or decreases in the northeast. A regional climate model is then evaluated for its ability to simulate historical fire weather in southeast Australia. It simulates observed spatial patterns of fire weather well, but has an average positive bias in annual cumulative FFDI of 381. A simple model of fuel load is next developed for use in a land surface model, using net primary productivity as a proxy. This model accounts for the effects of climate and carbon dioxide fertilisation. No trends in fuel load are evident in simulations of historical fuel load over Australia. Finally, these models are used to project both fire weather and fuel load in Australia under climate change and associated increasing carbon dioxide. Fuel load is consistently projected to increase in temperate, grassland and subtropical areas of Australia. The sign of change in fire weather projections is sensitive to model selection. However, the magnitude of increases is much larger than that of decreases and all models suggest a lengthening of the fire season. Overall this research suggests bushfire risk is likely to increase in Australia under climate change, with increased load likely to have a greater impact in load-limited areas such as grasslands. In contrast, fire weather increases are likely to be of greater significance in temperate forested areas in the southeast and southwest. Two key uncertainties in the evolution of Australian fire regimes are the trajectory of regional rainfall change and the impact of carbon dioxide fertilisation on vegetation growth.

ACKNOWLEDGEMENTS

At around 2pm on October 17, 2013, my two year old daughter lay in peaceful slumber on my bed, while I marshalled my strength to wake her and bundle her into the car to collect my four year old from pre-school. I stopped to enjoy the view from the bedroom window of our lower Blue Mountains home. We back onto bush, face north and are at the top of a ridge, so the views are pretty damn good.

Today the view was a little different. A large plume of smoke was on the horizon, very dark and very active at its base. Blessed with a keen intellect and razor sharp instincts, I reacted quickly and decisively by calling my wife and asking her what to do.

A few days later two hundred odd homes in the Springwood and Winmalee areas of New South Wales had been burnt to the ground. Schools were evacuated, my car was crammed with vital documents and photos, and the couches of my mother, parents in law and brother in law were all given a good work out. Meanwhile my bosses, colleagues in government and academia and even the media took a new interest in my work, the ‘hot’ topic of bushfires and climate change.

There’s nothing like coming face to face (or 1.4km as the crow flies) with the object of your study to give it new meaning. It underlined how much bushfires mean to people, here in Australia and around the world. And there’s nothing like a bushfire to remind you of what really matters in life.

Rebecca, you really, really matter. Thanks for your support, love, encouragement and tolerance. It’s hard being married to an eccentric genius; harder still to an eccentric fool.

Saskia and Freya, you matter. A lot. You are shining beacons of love and incredibility.

Andy, my excellent supervisor, you matter. I am so lucky that I got a supervisor who is smart, experienced, generous, supportive and unbelievably powerful.

Pete, you matter a lot. You got me into this thing and helped me to get out of it.

Jason, you also matter. Thanks for co-supervising and purveying fine modelling and computing know-how.

Thorough acknowledgements matter, at least a little bit. So let me go into some detail here.

I am very grateful to advice and support (metaphysical, material and financial) from colleagues at the Climate Change Research Centre, ARC Centre of Excellence for Climate System Science and Office of Environment and Heritage in all its incarnations. Never once did they hinder, impede, hamper or encumber me.

Thanks to Matt Adams, Bruce Chessman, Hugh Jones, Lee Bowling and Pete Smith, otherwise known as the Mourning Team. Morning tea with you all was a daily highlight and bottomless well of depressing realism. Matt in particular had to tolerate me not only over morning tea, but all other parts of the arduous public service working day. His bizarre support for perennial wooden spooners the Parramatta Eels stands as a testament to his loyalty, courage and reassuringly fragile grip on reality.

Ross Bradstock, Owen Price, Trent Penman, Penny Watson and Matthias Boer provided unrelenting expert advice, comradery and coauthorship, as well as a much needed dose of reality to my mainly modelling machinations.

Chris Lucas welcomed me to the wonderful world of Forest Fire Danger Index observations and even let me sit at the table with him to write a paper about it.

Sarah Perkins helped me access data from the World Climate Research Programme's (WCRP's) Coupled Model Intercomparison Project phase 3 (CMIP3) multi-model dataset. Jason Evans provided output from Regional Climate Model simulations. Jatin Kala and Claire Carouge went above, beyond and a little to the side in dragging my sorry carcass in to a position where I could actually run a land surface model. Vanessa Haverd provided me with BIOS2 model output.

I acknowledge the modelling groups, the Program for Climate Model Diagnosis and Intercomparison (PCMDI) and the WCRP’s Working Group on Coupled Modelling (WGCM) for their roles in making available the WCRP CMIP3 multi-model dataset. Support of this dataset is provided by the Office of Science, US Department of Energy. The NCI National Facility in Canberra, Australia, which is supported by the Australian Commonwealth Government, was used to run simulations used in this thesis.

I dedicate this PhD to my family, friends, colleagues and everyone else.

CONTENTS

LIST OF FIGURES

LIST OF TABLES

LIST OF ABBREVIATIONS

AWAP	Australian Water Availability Project
CABLE	Community Atmosphere Biosphere Land Exchange (model)
CMIP3/5	Coupled Model Intercomparison Project 3/5
CO_2	carbon dioxide
D&A	detection and attribution
DF	drought factor
DGVM	dynamic global vegetation model
FFDI	Forest Fire Danger Index
FWI	Fire Weather Index
GCM	global climate model
GHG	greenhouse gas
GPP	gross primary productivity
H	relative humidity
IPCC	Intergovernmental Panel on Climate Change
KBDI	Keetch-Byram Drought Index
L	fuel load
LAI	Leaf Area Index
LSM	land surface model
MERRA	Modern-Era Retrospective Analysis for Research and Applications
NNRP	NCEP NCAR Reanalysis Project
NPP	net primary productivity
PFT	plant functional type
r	rooting depth
R	fire rate of spread
RCM	regional climate model
RCP	representative concentration pathway
SRES	Special Report on Emissions Scenarios
T	temperature
v_{cmax}	maximum carboxylation rate
W	wind speed
WRF	Weather Research and Forecasting (model)

SUPPORTING PUBLICATIONS

Clarke H, Smith P, Pitman AJ (2011) Regional signatures of future fire weather over eastern Australia from global climate models. International Journal of Wildland Fire, 20, 550-562. DOI: 10.1071/WF10070

Clarke H, Smith PL, Lucas C (2013) Changes in Australian fire weather between 1973 and 2010. International Journal of Climatology, 33, 931-944. DOI 10.1002/joc.3480

Clarke H, Evans JP, Pitman AJ (2013) Fire weather simulation skill by the Weather Research and Forecasting (WRF) model over southeast Australia from 1985 to 2009. International Journal of Wildland Fire, 22, 739-756. DOI: 10.1071/WF12048

Clarke H, Pitman AJ, Kala J, Carouge C, Haverd V (submitted) Multidecadal wildfire fuel load over Australia simulated with a land surface model. International Journal of Wildland Fire.

Clarke H, Pitman AJ, Kala J, Carouge C, Haverd V, Evans JP (submitted) An investigation of future fuel load and fire weather in Australia. Climatic Change.

Chapter 1

Bushfires in Australia

Context, patterns, switches

The focus of this thesis is the question, how will climate change affect bushfire risk? Before considering the future, it is worth pausing briefly to consider the past. Fire has a long history on Earth, with evidence that fires occurred over 400 million years ago when terrestrial plants first appeared (Scott and Glasspool 2006). The evolution of humans marked a new period in the history of fire, as for the first time there was a species that could start fires, attempt to control or suppress them and change the flammability of the landscape (Marlon et al. 2008; Bowman et al. 2009; Pausas and Keeley 2009; Mooney et al. 2011; Bowman et al. 2013). Satellite imagery reveals the ubiquity of bushfires today, while also hinting at the complexity of contemporary fire regimes (Figure 1.1; NASA FIRMS 2014). Understanding the possible future of modern fire regimes requires a relatively new context to be taken into account – the onset of an era in which humans have become the chief agent of global environmental change (Crutzen 2002; Rockstrom et al. 2009). Recent warming of the climate system is unequivocal, humans are extremely likely to have been the dominant cause and continued greenhouse gas (GHG) emissions will cause further warming and changes (IPCC 2013).

Bushfires are a worldwide phenomenon and an active area of scientific research[1]. A major reason for research interest in bushfires is the adverse effects they can have. For example, the author of this thesis is employed by an organisation tasked with protecting “life, property and community assets from the adverse impacts of bushfires” (OEH 2012). The adverse effects of bushfires extend beyond the loss of lives and homes to a wide range of environmental, social and economic assets, such as biodiversity, iconic and threatened flora and fauna, carbon stocks and clean air and water (McAneney et al. 2009; Gill et al. 2013).

[1] The term ‘bushfire’ is distinctly Australian. Those searching for literature on bushfires are advised to consider alternatives, including but not limited to: bush fire (note the space), wildfire, wildland fire, vegetation fire, unplanned fire, biomass burning and vegetation-specific terms such as grass fire and forest fire.

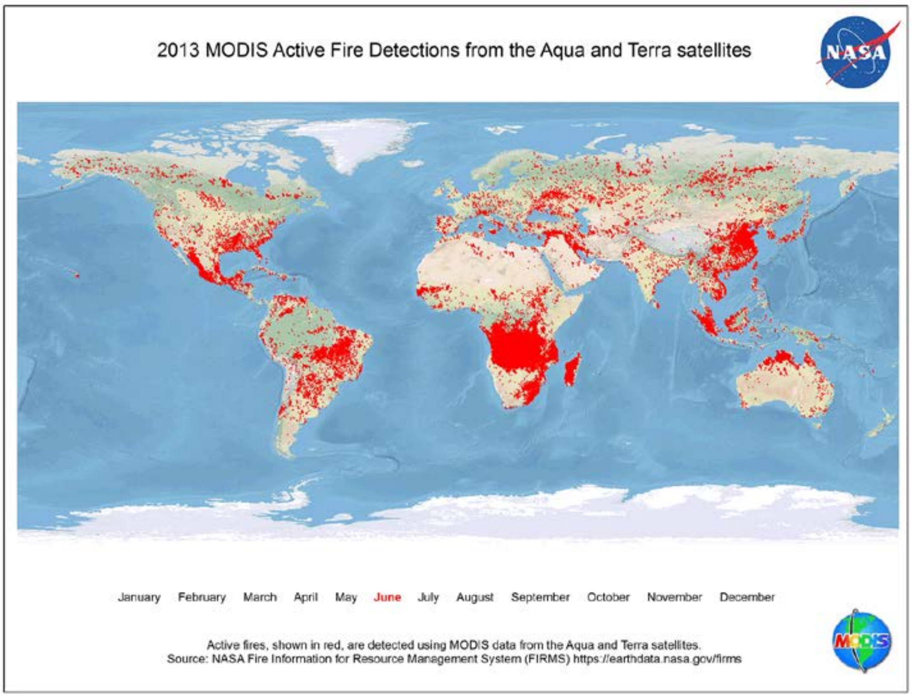

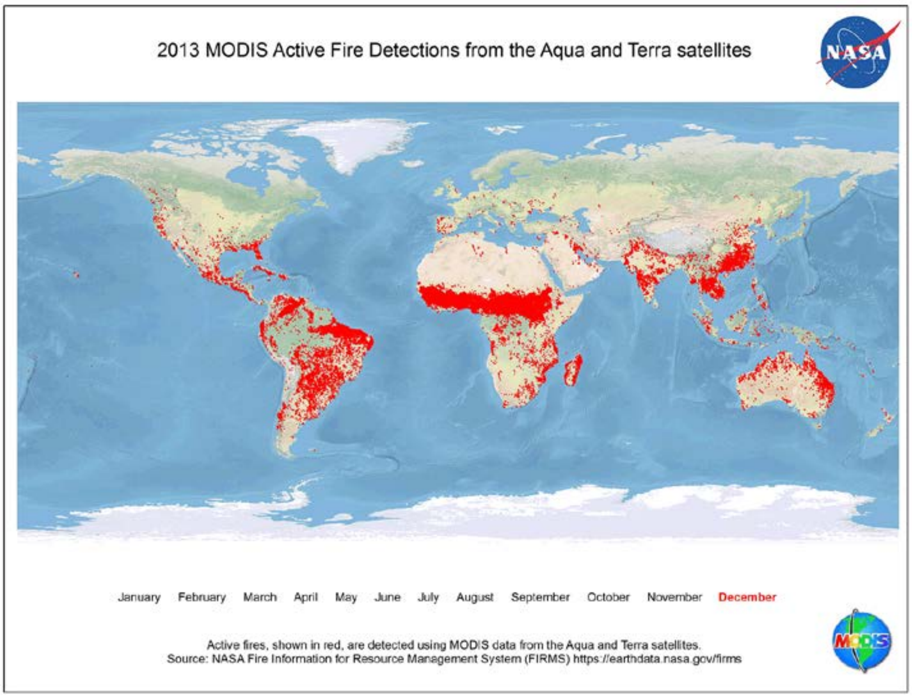

Figure 1.1 Fires detected by satellite in June (top) and December 2013 (bottom; NASA FIRMS 2014).

Our understanding of bushfire is frequently couched in the 'fire regime'[2] concept (Gill 1975). The concept has evolved since its introduction and now generally includes the prevailing timing (frequency and seasonality), size, severity and type (ground, surface, crown) of fires at a given location. Fire regimes vary greatly among ecosystems; it has been said that there are no fire adapted species *per se*, rather there are species adapted to specific fire regimes (Pausas and Keeley 2009). Variation in contemporary fire regimes can be traced to a large extent to variation in four drivers of bushfire incidence: the presence of sufficient biomass, the availability of biomass to burn, the presence of an ignition source and weather conditions conducive to the spread of fire (Archibald et al. 2009; Bradstock 2010). Given that each of these 'switches' must be on for a fire to occur, fire regimes can also be defined by the relative importance of each driver in limiting overall fire incidence. The 'four switches of fire' framework is a recurring theme in this thesis.

Recent studies have identified rainfall and fuel as particularly important in defining Australia's patterning of fire regimes. Russell-Smith et al. (2007) modelled the relationship between satellite-derived fire incidence data from 1997 to 2005 and a range of biophysical variables, finding rainfall seasonality to be the dominant influence, followed by vegetation (i.e. fuel) structure. Bradstock (2010) found that variation in available moisture and the dominance of either woody or herbaceous vegetation are the primary factors influencing fire regimes in much of Australia. Where fire depends on the accumulation of herbaceous fuels, available moisture in the months preceding the fire season limits fire incidence. In contrast, available moisture in the preceding days and weeks is the limiting factor where fire depends on the drying out of forest litter. The exception to this pattern is the tropics, where monsoonal rainfall is predictably followed by 'the dry', leading to the build up and subsequent drying out of fuel which often burns annually. Murphy et al. (2012) also identified the latitudinal gradient in summer monsoon rain activity as the major driver of Australia's fire regimes at a continental scale. The pictures of Australia's fire regimes developed by Russell-Smith et al. (2007) and Murphy et al. (2012) provide significant new detail compared to a frequently cited earlier version from Luke and McArthur (1978; Figure 1.2).

These continental assessments highlight the significance of regular, widespread burning in Australia's north, for instance with regard to carbon accounting and the global carbon cycle (Meyer et al. 2012; Haverd et al. 2013b; Poulter et al. 2014). Conversely, adopting the stance of fire as a problem to be dealt with (Gill et al. 2013) or a natural hazard to coexist with (Moritz et al. 2014) shifts attention to the infrequent but high intensity fire regimes associated with

[2] Krebs et al. (2010) give an interesting account of the history of the fire regime concept.

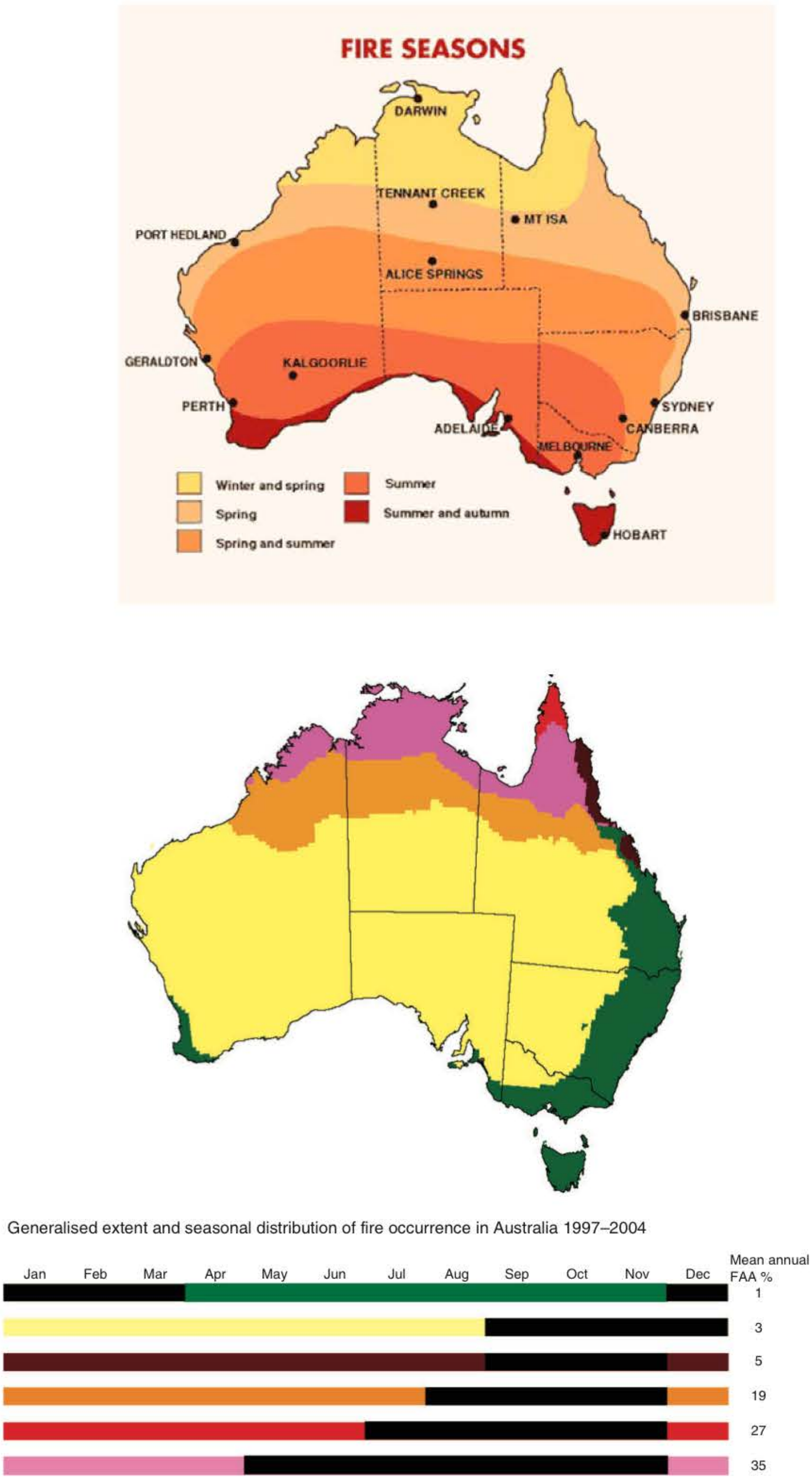

Figure 1.2 Models of different aspects of Australian fire regimes. Top is a widely cited schematic of bushfire seasonality (Luke and McArthur 1978). Bottom is a map and graph showing fire seasonality and extent derived by Russell-Smith et al. (2007). FAA stands for fire affected areas and corresponds to burned area.

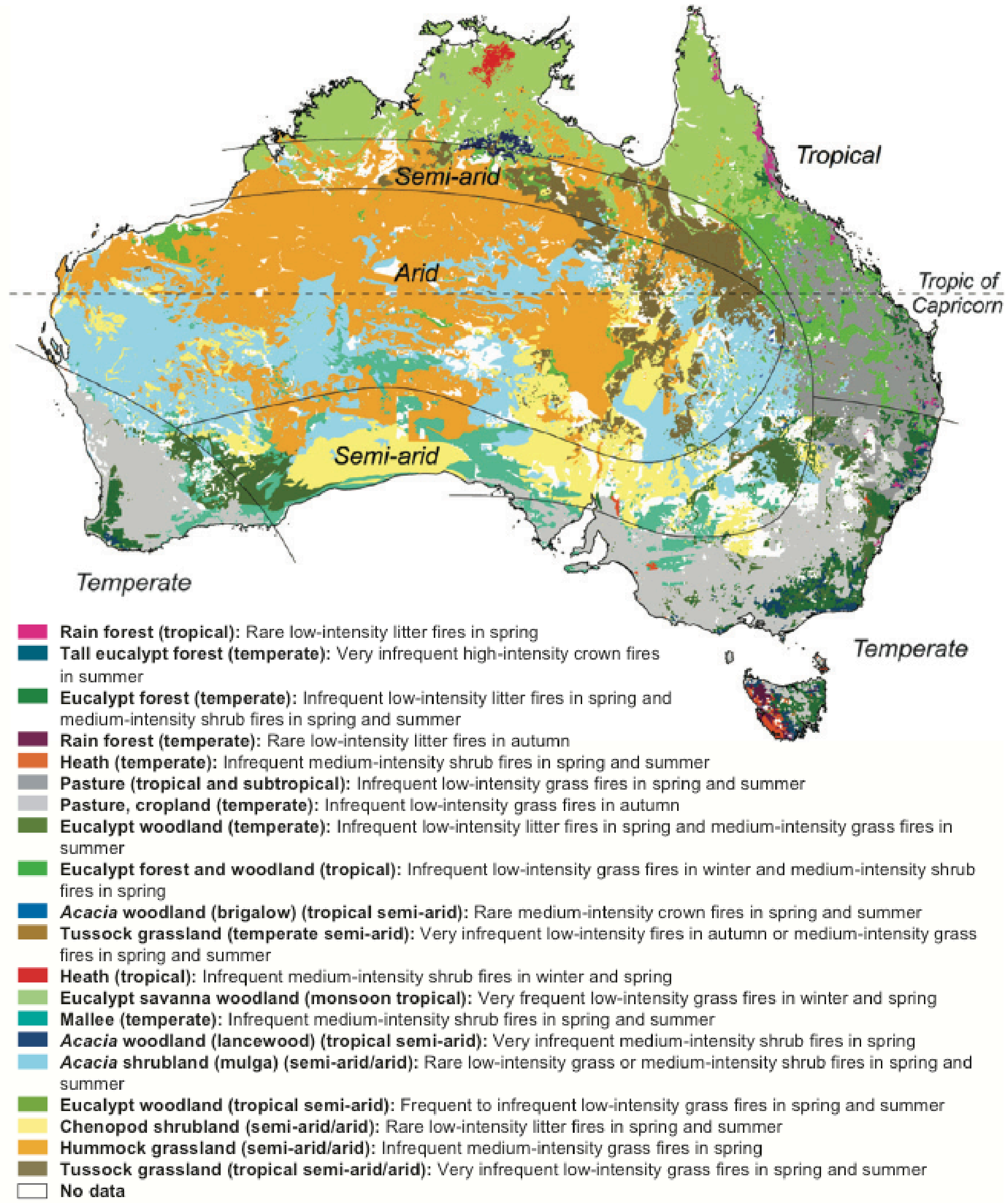

Figure 1.2 (continued) Model of Australian bushfire regime 'niches' from Murphy et al. (2012), encompassing vegetation type, fire frequency, fire intensity and seasonality. Niches are ordered according to decreasing annual net primary productivity.

eucalypt forests of Australia's southern and eastern extremities, because it is there that the majority of the Australian population lives. Particular attention is given to communities at the so-called wildland-urban interface (WUI), which are at greatest risk of the direct impacts of bushfires[3]. A national forum on fire research and policy priorities in 2003 nominated 'a better understanding of current fire regimes' as a major goal (Dovers et al. 2004). Over ten years on from the forum, major steps have been taken towards addressing this goal.

The 2003 forum identified another priority for both research and policy, which is the focus of this thesis: how can we improve our ability to forecast the impacts of climate change on bushfires, in particular at scales relevant to fire management? A number of studies have attempted to characterise potential responses of bushfire regimes to climate change, with significant impacts expected (Flannigan et al. 2009; Krawchuk et al. 2009; Bradstock 2010; Macias Fauria et al. 2011; Cary et al. 2012; Moritz et al. 2012; Bowman et al. 2014a). Given the complexity of bushfire, and its strong coupling to human systems, there are multiple pathways through which climate change may affect it (Hessl 2011; Bowman et al. 2013). One approach is to consider the impact of climate change on the drivers of fire incidence discussed earlier – fuel amount, fuel dryness, fire weather and ignition.

Fire weather is typically expressed through some combination of surface air temperature, precipitation, relative humidity[4] and wind speed. There are a number of different indices that integrate these meteorological variables into a single fire danger measure, for example the McArthur Forest Fire Danger Index (FFDI; Luke and McArthur 1978), the Canadian Forest Fire Weather Index System (FWI; Van Wagner 1987) and the United States National Fire Danger Ratings System (Deeming et al. 1977). Other metrics focus on the water and energy balance above the surface. The Haines Index (Haines 1988) and a variant adapted to Australia (Mills and McCaw 2010) link vertical atmospheric stability and humidity with erratic fire behaviour. The 850 hPa temperature gradient has been linked to extreme fire weather events over southeast Australia (Mills 2005a). There is a range of research focused on synoptic drivers of fire risk (e.g. Girardin et al. 2004; Crimmins 2006; Long 2006; Wastl et al. 2013; Papadopoulos et al. 2014 and references therein).

Numerous studies have projected changes in FFDI (e.g. Beer and Williams 1995; Cary and Banks 1999; Williams et al. 2001; Cary 2002; Lucas et al. 2007; Pitman et al. 2007; Bradstock et al. 2009; Fox-Hughes et al. 2014) and FWI (two recent examples are Bedia et al. 2013 and Lehtonen et al. 2014). Other elements of fire weather that have been related to climate change

[3] The building and construction guidelines of NSW, Australia, reserve a vivid term for those at highest level of bushfire risk: the flame zone.
[4] Relative humidity is actually a proxy for vapour pressure deficit, which directly influences fuel moisture. This proxy works best at low dew points and worst at high dew points and temperatures.

include atmospheric stability (Luo et al. 2013), synoptic patterns (Hasson et al. 2009; Grose et al. 2014) and modes of climate variability (Cai et al. 2009). By relating observed weather patterns to fire incidence or burned area, projected changes in weather are often used as a proxy for the presence of fire and its impacts (e.g. Amatulli et al. 2013; Mori and Johnson 2013).

Another of the four switches of fire, fuel dryness, can also be related to standard meteorological variables such as relative humidity and temperature[5]. Despite this, there are relatively few studies that focus on climate change impacts on fuel dryness as a driver of wildfire incidence (Matthews et al. 2011; Matthews et al. 2012). However, since FFDI and FWI incorporate measures of fuel dryness, studies of these indices contain implicit projections of climate change impacts on fuel dryness, even if their conclusions do not always emphasise this aspect. Fewer studies still have addressed climate change impacts on wildfire ignition sources. Such studies have focused on the only significant natural ignition source, lightning, through either model parameterisation (Price and Rind 1994; Goldammer and Price 1998; Krause et al. 2014) or a derived relationship between lightning and weather variables (Krawchuk et al. 2009; Penman et al. 2013). Although climate change per se is not expected to alter ignitions caused by humans, a number of studies have investigated the impacts of changes in variables linked to anthropogenic ignitions, such as population density or land use (Bistinas et al. 2013; Penman et al. 2013; Knorr et al. 2014; Price and Bradstock 2014).

In contrast to the direct use of meteorological variables for fire weather, fuel moisture and ignition risk assessment, attempts to predict changes in biomass growth or fuel load require a significant transformation of climate model data. The task is complicated by the need to factor in the potential response of vegetation to changes in atmospheric carbon dioxide (CO_2) concentration, in addition to climate (Karnosky 2003; Donohue et al. 2013). Reflecting this complexity, there are a number of different approaches to answering the question of how climate change affects wildfire fuel loads. Field and laboratory studies have examined the response of plants to elevated CO_2 in controlled environments, for instance through free air CO_2 enrichment (e.g. Barton et al. 2010). Similar to the other three switches, statistical relationships have been developed between current vegetation patterns and meteorological variables (Matthews et al. 2012; Thomas et al. 2014; Williamson et al. 2014). These relationships allow vegetation changes to be derived from projected changes in meteorological variables, but do not account for CO_2 effects. In contrast to these empirical studies, there is an active research community devoted to process-based approaches to fuel load and vegetation more broadly. These approaches include dynamic global vegetation models (DGVMs), landscape fire succession models and biogeochemical models. These models may represent

[5] Fuel dryness (i.e. fuel moisture) is of course commonly measured directly e.g. through field sampling

direct influences on fuel amount, such as litterfall, decomposition and fire incidence, as well as indirect causes like phenology, primary productivity, heat and moisture. Significantly, process-based models have the capacity to incorporate fertilisation effects of CO_2 on plant growth (e.g. Bala et al. 2013; Jiang et al. 2013).

Compared to the total number of studies of the impact of climate change on wildfire, relatively few attempt quantitative, integrated assessments of the impact of climate change on multiple fire drivers (Pechony and Shindell 2010; Kloster et al. 2012; Loepfe et al. 2012; Eliseev et al. 2014). In Australia, Bradstock (2010) provides a qualitative assessment of each of the four drivers, based on case studies of five fire regimes using quantitative and qualitative data. Bradstock (2010) concludes that increasing temperatures and dryness may lead to divergent impacts on fire activity across Australia, with potential increases in temperate forests, but decreases in areas where fires are currently limited by fuel amount rather than fire weather conditions. It is also noted that these trends could be confounded or reinforced by elevated CO_2 effects. Matthews (2012) estimates climate change impacts on fuel load, fuel moisture and fire weather at a single location in southeast Australia, finding increased fire weather and fuel moisture but decreased fuel amount, the latter through a litter accumulation model. King et al. (2011, 2012) examined climate change impacts on multiple wildfire drivers in forested and grassland regions of southeast Australia in two separate studies. While each examined potential changes in fire weather and fuel load, only the grassland study included fuel moisture (curing) as well as fertilisation effects of CO_2 (King et al. 2012), via a process-based grassland and water-balance model. Both studies projected increases in fire weather conditions and overall decreases in fuel load, which translated to increases in fire incidence and area burned in forests, but minimal changes in fire risk in grasslands.

To the author's knowledge, no previous studies have quantitatively addressed climate change impacts on fuel amount, fuel moisture, fire weather and ignitions across the landscape and at a scale relevant to decision makers, while incorporating fertilisation effects of CO_2 on vegetation. While this thesis does not attempt such a comprehensive endeavour, it examines a number of research avenues that build towards this goal.

Firstly, the thesis aims to explore climate change impacts on fire weather, as represented by the FFDI. Coupled climate models play a central role of in projecting future climate, making studies of fire weather an ideal research topic. FFDI can be calculated from meteorological variables obtained directly from global and regional climate models. There are also good scientific reasons for focusing on fire weather conditions, with evidence that weather can drive ignitions (Penman et al. 2013), fire severity (Bradstock et al. 2010), house loss (Blanchi et al. 2010) and fatalities (Blanchi et al. 2014). FFDI is chosen because of its considerable traction in the fire management community. It is used operationally by weather forecasters and fire agencies in Australia to declare fire weather warnings and total fire bans and to determine fire danger (the difficulty of putting out fires which may occur).

A natural reference point for any analysis or interpretation of projections of future fire weather is the existing or historical record of fire weather. Despite the widespread use of FFDI in climate projections research, there have been no peer-reviewed studies of existing spatial patterns or trends in this index in Australia. Chapter 3 aims to address this topic.

Chapter 4 aims to provide an initial estimate of the impact of climate change on FFDI using global climate models (GCMs). It builds on previous studies in a number of novel ways, making use of the evaluation of these climate models by Perkins et al. (2007) to select a subset that demonstrate skill in simulating the climate of Australia. These fire weather projections also aim to recognise the importance of rainfall in driving Australian fire regimes, by grouping results by regions of rainfall seasonality.

GCMs model the climate well at continental scales and above, but their ability to provide information about regional variations in climate is limited by their resolution and coarse representation of important regional climate drivers and offshore processes (e.g. the East Australian Current; Meehl et al. 2007b; Randall et al. 2007; Flato et al. 2013). Dynamical downscaling with regional climate models (RCMs) overcomes some of these limitations in providing information relevant to regional adaptation planning. They can operate at much finer spatial and temporal scales and contain additional information about a range of factors which are important in determining regional climate (such as more detailed topography). Since they are built on physical principles, dynamical RCMs allow for changes in the existing relationship between weather variables or climate drivers. A clear research direction therefore is to undertake high resolution modelling of fire weather. At the time of undertaking this research, only one Australian fire weather projection study (Lucas et al. 2007) used an (atmosphere only) RCM; the remainder were based on GCMs. Chapter 5 aims to lay the necessary groundwork for dynamically downscaled fire weather projections by undertaking an evaluation of the ability of a regional climate model to simulate observed FFDI.

The studies in Chapters 3 to 5 are limited by a lack of any link between increasing CO_2 levels, changes in plant growth and fuel load. The incorporation of more realistic representations of fire into global vegetation and climate change models has recently been cited as one of three keys to a better understanding of human-influenced fire regimes, along with better observational and historical data and a greater understanding of different cultural traditions of landscape burning (Bowman et al. 2011). The aim of the next phase of the thesis is to account for the effects of changing net primary productivity (NPP) under increased CO_2 conditions on fire risk.

To this end, Chapter 6 explores the use of NPP as a proxy for fuel load. NPP represents the rate of production of vegetation and changes in NPP are therefore associated with changes in the amount of vegetation and ultimately fuel load (Matthew 1997; Kindermann et al. 2008). The model of NPP as a proxy for fuel load is developed using a land surface model (LSM), which routinely simulates NPP. Equally importantly, the LSM used here provides the lower boundary conditions for the Australian coupled climate model used in numerical weather prediction and global intercomparisons (Kowalczyk et al. 2013).

Chapter 7 aims to draw together the research in Chapters 3 to 6 by developing the first relatively fine scaled (50 km horizontal resolution) continental assessment of the impact of climate change on two key drivers of bushfire risk, fire weather and fuel load, taking into account the interplay between increasing atmospheric CO_2 and plant growth. A key feature of the study is the use of an ensemble of GCMs and RCMs to sample, at least to some degree, the possible future change space. This ensemble is used to calculate projected changes in FFDI as well as force a land surface model, from which projected changes in fuel load are estimated.

Bushfires are an extremely diverse research topic and in focusing on fire weather and fuel load modelling, this thesis does not cover other important topics. The thesis does not consider bushfire ignitions, nor does it focus on fuel moisture – although the FFDI does contain an estimate of the moisture of fuel. By using FFDI, this research does not consider other important elements of weather such as synoptic patterns, atmospheric stability, wind direction and change, and local meteorological effects such as Foehn winds and topographic tunnelling. The model of fuel load developed here is necessarily simple, and does not take into account the complexity of Australian vegetation formations and fuel load dynamics, particularly their response to disturbance. Although fire weather conditions and fuel load both have significant impacts on fire behaviour, this thesis does not address the dynamics of fire, including characteristics like fire intensity and area burnt. An exception to the general omission of fire behaviour is the use of fire rate of spread, in Chapters 6 and 7, as a coarse measure of bushfire risk that integrates both weather and load. The diverse and complex consequences fire, including GHG emissions and changes in vegetation composition, are also beyond the scope of this thesis. Finally, this research does not address the human dimensions of fire, such as suppression, prescribed burning, smoke and the social and economic costs of bushfire. The scale of the projections developed here is not fine enough to facilitate detailed fire behaviour modelling or local fire weather forecasts. However, it is of a scale that can contribute to regional impact assessment and adaptation planning.

In summary, this thesis aims to contribute to the evidence base for understanding the impacts of climate change on fire weather conditions and fuel load in Australia. It does so by addressing four questions:

1. Are there significant trends in average or extreme fire weather within the observational record?

2. How is fire weather projected to change in different rainfall seasonality regions by skill-selected global climate models?

3. Can a simple model of fuel load be developed for use in the Australian land surface model, that accounts for both climate and atmospheric CO_2 effects on vegetation growth?

4. How are fire weather and fuel load projected to change at a relatively fine scale (50 km) by an ensemble of global and regional climate models, selected to span the possible future climate change space?

Chapter 2

Methods

Modelling the drivers of fire and climate

This thesis investigates the impact of climate change on two measures of bushfire risk, fire weather and fuel load. With the exception of Chapter 3, which focuses on observations, all of the studies contained herein use climate models to simulate past and future climate. These simulated climates are applied to measures of fire weather conditions and bushfire fuel load to arrive at estimates of the impact of the specified climate on these measures. Fire weather conditions are represented by an existing and widely used fire danger index. In contrast, a new and simple model of fuel load is developed for use in a land surface model (LSM), for the express purpose of facilitating estimates of the impact of climate change on load.

The first three sections address the use of global climate models (2.1), regional climate models (2.2) and reanalysis (2.3). The approach to bushfire risk is then addressed (2.4). Section 2.5 describes the calculation and use of FFDI as a measure of fire weather conditions. Section 2.6 describes the approach to fuel load, including the rationale for using an LSM (2.6.1), the development of a simple model (2.6.2-2.6.3) and its use (2.6.4-2.6.5). Section 2.7 describes the various analyses used throughout the thesis.

2.1 Global climate models

Global climate models (GCMs) are mathematical representations of the key processes of the Earth’s climate system, including the atmosphere, ocean and land surface, and are run on powerful computers (McGuffie and Henderson-Sellers 1987). The equations behind these models are based on well established physical laws such as conservation of mass, energy and momentum. Climate models are the main tools used to understand how earth’s climate system responds to various forcings and to project future climate on the scale of decades to centuries under different GHG emissions scenarios (Flato et al. 2013). There is a large research community dedicated to developing, running and evaluating climate models. The projections reported in the IPCC Fourth Assessment Report relied on trajectories of GHG emissions from the Special Report on Emissions Scenarios (SRES; Nakicenovic et al. 2000). Projections reported in the IPCC Fifth Assessment Report, which was released after the studies in this thesis were completed, use Representative Concentration Pathways (RCPs) instead of SRES emissions scenarios (Moss et al. 2010).

No GCMs are run as part of the research comprising this thesis. However, GCM output is used directly in Chapter 4 to project the impact of climate change on fire weather, and indirectly in Chapter 7 to supply the boundary conditions for a regional climate model (RCM) ensemble, from which climate change impacts on fire weather are estimated.

2.1.1 Fire weather projections from GCMs

For Chapter 4, daily climate model data over eastern Australia for maximum temperature, mean wind speed, average specific humidity and total precipitation are taken from the World Climate Research Program's (WCRP) Coupled Model Intercomparison Project phase 3 (CMIP3) multimodel dataset (Meehl et al. 2007a). The CMIP3 archive includes simulations of past, present and future climate. CMIP5 data were not available at the time of this and other studies in the thesis. Data from 1961 to 2000 are used to calculate present fire weather (i.e. 20th century for the purposes of the study in Chapter 4). Data from 2046 to 2065 and 2081 to 2100 are used to project climate for 2050 and 2100 respectively.

Only the A2 SRES emission scenario is used because at the time of the study it was the scenario closest to global emissions trends (Le Quéré et al. 2009) and for which daily data from multiple GCM simulations existed.

A key feature of Chapter 4 is the use of GCMs selected for their skill in representing the Australian climate. CSIRO, ECHO-G, IPSL and MRI are the models with the highest skill score over Australia, defined as the amount of overlap between observed and simulated probability density functions (PDFs) of daily temperature and precipitation (Perkins et al. 2007). MRI ranked fifth but daily data for the higher ranking MIROC-m were not available. One simulation is used per model because differences between individual model realisations were small (Perkins et al. 2007). Details of each climate model are available in Randall et al. (2007) and Perkins et al. (2007).

Another key element of the study in Chapter 4 is the aggregation of GCM output into rainfall seasonality zones. The study regions are adapted from the four major rainfall zones in eastern Australia: summer tropical (ST), summer (SU), uniform (UN) and winter (WI; Figure 2.1). These regions are based on differences between summer and winter rainfall (Australian Bureau of Meteorology 2005b). In the summer tropical (or 'summer dominant') zone, which occupies the upper half of the northeast state of Queensland (QLD), 50–70% of rainfall occurs in summer and winters are typically dry. Southeast QLD and northeast New South Wales (NSW) constitute the summer rainfall zone, receiving 30–40% of rainfall in summer and low rainfall in winter. The summer zone extends along or near the coast as far south as Sydney, NSW, with isolated patches in the southeast corner of NSW. To the south and west of the summer zone, precipitation occurs uniformly throughout the seasons. A patch of this uniform rainfall zone also occurs within the summer zone (Figure 2.1). The southwest of NSW and the majority of the southern state of Victoria fall within the winter rainfall zone, with a wet winter and low summer rainfall. Considerable areas of forest occur in all four zones.

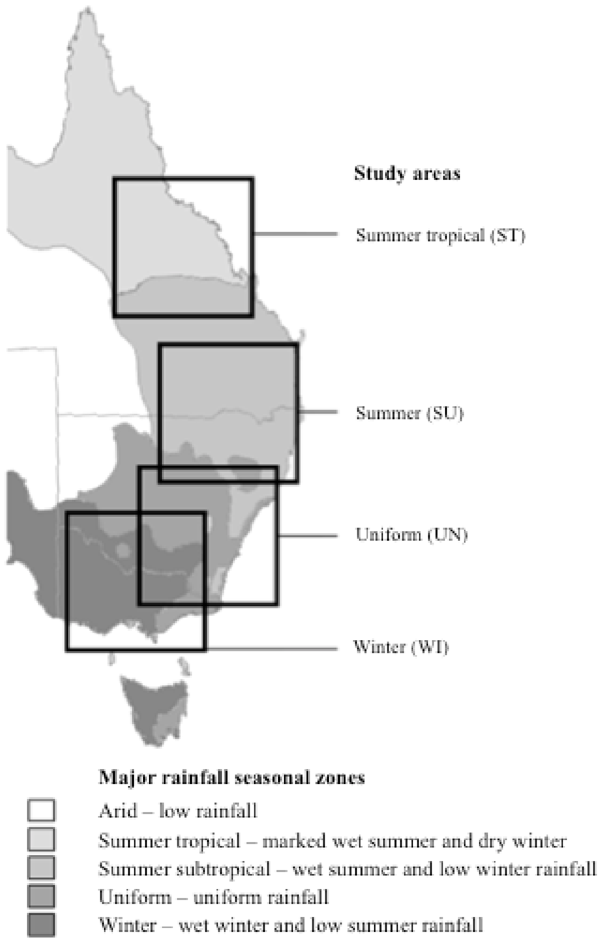

Figure 2.1 Rainfall seasonality regions (shaded; Australian Bureau of Meteorology 2005b) and study area (boxed) used in GCM-derived fire weather projections (Chapter 4).

To minimise overlap and maximise grid cell representation, a region size of 7° (~600 000 km^2) is used. This necessarily meant the exclusion of Tasmania and the inclusion of landscapes less prone to fire and a degree of overlap between rainfall zones, particularly in the south where rainfall zones are smaller. No ECHO-G grid cells fit in the uniform region and two CSIRO cells are counted towards separate regions (out of nine total grid cells in each). GCM grid-cell representation and other major features of the study areas are summarised in Table 2.1.

Table 2.1 Rainfall regions used in GCM-derived fire weather projections (Chapter 4).

Rainfall seasonality	Geographical area	Bounds (°)	Climate zones[1]	Number of model grid cells within region
Summer tropical (ST)	Northeast Queensland	17.5-24.5 S, 143.5-150.5 E	Tropical, subtropical, grassland	CSIRO (9), IPSL (2), ECHO-G (1), MRI (2)
Summer (SU)	Southeast Queensland, northeast New South Wales	25-32 S, 146.5-153.5 E	Subtropical, temperate, grassland	CSIRO (9), IPSL (2), ECHO-G (1), MRI (2)
Uniform (UN)	Mid- to southeast New South Wales	31-38 S, 145.5-152.5 E	Temperate, grassland	CSIRO (9), IPSL (1), ECHO-G (0), MRI (1)
Winter (WI)	Victoria, southwest New South Wales	33-40 S, 141.5-148.5 E	Temperate, grassland	CSIRO (9), IPSL (2), ECHO-G (1), MRI (4)

[1] Based on Köppen classification (Stern et al. 1999; Australian Bureau of Meteorology 2005a).

2.1.2 GCMs used to drive RCM ensemble for fire weather projections

A key feature of Chapter 7 is the use of global and regional climate model ensemble. Four GCMs are downscaled using three configurations of WRF resulting in a 12 member ensemble (Figure 2.2; Evans et al. 2014). GCMs were selected in three steps. First, a large set drawn from the CMIP3 (Meehl et al. 2007a) was evaluated in order to remove the worst performing models. Second, remaining models were ranked according to their independence following Bishop and Abramowitz (2013). Last, GCMs were placed within the future change space (defined by projected change in temperature and precipitation) and the most independent models that span that space were chosen. The GCM choices were MIROC3.2-medres, ECHAM5, CCCM3.1 and CSIRO-Mk3.0. The GCMs are downscaled for present (1990–2008) and, using the A2 SRES emissions scenario (Nakicenovic et al. 2000) future (2060–2078) time periods.

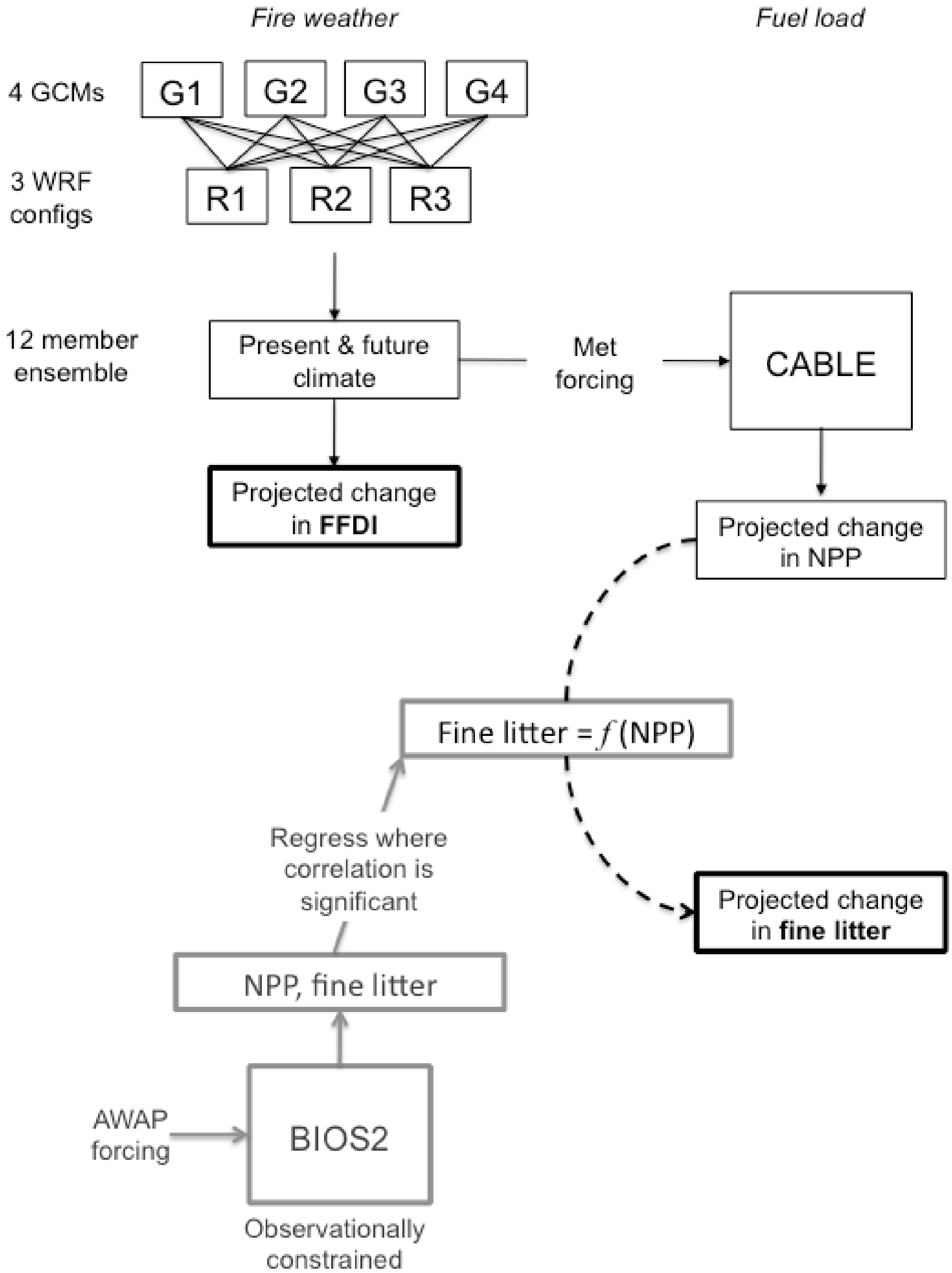

Figure 2.2 Methods for projecting fire weather and fuel load (Chapter 7). FFDI is calculated from a global and regional climate model ensemble spanning present (1990-2008) and future (2060-2078) periods. The same ensemble supplies the meteorological forcing to the land surface model CABLE, yielding NPP. Based on the relationship between fine litter and NPP in the BIOS2 modelling environment, fine litter is calculated from NPP in CABLE.

2.2 Regional climate models

As discussed in the Chapter 1, dynamical downscaling with RCMs overcomes some of the limitations of global climate models in providing information relevant to regional adaptation planning (Evans et al. 2012a). No RCMs are run as part of the research comprising this thesis. However, RCM output is used to calculate FFDI for the studies in Chapters 5 and 7. RCM output is also used in Chapter 7 to supply the meteorological forcing for LSM simulations, the output of which is used to calculate fuel load.

2.2.1 WRF Model

All regional climate model output used in this thesis is derived from the Weather Research and Forecasting (WRF) model, an open source atmospheric simulation system that can be used as an RCM (Skamarock et al. 2008). The design of WRF allows for the effective creation of many different RCMs through the selection of different model physical parameterisations. WRF has been shown to skilfully reproduce the observed spatial patterns of surface temperature and precipitation (Evans and McCabe 2010) and the diurnal rainfall cycle (Evans and Westra 2012) from the late 20th to early 21st century in southeast Australia. Another more practical reason for selecting WRF was the availability of output from simulations which were beyond my capacity to reproduce.

2.2.2 Simulation of historical fire weather by an RCM – WRF setup

In the study in Chapter 5, the Advanced Research WRF (ARW) version 3 is used. WRF is run from 1 November 1984 to 31 December 2009, excluding the first two months which are discarded as model spin-up. The model timestep is 1 min. Model top pressure is 50 hPa. The monthly atmospheric CO_2 concentration changes monthly from measurements at Baring Head, New Zealand (Evans and McCabe 2010). Sea surface temperatures are continuously updated and deep soil moisture varies dynamically throughout the simulation according to the physics embodied in the Noah land surface model. The following physics schemes are used: WRF single moment 5-class microphysics scheme; the rapid radiative transfer model (RRTM) longwave radiation scheme; the Dudhia shortwave radiation scheme; Monin-Obukhov surface layer similarity; Noah land-surface scheme; Yonsei University boundary layer scheme; Kain-Fritsch cumulus physics scheme and Rayleigh damping in the upper 5 km of the atmosphere. The model has 30 vertical levels spaced closer together in the planetary boundary layer. The physics schemes used here are chosen as a compromise between schemes that have been found to a) perform well in other studies (Evans and McCabe 2010; Evans et al. 2012b), b) represent the required physical processes and c) be computationally efficient enough to perform long simulations.

A key feature of the study in Chapter 5 is the comparison of two WRF simulations with different horizontal resolution. Two domains are used with one-way nesting. The parent and nested domain have respective horizontal grid spacings of 50 and 10 km. The two simulations are referred to as WRF50 and WRF10. The lateral boundary conditions of the parent domain are provided by reanalysis data (see section 2.3 below). The outermost six horizontal layers of both nests were discarded from the analysis to minimise lateral boundary effects.

2.2.3 Fire weather projections from RCMs – WRF setup

The WRF simulations in Chapter 7 are part of a study of the impact of climate change on fire weather and fuel load (Figure 2.2). The 12 member regional climate model ensemble used in Chapter 7 was built from 4 GCMs (see section 2.1.2 above) and 3 RCMs created by using different configurations of WRF (Evans et al. 2014). RCMs were selected using a similar process to that used to select GCMs. A large set consisting of different physical parameterisations was evaluated in order to remove the worst performing RCMs. From the better performing models, a subset was chosen such that each chosen RCM is as independent as possible from the other RCMs. The three selected model configurations are shown in Table 2.2.

Table 2.2 Configuration of RCMs selected for ensemble (Chapter 7; from Evans et al. 2014).

Ensemble member	Planetary boundary layer physics / surface layer physics	Cumulus physics	Microphysics	Short wave / long wave radiation physics
R1	MYJ / Eta similarity	KF	WDM 5 class	Dudhia / RRTM
R2	MYJ / Eta similarity	BMJ	WDM 5 class	Dudhia / RRTM
R3	YSU / MM5 similarity	KF	WDM 5 class	CAM / CAM

The RCM was run at 50 km resolution over the CORDEX AustralAsia region (Giorgi et al. 2009), which includes Australia, New Zealand, Indonesia, Papua New Guinea and large parts of the Indian, Southern and Pacific Oceans. Analysis is restricted to output over the Australian continent including Tasmania, bounded in the southwest at (44.75S, 110.5E) and in the northeast at (10.00S, 158.75E).

2.3 Reanalysis

Reanalyses are analyses of meteorological and oceanographic variables, created by incorporating observations of these quantities into modelling systems that are similar to climate models (Kalnay 2003). They can be contrasted with analyses, which are used in operational weather forecasting but are not consistent over long periods of time due to changes in the methods used to create them. By incorporating observations using a common method, reanalyses produce a long term, gridded estimate of the state of the climate that is as close to reality as possible.

No reanalyses are created for this thesis, but reanalysis output is used in Chapter 5 to calculate FFDI and provide the lateral boundary conditions to an RCM simulation. Modified reanalysis output is used in Chapter 6 to force an LSM, from which fuel load is estimated.

2.3.1 Reanalysis used to drive RCM simulation of historical fire weather

Chapter 5 presents an evaluation of the ability of WRF to simulate FFDI in southeast Australia. Reanalysis lateral boundary conditions are used to drive WRF, which minimises error inheritance and allows identification of positive and negative features of the RCM simulation in a reasonably controlled environment. The lateral boundary conditions of the parent domain are provided by 6-hourly National Centers for Environmental Prediction (NCEP) and National Center for Atmospheric Research (NCAR) reanalysis project data (NNRP; Kalnay et al. 1996) at a grid spacing of 250 km. The regional climate produced by the WRF simulation driven by the NNRP reanalysis has been extensively evaluated on time scales ranging from diurnal to interannual (Evans and McCabe 2010; Evans and Westra 2012). This simulation was found to be a good representation of the observed regional climate.

2.3.2 Reanalysis used to drive LSM simulation of historical fuel load

Chapter 6 presents a model for estimating fuel load over Australia. Similar to Chapter 5, reanalysis output is used in order to provide a long term estimate of the climate that is as close to reality as possible. A key difference is that the reanalysis data in Chapter 6 is bias corrected.

The LSM used in Chapter 6 is forced with meteorological data sourced from the Modern-Era Retrospective Analysis for Research and Applications (MERRA) reanalysis (Rienecker et al. 2011) at 3-hourly intervals and integrated from 1980 to 2008. The forcing variables include incoming longwave and shortwave radiation, air temperature, specific humidity, surface pressure, wind speed, and precipitation. The MERRA reanalysis was bias corrected for precipitation following Decker et al. (2013) using the Bureau of Meteorology's Australian Water Availability Project (AWAP) gridded precipitation dataset (Grant et al. 2008; Jones et al. 2009).

2.4 Perspectives on bushfire risk

In this thesis bushfire risk is considered through the lens of four major drivers of bushfire incidence: fuel load, fuel dryness, fire weather and an ignition source (Archibald et al. 2009; Bradstock 2010). These drivers of fire incidence can be considered switches, all of which need to be on for a bushfire to occur. One variation of this combines fuel amount and fuel dryness into a single switch (fuel) while adding a new switch, humans. This recognises the many ways humans influence fire, including by fragmenting the landscape, changing vegetation and actively suppressing fire. Although worthy of investigation, the role of humans is beyond the scope of this thesis. Other models of fire incidence include those of Preisler et al. (2004), Pechony and Shindell (2010), Guyette et al. (2012) and process-based fire models such as Thonicke et al. (2010).

Regional variation in fire regimes can be characterised in part by variation in which of the four switches tends to limit overall fire incidence. The four switches also provide a potential focus for climate change impact studies. Projected changes take on extra significance when they are to a switch that limits overall fire incidence for the fire regime in question. This thesis examines two of the four switches of fire: fire weather conditions and fuel load. A third switch, fuel dryness, is addressed only indirectly as a component of the fire weather index used.

By choosing drivers of bushfire incidence, this thesis focuses on the preconditions for fire. Other frameworks for understanding bushfire risk, and risk more generally, include both the probability of fire occurring and its consequences (e.g. Jones et al. 2012). These consequences might include impacts on human life and property, or more broadly on social, economic and natural systems. A focus on impacts suggests additional pathways for reducing bushfire risk beyond minimising fire occurrence, such as not locating properties and infrastructure in bushfire prone landscapes (reducing exposure) or using more fire resistant materials in building construction (reducing vulnerability). There are a wide range of programs, accompanied by a growing body of research, that address bushfire risk through preparedness. In Australia, this has focused on risk perception, homeowner preparedness and response during fires, and community safety (Moritz et al. 2014). In contrast, much work in the United States has been devoted to understanding the social acceptance of fuel reduction on public and private lands, and other risk minimisation techniques. The public response during and after fires is also beginning to receive more attention in the United States.

2.5 The McArthur Forest Fire Danger Index

In this thesis, fire weather conditions are represented using the Forest Fire Danger Index, known variously as the FFDI, McArthur FFDI, Fire Danger Index (FDI) and Fire Danger Rating (FDR). It was empirically derived in the late 1960s to relate weather conditions to expected fire behaviour and rate of spread (Luke and McArthur 1978). The FFDI combines observations of temperature, relative humidity and wind speed with an estimate of the fuel state: the 'drought factor'. The latter depends largely on daily rainfall and the amount of time since the last rain.

FFDI[1] was originally calculated using a set of cardboard wheels which the user turned to match the observations (the Forest Fire Danger Meter; Figure 2.3). Turning the wheels on the meter yielded a number (the FFDI) as well as a category corresponding to this number. Initially the highest category was "Extreme", corresponding to FFDI values between 50 and 100 (Figure 2.3). An FFDI of 100 was thought to indicate 'the near worst possible fire conditions that are likely to be experienced in Australia' (Luke and McArthur 1978). This notional upper bound was based on observations made during the 1939 Black Friday fires in Victoria: temperature of 40°C, relative humidity of 15%, 10 minute averaged wind speed of 55 km h^{-1} and at least six to eight weeks of drought. However, these conditions have been exceed in the observational record (Lucas 2010) and after the 2009 Black Saturday fires in Victoria the FFDI categories and thresholds were revised in many jurisdictions, including NSW, as follows: 0–11 (low/moderate), 12–24 (high), 25–49 (very high), 50–74 (severe), 75–99 (extreme) and 100+ (catastrophic).

Today the FFDI is used operationally by weather forecasters and fire agencies in Australia to declare fire weather warnings and total fire bans and to determine fire danger (the difficulty of putting out fires which may occur) and associated operational preparedness requirements.

[1] When describing FFDI as a value, rather than a fire weather index, no definite article is used.

2.5.1 Calculation of FFDI

Although the meters shown in Figure 2.3 are still used operationally (Lucas 2010), they have been reverse engineered to obtain equations by which FFDI is now more commonly calculated (Noble et al. 1980). The basic equation for FFDI is:

$$FFDI = 2 \times \exp(0.987 \times \ln(DF) - 0.0345 \times H + 0.0338 \times T + 0.0234 \times V - 0.45) \qquad (1)$$

where *DF* is the drought factor, *T* is the temperature (°C), *V* the wind speed (km h^{-1}) and *H* the relative humidity (%). Continuously recording weather stations make it possible to calculate FFDI at any time of day and to establish the daily maximum value. By convention, however, daily FFDI is calculated from daily maximum surface air temperature and 3pm local time (LT) values of relative humidity and wind speed, with wind speed calculated as an average of the previous 10 minutes at a height of 10m. The aim is to capture the period of highest fire danger in the day, which is often but not always around 3pm (Fox-Hughes 2011).

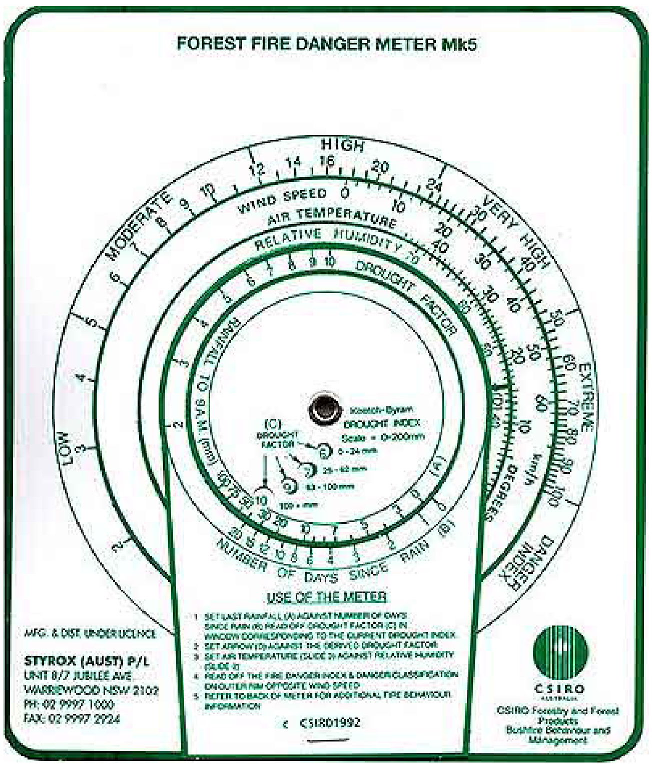

Figure 2.3 A McArthur Mk 5 Forest Fire Danger Meter (CSIRO 2011).

In contrast to the relatively simple formulation of T, V and H, the drought factor is more complex[2]. It is an empirical estimate of the state of the fuel, incorporating soil moisture deficit and recent daily rainfall. In the form used here, *DF* is calculated following the methodology described in Griffiths (1999) and Finkele et al. (2006). This method uses the Keetch-Byram Drought Index (KBDI; Keetch and Byram 1968) as its input for soil moisture deficit.

The drought factor is dimensionless, ranging between 0 and 10 and is calculated as:

$$DF = 10.5 \times (1 - \exp(-(\mathrm{KBDI}/30)/40) \times (41X^2 + X)/(40X^2 + X + 1) \qquad (2)$$

where X expresses the influence on the drought factor of past rainfall. X is defined as:

$$X = N^{1.3} / (N^{1.3} + P - 2) \quad \text{for } N \geq 1 \text{ and } P > 2 \qquad (3)$$
$$X = 0.8^{1.3} / (0.8^{1.3} + P - 2) \quad \text{for } N = 0 \text{ and } P > 2$$
$$X = 1 \text{ for } P \leq 2$$

where P is the past rainfall amount and N is the number of days since it fell. A rainfall event is defined as a set of consecutive days, each with rainfall above 2 mm, within the last 20 days. P is the sum of rainfall within the event and N is the number of days since the day with the largest daily rainfall amount within the rain event. In operational use, the above algorithm has been found to increase the drought factor too quickly in prolonged dry periods after significant rain events (Finkele et al. 2006). A correction applied by the Australian Bureau of Meteorology is used, which calculates X as the minimum of Eqn 3 and the limiting function X_{lim}, defined as:

$$X_{\mathrm{lim}} = 1/(1 + 0.1135 \times \mathrm{KBDI}) \quad \text{for KBDI} < 20 \qquad (4)$$
$$X_{\mathrm{lim}} = 75/(270.525 + 1.267 \times \mathrm{KBDI}) \quad \text{for KBDI} \geq 20$$

The FFDI methodology ignores local variations in fuel amounts and types, as well as the slope of the terrain, factors that significantly impact fire behaviour. However, the goal here is to understand the weather and climate aspects of the issue. Uncertainties in the amounts of historical grassland curing make the use of GFDI problematic. In any case, future climate projections show a great deal of overlap in the behaviour of the GFDI and FFDI (Hennessy et al. 2005). Furthermore, a comparison of FFDI with the widely used Canadian FWI shows considerable similarities between the two (Dowdy et al. 2010).

[2] Complex enough to have inspired the creation of simpler alternatives (Sharples and McRae 2009)

2.5.2 Analysis of historical trends in FFDI

Chapter 3 presents a study of historical trends in FFDI in Australia. The observations are drawn from Australia's first high quality observational FFDI dataset. This dataset has daily time resolution and is created using observations of maximum daily temperature and wind speed and relative humidity as measured at 1500 LT. The drought factor is calculated using daily rainfall measurements collected at 0900 LT.

A major feature of this dataset is the use of homogenisation. When investigating the long-term behaviour of any climate variable, the homogeneity of the dataset is important. Homogeneous data are those which are free from artificial trends or discontinuities, such as those caused by station relocations, instrument changes and/or changes in observational practices. Lucas (2010) examined the homogeneity of the FFDI dataset and its components. While all the individual datasets show some degree of inhomogeneity, those in the wind speed data have the largest impact on the FFDI. These inhomogeneities in the wind speed arise from the changing local environment of the wind measurement as well as the changing instrumentation used to record wind speeds (see also Jakob 2010), particularly those associated with the modernization of the observing network and the introduction of Automatic Weather Stations (AWS). Further, before the introduction of the AWS, wind reports at many of the rural stations in the dataset were made through visual estimates of the effects of wind on vegetation. The quality of these measurements is greatly dependent on the skill of the observer, and they often show many inhomogeneities. They are also often inconsistent with later records made with the modern AWS instrumentation, with very different means, variance and skewness characteristics. As a general rule, the mean of past wind speed measurements is lower than those measured with contemporary AWS anemometers. However, there are exceptions.

Lucas (2010) described a correction methodology for the wind inhomogeneities, applicable to statistics of the FFDI distribution rather than individual observations. Breakpoints in the wind speed time series are identified using two-phase regression similar to that described by Easterling and Peterson (1995). The bulk change in FFDI (ΔFFDI) at a given percentile level (e.g. median or 90th percentile) for a given change in wind speed (ΔV) is given by:

$$\Delta FFDI = 0.0234 \times FFDI \times \Delta V \qquad (5)$$

Past FFDI values are adjusted so that they are in relative homogeneity with contemporary measurements. The sensitivity of this homogenization methodology was discussed in Lucas (2010). It was found to adequately account for changes in the FFDI distribution at most percentile levels. However, this was not true at the extreme upper ends of the FFDI distribution, where the changes to the variance and the skewness of the winds had a significant effect. This generally occurred at percentile levels above 90%; the homogenization correction at higher levels is subject to more uncertainty. A scheme based on similar principles is determined for ΣFFDI. For this variable, an amount of adjustment is estimated by integrating Equation (2) multiplied by the observed relative frequency of occurrence of each value of FFDI over the observed FFDI distribution. This is done individually for each station.

A subset of the Lucas (2010) dataset is used, based on two criteria: 1) Stations that contain wind speed measurements based on visual estimates are excluded; 2) Stations with 365 or more total missing days are excluded. Applying these criteria results in 38 stations being selected for this analysis (Figure 2.4, Table 2.3). There is considerable overlap between the two sets of stations that fail to meet the criteria. Stations with visually estimated winds are mostly rural, where in general there are more missing data. The stations chosen tend to be located in the more populated areas, often at airports or meteorological offices. While the number of stations is approximately halved, the national coverage of the complete dataset is maintained, albeit with gaps in northern Queensland (QLD) and along the eastern border of Western Australia (WA).

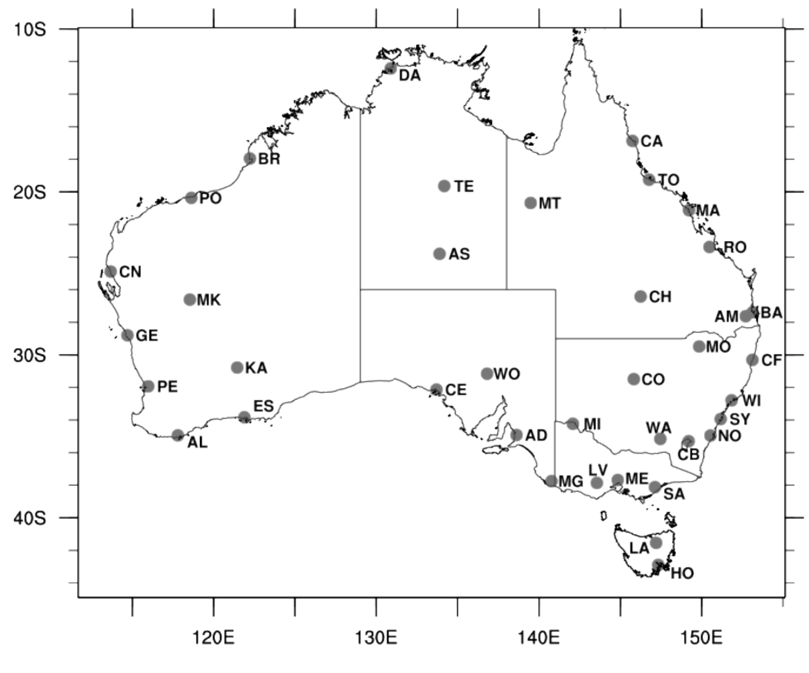

Figure 2.4 Stations used to analyse historical FFDI trends (Chapter 3). See Table 2.3 for key. The marker for Laverton (LV) has been moved west to avoid overlap with Melbourne Airport.

Table 2.3 Stations used to analyse historical FFDI trends (Chapter 3).

Station (Abbreviation)	State	Latitude (°)	Longitude (°)
Adelaide (AD)	SA	-34.92	138.62
Albany Airport (AL)	WA	-34.94	117.80
Alice Springs (AS)	NT	-23.80	133.89
Amberley (AM)	QLD	-27.63	152.71
Brisbane Airport (BA)	QLD	-27.39	153.13
Broome (BR)	WA	-17.95	122.23
Cairns (CA)	QLD	-16.87	145.75
Canberra (CB)	ACT	-35.30	149.20
Carnarvon (CN)	WA	-24.89	113.67
Ceduna (CE)	SA	-32.13	133.70
Charleville (CH)	QLD	-26.42	146.25
Cobar (CO)	NSW	-31.49	145.83
Coffs Harbour (CF)	NSW	-30.31	153.12
Darwin (DA)	NT	-12.42	130.89
Esperance (ES)	WA	-33.83	121.89
Geraldton (GE)	WA	-28.80	114.70
Hobart (HO)	TAS	-42.89	147.33
Kalgoorlie (KA)	WA	-30.78	121.45
Launceston Airport (LA)	TAS	-41.54	147.20
Laverton (LV)	VIC	-37.86	144.76
Mackay (MA)	QLD	-21.12	149.22
Meekatharra (MK)	WA	-26.61	118.54
Melbourne Airport (ME)	VIC	-37.68	144.84
Mildura (MI)	VIC	-34.23	142.08
Moree (MO)	NSW	-29.49	149.85
Mt Gambier (MG)	SA	-37.75	140.77
Mt Isa (MT)	QLD	-20.68	139.49
Nowra (NO)	NSW	-34.95	150.54
Perth Airport (PE)	WA	-31.93	115.98
Port Hedland (PO)	WA	-20.37	118.63
Rockhampton (RO)	QLD	-23.38	150.48
Sale (SA)	VIC	-38.12	147.13
Sydney Airport (SY)	NSW	-33.94	151.17
Tennant Creek (TE)	NT	-19.64	134.18
Townsville (TO)	QLD	-19.25	146.77
Wagga (WA)	NSW	-35.16	147.46
Williamtown (WI)	NSW	-32.79	151.84
Woomera (WO)	SA	-31.16	136.81

2.5.3 Use of historical FFDI to evaluate an RCM simulation

Chapter 5 presents an evaluation of the regional climate model WRF's ability to simulate observed FFDI in southeast Australia. The observations used for the evaluation are drawn from the same FFDI dataset used in Chapter 3. As stated above, the observations used in Chapter 3 are subject to a correction for wind inhomogeneities that is applicable to the statistics of the

FFDI distribution, rather than individual observations. The methodology breaks down at the extreme upper ends of the FFDI distribution, typically above the 90th percentile. However, the evaluation criteria employed in Chapter 5 require observations with daily time resolution and include values occurring less frequently than those at the 90th percentile. In order to retain data with daily resolution uncorrected data is used. This leads to an underestimate of average FFDI values by ~5% for the period of this study (corrected and uncorrected data supplied by Chris Lucas, Bureau of Meteorology).

All weather stations from Lucas (2010) that fall within the regional climate model domains are used for the analysis; 35 in total (Figure 2.5, Table 2.4). All stations are missing some observational data (Table 2.4).

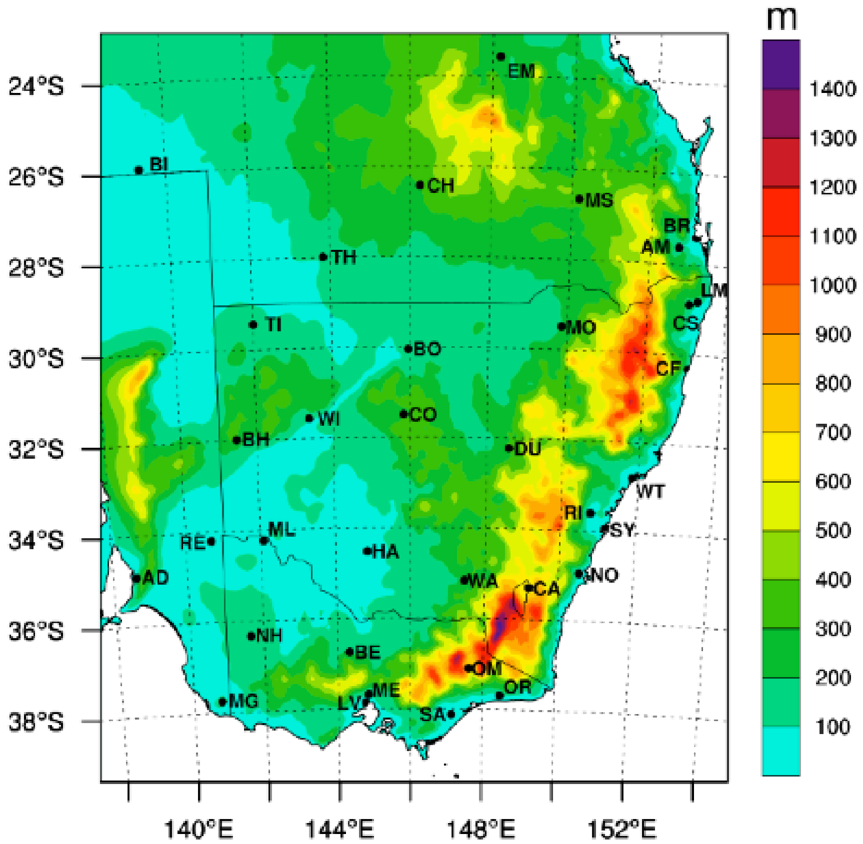

Figure 2.5 WRF domain showing elevation and stations used to evaluate WRF (Chapter 5). See Table 2.4 for key.

Table 2.4 Stations used to evaluate WRF (Chapter 5), including missing data.

Station (Abbreviation)	Station location (°) Lat	Lon	Total days missing (years missing >90 days)
Adelaide (AD)	-34.92	138.62	16
Amberley (AM)	-27.63	152.71	259
Bendigo (BE)	-36.74	144.33	57
Birdsville (BI)	-25.9	139.35	652 (1997)
Bourke (BO)	-30.04	145.95	561 (1998)
Brisbane (BR)	-27.39	153.13	7
Broken Hill (BH)	-31.98	141.47	708 (1985, 1991)
Canberra (CA)	-35.3	149.2	16
Casino (CS)	-28.88	153.05	1012 (1985-86)
Charleville (CH)	-26.42	146.25	27
Cobar (CO)	-31.49	145.83	80
Coffs Harbour (CF)	-30.31	153.12	18
Dubbo (DU)	-32.22	148.58	298
Emerald (EM)	-23.57	148.18	159
Hay (HA)	-34.52	144.85	441 (1991)
Laverton (LV)	-37.86	144.76	21
Lismore (LM)	-28.81	153.26	680 (1986-87)
Melbourne (ME)	-37.68	144.84	19
Mildura (ML)	-34.23	142.08	10
Miles (MS)	-26.66	150.18	530 (1987)
Moree (MO)	-29.49	149.85	24
Mt Gambier (MG)	-37.75	140.77	8
Nhill (NH)	-36.33	141.64	104
Nowra (NO)	-34.95	150.54	246
Omeo (OM)	-37.1	147.6	1021 (1986, 2002, 2009)
Orbost (OR)	-37.69	148.47	47
Renmark (RE)	-34.2	140.68	173 (1988)
Richmond (RI)	-33.6	150.78	29
Sale (SA)	-38.12	147.13	101
Sydney (SY)	-33.94	151.17	6
Thargomindah (TH)	-27.99	143.82	345
Tibooburra (TI)	-29.44	142.01	131
Wagga (WA)	-35.16	147.46	13
Wilcannia (WI)	-31.56	143.37	1057 (1985, 1988-92, 1996)
Williamtown (WT)	-32.79	151.84	9

2.5.4 Calculation of FFDI from climate models

FFDI is computed at each model grid cell using Equations 1-4 above. Due to limitations in the available model data, there are some departures from the standard method for calculating FFDI. The study in Chapter 4 calculates FFDI from skill-selected global climate models (GCMs). Departures from the standard method include the use of daily average wind speed and humidity, derivation of wind speed from GCM-simulated north and east vectors, and derivation of relative humidity from GCM-simulated specific humidity and temperature. The use of daily mean, rather than 3pm, relative humidity is likely to lead to underestimates of FFDI. The effect of using daily mean wind speed is less clear because, unlike temperature (relative humidity), wind speed is not generally assumed to be greatest (lowest) around 3pm. However, no quantitative analysis of these effects was conducted. In addition, for some models surface humidity data is not available so was calculated based on a simple linear relationship found to exist between GCM humidity at surface (1000 hPa) and 925 hPa over land.

The studies in Chapters 5 and 7 calculate FFDI from a regional climate model (RCM). Departures from the standard method include the derivation of wind speed from RCM-simulated north and east wind vectors and the derivation of relative humidity from RCM-simulated specific humidity, temperature and air pressure. Further, wind speed values are instantaneous, not 10 minute averages.

2.6 Fuel load

Bushfire fuel load is connected to a wide range of human and natural systems, with each system emphasising different aspects of load. Fire fighters and communities are directly affected by fuel load because it affects fire behaviour – including rate of spread, flame height and spotting – and the resulting probability of suppression (Watson 2009). Since fires typically ignite in fuels found on the surface, fuel load is often defined as surface fuel – primarily litter, the dead leaves and twigs that have been shed from living and dead plants (Watson 2009). The need to improve our understanding of fire behaviour has led to a more nuanced approach to fuel modelling, stressing the importance of different layers of fuel and the spaces between them, rather than the total mass of surface fuel (e.g. Cheney et al. 1992; Gould et al. 2007; Hines et al. 2010; Zylstra 2011). Establishing links between vegetation types and typical fuel load levels has contributed significantly to the management of fire across the landscape (e.g. Watson 2012). Where vegetation mapping allows, these links provide an estimate of average or baseline conditions. By adding information about the evolution of fuel load over time, particularly its buildup since the last fire, fire managers make decisions and allocate scarce resources for conducting planned burns (Penman et al. 2011). Wildfires and controlled burns are an important source of local and regional air pollution, with significant human health impacts including an estimate of over 330,000 deaths annually due to bushfire smoke (Johnson et al. 2012; Johnston and Bowman 2013). Studies of biomass burning emissions more broadly emphasise specific aspects of fuel load (e.g. dryness, structure, vegetation type) that influence (e.g. Russell-Smith et al. 2009). Finally, at both global and regional scales, wildfires influence the carbon cycle, releasing large quantities of carbon into the atmosphere, which slowly return during vegetation regrowth

(Haverd et al. 2013c; Poulter et al. 2014). In Indonesia, for example, emissions from a single year of peat fires were equivalent to 20-40% of global fossil fuel emissions (Page et al. 2012).

2.6.1 CABLE model and the rationale for using an LSM to model fuel load

Fuel load models vary widely in how they derive load, with mechanisms represented empirically at one end of the spectrum to process-based approaches at the other (Adams et al. 2013). A key aim of process-based models is to provide physically consistent and spatially and temporally continuous estimates of many different variables across the entire landscape. Process-based approaches to fuel load dynamics are incorporated in several major classes of models, including dynamical global vegetation models (DGVMs), landscape fire succession models and biogeochemical models. These models allocate carbon or total biomass into multiple litter pools based on the balance of litterfall and decomposition (e.g. Wang et al. 2010; Keane et al. 2011). Litterfall is typically linked to phenology and primary productivity, while decomposition is determined by a combination of heat and moisture.

LSMs provide process-based simulations of fluxes of heat, water and carbon between the land surface and the atmosphere. The Community Atmosphere Biosphere Land Exchange (CABLE; Wang et al. 2011) model is a sophisticated LSM that can be run as an offline model with prescribed meteorology (e.g. Kala et al. 2014) or fully coupled to an atmospheric model within a global or regional climate model (e.g., Hirsch et al. 2014). CABLE has been extensively evaluated (Abramowitz et al. 2008; Wang et al. 2011) and has been used at site-specific, (Abramowitz et al. 2007), regional (Cruz et al. 2010) and global (Pitman et al. 2011; Zhang et al. 2011; Lorenz et al. 2014) scales.

Critically, CABLE also provides the lower boundary condition for the Australian Community Climate and Earth System Simulator (ACCESS) coupled climate model used in numerical weather prediction (NWP) and global intercomparisons, including the Australian contribution to CMIP5 (Kowalczyk et al. 2013). The use of CABLE in this context provides an advantage over other process-based models that provide explicit measures of fuel load but are not routinely used for NWP or in IPCC assessments. The aim of Chapter 6 is to develop a simple model of fuel load that can be incorporated into the operational LSM used in Australia.

2.6.2 Development of a simple fuel load model

The model developed in Chapter 6 uses net primary productivity (NPP), which is routinely simulated by LSMs, as a proxy for fuel load, which is not. The rationale for using NPP as a proxy for fuel load is well founded. NPP represents the rate of production of vegetation and changes in NPP are therefore associated with changes in the amount of vegetation and ultimately fuel load (Matthew 1997; Kindermann et al. 2008). Since fuel load is usually considered as a subset of total plant matter (e.g. foliage and small twigs in forests), it is proportional to, rather than equivalent to, total accumulated NPP. Chapter 7 uses this model to project the response of fuel load to climate change.

The fuel load model is developed in two parts (Figure 2.6). Part A aims to derive the relationship between fuel load and NPP. This ideally requires observations of both quantities at a sufficiently long time-scale and over a range of ecosystem/vegetation types. Since these datasets are not available, the next best source of fuel load and NPP data is from an ecosystems model, ideally one that has been constrained using observations. One such modelling environment, BIOS2 (Haverd et al. 2013a), includes a biogeochemical model that includes fine litter pools, and is constrained by multiple observational datasets, including litter observations and flux tower measurements. BIOS2 is not designed to be coupled to a climate model and cannot be used in ACCESS. The routine use of CABLE in Australia, including coupled to ACCESS and regional climate models, provides the rationale for part B of the study, which aims to simulate fuel load in CABLE by using the BIOS2 relationship between fuel load and NPP derived in Part A. The fuel load generated will be consistent with CABLE's simulation of NPP. Finally, uncertainty in the estimation of fuel load in CABLE is examined by varying three key vegetation parameters that have a large influence on NPP.

2.6.3 Linking fuel load with NPP

BIOS2 is a system for modelling the coupled energy, water and carbon balances of the Australian continent at fine spatial (0.05°, 5 km) and temporal (hourly) scales (Haverd et al. 2013a). BIOS2 is limited to the Australian continent and cannot be coupled to the global ACCESS model. BIOS2 is partly based on the land surface model CABLE, but with some important differences (see Part B for a description of the CABLE model). BIOS2 does not use CABLE's default modules for soil processes and carbon. Instead, it uses the SLI soil model (Haverd and Cuntz 2010) and the CASA-CNP biogeochemical model (Wang et al. 2010). CASA-CNP allocates the carbon cycling through the terrestrial ecosystem into plant, litter and soil pools. There are three litter pools: metabolic, structural and coarse woody debris. BIOS2 was run from 1990 to 2011 using meteorological forcing from the AWAP dataset.

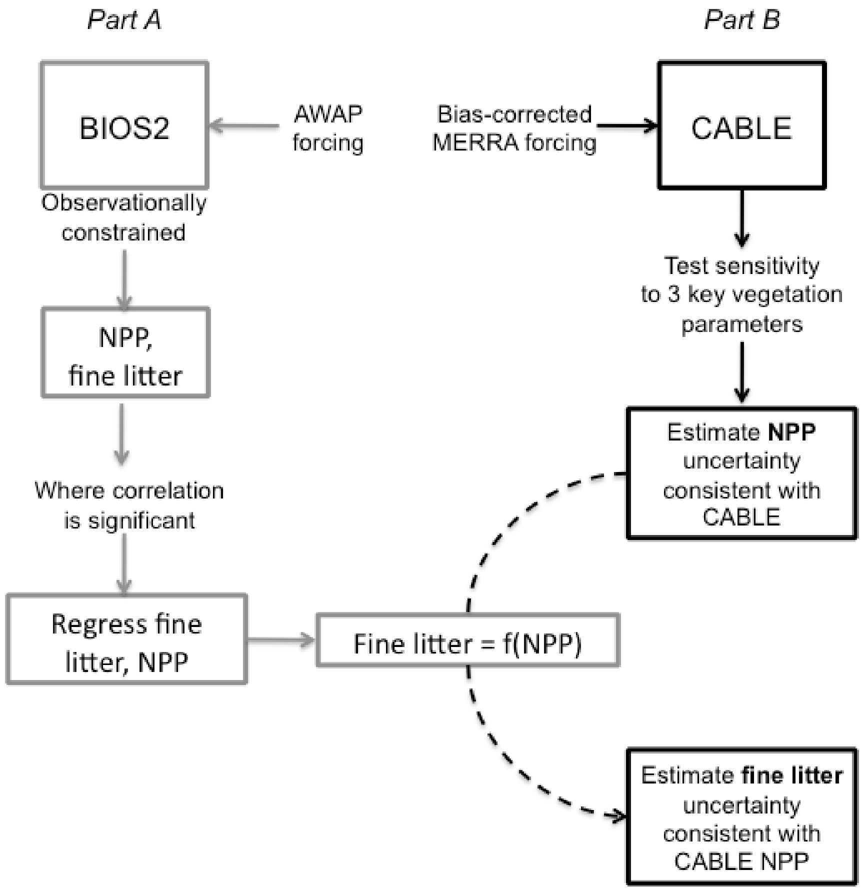

Figure 2.6 Methods for developing a simple fuel load model (Chapter 6). By linking fuel load and NPP in BIOS2 (Part A), fuel load can be calculated from NPP in CABLE (Part B).

AWAP data are downscaled from daily to hourly time steps (on the half-hour) using a weather generator within BIOS2. The BIOS2 simulations used here were also constrained by observations of a wide variety of variables including streamflow, evapotranspiration, net ecosystem production and litterfall. The use of observational constraints along with the best available gridded observations for Australia (AWAP) means the simulations by BIOS2 are likely the best available estimates of quantities such as fuel load that are not measured often enough or over a large enough sample, to provide a direct observational dataset.

Fuel load is defined as fine litter, which is the sum of the metabolic (easily broken down) and structural (resistant) litter pools (e.g. Wang et al. 2010; Haverd et al. 2013a). BIOS2 divides vegetation cover in each grid cell into persistent (mostly woody) and recurrent (mostly grassy) fractions based on partitioning of remotely sensed estimates of the fraction of photosynthetic absorbed radiation (fPAR; see Haverd et al. 2013a). Woody fine litter is mostly along the southwest and southeast coast and in Tasmania, where most of the evergreen broadleaf forests are found. Grassy fine litter is mostly within the agricultural regions of the southwest and southeast wheat belts and parts of the northern tropical savannas.

To obtain the relationship between NPP and fuel load for BIOS2, the relationship between annual NPP and fine litter for the period 1990 to 2011 is calculated using the Pearson product-moment correlation coefficient. BIOS2's fine litter values are also compared with NPP values in the preceding year i.e. lag-1 correlation, on the grounds that it should be on the order of one seasonal cycle before NPP is translated into fine litter load. NPP and fine litter are not separated into grassy and woody fractions; instead the total of both grassy and woody fractions is used in all analyses. Fine litter is related to NPP using ordinary least squares linear regression, with NPP taken as the independent variable. There is a generally high correlation between the two variables, and no clear evidence for a nonlinear relationship. For each model grid cell with a significant ($p < 0.05$) lag-1 correlation, a linear model is calculated.

To understand regional variation in model output, a modified Köppen climate classification is used, which separates Australia into 6 mostly-contiguous and climatically similar regions (Figure 2.7; Stern et al. 1999). The Köppen zones are: equatorial, tropical, subtropical, desert, grassland and temperate. A linear model is developed for each of these climate zones. Although one of the climate zones is called 'grassland', there is no separation of woody and grassy fractions in this or any other climate zone in this analysis. These zones are applied to fuel load simulations in Chapter 6 and both fuel load and FFDI simulations in Chapter 7.

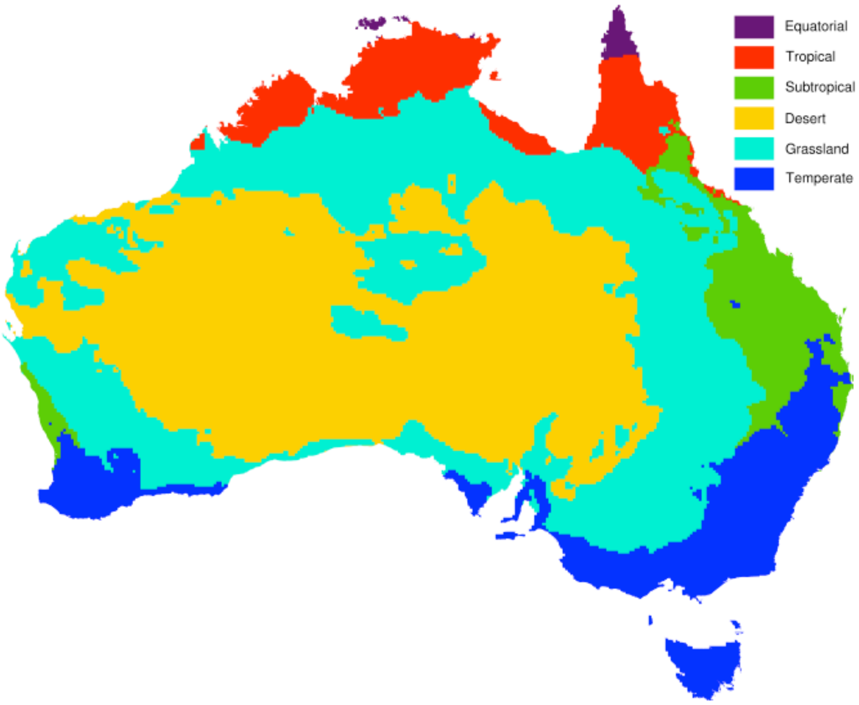

Figure 2.7 Köppen zones used to regionalise model output (Chapters 6, 7; Stern et al. 1999).

2.6.4 Simulation of historical fuel load by an LSM – CABLE setup

The version used in this study is CABLEv1.4b. In CABLEv1.4b, the one-layered, two-leaf canopy radiation module of Wang and Leuning (1998) is used for sunlit and shaded leaves and the canopy micrometeorology module of Raupach (1994) is used for computing surface roughness length, zero-plane displacement height, and aerodynamic resistance. The model also consists of a surface flux module to compute the sensible and latent heat flux from the canopy and soil, the ground heat flux, as well as net photosynthesis. A soil module is used for the transfer of heat and water within the soil and snow, and an ecosystem carbon module based on Dickinson et al. (1998) is used for the terrestrial carbon cycle. A detailed description of CABLE is provided by Wang et al. (2011). CABLE, like most LSMs, uses plant functional types (PFTs), as opposed to the partitioning of cells between recurrent and persistent vegetation as BIOS2 does. This implementation of CABLE uses fixed PFTs derived from the International Geosphere–Biosphere Programme (IGBP) land-use classification map.

CABLEv1.4b is used within the National Aeronautics and Space Administration Land Information System version 6.1 (LIS-6.1; Kumar et al. 2006, 2008), a flexible software platform designed as a land surface modelling and hydrological data assimilation system. A grid resolution of 0.25° is utilized, covering Australia. Monthly CO_2 concentrations are prescribed using measurements from Baring Head, New Zealand (Keeling et al. 2005).

Using CABLE in this way provides NPP consistent with the meteorological forcing and the LSM. In order to estimate uncertainty in NPP from CABLE, and hence fuel load, a series of sensitivity experiments are carried out using the upper, lower and middle estimates of three vegetation parameters that influence NPP. Lu et al. (2013) conducted an extensive parameter sensitivity analysis of CABLE and found that globally, the most important parameters affecting gross primary production (GPP), and therefore affecting NPP, are the maximum carboxylation rate (v_{cmax}, the maximum ribulose-1,5-bisphosphate carboxylation rate of the leaves at the canopy top at a leaf temperature of 25°C), followed by Leaf Area Index (LAI, the total one-sided surface area of leaf per ground surface area). v_{cmax} partially determines the rate of photosynthesis and hence GPP and thereby NPP and is estimated as a function of leaf nitrogen per unit leaf area. LAI affects photosynthesis directly in the ecosystem carbon module, where it also affects GPP and to a lesser extent autotrophic respiration. Finally, the rooting depth (r) was varied. NPP is partially dependent on soil moisture since transpiration cannot occur in the absence of water. Varying r changes the amount of water available for transpiration and photosynthesis and therefore, GPP and NPP. Root depths are not well known and therefore r remains a parameter that is uncertain but important.

Kala et al. (2014) examined the influence of realistic interannual variations in LAI on the surface energy and carbon balance in CABLE. They generated a 15 member monthly LAI ensemble, based on the Moderate Resolution Imaging Spectroradiometer (MODIS) LAI product and gridded observations of temperature and precipitation. The maximum, mean and minimum LAI ensemble members from Kala et al. (2014) are used for these simulations to capture the variability of LAI. Upper and lower estimates of v_{cmax} values are derived from Kattge et al. (2009). Since the values in Kattge et al. (2009) did not exactly match the default CABLE values for each plant functional type, CABLE values are varied by the ratio of standard deviation to mean values as shown in Table 3 of Kattge et al. (2009). Upper and lower estimates for *r* are derived by varying default values by the standard deviation of the default *r* values for all plant functional types (0.015). The key 1 = low, 2 = default (v_{cmax}, *r*) or mean (LAI), 3 = high is used to describe these experiments. For example, L3V1R2 refers to the ensemble member with a high LAI parameter value, a low v_{cmax} parameter value, and the default *r* value.

2.6.5 Fuel load projections from an LSM – CABLE setup

The CABLE simulations in Chapter 7 are part of a study of the impacts of climate change on fire weather and fuel load (Figure 2.2). The version used in this study is CABLE v2.0. A detailed description of CABLE is provided by Wang et al. (2011). CABLE is used within LIS-6.1 (Kumar et al. 2006, 2008). A grid resolution of 0.25° is utilized, covering Australia. 12 offline simulations are run, each forced with meteorological data from one of the 12 regional climate model ensemble members described above. The emissions scenarios used in WRF (i.e. present day and SRES A2) are also used with CABLE. LAI is prescribed using the mean of the 15 member monthly LAI ensemble described above (Kala et al. 2014). The same LAI prescribed for present day simulations is also used for future projections. The use of prescribed LAI i.e. the inability of LAI to respond to variations in surface climate or atmospheric CO_2, is a limitation of this study. It is likely to dampen variation in NPP due to changes in LAI but the overall effect is expected to be small.

2.7 Analysis

The FFDI analyses in Chapters 3, 4 and 5 include measures of mean and extreme FFDI. Chapters 3, 4 and 7 include measures of FFDI seasonality. Chapter 7 includes measures of mean FFDI and fuel load, as well as seasonality of both variables. Chapters 6 and 7 also introduce fire rate of spread, as a simple way of incorporating the influence of both load and fire weather on a measure of bushfire risk.

2.7.1 Analysis of trends in historical fire weather

To analyse the long-term trends of fire weather in Australia, daily data are further summarized on both annual and seasonal time scales. Across much of Australia, the peak fire season occurs during the summer half of the year, roughly from September to March (Luke and McArthur 1978; but see also second two parts of Figure 1.2). To accommodate this, a 'fire year' is chosen to run from 1 July to 30 June of the following year for the annual calculations. The variables chosen to summarize the fire weather climate are:

1. Annual cumulative FFDI (ΣFFDI): This variable is calculated as the sum of all daily FFDI values over the entire fire year (Beer and Williams 1995). It provides a useful metric to compare relative levels of fire weather danger over long time periods and/or different spatial areas. Cumulative FFDI is computed from the 1973–1974 through the 2009–2010 fire years, a total span of 37 years.

2. Annual 90th percentile FFDI: The daily values during a fire year are sorted, and the 36th highest value is chosen. This variable is indicative of the extreme end of the fire weather spectrum, times when the largest, most intense wildfires are more likely to occur and be more active. This variable is computed over the same period as ΣFFDI.

3. Seasonal median and 90th percentile FFDI: The median and 90th percentile FFDI over the standard southern hemisphere meteorological seasons are chosen (i.e. December–January–February (DJF), March–April– May (MAM), etc.). Each season is approximately 90 days long. This variable provides information on any potential changes in the annual timing of the fire season. It is available from MAM 1973 through DJF 2011.

The trends in Chapter 3 are estimated by using ordinary least squares linear regression with time taken as the independent variable. There is no physical reason why trends in fire weather should be strictly linear. Rather, this method is chosen as it is simple, widely used and easily understood. The possibility of more complex trend shapes cannot be excluded. The 95th percentile confidence interval for linear trends is also calculated for each time series. The F - statistic ($p < 0.05$), a comparison of the variance explained by the linear fit and the total variance of the system, is examined as an indicator of the significance of the trend.

The calculation of climate trends is sensitive to the choice of start and end dates of the calculation. The robustness of trends calculated here is examined with some simple sensitivity tests. These are:

1. changing the start and end dates by 1, 5 and 10 years and
2. randomly removing increasing numbers of stations and in each case re-calculating trends.

2.7.2 Analysis of fire weather projections from GCMs

Bootstrapping is a statistical method to increase the sample size by randomly selecting data values from the original dataset to create a new set of observations of specified size, making it possible to put confidence bounds on sample parameters. Standard, with-replacement bootstrapping techniques are used to create 1000 bootstrap samples for each GCM, region and scenario. These are used to calculate the 95% confidence interval for mean monthly FFDI, defined as the average of daily values in each month. Thus, where models project changes that are large relative to the confidence bounds shown by the bootstrapping, these changes are likely to be significant.

A two-sided Kolmogorov–Smirnov test ($p < 0.05$) is used to provide a statistical basis on which to judge the difference between the distributions of monthly FFDI, based on all daily values, in each scenario. The null hypothesis is that there is no difference between the FFDI in 2050 or 2100 and the 20th century i.e. that the two FFDI samples are from the same population. Years are defined from July to June in order to encompass the spring–summer fire season.

The probability of property destruction has been found to approach 1 when FFDI exceeds 40, given a fire is burning at the time (Bradstock and Gill 2001). A measure of days per month with FFDI above 40 is therefore empirically based and policy-relevant, while also permitting analysis of seasonal changes. Bradstock and Gill’s study is based on data from the Sydney region of NSW, but a value of 40 is used throughout all regions as no better estimate existed at the time of the analysis. However, Blanchi et al. (2010) report a value of 50 may be appropriate for forested areas – this value is used in Chapters 5 and 7.

There are also several different measures of bushfire season length. State (regional) governments employ statutory definitions of fire season timing, e.g. for issuing fire permits, but State boundaries do not align well with these study areas (Figure 2.1). Lucas et al. (2007)

proposed a method of determining the start and end of the fire season by using a threshold of the average date of the first and last 3 days with FFDI over 25. This simple method yielded reasonable results for some cities but failed for others, and baseline differences between GCMs mean it is not universally applicable to these results. Therefore an internal measure of fire seasonality is used: the peak months of mean and extreme FFDI as calculated above. Calculating the percentage change in mean monthly FFDI allows an analysis of seasonal changes in fire weather independent of model baselines.

2.7.3 Analysis of an RCM's ability to simulate fire weather

The variables chosen to summarise and evaluate the fire weather climate are:

1. Annual cumulative FFDI (ΣFFDI) – see section 2.7.1 above. ΣFFDI is calculated as the average over the period 1985–2009.

2. Days per year over 50 – this variable is indicative of extreme conditions. The largest, most intense wildfires are more likely to happen on these days and any fires that do occur are unlikely to be controllable. It has been found that 90% of property loss from major fires in Australia occurred during times when FFDI was above 50 (Blanchi et al. 2010). Days per year over 50 is calculated over the same time period as ΣFFDI. Although there is great interest in FFDI categories above 50 (namely 75 and 100) the sample size at many stations is too small to draw robust conclusions.

3. Skill score for FFDI and underlying variables – also known as the overlap statistic of the PDF (Perkins et al. 2007). It is calculated by taking the area under the curve defined by the minimum of the modelled and observed PDFs. Expressed in terms of the empirical bins used:

$$\text{Skill score} = \sum_{1}^{n} \min(Z_{\mathrm{m}}, Z_{\mathrm{o}}) \qquad (6)$$

where n is the number of bins used to calculate the PDF, Z_{m} is the relative frequency of values in a given bin from the model and Z_{o} is the relative frequency of values in a given bin from the observations. Skill score ranges from zero to one, with zero indicating no overlap and one indicating identical PDFs. It is multiplied by 100 to simplify visual interpretation. This metric is useful as it is quite robust to sampling errors or random errors in the observations and it measures more than just the mean: simulation of an entire PDF demonstrates an ability to simulate values at the tails of the distribution as well as at the centre. However, skill scores do not indicate the sign of bias and are increasingly insensitive to errors as values become rarer.

Bias and root mean square error (RMSE) are calculated for annual cumulative FFDI and days per year with FFDI over 50 at each station. In order to investigate potential sources of WRF error, FFDI is also recalculated after replacing WRF values with observed values for the variables underlying FFDI. One limitation of this approach is that the variables are not independent, particularly in the case of relative humidity and temperature, so changing one without changing the other(s) may lead to physical inconsistencies. Proportional error is defined here as: the absolute value of (WRF − Observed) ÷ Observed. The effect of substituting observed data is labelled *Improvement*, defined as:

$$(|\mathrm{WRF} - \mathrm{Observed}| - |WRF_S - \mathrm{Observed}|) \div |\mathrm{WRF} - \mathrm{Observed}| \qquad (7)$$

where WRF_S is WRF with one variable substituted with either observed drought factor (*DF*), maximum temperature (*T*), wind speed (*W*) or relative humidity (*H*). A negative value of *Improvement* implies that model accuracy has deteriorated with substitution relative to the original model value. Generally, *Improvement* behaves as follows:

As |WRFS − Observed| → 0, *Improvement* → 1

As |WRF − Observed| → 0, *Improvement* → -∞

As |WRFS − Observed| → |WRF − Observed|, *Improvement* → 0

For |WRF − Observed| » |WRFS − Observed|, Improvement → 1

2.7.4 Analysis of LSM simulations of historical fuel load

Mean annual continental NPP is used to describe the overall effect of varying each of the vegetation parameters used in the sensitivity analysis. Fine litter in CABLE is derived for both individual grid cells as well as for each climate zone. Results are illustrated using either all ensemble members, or a sample of the lowest, highest and default ensemble members. Annual fine litter anomaly time series are calculated to examine the impact of parameter variation on the temporal evolution of fuel load. Additionally, to frame changes in fuel load linked with NPP with changes in meteorological forcing, the relative impact of load and weather in forested areas is examined using rate of spread of fire (McArthur 1967). The rate of spread (R, in km h^{-1}) is defined as

$$R = 0.0012 \times F \times L \ (4) \qquad (8)$$

where F is the McArthur Forest Fire Danger Index (FFDI) and L is load in t ha^{-1}.

This provides a simple way of comparing the impact of changes in load and fire weather conditions. Analysis is restricted to the temperate region, which contains the forest types in which this rate of spread function was calibrated. The rate of spread in grassland is calculated differently to forests, and commonly used models of rate of spread draw on fuel moisture and weather but not fuel amount (Cheney et al. 1998; Sharples and McRae 2013). Because fuel load is not a significant driver of the rate of spread of grass fires, compared to fuel moisture and weather, no comparison is made of the relative influence of load and weather on grassland fire rate of spread.

2.7.1 Analysis of projections of fire weather and fuel load

Mean annual continental values are used to describe the overall impact of climate change, as well as variation between ensemble members. Mean annual values are calculated for each climate zone to understand regional variation in these results. To explore changes in seasonality mean monthly values are calculated. As in Chapter 6, to frame changes in fuel load with changes in meteorological forcing the rate of spread of fire (McArthur 1967) in the temperate region is examined.

Chapter 3 Overview

Analysis of historical trends in fire weather

A natural reference point for any analysis or interpretation of projections of future fire weather is the existing or historical record of fire weather. Despite the widespread use of FFDI as a measure of fire weather in climate projections research, there have been no peer-reviewed studies of existing spatial patterns or trends in this index in Australia.

Although trends have been recorded in some of the variables from which FFDI is constructed, none of these correspond to the precise formulation of each variable in the FFDI equation. The creation of the first high quality historical data-set of FFDI (Lucas, 2010b) was the catalyst for Chapter 3, an analysis of observations of FFDI. In particular, the question was posed, given the observed and regionally varied changes in the Australian climate, do we observe any significant trends in average and extreme fire weather and if so, what are their spatial patterns? Some trends from this data-set have previously been reported in the context of a study on climate change projections for southeastern Australia (Lucas *et al*., 2007). This earlier work was expanded upon by including more recent data, additional stations from the entire continent, and correcting for inhomogeneities in the wind record.

The work reported here has been published in the peer reviewed literature and is reproduced exactly as published:

Clarke H, Smith PL, Lucas C (2013) Changes in Australian fire weather between 1973 and 2010. International Journal of Climatology, 33, 931-944. DOI 10.1002/joc.3480

Author contributions

I led this project. Peter Smith (PS; then my immediate work supervisor) conceived the study, which was then refined in scope by myself and Chris Lucas (CL; Bureau of Meteorology). CL provided the data. I was jointly responsible for the experimental design with CL, incorporating feedback from PS. I conducted the analysis and prepared the figures, incorporating feedback from PS and CL. I drafted the paper and rewrote it following comments by PS and CL. I led the revisions following external review by two anonymous referees, incorporating contributions from PS and CL.

INTERNATIONAL JOURNAL OF CLIMATOLOGY
Int. J. Climatol. **33**: 931–944 (2013)
Published online 11 April 2012 in Wiley Online Library
(wileyonlinelibrary.com) DOI: 10.1002/joc.3480

RMetS
Royal Meteorological Society

Changes in Australian fire weather between 1973 and 2010

Hamish Clarke[a,b]* Christopher Lucas[c] and Peter Smith[a]
[a] *Climate Change Science Section, NSW Office of Environment and Heritage, Sydney, Australia*
[b] *Climate Change Research Centre, University of NSW, Sydney, Australia*
[c] *Centre for Australian Weather and Climate Research, a partnership between the Bureau of Meteorology and CSIRO, Melbourne, Australia*

ABSTRACT: A data set of observed fire weather in Australia from 1973–2010 is analysed for trends using the McArthur Forest Fire Danger Index (FFDI). Annual cumulative FFDI, which integrates daily fire weather across the year, increased significantly at 16 of 38 stations. Annual 90th percentile FFDI increased significantly at 24 stations over the same period. None of the stations examined recorded a significant decrease in FFDI. There is an overall bias in the number of significant increases towards the southeast of the continent, while the largest trends occur in the interior of the continent and the smallest occur near the coast. The largest increases in seasonal FFDI occurred during spring and autumn, although with different spatial patterns, while summer recorded the fewest significant trends. These trends suggest increased fire weather conditions at many locations across Australia, due to both increased magnitude of FFDI and a lengthened fire season. Although these trends are consistent with projected impacts of climate change on FFDI, this study cannot separate the influence of climate change, if any, with that of natural variability.

KEY WORDS wildland fire; bush fire; wildfire; Forest Fire Danger Index; observations; trends

Received 5 July 2011; Revised 16 January 2012; Accepted 11 March 2012

1. Introduction

The probability of wildland fire is driven by the amount and dryness of fuel, ambient weather and ignitions (Archibald *et al*., 2009). Fire regimes can be characterized in part by differences in these drivers – for instance those ecosystems where wildland fire occurrence is limited by the amount of fuel and those where it is limited by a combination of fuel availability and ambient weather (Bradstock, 2010). Humans have a substantial and diverse impact on fuel and ignitions across the globe, for instance through land clearing, active fire suppression and burning off of agricultural debris. In contrast, there is no clear human imprint on fire weather – yet. Each of the drivers of wildland fire is highly sensitive to changes in climatic conditions, but fire weather is one of the first phenomena that could be expected to show a response to existing trends in climate change. The effects of climate change on biomass growth and fuel availability are complex and because of the nature of climate variability and human influence it may take decades for this to be clearly discernible.

Fire weather is typically expressed through some combination of surface air temperature, precipitation, relative humidity and wind speed. There are a number of different indices that integrate these meteorological variables into a single fire danger measure, for example the McArthur Forest Fire Danger Index (FFDI; Luke and McArthur, 1978), the Canadian Forest Fire Weather Index System (FWI; Van Wagner, 1987) and the United States National Fire Danger Ratings System (NFDRS; Deeming *et al*., 1978). Other metrics focus on the water and energy balance above the surface. The Haines Index (Haines, 1988) and a variant adapted to Australia (Mills and McCaw, 2010) link vertical atmospheric stability and humidity with erratic fire behaviour. The 850 hPa temperature gradient has been linked to extreme fire weather events over southeastern Australia (Mills, 2005).

Some trends have been observed in the variables underlying fire weather indices. Since 1960, the mean temperature in Australia has increased by about 0.7 °C. The entire country has experienced warming, in some areas by 1.5–2 °C (CSIRO and Bureau of Meteorology, 2010). Warming has occurred in all seasons; however, the strongest warming has occurred in spring (about 0.9 °C) and the weakest in summer (about 0.4 °C). There has been an increase in the number of record hot days and a decrease in the number of record cold days each decade since 1960 (Alexander and Arblaster, 2009; CSIRO and Bureau of Meteorology, 2010). The increase in temperature has been formally attributed to anthropogenic increases in greenhouse gases (Stott, 2003; Nicholls, 2006). Australian rainfall patterns are highly variable, with no consistent sign of change across the country and trends that depend more on start points. In southwestern Australia, a significant decline in rainfall since the 1970s has been attributed to a combination of natural variability and anthropogenic greenhouse gases (Timbal *et al*., 2006; Bates *et al*., 2008). Decreases in rainfall since 1960

* Correspondence to: H. Clarke, Climate Change Science Section, NSW Office of Environment and Heritage, PO Box 3720, Parramatta, NSW 2124, Australia. E-mail: h.clarke@student.unsw.edu.au

have also occurred in southeast Australia, while there was an increasing trend over northwestern Australia over the same period. Between 1957 and 2003, dew point temperature either remained the same or increased over much of Australia, with a national averaged trend of 0.1 °C per decade (Lucas, 2010a). These results are broadly similar to those from a global humidity data set with 5° resolution (Willett *et al*., 2007), although its starting point (1973) coincides with an exceptionally wet period over Australia, leading to more negative trends. From 1975 to 2006, there has been a small stilling trend in wind speed of -0.009 m s^{-1} year^{-1} across Australia (McVicar *et al*., 2008). This trend is widespread, with almost 90% of the 0.1° resolution grid cells showing a decline, and 58% of them a significant decline. These trends have occurred in the presence of considerable interannual fluctuations in the Australian climate, due to the El Niño-Southern Oscillation (ENSO) and other drivers of climate variability (Risbey *et al*., 2009).

Furthermore, the meteorological variables described above do not match exactly with those used in the calculation of the FFDI, which is used operationally by weather forecasters and fire agencies in Australia to declare fire weather warnings and total fire bans and to determine fire danger (the difficulty of putting out fires which may occur). The Australian humidity data set (Lucas, 2010a) is for dew point temperature, has monthly resolution and has been homogenized for measurements at 0900 local time (LT). FFDI uses relative humidity typically calculated at 1500 LT, when relative humidity is close to a minimum. The wind trends reported by McVicar *et al*. (2008) are based on total daily wind run, whereas FFDI uses wind speed at 1500 LT, averaged over the previous 10 min. Moreover, in the calculation of FFDI each variable is weighted differently (see Section 2), such that a one unit increase in one variable does not equate to a one unit increase in another, for example. Therefore, it is only in cases where just a single variable has changed, or where the direction of trend in all variables effectively coincides (i.e. temperature and wind speed increasing, relative humidity and precipitation decreasing) that we may state with confidence that a change in fire weather is likely. The impact of a given change in fire weather – for example in extreme values of the FFDI at a certain time of year – will be moderated by regional differences in fire seasonality as well as the relative importance of fire weather among fire limiting processes (Bradstock, 2010).

The creation of Australia's first high-quality observational FFDI data set (Lucas, 2010b) presents an opportunity to pose the question: Given the observed and regionally varied changes in the Australian climate, do we observe any significant trends in average and extreme fire weather and if so, what are their spatial patterns? Some trends from this data set have previously been reported in the context of a study on climate change projections for southeastern Australia (Lucas *et al*., 2007). We expand upon this earlier work on by including more recent data, additional stations from the entire continent and correcting for inhomogeneities in the wind record (see Section 2). Finally, an examination of historical trends should add value to the interpretation of existing and future projections of fire weather in Australia under climate change.

2. Data and methods

2.1. Study area

Australian fire regimes are highly seasonal in nature. In the forested southeast and southwest, summer and spring are the dominant fire seasons, while in the savanna landscapes of monsoonal northern Australia fire danger peaks late in the winter dry season (Luke and McArthur, 1978). The roughly latitudinal gradient in continental scale fire patterning is explained to a large extent by rainfall seasonality (Russell-Smith *et al*., 2007).

2.2. Fire weather and climate variables

For this study, FFDI is chosen to quantify fire weather conditions. This index was empirically derived in the late 1960s to relate weather conditions to expected fire behaviour and rate of spread. A series of threshold values are used to determine fire danger ratings: 0–11 (low/moderate), 12–24 (high), 25–49 (very high), 50–74 (severe), 75–99 (extreme) and 100+ (catastrophic). The FFDI – or its similarly derived counterpart the Grassland Fire Danger Index (GFDI) – is widely used across Australia as the basis for fire weather warnings issued by fire agencies. The methods of calculation used in this study are described by Lucas (2010b).

FFDI utilizes standard weather observations of temperature, relative humidity, 10 min averaged wind speed and rainfall to estimate the fire weather conditions. The basic equation for FFDI is given by Noble *et al*. (1980):

$$\begin{aligned}\mathrm{FFDI} = 2 \times \exp(0.987 \times \ln(\mathrm{DF}) - 0.0345 \\ \times H + 0.0338 \times T + 0.0234 \times V - 0.45)\end{aligned} \quad (1)$$

where DF is the drought factor, T is the temperature (°C), V the wind speed (km h^{-1}) and RH the relative humidity (%). In the formulation used here, fully described in Lucas (2010b), a fire weather data set with daily time resolution is created using observations of maximum temperature and V and RH as measured at 1500 LT. The drought factor, an empirical estimate of the state of the fuel, is calculated following the methodology described in Griffiths (1999) and uses the Keetch–Byram Drought Index (Keetch and Byram, 1968) as its input for soil moisture deficit, based on rainfall measurements collected at 0900 LT.

The methodology described in Lucas (2010b) provides a consistently calculated fire weather data set. The methodology ignores local variations in fuel amounts and types, as well as the slope of the terrain. These factors have a significant impact on the fire behaviour. While this presents problems for understanding the exact details of fire behaviour, our goal is to understand the weather and climate aspects of the issue. Uncertainties in the amounts of historical grassland curing make the use of GFDI problematic. In any case, future climate projections show a great deal of overlap in the behaviour of the GFDI and FFDI (Hennessy *et al*., 2005). Furthermore, a comparison of FFDI with the widely used Canadian FWI shows considerable similarities between the two (Dowdy *et al*., 2010).

To analyse the long-term trends of fire weather in Australia, these daily data are further summarized on both annual and seasonal time scales. Across much of Australia, the peak fire season occurs during the summer half of the year, roughly from September to March (Luke and McArthur, 1978). To accommodate this, a 'fire year' is chosen to run from 1 July to 30 June of the following year for the annual calculations. The variables chosen to summarize the fire weather climate are:

1. *Annual cumulative FFDI (ΣFFDI)*: This variable is calculated as the sum of all daily FFDI values over the entire fire year (Beer and Williams, 1995). It provides a useful metric to compare relative levels of fire weather danger over long time periods and/or different spatial areas. Cumulative FFDI is computed from the 1973–1974 through the 2009–2010 fire years, a total span of 37 years.
2. *Annual 90th percentile FFDI*: The daily values during a fire year are sorted, and the 36th highest value is chosen. This variable is indicative of the extreme end of the fire weather spectrum, times when the largest, most intense wildfires are more likely to occur and be more active. This variable is computed over the same period as ΣFFDI.
3. *Seasonal median and 90th percentile FFDI*: The median and 90th percentile FFDI over the standard southern hemisphere meteorological seasons are chosen (i.e. December–January–February (DJF), March–April–May (MAM), etc.). Each season is approximately 90 d long. This variable provides information on any potential changes in the annual timing of the fire season. It is available from MAM 1973 through DJF 2011.

2.3. Data homogenization and station selection

When investigating the long-term behaviour of any climate variable, the homogeneity of the data set is important. Homogeneous data are those which are free from artificial trends or discontinuities, such as those caused by station relocations, instrument changes and/or changes in observational practices. Lucas (2010b) examined the homogeneity of the FFDI data set and its components. While all the individual data sets show some degree of inhomogeneity, those in the wind speed data have the largest impact on the FFDI. These inhomogeneities in the wind speed arise from the changing local environment of the wind measurement as well as the changing instrumentation used to record wind speeds (see also Jakob, 2010), particularly those associated with the modernization of the observing network and the introduction of Automatic Weather Stations (AWS). Further, before the introduction of the AWS, wind reports at many of the rural stations in the data set were made through visual estimates of the effects of wind on vegetation. The quality of these measurements is greatly dependent on the skill of the observer, and they often show many inhomogeneities. They are also often inconsistent with later records made with the modern AWS instrumentation, with very different means, variance and skewness characteristics. As a general rule, the mean of past wind speed measurements is lower than those measured with contemporary AWS anemometers. However, there are exceptions.

Lucas (2010b) described a correction methodology for the wind inhomogeneities, applicable to statistics of the FFDI distribution rather than individual observations. Breakpoints in the wind speed time series are identified using two-phase regression similar to that described by Easterling and Peterson (1995). The bulk change in FFDI (ΔFFDI) at a given percentile level (e.g. median or 90th percentile) for a given change in wind speed (ΔV) is given by:

$$\Delta \text{FFDI} = 0.0234 \times \text{FFDI} \times \Delta V \qquad (2)$$

Past FFDI values are adjusted so that they are in relative homogeneity with contemporary measurements. The sensitivity of this homogenization methodology was discussed in Lucas (2010b). It was found to adequately account for changes in the FFDI distribution at most percentile levels. However, this was not true at the extreme upper ends of the FFDI distribution, where the changes to the variance and the skewness of the winds had a significant effect. This generally occurred at percentile levels above 90%; the homogenization correction at higher levels is subject to more uncertainty.

A scheme based on similar principles is determined for ΣFFDI. For this variable, an amount of adjustment is estimated by integrating Equation (2) multiplied by the observed relative frequency of occurrence of each value of FFDI over the observed FFDI distribution. This is done individually for each station resulting in a unique correction factor at each location.

The data set described in Lucas (2010b) was comprised of 77 individual stations. However, many of these stations were not suitable for use in this analysis. Two criteria are used in this study:

1. Stations that contain wind speed measurements based on visual estimates are excluded. In many cases, the wind speed time series at these stations show frequent changes in the mean and considerable differences compared to later instrumental observations, suggesting that they are unreliable. Furthermore, differences in the statistical distributions make the homogenization more subject to uncertainty.

2. Stations with more than 1 year (365 d) of cumulative missing observations between 1973 and 2010 are excluded. This is equivalent to a record that is 98% complete.

Applying these criteria results in 38 stations selected for this analysis (Table I). There is considerable overlap between the two sets of stations that fail to meet the criteria. Stations with visually estimated winds are mostly rural, where in general there are more missing data. The stations chosen tend to be located in the more populated areas, often at airports or meteorological offices. The locations of the chosen stations are shown in Figure 1. While the number of stations is approximately halved, the national coverage of the complete data set is maintained, albeit with some gaps in northern Queensland (QLD) and in the desert regions along the eastern border of Western Australia (WA).

Table I. List of stations used in this study.

Station (Abbreviation)	State	Latitude (°)	Longitude (°)
Adelaide (AD)	SA	−34.92	138.62
Albany Airport (AL)	WA	−34.94	117.80
Alice Springs (AS)	NT	−23.80	133.89
Amberley (AM)	QLD	−27.63	152.71
Brisbane Airport (BA)	QLD	−27.39	153.13
Broome (BR)	WA	−17.95	122.23
Cairns (CA)	QLD	−16.87	145.75
Canberra (CB)	ACT	−35.30	149.20
Carnarvon (CN)	WA	−24.89	113.67
Ceduna (CE)	SA	−32.13	133.70
Charleville (CH)	QLD	−26.42	146.25
Cobar (CO)	NSW	−31.49	145.83
Coffs Harbour (CF)	NSW	−30.31	153.12
Darwin (DA)	NT	−12.42	130.89
Esperance (ES)	WA	−33.83	121.89
Geraldton (GE)	WA	−28.80	114.70
Hobart (HO)	TAS	−42.89	147.33
Kalgoorlie (KA)	WA	−30.78	121.45
Launceston Airport (LA)	TAS	−41.54	147.20
Laverton (LV)	VIC	−37.86	144.76
Mackay (MA)	QLD	−21.12	149.22
Meekatharra (MK)	WA	−26.61	118.54
Melbourne Airport (ME)	VIC	−37.68	144.84
Mildura (MI)	VIC	−34.23	142.08
Moree (MO)	NSW	−29.49	149.85
Mt Gambier (MG)	SA	−37.75	140.77
Mt Isa (MT)	QLD	−20.68	139.49
Nowra (NO)	NSW	−34.95	150.54
Perth Airport (PE)	WA	−31.93	115.98
Port Hedland (PO)	WA	−20.37	118.63
Rockhampton (RO)	QLD	−23.38	150.48
Sale (SA)	VIC	−38.12	147.13
Sydney Airport (SY)	NSW	−33.94	151.17
Tennant Creek (TE)	NT	−19.64	134.18
Townsville (TO)	QLD	−19.25	146.77
Wagga (WA)	NSW	−35.16	147.46
Williamtown (WI)	NSW	−32.79	151.84
Woomera (WO)	SA	−31.16	136.81

2.4. Trend analysis

The trends in this study are estimated by using ordinary least squares linear regression with time taken as the independent variable. There is no physical reason why trends in fire weather should be strictly linear. Rather, this method is chosen as it is simple, widely used and easily understood. The possibility of more complex trend shapes cannot be excluded. The 95th percentile confidence interval for linear trends was also calculated for each time series. The F-statistic ($p < 0.05$), a comparison of the variance explained by the linear fit and the total variance of the system, was examined as an indicator of the significance of the trend.

The calculation of climate trends is sensitive to the choice of start and end dates of the calculation. The robustness of trends calculated here is examined with some simple sensitivity tests. These are:

1. changing the start and end dates by 1, 5 and 10 years and
2. randomly removing increasing numbers of stations and in each case re-calculating trends.

3. Results

3.1. Annual statistics

The time series of wind-corrected ΣFFDI anomaly for each station in this study is shown in Figure 2. Although there is considerable interannual variability throughout the record, a clear upward trend is apparent at many of the stations and in the nationally averaged anomaly. Many of the lowest values at individual stations are observed in the early 1970s. There is evidence of a 'jump' in ΣFFDI at many stations after 2000, as noted in Lucas *et al*. (2007) for southeastern Australia. Some degree of coherence is seen in the signal, with peaks and troughs in the individual time series tending to occur simultaneously. This coherent interannual variability is broadly consistent with the known modulation of the fire-weather climate by ENSO (Williams and Karoly, 1999). El Niño years (e.g. 1982–1983, 1997–1998, 2002–2003, 2006–2007) are often higher than normal; La Niña periods (e.g. 1973–1975, 1998–2000) show negative anomalies.

Table II lists the trend values of ΣFFDI at individual stations. Mean values for ΣFFDI and all other metrics used here are shown in Table III to aid interpretation of these trends. Sixteen of 38 stations show a significant positive trend; none show a negative trend, significant or otherwise. The multi-station mean shows that on average across Australia, there has been an increase in annual cumulative FFDI since 1973 of 212 points per decade. This increase is not an artefact of the correction procedure. At 36 of 38 stations, the trend in ΣFFDI is reduced by the correction process, many times by over 50% of its original value. The two stations where the correction procedure results in an increased trend occur at Albany Airport and Mackay although the magnitude

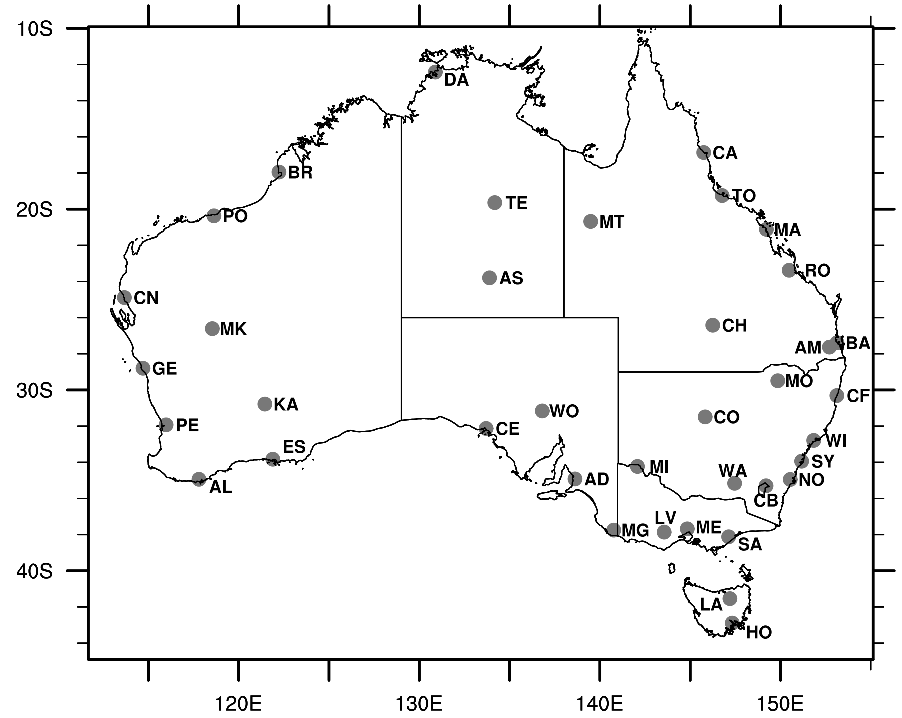

Figure 1. Map of station locations. See Table I for key. The marker for Laverton (LA) has been moved west to avoid overlap with Melbourne Airport.

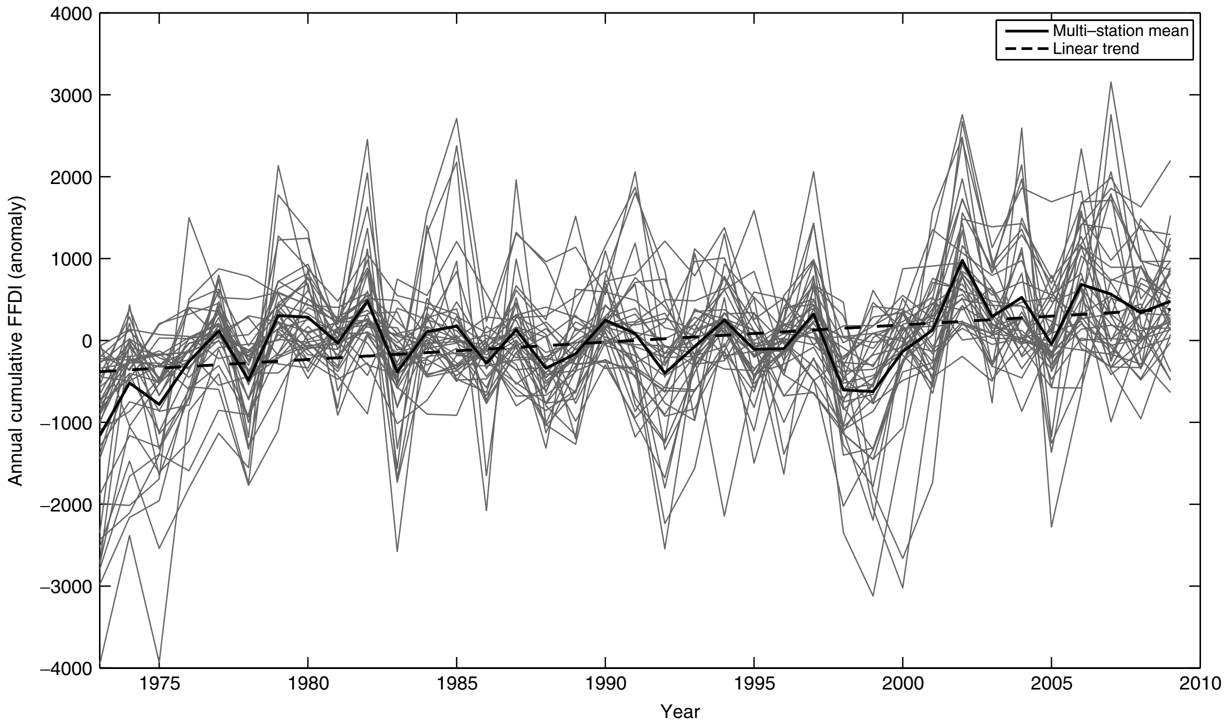

Figure 2. Time series of annual cumulative FFDI anomaly at each station. The thick line indicates the multi-station mean. The thick dotted line indicates the linear trend.

is small and the trend is near-zero before and after correction. As previously noted (see Section 2), this is consistent with the known historical shortcomings and tendencies in the observed wind speed data.

The spatial pattern of the trends in ΣFFDI is shown in Figure 3. An area of large, significant positive trend is seen in the southeast of the country, extending from Alice Springs southeastwards through South Australia (SA), western New South Wales (NSW), Victoria (VIC) and into northern Tasmania (TAS). With the exception of the Tasmanian station, trends in this region are well above 100 points per decade and at their strongest

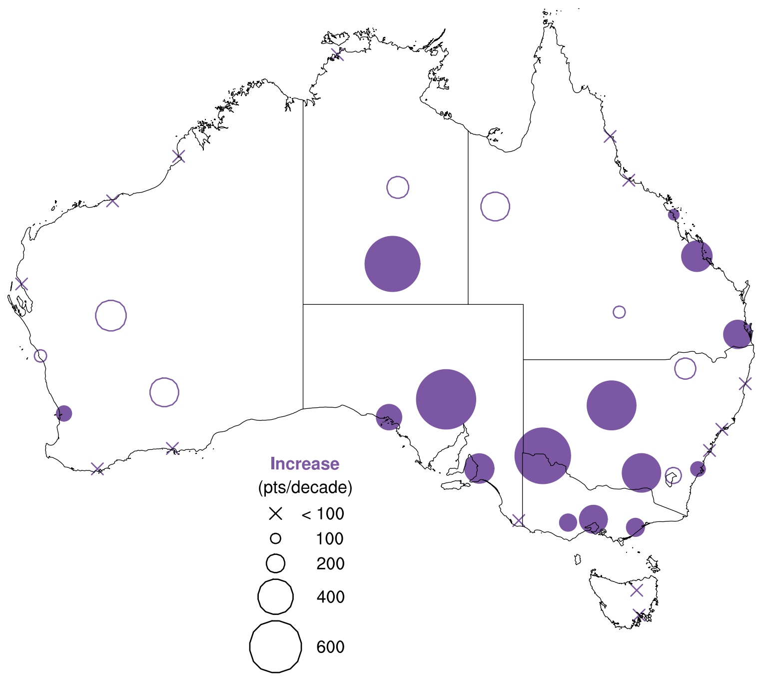

Figure 3. Map of trend magnitude in annual cumulative FFDI. Marker size is proportional to the magnitude of trend. Reference sizes are shown in the legend. Filled markers represent trends that are statistically significant. The marker for Laverton has been moved west to avoid overlap with Melbourne Airport. This figure is available in colour online at wileyonlinelibrary.com/journal/joc

exceed 600 points per decade. Furthermore, trends at Mt Isa in western QLD and Moree in northern NSW are significant if the 90% ($p < 0.10$) level is considered. Outside of this region, an area of significant trends is noted in southeast QLD at Mackay, Rockhampton and Amberley. However, the coastal Brisbane Airport does not show a significant trend. Perth Airport in Western Australia has a significant positive trend in ΣFFDI; Kalgoorlie and Esperance have trends that are significant at the 90% level. Across much of tropical north Australia small and insignificant trends are observed. Coastal regions of New South Wales, including Sydney, Williamtown and Coffs Harbour also have small insignificant trends.

Figure 4 shows the time series of the annual 90th percentile FFDI anomaly at each station. The shape of the time series shares many traits with the time series of ΣFFDI shown in Figure 2. The interannual variability shows the same pattern, with higher values generally found during El Niño years and an overall upward trend. Figure 5 shows the spatial pattern of the trends and Table II shows the magnitude of the trend at each station. The spatial pattern of the trends is very similar to that of ΣFFDI, with strong upward trends identified across the southeast portion of the continent. A few stations that did not have significant trends in ΣFFDI showed significant trends in annual 90th percentile FFDI, especially along the New South Wales and Queensland coasts. Five stations recorded an annual increase of 0.27 or greater, which equates to a rise since 1973 of at least 10 points in the value exceeded on the 36 highest fire danger days of the year. No significant decreases were observed. Trends in annual 95th percentile levels were also computed (not shown). As a general rule, trends are larger at the high percentile levels, which suggests that the overall shape of the distribution is changing, rather than merely shifting to the right due to a change in the mean.

Trends in the multi-station mean ΣFFDI and 90th percentile FFDI show similar sensitivity to the selection of start and end points (Figure 6). The trend in both measures remains positive when 1, 5 and 10 years are removed from the start or end of the record. However, the trend is no longer significant when the end point occurs 10 years earlier. This gives an indication of the magnitude of the apparent ‘jump’ in values in the post-2000 years. In the case of ΣFFDI, delaying the start date by 5 years results in a trend whose lower 95% confidence bound is just below 0, which points to a period of relatively low fire weather conditions during the mid-1970s. Randomly removing individual stations has no material effect on trends until well in excess of 50% are removed (data not shown). This fits in with the suggestion of a spatial coherence in the signal between individual station time series shown in Figures 2 and 4.

3.2. Seasonal statistics

The spatial distribution of trends in seasonal 90th percentile FFDI for each of the four meteorological seasons is shown in Figure 7. Table III shows the values at individual stations for both the median and 90th percentile FFDI. The seasonal patterns show a wider variety of changes compared to the annual values shown previously. During winter, trends in both median and 90th percentile FFDI are almost uniformly positive, the exception being Brisbane Airport. For the 90th percentile FFDI

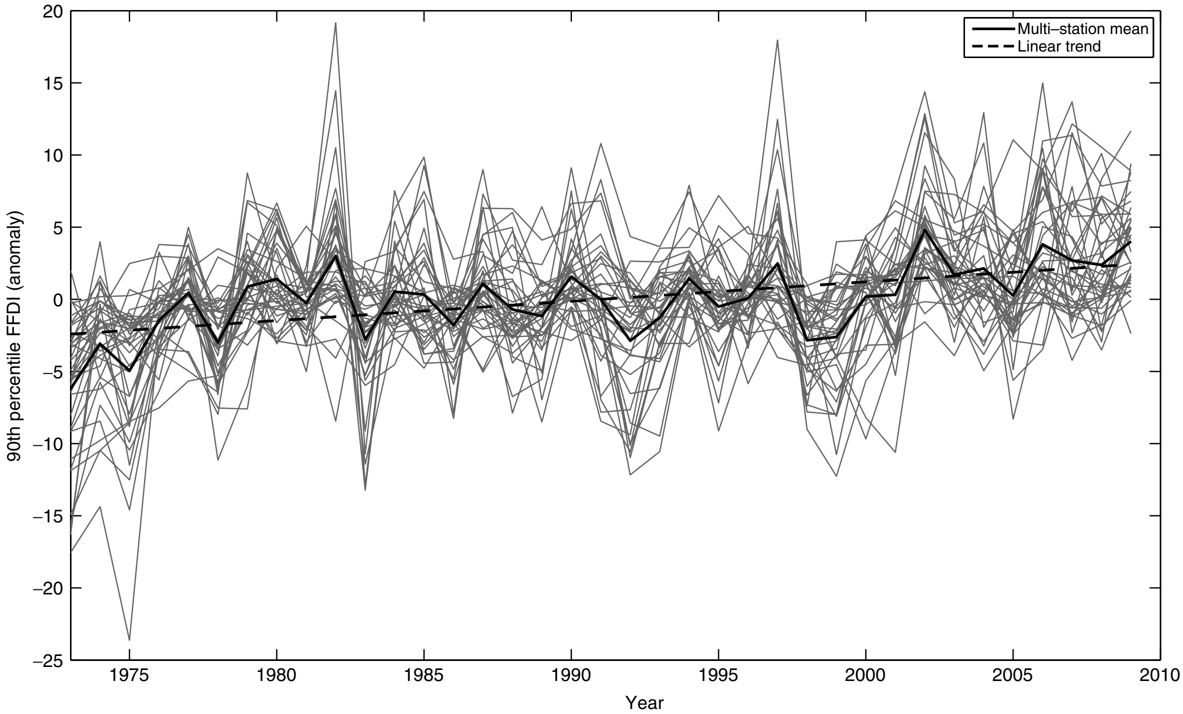

Figure 4. Time series of annual 90th percentile FFDI anomaly at each station. The thick line indicates the multi-station mean. The thick dotted line indicates the linear trend.

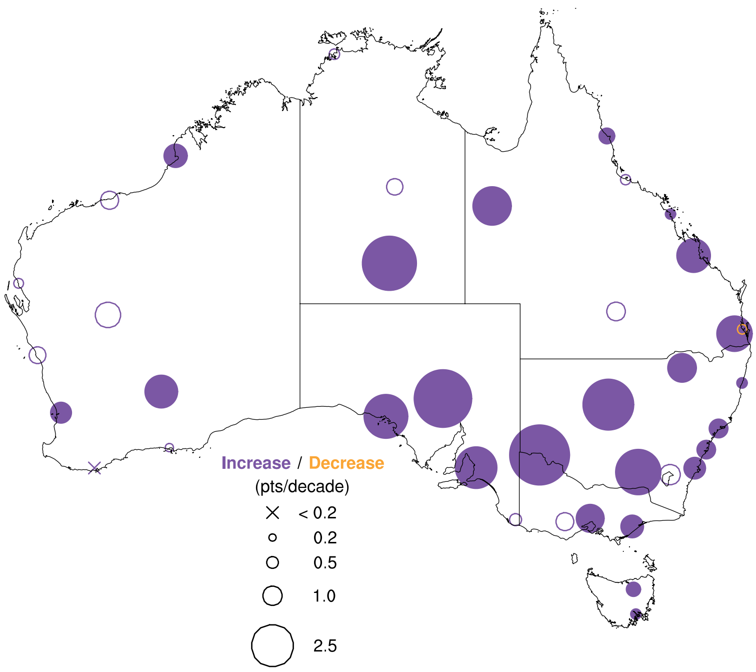

Figure 5. Map of trend in annual 90th percentile FFDI. Marker size is proportional to the magnitude of trend. Reference sizes are shown in the legend. Filled markers represent trends that are statistically significant. The marker for Laverton has been moved west to avoid overlap with Melbourne Airport. This figure is available in colour online at wileyonlinelibrary.com/journal/joc

(median FFDI), 17 (15) stations recorded significantly positive trends, and an additional 4 (6) at the $p < 0.10$ level. The stations with significant trends are spread out across the country, although the largest trends are found northwards of about 31 °S. Smaller trends, significant or otherwise, are found in the southeast and in northern coastal Queensland.

The largest trends overall are seen in spring, for both median and 90th percentile FFDI. Most significant changes in FFDI are found in the southern half of mainland Australia, particularly in the southeast. Tasmania is an exception here. Many non-significant, but large-valued, trends are noted in the central latitudes of the country. In several cases, these are significant

Table II. Trends (points/decade) in annual cumulative and 90th percentile FFDI and seasonal median and 90th percentile FFDI. Shading indicates trends are significant at the 95% level.

Station	Annual ∑ FFDI	Annual 90%	Seasonal 50%				Seasonal 90%			
			JJA	SON	DJF	MAM	JJA	SON	DJF	MAM
Adelaide	330	2.49	0.13	0.66	1.09	0.70	0.41	2.21	2.47	2.49
Albany Airport	30	0.00	0.09	0.15	−0.30	0.06	0.23	0.32	−0.43	0.33
Alice Springs	638	3.33	0.96	2.31	1.55	2.36	1.34	3.09	1.08	2.62
Amberley	317	2.08	0.98	0.61	0.49	1.28	2.23	1.63	0.66	1.6
Brisbane Airport	0	−0.36	−0.15	−0.15	−0.10	0.23	0.34	0.94	−0.51	−0.05
Broome	50	1.27	0.83	0.07	−0.17	0.05	2.21	0.55	−0.43	1.39
Cairns	49	0.77	0.22	0.21	−0.34	0.36	0.56	0.51	−0.36	1.2
Canberra	170	1.07	0.14	0.61	−0.43	0.92	0.25	1.1	−0.07	1.83
Carnarvon	60	0.37	0.44	0.23	−0.25	0.25	1.64	0.43	−0.65	0.94
Ceduna	282	2.64	0.36	0.84	0.55	0.85	1.42	3.78	1.74	3.31
Charleville	122	0.96	0.84	1.10	−1.46	1.20	1.52	1.51	−1.61	1.38
Cobar	564	3.11	0.57	2.08	1.30	1.05	1.65	3.43	1.74	1.13
Coffs Harbour	48	0.42	0.13	−0.08	0.12	0.21	0.25	0.16	0.45	0.34
Darwin	59	0.42	0.64	0.40	−0.07	0.04	0.46	0.21	−0.12	0.23
Esperance	94	0.27	0.13	0.21	0.10	0.15	0.44	0.43	0.07	0.73
Geraldton	126	0.84	0.63	0.68	0.16	0.74	1.81	2.04	−1.5	2.48
Hobart	48	0.41	0.19	0.25	0.11	0.27	0.24	0.38	0.49	0.42
Kalgoorlie	323	1.90	0.80	1.84	0.61	0.53	1.94	2.69	1.87	1.12
Launceston Airport	85	0.67	0.07	0.21	0.41	0.42	0.15	0.38	0.16	0.87
Laverton	183	0.91	0.29	0.69	0.09	0.17	0.3	2.1	0.77	0.26
Mackay	105	0.41	0.05	0.19	−0.05	0.35	0.2	0.16	0.21	0.42
Meekatharra	346	1.41	1.20	2.27	0.40	0.73	1.63	1.86	1.05	−0.01
Melbourne Airport	312	1.58	0.40	1.06	0.37	0.43	0.85	3.32	1.58	0.89
Mildura	645	3.72	0.57	1.99	1.67	1.20	0.95	4.17	2.77	2.62
Moree	231	1.63	0.91	0.98	0.05	1.21	2.16	2.3	0.62	1.24
Mt Gambier	70	0.52	0.01	0.18	−0.06	0.14	0.11	1.07	0.34	0.91
Mt Isa	323	2.28	1.28	2.00	−0.76	1.32	1.4	1.88	0.26	1.5
Nowra	153	1.16	0.51	0.62	0.16	0.69	0.71	1.83	−0.07	1.28
Perth Airport	160	1.11	0.32	0.59	0.89	0.75	1.06	1.77	0.78	1.56
Port Hedland	82	0.92	0.95	0.04	0.13	0.67	1.53	1.05	−0.24	1.32
Rockhampton	343	1.96	0.53	0.94	0.25	0.90	2.15	1.91	0.74	2.07
Sale	193	1.23	0.39	0.82	0.16	0.64	0.9	1.79	0.02	1.23
Sydney Airport	27	0.96	0.18	0.48	0.22	0.31	0.31	2.34	0.64	0.57
Tennant Creek	240	0.81	0.80	0.89	−0.23	1.24	0.1	0.42	−1.39	0.58
Townsville	1	0.40	0.05	0.07	−0.18	0.71	0.38	0.06	−0.17	1.01
Wagga	439	2.74	0.22	1.49	1.09	1.30	0.32	2.85	2.21	1.46
Williamtown	87	0.97	0.11	0.24	0.35	0.22	0.65	1.86	0.4	−0.02
Woomera	689	3.56	0.92	2.67	2.33	1.38	2.31	4.58	3.08	2.58

at the $p < 0.10$ level. While median trends are smaller than 90th percentile trends in almost all cases, southeastern New South Wales shows a striking disparity in this regard. In the tropical north, trends in both the median and 90th percentile FFDI are small during this season.

The fewest significant trends are observed during DJF (the summer), with only 3 (5) stations significant for the seasonal 90th percentile FFDI (median FFDI). These are found in southern portions of the country, at Adelaide, Mildura and Woomera, with Ceduna and Perth included for the median. Generally weak and insignificant negative trends are seen during this season in the northern portions of the country. Significant trends are more frequent during MAM and are seen along eastern Australia from coastal north QLD extending southwards into Tasmania. A greater number of significant trends are seen in the median than 90th percentile FFDI during autumn, especially in southeastern NSW. Prominent trends in the 90% level are also noted in a region centred on South Australia. Sites along the west coast also show significant trends.

4. Discussion and conclusions

4.1. Trends in fire weather

Fire weather, as depicted by the FFDI, has increased across much of Australia since 1973. Statistically significant increases in annual cumulative FFDI, observed at two fifths of the sites in the data set, are concentrated in the south and southeast of Australia. The largest absolute changes occur in the hot, arid interior of the continent, although some of the largest proportional increases

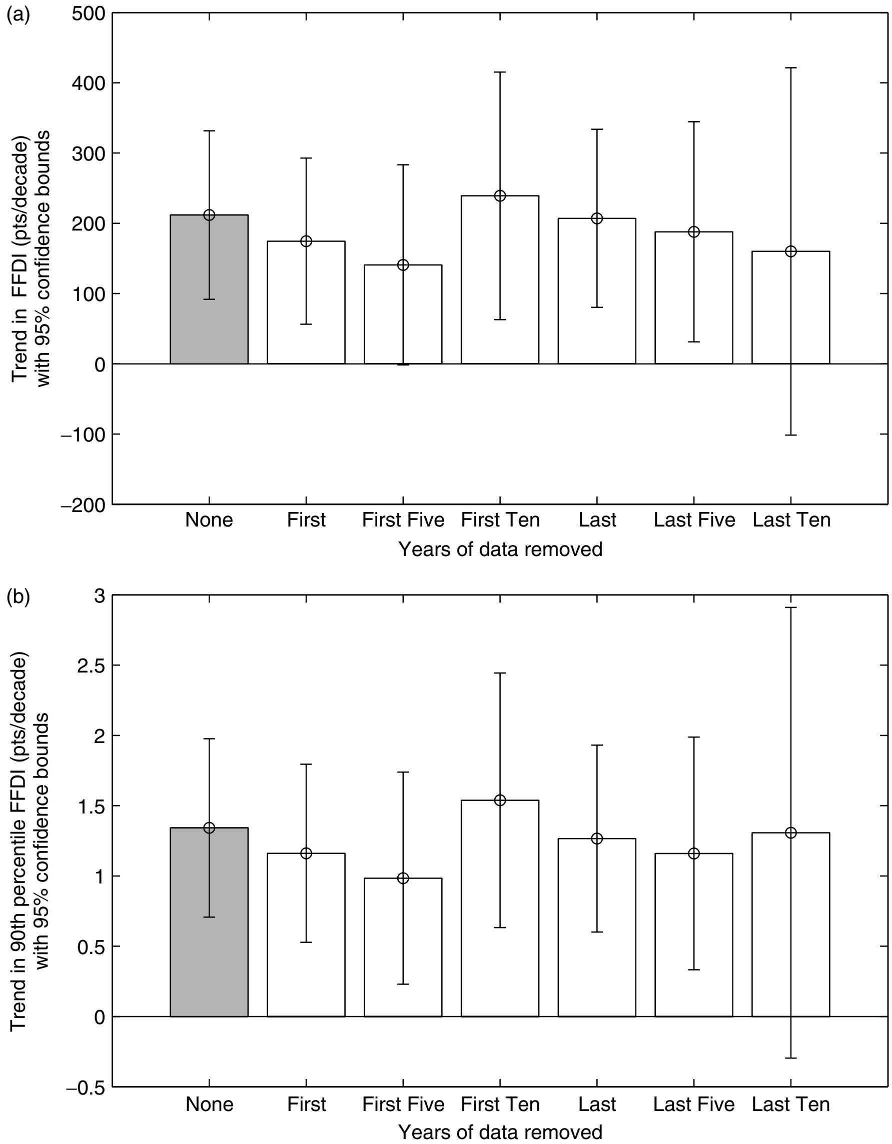

Figure 6. Sensitivity of multi-station mean trend values in (a) annual cumulative FFDI and (b) annual 90th percentile FFDI (points/decade) to variation in the start and end points of the time series. Whiskers indicate 95% confidence intervals for trend values.

occurred in coastal areas, where average annual cumulative FFDI is relatively low – Melbourne and Adelaide recorded increases of 49% or more over the duration of the record. Although no significant decreases in annual cumulative FFDI were observed, large areas did not record a significant increase: much of the north and west of the country, as well as most of the eastern seaboard.

While annual cumulative FFDI provides a good standalone estimate of changes to fire weather, it masks their distribution and timing. The upper tails are changing more quickly than the centre, such that changes to the annual 90th percentile FFDI account for 20–30% of the total change on average. It is at these upper tails of the FFDI distribution that fire weather conditions are greatest. There are also distinct seasonal changes and associated spatial patterns, even in regions which do not show a significant increase in the annual figures. The largest changes by magnitude have occurred in the spring, with large changes on southern parts of the mainland, particularly Victoria, South Australia and New South Wales. An increase in the upper tails of the distribution is particularly dominant here. There are similarities here with temperature trends in Australia since 1960, which have increased the most in spring and the least in summer (CSIRO and Bureau of Meteorology, 2010). Based on the weather station data used in this study, relative humidity shows a similar pattern of larger increases in spring. The bias towards larger increases in spring compared to other seasons is slightly more pronounced for temperature than for relative humidity and FFDI.

The fewest significant trends are observed in summer. Trends in the 90th percentile summer FFDI are large across the south, but often not significant because of the large interannual variability. In the tropical north, weak negative trends occur during summer, which is not part of the fire season. Widespread changes occur in both autumn and spring, but are of larger magnitude during spring. Changes in the winter are comparatively small

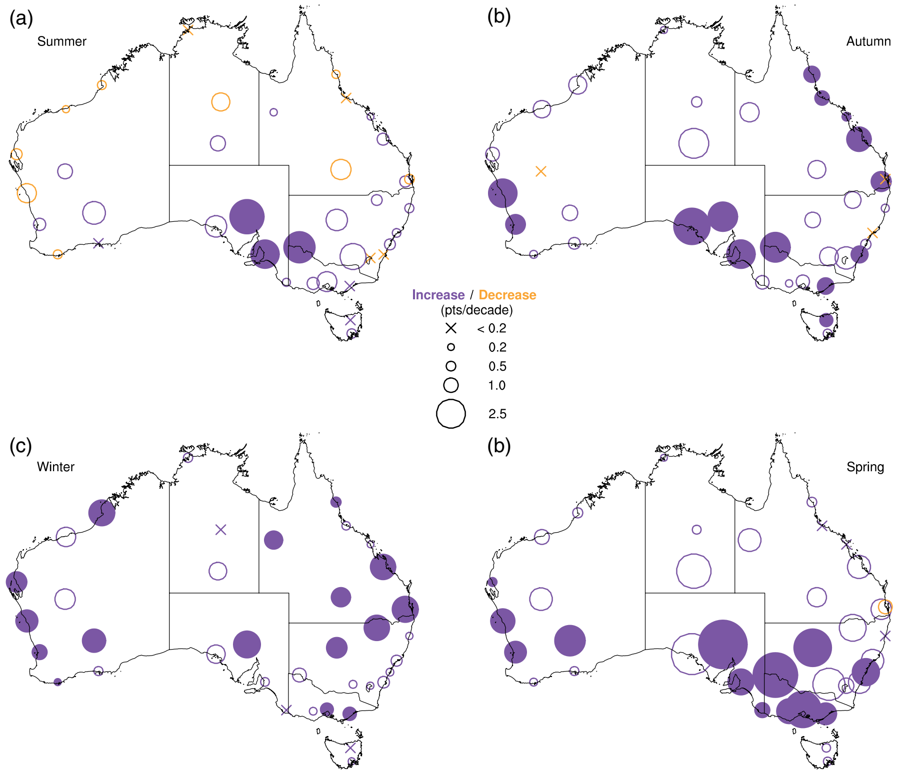

Figure 7. Map of trend in seasonal median FFDI. Marker size is proportional to the magnitude of trend. Reference sizes are shown in the legend. Filled markers represent trends that are statistically significant. The marker for Laverton has been moved west to avoid overlap with Melbourne Airport. This figure is available in colour online at wileyonlinelibrary.com/journal/joc

but widespread, and occur at lower latitudes than the bulk of spring and autumn increases. The general spatial coherence of these changes suggests that these are not effects of 'spurious significance' but real phenomena. At most locales, the largest trends are observed in the season before the peak of the fire season, which indicates a lengthening fire season across southern Australia. An increase in fire season length has also been found in Ontario, Canada, due in contrast to a delayed end to the fire season (Woolford *et al*., 2010). It should be noted that FFDI values are a nonlinear indication of fire weather conditions; the magnitude of change must be interpreted with respect to local baseline values and fire danger rating thresholds.

There are a number of difficulties in separating the contribution from each of the variables constituting FFDI towards the observed trends. One method, adapted from Lucas (2010b; see also Dowdy *et al*., 2010), is to take the partial derivative of the FFDI equation with respect to each variable (they are differently weighted) and substitute the change in each variable, as derived from ordinary least squares regression. This approach suggests that decreases in relative humidity have played the largest role in the average changes observed here and that the direct effect of temperature has played a relatively small role (data not shown). In southeastern Australia, drought factor – an estimate of fuel dryness – appears to be a significant factor in the observed trends. This observation is particularly noteworthy in Victoria (e.g. Laverton, Melbourne and Mildura), where severe drought conditions have prevailed between 1996 and late-2010 (Murphy and Timbal 2008; Timbal 2009). However, this method is based on average changes and does not capture influences across the distribution, particularly at the important upper end. It must also rule out wind speed, as the methodology used here to correct inhomogeneities in the wind record has the effect of removing any trends. Moreover, the decreasing trend in relative humidity is influenced by the data set commencing during a relatively wet period. Ultimately, any attempt at attributing changes in FFDI to individual variables must recognize that the variables are not independent. Relative humidity and temperature are strongly linked and it is possible that changes in relative humidity are more attributable to temperature than actual water vapour amounts. In addition, while the drought factor is based largely on recent rainfall, temperature is also a contributing factor in its calculation.

These increases in FFDI do not necessarily equate to an increased chance of wildland fire occurrence. The changes will have manifested differently depending on local fire dynamics. In the north and widespread arid regions, wildland fire is limited more by fuel availability than the immediate weather (Bradstock, 2010). Rainy years – such as the strong La Niña event of 2010 – can bring enhanced fire danger in the following year(s). This can lead to a situation where 1 or 2 years of very low cumulative FFDI are followed by a period of increased fire weather conditions, such as the central Australian fires in the 1970s and early 2000s (Griffin

Table III. 1973–2010 mean values (in points FFDI) for ΣFFDI, annual 90th percentile FFDI and seasonal median and 90th percentile FFDI.

Station	Annual ∑FFDI	Annual 90%	Seasonal 50%				Seasonal 90%			
			JJA	SON	DJF	MAM	JJA	SON	DJF	MAM
Adelaide	2875	18.6	1.9	4.3	10.3	5.7	5.7	15.7	28.2	17.5
Albany Airport	1414	8.6	1.0	1.9	6.1	3.9	3.3	5.0	11.9	10.8
Alice Springs	9329	45.8	12.1	26.6	29.6	17.7	25.5	48.1	51.4	36.9
Amberley	3378	17.9	7.1	8.6	4.7	5.7	17.6	21.8	14.1	14.0
Brisbane Airport	2068	10.6	5.1	5.5	3.4	3.9	13.0	12.3	8.5	8.8
Broome	4496	27.1	17.0	8.2	4.2	8.3	29.9	30.7	9.3	24.8
Cairns	1919	10.8	5.9	5.9	1.1	1.6	11.1	12.3	7.4	7.5
Canberra	2693	17.3	2.4	4.1	8.5	4.8	5.7	14.7	27.1	13.7
Carnarvon	3658	18.1	6.1	8.6	8.9	8.1	16.6	18.3	18.7	18.2
Ceduna	4984	30.9	4.9	8.3	10.2	7.9	17.0	35.4	39.5	26.9
Charleville	6582	34.5	9.8	20.1	18.8	13.9	19.3	38.6	40.3	28.5
Cobar	5191	29.5	4.9	12.7	20.2	10.5	11.8	30.7	39.8	22.5
Coffs Harbour	1397	7.8	3.4	3.4	2.0	1.5	8.5	9.0	6.6	5.4
Darwin	3510	22.1	14.9	8.3	0.6	5.1	27.1	17.6	5.3	17.9
Esperance	1905	10.2	1.9	3.3	6.3	4.7	6.9	9.0	12.8	13.1
Geraldton	4412	27.5	2.7	6.5	13.1	10.4	10.1	18.8	42.6	31.4
Hobart	1458	7.9	1.6	2.6	4.2	2.9	4.1	7.0	10.7	7.6
Kalgoorlie	6059	34.1	6.7	16.7	22.3	11.2	17.0	37.2	44.9	27.6
Launceston Airport	1396	9.0	1.0	2.3	6.2	3.0	2.3	5.9	13.3	8.8
Laverton	2185	12.7	2.3	3.2	5.6	3.9	6.0	11.8	21.1	12.3
Mackay	1110	6.5	3.0	5.1	1.8	1.7	6.6	8.4	7.0	5.1
Meekatharra	8467	44.9	10.0	26.6	35.0	17.9	22.7	47.1	56.5	36.8
Melbourne Airport	2591	15.1	2.4	3.5	6.8	4.5	5.9	13.2	25.0	14.3
Mildura	5121	29.4	4.8	12.2	20.2	10.1	12.1	31.6	40.1	24.1
Moree	4696	24.5	5.9	10.8	11.9	10.2	12.9	28.6	27.6	20.7
Mt Gambier	2097	12.7	0.9	2.2	7.7	3.7	2.6	7.6	22.5	13.6
Mt Isa	8447	41.0	18.0	29.4	14.2	17.1	28.7	47.6	40.4	30.8
Nowra	2022	11.2	3.2	3.5	3.4	2.9	9.1	15.0	11.7	8.6
Perth Airport	3805	24.8	1.3	4.8	16.2	9.0	5.8	14.4	35.1	24.2
Port Hedland	7722	38.5	17.2	22.3	11.3	15.2	32.1	46.0	30.5	32.0
Rockhampton	3329	16.9	8.1	9.7	6.0	7.3	17.3	21.1	14.2	14.5
Sale	2010	10.9	2.1	3.0	5.3	3.5	5.9	10.0	15.8	10.2
Sydney Airport	2370	12.7	3.0	4.3	4.2	2.9	10.3	15.2	12.9	9.0
Tennant Creek	8710	41.6	20.3	31.5	18.3	19.8	31.2	47.8	45.4	36.6
Townsville	2883	13.7	7.6	8.2	2.9	5.6	16.1	13.8	10.0	11.6
Wagga	3639	23.8	1.8	4.1	15.8	7.0	5.0	18.5	36.8	18.8
Williamtown	2100	12.8	2.6	4.2	4.4	2.4	9.8	16.7	15.8	8.9
Woomera	7615	40.9	8.1	19.6	27.9	14.9	20.1	46.8	50.8	31.4

et al., 1983; Edwards *et al*., 2008). Conversely, the Black Saturday forest fires of February 2009 in Victoria, in the country's temperate southeast, were driven by some of the highest FFDI values on record, against a background of severe drought conditions in the preceding months and years (McCaw *et al*., 2009; National Climate Centre, 2009). Regional differences in fire frequency will also lead to different sample sizes from which to detect potential impacts of changes in fire weather. In the north, some parts of the tropical savanna woodlands and grasslands burn on an annual basis, while fires in temperate heathlands and dry sclerophyll forests have inter-fire intervals of 7 to 30 years (Beeton *et al*., 2006). Fires in wet sclerophyll forests are less frequent but often of extremely high intensity when they do occur, especially in the southern temperate areas.

4.2. Natural variability and climate change

The observed trends in fire weather occurred against a backdrop of considerable interannual variability. A primary mechanism driving this variability across Australia is ENSO. There is a strong positive relationship between El Niño events and fire weather conditions in southeast and central Australia (Williams and Karoly, 1999; Verdon *et al*., 2004; Lucas, 2005). Despite the strong relationships, ENSO only explains 15–35% of the year to year variance in FFDI (Lucas *et al*., 2007). A link has recently been found between positive Indian Ocean Dipole (pIOD) events, which have trended upwards since 1950, and significant fire seasons in the country's southeast (Cai *et al*., 2009). Another possible driver of variability is the Southern Hemisphere Annular Mode (SAM). The effect of SAM on Australia varies with the season; the positive phase of SAM corresponds with generally higher summer rainfall in north-central and south-east Australia and lower winter rainfall in south-east and south-west Australia (Hendon *et al.*, 2007).

Sources of interannual variability are in turn subject to longer term interdecadal circulation variations such as the Interdecadal Pacific Oscillation (IPO; Folland *et al.*, 1999; Power *et al.*, 1999). Long-term fluctuations with a period of around 20 years are apparent at a few stations in southeast Australia with data extending back to the 1940s (Lucas *et al.*, 2007). These longer time series also highlight the importance of start date selection in a highly variable climate. The 1940s were a period of relatively high fire danger and the observed trends since then are much lower. Although we find the choice of start and end dates has a relatively small effect on the positive trends in fire danger, the fact remains that the period 1973–1975 was one of the wettest across Australia.

Is climate change a plausible contributor to the trends observed here? Studies of the impacts of elevated atmospheric carbon dioxide on future fire weather show considerable global variation, including decreases in some areas, but the potential for large increases in many areas (e.g. increases of up to 95% in a daily fire severity rating by 2070 in western Canada during summer; Nitschke and Innes, 2008; see Flannigan *et al.*, 2009 for other examples). A number of early Australian studies on the effects of climate change using global climate model (GCM) simulations found widespread increases in fire weather under increased atmospheric carbon dioxide (Beer and Williams, 1995; Cary and Banks, 1999; Williams *et al.*, 2001; Cary, 2002). Building on the work of Hennessy *et al.* (2005), Lucas *et al.* (2007) projected increases in annual FFDI of up to 30% by 2050 over historical levels in southeast Australia, and up to a trebling in the number of days per year where the uppermost values of the index are exceeded. The largest changes occurred in the arid and semi-arid interior of NSW and northern Victoria, with the smallest changes in coastal areas and Tasmania. They also found that in many cases, fire weather conditions during the 2000s far exceeded the projections for 2050. The southeast of Australia is a hotspot for future increases in fire weather conditions according to other studies, in terms of both FFDI (Clarke *et al.*, 2011) and a synoptic marker of extreme fire events (Hasson *et al.*, 2009). Observed increases in FFDI over southeast Australia match these projections well. Another area of agreement is Tasmania, which has recorded little to no increases in FFDI and was projected to continue to do so by Lucas *et al.* (2007). There is less consistency in projections for other areas: in tropical northeast Australia, some studies have projected no change or decreases in mean and extreme FFDI (Clarke *et al.*, 2011) while others located the largest increases in this region (Pitman *et al.*, 2007). Observations for tropical north Australia correspond more closely to the former, with smaller increases or no significant trends in much of tropical northern Australia. Detailed spatial projections are lacking for much of central and Western Australia.

These projections should be interpreted in light of known flaws in climate models' ability to simulate important modes of variability (Guilyardi *et al.*, 2009) and their interaction (Cai *et al.*, 2011). There is further uncertainty about the potential effect climate change will have on these modes and thus indirectly on future fire weather conditions. For instance, it is believed that climate change will impact the physical processes that underpin ENSO, but it is not known whether this will lead to more or less events or a change in their intensity (Collins *et al.*, 2010). An additional source of doubt in future projections of the probability of wildland fire occurrence is the response of fuel load to climate change, with potentially competing effects of increased carbon dioxide fertilization and changes in both magnitude and variability of temperature and precipitation (Medvigy *et al.*, 2010; Zhang *et al.*, 2010; Matthews *et al.* 2011). As discussed above, the relative importance of fire weather with respect to other limiting factors (such as fuel load) in determining overall chance of wildland fire occurrence depends on prevailing fire regimes.

The total change predicted by the trends is typically smaller than the range of interannual variability, which can be quite large depending on the location and season. Despite this, there is a consistency between the increases in FFDI observed since 1973 and projections of increased fire weather conditions due to climate change. One hypothesis, after Lucas *et al.* (2007) is that we are currently experiencing an upswing in fire weather conditions due to some natural forcing with an interdecadal time scale, and that this is being exacerbated by the subtle, ongoing effects of climate change. In this respect, it is noteworthy that the 2010/2011 fire season has seen some of the lowest measures of FFDI on record in some areas. Additional data in the coming years will reveal whether this is a natural fluctuation in the face of a steadily increasing trend, or part of a longer lasting decline in FFDI values.

Acknowledgements

Andy Pitman, Andrew Dowdy, Graham Mills and two anonymous reviewers provided helpful comments on the manuscript.

References

Archibald S, Roy DP, van Wilgen BW, Scholes RJ. 2009. What limits fire? An examination of drivers of burnt area in Southern Africa. *Global Change Biology* **15**: 613–630.

Alexander L, Arblaster J. 2009. Assessing trends in observed and modelled climate extremes over Australia in relation to future projections. *International Journal of Climatology* **29**: 417–435.

Bates BC, Hope P, Ryan B, Smith I, Charles S. 2008. Key findings from the Indian Ocean Climate Initiative and their impact on policy development in Australia. *Climatic Change* **89**(3–4): 339–354.

Beer T, Williams A. 1995. Estimating Australian forest fire danger under conditions of doubled carbon dioxide concentrations. *Climatic Change* **29**: 169–188.

Beeton RJS, Buckley KI, Jones GJ, Morgan D, Reichelt RE, Trewin D. 2006. Australia State of the Environment. *Independent report to the Australian Government Minister for the Environment and Heritage*. Department of the Environment and Heritage: Canberra.

Bradstock RA. 2010. A biogeographic model of fire regimes in Australia: current and future implications. *Global Ecology and Biogeography* **19**: 145–158.

Cai W, Cowan T, Raupach M. 2009. Positive Indian Ocean Dipole events precondition southeast Australia bushfires. *Geophysical Research Letters* **36**: L19710.

Cai W, Sullivan A, Cowan T. 2011. Interactions of ENSO, IOD, and the SAM in CMIP3 models. *Journal of Climate* **24**: 1688–1704.

Cary GJ. 2002. Importance of changing climate for fire regimes in Australia. In *Flammable Australia – The Fire Regimes and Biodiversity of a Continent*. Bradstock R, Williams J, Gill M (eds). Cambridge University Press: Cambridge, UK.

Cary GJ, Banks JCG. 1999. Fire regime sensitivity to global climate change: an Australian perspective. In *Biomass Burning and Its Inter-Relationships With the Climate System*. Innes J, Beniston M, Verstraete M (eds). Kluwer: Boston, USA.

Clarke HC, Smith PL, Pitman AJ. 2011. Regional signatures of future fire weather over Eastern Australia from Global Climate Models. *International Journal of Wildland Fire* **20**: 550–562.

Collins M, An SI, Cai W, Ganachaud A, Guilyardi E, Jin FF, Jochum M, Lengaigne M, Power S, Timmermann A, Cecchi G, Wittenberg A. 2010. The impact of global warming on the tropical Pacific ocean and El Niño. *Nature Geoscience* **3**(6): 391–397.

CSIRO, Australian Bureau of Meteorology. 2010. State of the Climate. Retrieved 5 July 2011. http://www.bom.gov.au/inside/eiab/State-of-climate-2010-updated.pdf.

Deeming JE, Burgan RE, Cohen JE. 1978. *The National Fire-Danger Rating System*. Doc. No. A 13.88:INT-39. Dept. of Agriculture, Forest Service, Intermountain Forest and Range Experiment Station Ogden: Utah.

Dowdy AJ, Mills GA, Finkele K, de Groot W. 2010. Index sensitivity analysis applied to the Canadian Forest Fire Weather Index and the McArthur Forest Fire Danger Index. *Meteorological Applications* **17**: 298–312.

Easterling DR, Peterson TC. 1995. A new method for detecting undocumented discontinuities in climatological time series. *International Journal of Climatology* **15**: 369–377.

Edwards GP, Allan GE, Brock C, Duguid A, Gabrys K, Vaarzon-Morel P. 2008. Fire and its management in central Australia. *The Rangeland Journal* **30**: 109–121.

Flannigan MD, Krawchuk MA, De Groot WJ, Wotton BM, Gowman LM. 2009. Implications of changing climate for global wildland fire. *International Journal of Wildland Fire* **18**: 483–507.

Folland CK, Parker DE, Colman AW, Washington R. 1999. Large scale modes of ocean surface temperatures since the late nineteenth century. In *Beyond El Niño: Decadal and interdecadal Climate Variability*. Navarra A (ed). Springer-Verlag: Berlin, Germany.

Griffiths D. 1999. Improved formula for the drought factor in McArthur's Forest Fire Danger Meter. *Australian Forestry* **62**: 202–206.

Guilyardi E, Wittenberg A, Fedorov A, Collins M, Wang C, Capotondi A, van Oldenborgh GJ, Stockdale T. 2009. Understanding El Niño in ocean–atmosphere general circulation models: Progress and challenges. *Bulletin of the American Meteorological Society* **90**: 325–340.

Haines DA. 1988. A lower atmospheric severity index for wildland fires. *National Weather Digest* **13**: 23–27.

Hasson AEA, Mills GA, Timbal B, Walsh K. 2009. Assessing the impact of climate change on extreme fire weather events over Southeastern Australia. *Climate Research* **39**: 159–172.

Hendon HH, Thompson DWJ, Wheeler M. 2007. Australian rainfall and surface temperature variation associated with the Southern Hemisphere Annular Mode. *Journal of Climate* **20**: 2452–2467.

Hennessy K, Lucas C, Nicholls N, Bathols J, Suppiah R, Ricketts J. 2005. *Climate change impacts on fire-weather in south-east Australia*. Consultancy report for the New South Wales Greenhouse Office, Victorian Department of Sustainability and Environment, ACT Government, Tasmanian Department of Primary Industries, Water and Environment and the Australian Greenhouse Office. CSIRO and Bureau of Meteorology: Victoria.

Jakob D. 2010. Challenges in developing a high-quality surface wind-speed data-set for Australia. *Australian Meteorological and Oceanographic Journal* **60**: 227–236.

Keetch JJ, Byram GM. 1968. *A drought index for forest fire control.* Research Paper SE-38. USDA Forest Service: Ashville, NC.

Lucas C. 2005. *Fire climates of Australia: Past, present and future*. Proceedings, 6th Symposium on Fire and Forest Meteorology, Canmore, Alberta, Canada, 25–27 October 2005. Retrieved 5 July 2011. http://ams.confex.com/ams/pdfpapers/97592.pdf.

Lucas C. 2010a. A high-quality historical humidity database for Australia. CAWCR Technical Report No. 24. CSIRO and Bureau of Meteorology: Victoria.

Lucas C. 2010b. On developing a historical fire weather data-set for Australia. *Australian Meteorological and Oceanographic Journal* **60**: 1–14.

Lucas C, Hennessy K, Mills G, Bathols J. 2007. *Bush fire weather in southeast Australia: recent trends and projected climate change impacts.* Consultancy Report prepared for The Climate Institute of Australia. Bush fire Cooperative Research Centre: Victoria.

Luke R, McArthur A. 1978. *Bush fires in Australia*. Australian Government Publishing Service: Canberra.

Matthews S, Nguyen K, McGregor JL. 2011. Modelling fuel moisture under climate change. *International Journal of Climate Change Strategies and Management* **3**(1): 6–15, DOI: 10.1108/17568691111107916.

McCaw L, Mills G, Sullivan A, Hurley R, Ellis P, Matthews S, Plucinski M, Pippen B, Boura J. 2009. Fire behaviour investigation. In *Victorian 2009 Bushfire Research Response Final Report*. Bushfire CRC: Victoria.

McVicar TR, Van Niel TG, Li LT, Roderick ML, Rayner DP, Ricciardulli L, Donohue RJ. 2008. Wind speed climatology and trends for Australia, 1975–2006: Capturing the stilling phenomenon and comparison with near-surface reanalysis output. *Geophysical Research Letters* **35**: L20403.

Medvigy D, Wofsy SC, Munger JW, Moorcroft PR. 2010. Responses of terrestrial ecosystems and carbon budgets to current and future environmental variability. *Proceedings of the National Academy of Sciences of the United States of America* **107**(18): 8275–9280.

Mills GA. 2005. A re-examination of the synoptic and mesoscale meteorology of Ash Wednesday 1983. *Australian Meteorological Magazine* **54**: 35–55.

Mills GA, McCaw L. 2010. Atmospheric Stability Environments and Fire Weather in Australia – extending the Haines Index. CAWCR Technical Report No. 20. CSIRO and Bureau of Meteorology: Victoria.

Murphy BF, Timbal B. 2008. A review of recent climate variability and climate change in southeastern Australia. *International Journal of Climatology* **28**: 859–879.

National Climate Centre. 2009. The exceptional January–February 2009 heatwave in south-eastern Australia. Special Climate Statement 17. Bureau of Meteorology: Victoria.

Nicholls N. 2006. Detecting and attributing Australian climate change: a review. *Australian Meteorological Magazine* **55**: 199–211.

Nitschke CR, Innes JL. 2008. Climatic change and fire potential in south-central British Columbia, Canada. *Global Change Biology* **14**: 841–855.

Noble IR, Barry GAV, Gill AM. 1980. McArthur's fire danger meters expressed as equations. *Australian Journal of Ecology* **5**: 201–203.

Pitman AJ, Narisma GT, McAneney J. 2007. The impact of climate change on the risk of forest and grassland fires in Australia. *Climatic Change* **84**: 383–401.

Power SB, Casey T, Folland C, Colman A, Mehta V. 1999. Interdecadal modulation of the impact of ENSO on Australia. *Climate Dynamics* **15**: 319–324.

Risbey JS, Pook MJ, McIntosh PC. 2009. On the remote drivers of rainfall variability in Australia. *Monthly Weather Review* **137**(10): 3233–3253.

Russell-Smith J, Yates CP, Whitehead PJ, Smith R, Craig R, Allan GE, Thackway R, Frakes I, Cridland S, Meyer MCP, Gill AM. 2007. Bushfires 'down under': patterns and implications of contemporary Australian landscape burning. *International Journal of Wildland Fire* **16**: 361–377.

Stott PA. 2003. Attribution of regional-scale temperature changes to anthropogenic and natural causes. *Geophysical Research Letters* **30**: 1728.

Timbal B. 2009. The continuing decline in southeast Australian rainfall: update to May 2009. CAWCR Research Letters Issue 5, July 2009. CSIRO and Bureau of Meteorology: Victoria.

Timbal B, Arblaster JM, Power S. 2006. Attribution of the late-twentieth-century rainfall decline in southwest Australia. *Journal of Climate* **19**: 2046–2062.

Van Wagner CE. 1987. *Development and Structure of the Canadian Forest Fire Weather Index System.* Technical Report 35. Canadian Forestry Service: Ottawa, ON.

Verdon DC, Kiem AS, Franks SW. 2004. Multi-decadal variability of forest fire risk – eastern Australia. *International Journal of Wildland Fire* **13**: 165–171.

Willett KM, Gillett NP, Jones PD, Thorne PW. 2007. Attribution of observed surface humidity changes to human influence. *Nature* **449**: 710–713.

Williams AAJ, Karoly DJ. 1999. Extreme fire weather in Australia and the impact of the El Niño-Southern Oscillation. *Australian Meteorological Magazine* **48**: 15–22.

Williams AAJ, Karoly DJ, Tapper N. 2001. The sensitivity of australian fire danger to climate change. *Climatic Change* **49**: 171–191.

Woolford DG, Cao J, Dean CB, Martell DL. 2010. Characterizing temporal changes in forest fire ignitions: looking for climate change signals in a region of the Canadian boreal forest. *Environmetrics* **21**: 789–800.

Zhang C, Hanqin T, Wang Y, Zeng T, Liu Y. 2010. Predicting response of fuel load to future changes in climate and atmospheric composition in the Southern United States. *Forest Ecology and Management* **260**: 556–564.

Chapter 3 Summary

Analysis of historical trends in fire weather

The observational record of FFDI in Australia is marked by clear interannual variability. There is a spatial coherence to this variability, suggesting common drivers in its evolution amongst the 38 stations that comprise the high quality FFDI dataset. Against this backdrop of variability, 16 of 38 stations recorded a significant increase in average fire weather conditions between 1973 and 2010. No decreases were recorded at any station. Over the same period, 24 of 38 stations recorded a significant increase in high fire danger conditions. Again, no decreases were recorded. These trends are largely robust to variation of the starting and ending points from which they are calculated.

The period of these observations coincides with an era of unprecedented rates of global warming, including increases in temperature across Australia. Although no formal attribution of FFDI was conducted, observations of either increased or unchanged levels of fire danger are consistent with early studies of the influence of climate change over fire weather in Australia. The next chapter aims to build on these earlier studies to further investigate the changes in FFDI projected by global climate models over Australia.

Chapter 4 Overview

Projections of fire weather from global climate models

Global climate models (GCMs) are the major tools for understanding the potential evolution of the earth's climate system under different scenarios over the coming decades and centuries. They have evolved significantly since their inception, incorporating additional physical processes, uniting atmospheric, ocean and land systems and improving in skill. They also provide outputs from which FFDI can be calculated.

Several previous studies have investigated the broad impacts of climate change on FFDI in Australia. The work in Chapter 4 describes these studies and then build on them in a number of novel ways:

- It uses GCMs selected for their skill in representing the Australian climate, increasing confidence in model projections,
- It takes daily model output to create a daily FFDI time series, avoiding bias from analyses based on averages and increasing the amount of data available, and
- It examines regional variation in fire weather changes using rainfall seasonality zones, which are simple and climatically relevant.

The work reported here has been published in the peer reviewed literature and is reproduced exactly as published:

Clarke H, Smith P, Pitman AJ (2011) Regional signatures of future fire weather over eastern Australia from global climate models. International Journal of Wildland Fire, 20, 550-562. DOI: 10.1071/WF10070

Author contributions

I led this project. This project was conceived over several months through discussions between Andy Pitman (AP; my PhD Supervisor), Peter Smith (then my immediate work supervisor) and myself. The experiments were jointly designed by AP, PS and myself. I conducted the analysis and prepared the figures, then revised these after comments from AP and PS. I drafted the paper and revised it following several iterations of comments from AP and PS. I led the response to the reviewers' comments, incorporating comments from AP and PS.

Errata

An examiner noted the following error in the published paper:

p552 “in most of cases” should read “in most cases”

CSIRO PUBLISHING

International Journal of Wildland Fire **2011**, *20*, 550–562 www.publish.csiro.au/journals/ijwf

Regional signatures of future fire weather over eastern Australia from global climate models

Hamish G. Clarke[A,B,C], *Peter L. Smith*[A] *and Andrew J. Pitman*[B]

[A]NSW Department of Environment, Climate Change and Water, Climate Change Science Section, PO Box 3720, Parramatta, NSW 2124, Australia.
[B]University of NSW, Climate Change Research Centre, Sydney, NSW 2052, Australia.
[C]Corresponding author. Email: h.clarke@student.unsw.edu.au

Abstract. Skill-selected global climate models were used to explore the effect of future climate change on regional bushfire weather in eastern Australia. Daily Forest Fire Danger Index (FFDI) was calculated in four regions of differing rainfall seasonality for the 20th century, 2050 and 2100 using the A2 scenario from the Special Report on Emissions Scenarios. Projected changes in FFDI vary along a latitudinal gradient. In summer rainfall-dominated tropical north-east Australia, mean and extreme FFDI are projected to decrease or remain close to 20th century levels. In the uniform and winter rainfall regions, which occupy south-east continental Australia, FFDI is projected to increase strongly by 2100. Projections fall between these two extremes for the summer rainfall region, which lies between the uniform and summer tropical rainfall zones. Based on these changes in fire weather, the fire season is projected to start earlier in the uniform and winter rainfall regions, potentially leading to a longer overall fire season.

Additional keywords: climate projections, fire seasonality, Forest Fire Danger Index.

Introduction

Regional variation in the drivers of bushfire risk – biomass growth, the fuel's availability for burning, ambient weather and ignitions – has led to a distinct pattern of fire regimes across Australia (Bradstock 2010). In the south-east and south-west, summer and spring are the dominant fire seasons, whereas in northern Australia, fire danger peaks late in the winter dry season (Fig. 1*a*; Luke and McArthur 1978). In the north, some parts of the tropical savanna woodlands and grasslands burn on an annual basis, whereas fires in temperate heathlands and dry sclerophyll forests have interfire intervals of 7 to 30 years. Fires in wet sclerophyll forests are less frequent but often of extremely high intensity when they do occur, especially in the southern temperate areas. Fires are absent or very rare in rainforest for both temperate and tropical regions and of low intensity in the absence of disturbances such as cyclones or logging (Beeton *et al*. 2006).

Climate change adds a layer of complexity to this existing pattern of fire regimes, and to the challenge of bushfire prediction. There has been a growing effort to characterise potential responses of bushfire regimes across the globe to climate change (see Flannigan *et al*. 2009 for a review). Although dominated by North American studies, the current consensus is that climate change will lead to an increase in fire risk globally, partially offset by decreased risks in some areas. Several different aspects of bushfire have been explored, including fire weather, area burned, fire occurrence, fire season and fire intensity.

Within Australia, the focus of most climate change studies has been fire weather, frequently depicted by the McArthur Forest Fire Danger Index (FFDI; Luke and McArthur 1978). The FFDI is an exponential function of dryness, temperature, wind speed and humidity. Several early Australian studies on the effects of climate change using global climate model (GCM) simulations found an increase in bushfire weather under increased atmospheric carbon dioxide (CO_2) (Beer and Williams 1995; Cary and Banks 1999; Williams *et al*. 2001; Cary 2002).

Lucas *et al*. (2007) used a 'change factor' approach to convert observed daily weather time series in south-east Australia into new series centred on 2020 and 2050, using an atmosphere-only regional climate model (CCAM), driven at the boundaries by two versions of the CSIRO GCM. They calculated monthly decile changes per degree of global warming for each weather variable, based on the upper and lower projection bounds from the Intergovernmental Panel on Climate Change's (IPCC's) Fourth Assessment Report (AR4, IPCC 2007). By 2050, annual FFDI was projected to increase by up to 30%, whereas the uppermost values of the index were projected to increase by up to 300%. The largest changes occurred in the arid and semiarid interior of NSW and northern Victoria, where fire danger from forest or grassland fire is usually low owing to negligible fuels in most years. Alternatively, along the near-coastal regions where most forests are distributed, little or no change in fire weather was simulated. These findings, along with a modified FFDI split into ambient and drought components, were used by Bradstock *et al*. (2009) to predict a 20–84% increase in potential large ($\geq$1000 ha) fire ignition days in the Blue Mountains and Central Coast regions, both located near Sydney in NSW, by 2050.

 10.1071/WF10070 1049-8001/11/040550

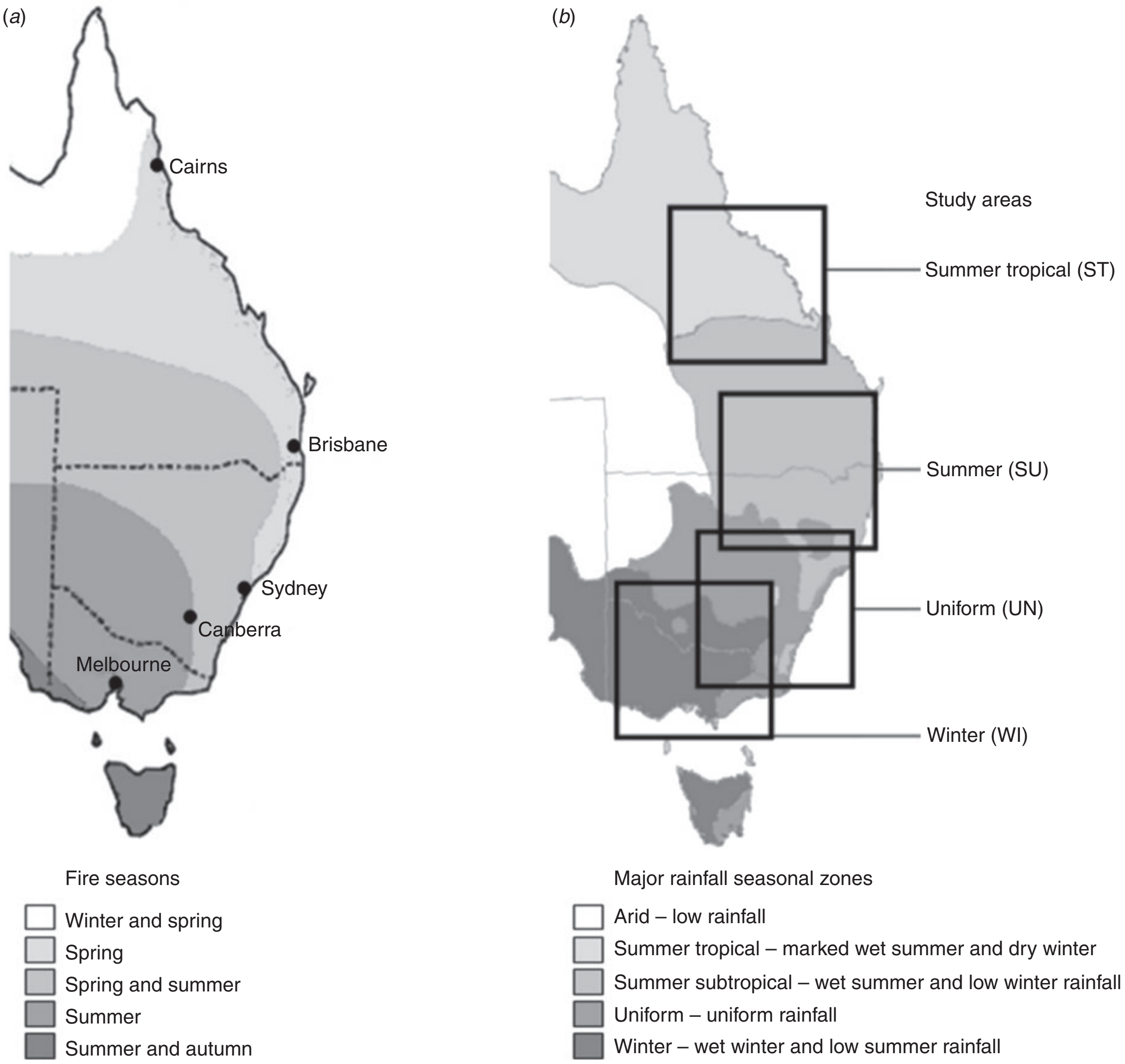

Fig. 1. (*a*) Bushfire seasonality in eastern Australia (from Luke and McArthur 1978). (*b*) Rainfall seasonality regions (shaded; from Australian Bureau of Meteorology 2005*b*) and study area (boxed).

In contrast, Pitman *et al*. (2007) directly used output from a regional climate model (RAMS, Pielke *et al*. 1992), driven at the boundaries by the CSIRO GCM, to calculate the change in FFDI and grassland fire danger index in January throughout Australia in 2050 and 2100. FFDI increased under both low–moderate (B2) and relatively high (A2) emissions scenarios from the Special Report on Emissions Scenarios (SRES, Nakicenovic *et al*. 2000). To move away from considering averages, Pitman *et al*. (2007) also calculated the FFDI probability density function (PDF), which describes the relative likelihood of a variable taking any given value within its distribution, at a single point in NSW. For example, on the western slopes of the Great Dividing Range, 29.885°S, 149.104°E, they found a 25% increase in 2050, a further 20% increase in 2100 under the B2 scenario and a dramatically higher risk again under the A2 scenario compared with the present day. These values represent maxima, as the drought factor was fixed at its uppermost value of 10 for the study.

Hasson *et al*. (2009) also investigated the effect of climate change on fire weather. However, rather than using FFDI, they examined a synoptic feature characteristic of some of the most extreme fire events in south-east Australia over the last 50 years: strong cold fronts over the Southern Ocean moving towards the area. Intensification of these fronts generates ideal bushfire conditions, because of a northerly prefrontal jet that advects hot, dry gusty winds southwards. Using an 850-hPa temperature gradient as a proxy, they calibrated output from 10 AR4 GCMs against reanalysis datasets to predict changes in the frequency of extreme cold fronts in 2050 and 2100 under the A2 and B1 SRES scenarios. Overall, the results suggested a doubling in the number of extreme cold fronts – and hence extreme fire weather – by 2050, from approximately one every

2 years to one per year. By 2100, this increases to between one and two events per year.

The ability of climate models to simulate observed climate must be considered when evaluating projections against a model baseline. Perkins *et al*. (2007) reasoned that the better a model can simulate the entire PDF of a variable – i.e. not just the average but the range and relative probability of all values – the more confidence there is in the model's projections under future climate change. This is because even at $2 \times CO_2$ in 2100, the future PDF still substantially overlaps a current PDF. Perkins *et al*. (2007) partitioned Australia into 12 regions and evaluated the capacity of 16 AR4 models to simulate observed PDFs for minimum temperature, maximum temperature and precipitation for each region. Many of the models show considerable skill in representing observed PDFs over Australia, more so for temperature than precipitation. Similar results have been found with indices of climate extremes (Alexander and Arblaster 2009). There is less knowledge about GCM skill over Australia in simulating the other two variables from which FFDI is calculated: wind speed and humidity. On a global scale, models show significant and increasing skill in representing large-scale distributions of both variables (Randall *et al*. 2007) but no detailed evaluation exists for Australia owing to limited observational data.

The aim of this paper is to explore the effect of climate change on one of the key drivers of fire regimes over eastern Australia – fire weather. Rather than using an adjusted historical time series, we use GCMs to directly calculate FFDI, which does not assume a linear relationship between annual mean global warming and regional climate (i.e. temperature, precipitation, humidity and wind speed). We use rainfall seasonality zones as the basis for exploring regional variation in fire weather. Rainfall seasonality is a major driver of existing fire regimes (see e.g. Bradstock 2010) and there are four major rainfall zones along the eastern third of Australia, which matches the resolution of GCMs well.

Our approach differs from existing studies in that it:

- uses GCMs selected for their skill in representing the Australian climate, increasing confidence in model projections,
- takes daily model output to create a daily FFDI time series, avoiding bias from analyses based on averages and increasing the amount of data available, and
- examines regional variation in fire weather changes using rainfall seasonality zones, which are simple and climatically relevant.

Methods

Climate model data

Daily climate model data over eastern Australia for maximum temperature, mean wind speed, average specific humidity and total precipitation were taken from the World Climate Research Program's (WCRP) Coupled Model Intercomparison Project phase 3 (CMIP3) multimodel dataset. The CMIP3 archive includes simulations of past, present and future climate. Data from 1961 to 2000 were used to calculate present fire weather (i.e. 20th century for the purposes of the present study). Data from 2046 to 2065 and 2081 to 2100 were used to project climate for 2050 and 2100 respectively. The use of daily data avoids biases that may accompany analyses based only on averages or other summary statistics. Only the A2 SRES emission scenario was used because it is the scenario closest to – although presently tracking below – global emissions trends and for which daily data from multiple GCM simulations exist (Le Quéré *et al*. 2009).

The four models selected were CSIRO, ECHO-G, IPSL and MRI. These were the models with the highest skill score over Australia, defined by Perkins *et al*. (2007) as the amount of overlap between observed and simulated PDFs. MRI ranked fifth but was included because daily data for all variables were not available for MIROC-m, which would otherwise have been used. One simulation was used for each model. Details of each climate model are available in Randall *et al*. (2007) and Perkins *et al*. (2007).

Study area

The study regions are adapted from the four major seasonal rainfall zones in eastern Australia: summer tropical (ST), summer (SU), uniform (UN) and winter (WI) (Fig. 1*b*). These regions are based on differences between summer and winter rainfall (Australian Bureau of Meteorology 2005*b*). In the summer tropical (or 'summer dominant') zone, which occupies the upper half of the north-eastern state of Queensland (QLD), 50–70% of rainfall occurs in summer and winters are typically dry. South-east QLD and north-east New South Wales (NSW) constitute the summer rainfall zone, receiving 30–40% of rainfall in summer and low rainfall in winter. The summer zone extends along or near the coast as far south as Sydney, NSW, with isolated patches in the south-east corner of NSW. To the south and west of the summer zone, precipitation occurs uniformly throughout the seasons. A patch of this uniform rainfall zone also occurs within the summer zone (Fig. 1*b*). The south-west of NSW and the majority of the southernmost continental state of Victoria fall within the winter rainfall zone, with a wet winter and low summer rainfall. Considerable areas of forest occur in all four zones.

GCM grid cells differ in size with CSIRO having the highest resolution ($\sim 1.9° \times 1.9°$) and ECHO-G the lowest ($\sim 3.9° \times 3.9°$). Models also differ in the location of their boundaries. To minimise overlap and maximise grid cell representation, a region size of 7° ($\sim$600 000 km^2) was used. This necessarily meant the exclusion of Tasmania and the inclusion of landscapes less prone to fire and a degree of overlap between rainfall zones, particularly in the south where rainfall zones are smaller. No ECHO-G grid cells fitted in the uniform region and two CSIRO cells were counted towards separate regions (out of nine total grid cells in each). GCM grid-cell representation and other major features of the study areas are summarised in Table 1.

Forest fire danger index (FFDI)

Daily FFDI values were calculated as:

$$\begin{aligned} FFDI = 2 \times \exp(&0.987 \times \ln(DF) - 0.0345 \times H + 0.0338 \\ &\times T + 0.0234 \times V - 0.45) \end{aligned} \quad (1)$$

where DF is a drought factor, H is relative humidity (%), T is maximum temperature (°C), and V is wind speed in the open at a height of 10 m (km h^{-1}) (Noble *et al*. 1980). Continuously

Table 1. Characteristics of the four study areas based on rainfall seasonality zones

Climate zones are based on Köppen classification (Australian Bureau of Meteorology 2005*a*)

Rainfall seasonality	Geographical area	Bounds (°)	Climate zones	Number of model grid cells within region
Summer tropical (ST)	North-east Queensland	17.5–24.5°S, 143.5–150.5°E	Tropical, subtropical, grassland	CSIRO (9), IPSL (2), ECHO-G (1), MRI (2)
Summer (SU)	South-east Queensland, north-east New South Wales	25–32°S, 146.5–153.5°E	Subtropical, temperate, grassland	CSIRO (9), IPSL (2), ECHO-G (1), MRI (2)
Uniform (UN)	Mid- to south-east New South Wales	31–38°S, 145.5–152.5°E	Temperate, grassland	CSIRO (9), IPSL (1), ECHO-G (0), MRI (1)
Winter (WI)	Victoria, south-west New South Wales	33–40°S, 141.5–148.5°E	Temperate, grassland	CSIRO (9), IPSL (2), ECHO-G (1), MRI (4)

recording weather stations make it possible to calculate FFDI at any time of day and to establish the daily maximum value. This is not possible with GCM data as wind speed and humidity are provided as daily averages. The drought factor is dimensionless, ranging between 0 and 10 and was calculated using the Keetch–Byram Drought Index (KBDI; Keetch and Byram 1968), following Griffiths (1999), as:

$$DF = 10.5 \times (1 - \exp(-(\mathrm{KBDI}/30)/40)) \times (41X^2 + X)/(40X^2 + X + 1) \qquad (2)$$

where X expresses the influence on the drought factor of past rainfall. X is defined as:

$$X = N^{1.3}/(N^{1.3} + p - 2) \text{ for } N \geq 1 \text{ and } p > 2$$

$$X = 0.8^{1.3}/(0.8^{1.3} + p - 2) \text{ for } N = 0 \text{ and } p > 2$$

$$X = 1 \text{ for } p \leq 2 \qquad (3)$$

where p is the sum of rainfall within the last rain event and N is the number of days since the day with the largest daily rainfall amount within the rain event. A rainfall event is defined as a set of consecutive days, each with rainfall above 2 mm, within the last 20 days. In operational use, the above algorithm has been found to increase the drought factor too quickly in prolonged dry periods after significant rain events. We use a correction applied by the Australian Bureau of Meteorology (Finkele *et al*. 2006), which calculates X as the minimum of Eqn 3 and the limiting function X_{lim}, defined as:

$$X_{\mathrm{lim}} = 1/(1 + 0.1135 \times \mathrm{KBDI}) \text{ for KBDI} < 20$$

$$X_{\mathrm{lim}} = 75/(270.525 + 1.267 \times \mathrm{KBDI}) \text{ for KBDI} \geq 20 \qquad (4)$$

Wind speed was derived from GCM-simulated north and east vectors. GCMs produce specific humidity at several different atmospheric pressure levels. For all models except ECHO-G, a significant proportion of surface humidity data was not available. It was found that a simple linear relationship exists between GCM humidity at surface (1000 hPa) and 925 hPa over land. Missing surface humidity was calculated using this relationship. Relative humidity was calculated from GCM-specific humidity and temperature, capped at 100. All calculations were performed using *MatLab* (see http://www.mathworks.com).

Data analysis

Bootstrapping is a statistical method to increase the sample size by randomly selecting data values from the original dataset to create a new set of observations of specified size, making it possible to put confidence bounds on sample parameters. We used standard, with-replacement bootstrapping techniques to create 1000 bootstrap samples for each model, region and scenario. We used these to calculate the 95% confidence interval for mean monthly FFDI, defined as the average of daily values in each month. Thus, where models project changes that are large

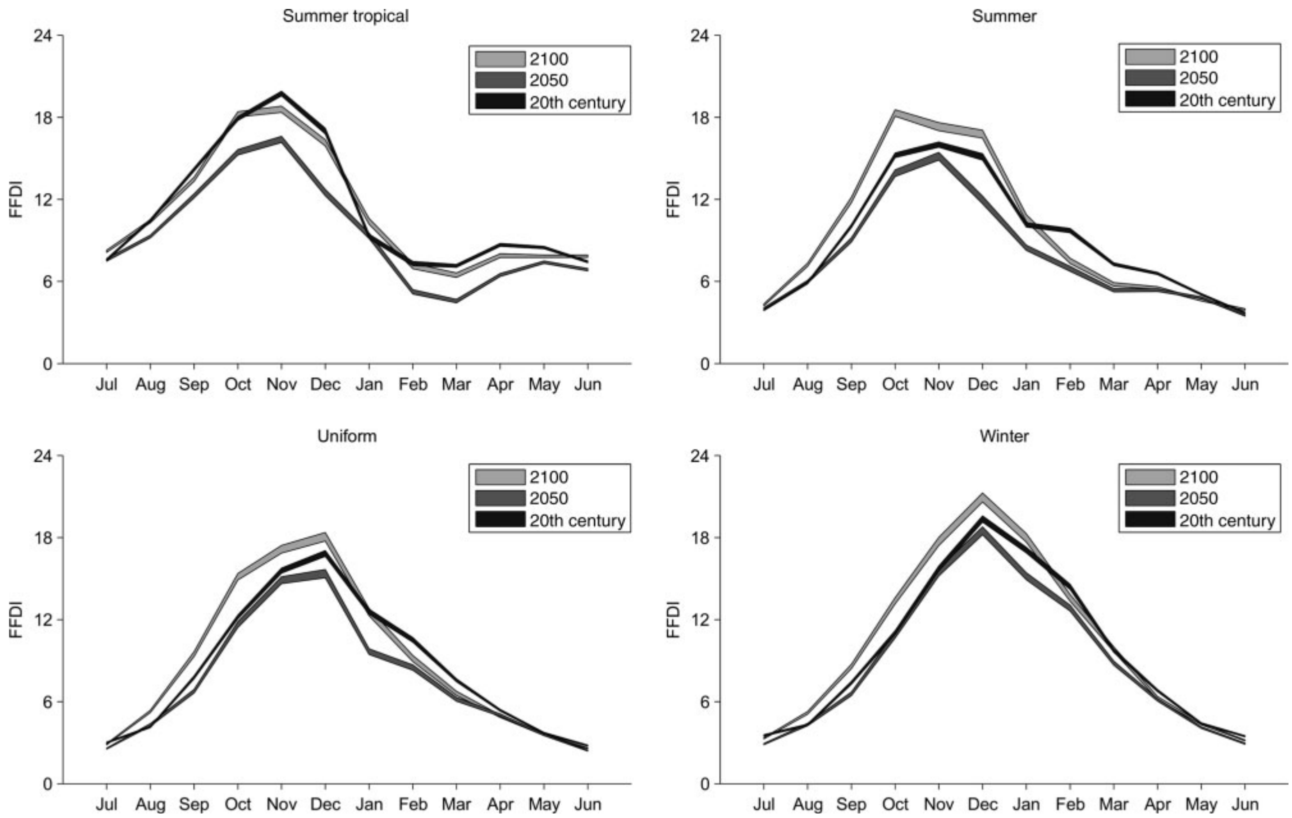

Fig. 2. Mean monthly forest fire danger index (FFDI) for each scenario from the CSIRO model in each region. The width of each line provides a 95% confidence interval for the mean estimate derived using bootstrapping (see Methods).

relative to the confidence bounds shown by the bootstrapping, these changes are likely to be significant.

We used a two-sided Kolmogorov–Smirnov test ($P = 0.05$) to provide a statistical basis on which to judge the difference between the distributions of monthly FFDI, based on all daily values, in each scenario. The null hypothesis was that there is no difference between the FFDI in 2050 or 2100 and the 20th century i.e. that the two FFDI samples are from the same population. Years are defined from July to June in order to encompass the spring–summer fire season.

There are several ways to investigate extreme values in the distribution of FFDI, including return values (annual, decadal or otherwise), percentile values (e.g. 90th, 99th) and days (per month, season or year) over some threshold. The probability of property destruction has been found to approach 1 when FFDI exceeds 40, given a fire is burning at the time (Bradstock and Gill 2001). A measure of days per month with FFDI above 40 is therefore empirically based and policy-relevant, while also permitting analysis of seasonal changes. Bradstock and Gill's study is based on data from the Sydney region of NSW, but we used a value of 40 throughout all regions as no better estimate existed at the time of the analysis. However, Blanchi *et al.* (2010) report a value of 50 may be appropriate for forested areas.

There are also several different measures of bushfire season length. State (regional) governments employ statutory definitions of fire season timing, e.g. for issuing fire permits, but State boundaries do not align well with our study areas (Fig. 1). Lucas *et al.* (2007) proposed a method of determining the start and end of the fire season by using a threshold of the average date of the first and last 3 days with FFDI over 25. This simple method yielded reasonable results for some cities but failed for others, and baseline differences between GCMs mean it is not universally applicable to our results. We therefore used an internal measure of fire seasonality: the peak months of mean and extreme FFDI as calculated above. Calculating the percentage change in mean monthly FFDI allows an analysis of seasonal changes in fire weather independent of model baselines.

Results

Mean monthly FFDI

Figs 2–5 show the bootstrapped 95% confidence interval for mean monthly FFDI by region and scenario for each model. Seasonal variation is apparent in all models, with mean monthly values reaching a maximum earlier in the ST and SU regions than in the UN and WI regions, although there are intermodel differences.

CSIRO results are shown in Fig. 2. In the ST region, mean FFDI peaks in November in each scenario. FFDI is projected to decrease throughout the year by 2050. By 2100, the projected monthly FFDI increases from the 2050 projections to be very similar to the 20th century levels. Thus, in the CSIRO model, the future mean monthly FFDI either decreases or shows negligible change relative to the 20th century simulations in the ST region.

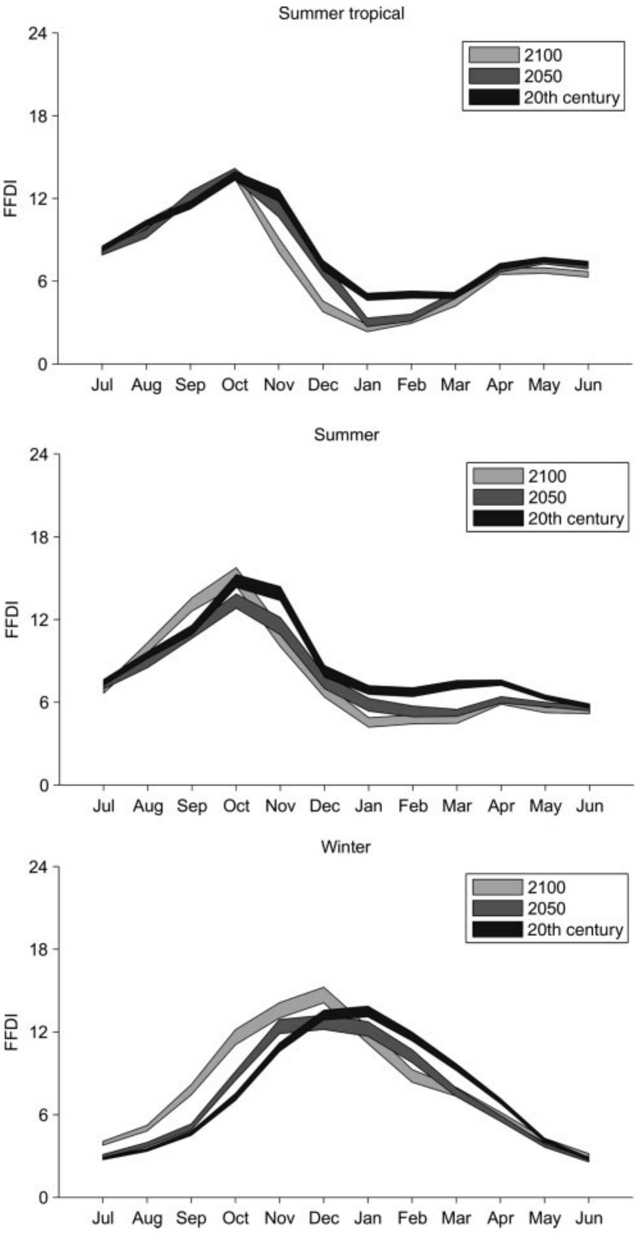

Fig. 3. As in Fig. 2 but for the ECHO-G model. No ECHO-G results were obtained for the uniform region (see Methods).

Decreases by 2050 are also projected in the SU, UN and WI regions (Fig. 2). These decreases occur predominantly later in the fire season than earlier, i.e. after the peak month. These changes follow a latitudinal gradient, with the largest decreases projected in the northernmost ST region and the smallest decreases projected in the southernmost WI region. However, in each region, by 2100, the mean FFDI is projected to either return to levels similar to 20th century (ST region) or to increase above 20th century levels (SU, UN and WI regions). Where the mean FFDI is projected to increase above 20th century levels by 2100, this increase occurs predominantly earlier in the fire season. In addition, the peak of the mean FFDI is higher by 2100 in the SU, UN and WI regions, suggesting more severe fire weather during the fire season. The combination of increased values earlier in the fire season and similar values later suggests an extension of the fire season through an earlier onset by 2100.

Results for ECHO-G are shown in Fig. 3. As with CSIRO, mean monthly FFDI is projected to decrease by 2050 in the ST, SU and WI regions (Fig. 3), mostly later in the fire season. No results were obtained from ECHO-G for the UN region, as it had no grid cells that fell entirely within this region. By 2100, mean monthly FFDI is projected to decline in the ST region (Fig. 3) through further decreases after the peak fire month. A similar pattern is evident by 2100 in the SU region (Fig. 3), although decreases in mean monthly FFDI later in the year are partly offset by increases earlier in the year. By 2100 in the WI region (Fig. 3), there is both an overall increase in monthly FFDI, particularly in the first half of the year, and a clear shift forwards in the fire season, with higher values earlier in the season and marginally lower values later. The key results from the ECHO-G model are therefore the projection of an earlier end to the fire season in all three regions. This is offset by an earlier start to the fire season in the SU region, and both an earlier start and higher overall values in the WI region by 2100.

Fig. 4 shows results for the IPSL model. Little change is projected in the ST region by 2050 and 2100 and, because most changes are within the confidence bounds estimated with bootstrapping, these are likely the result of model variability. The SU region follows a similar pattern, but with a more marked increase in mean FFDI early in the fire season by 2100 (Fig. 4). Large increases in FFDI are projected throughout the year by 2050 and 2100 in the UN and WI regions (Fig. 4), with the largest increases occurring in the WI region. These changes are large relative to the confidence bounds estimated via bootstrapping.

MRI results are shown in Fig. 5. In the ST and SU regions, monthly FFDI changes little during the peak fire danger months, and those changes that are projected fall largely within the confidence bounds estimated via bootstrapping. By 2050 and 2100 in the UN and WI regions (Fig. 5), there is an increase in mean FFDI during the peak fire months and earlier in the season, suggesting a longer fire season with more severe fire weather. These are clearly different from the 20th century projections and are clearly differentiated in the bootstrapped confidence bounds.

The monthly distribution of FFDI in 2050 and 2100 was significantly different from the 20th century distribution in most of cases ($P < 0.05$ for 96 of 96 CSIRO, 92 of 96 IPSL, 58 of 72 ECHO-G and 74 of 96 MRI comparisons). Although they represent a small fraction overall, cases where the distributions were not found to be significantly different are biased towards 2050–20th century comparisons (65% of not-significant results) and ST and SU regions (combined 70% of not-significant results).

Considering all models and both 2050 and 2100 timeframes, mean monthly FFDI is projected to decrease or remain similar to 20th century levels in the ST region, but increase in the UN and WI regions, with changes in the SU region falling in between. The strongest increases in FFDI occur early in the season, suggesting an extended fire season through an earlier start in the UN and WI regions. Despite these similarities, models vary considerably in the magnitude of FFDI. MRI (Fig. 5) has the consistently highest mean FFDI values, peaking between 20 and

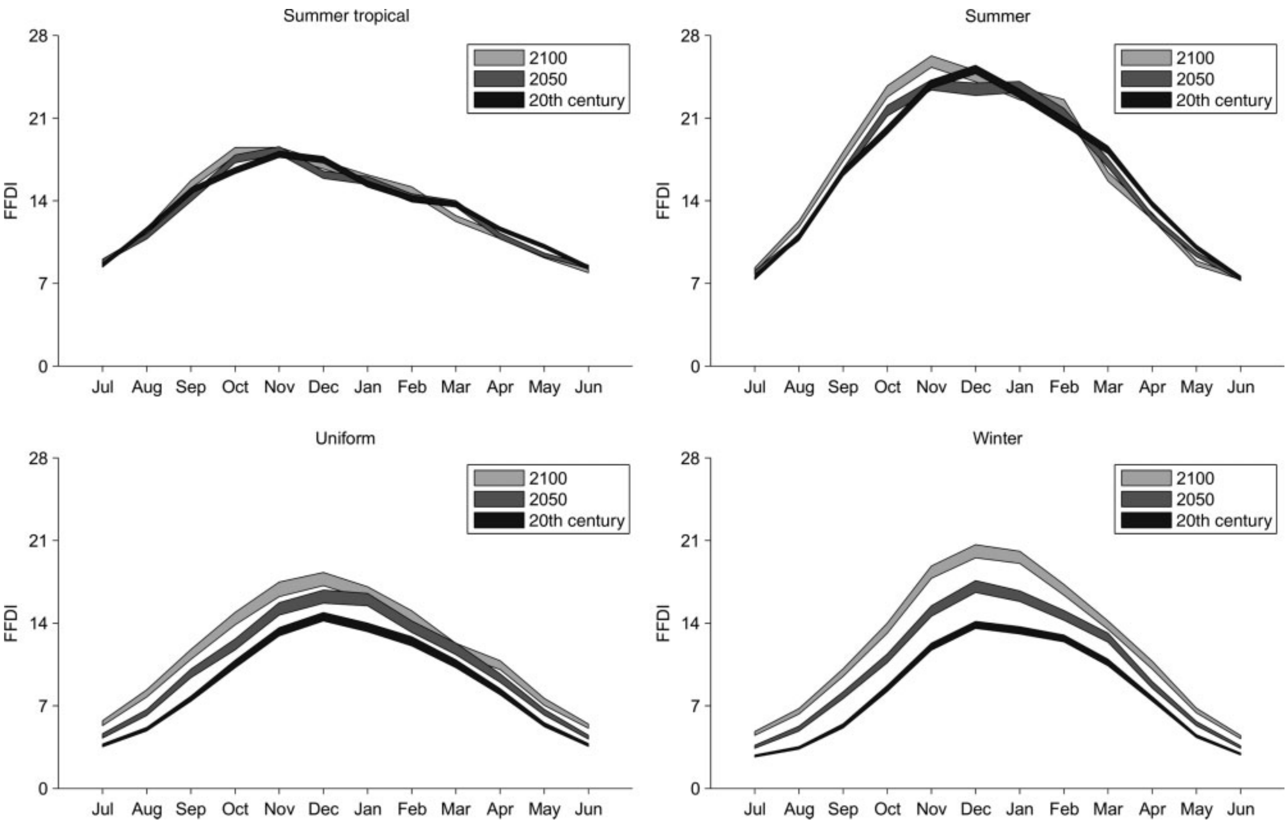

Fig. 4. As in Fig. 2 but for the IPSL model.

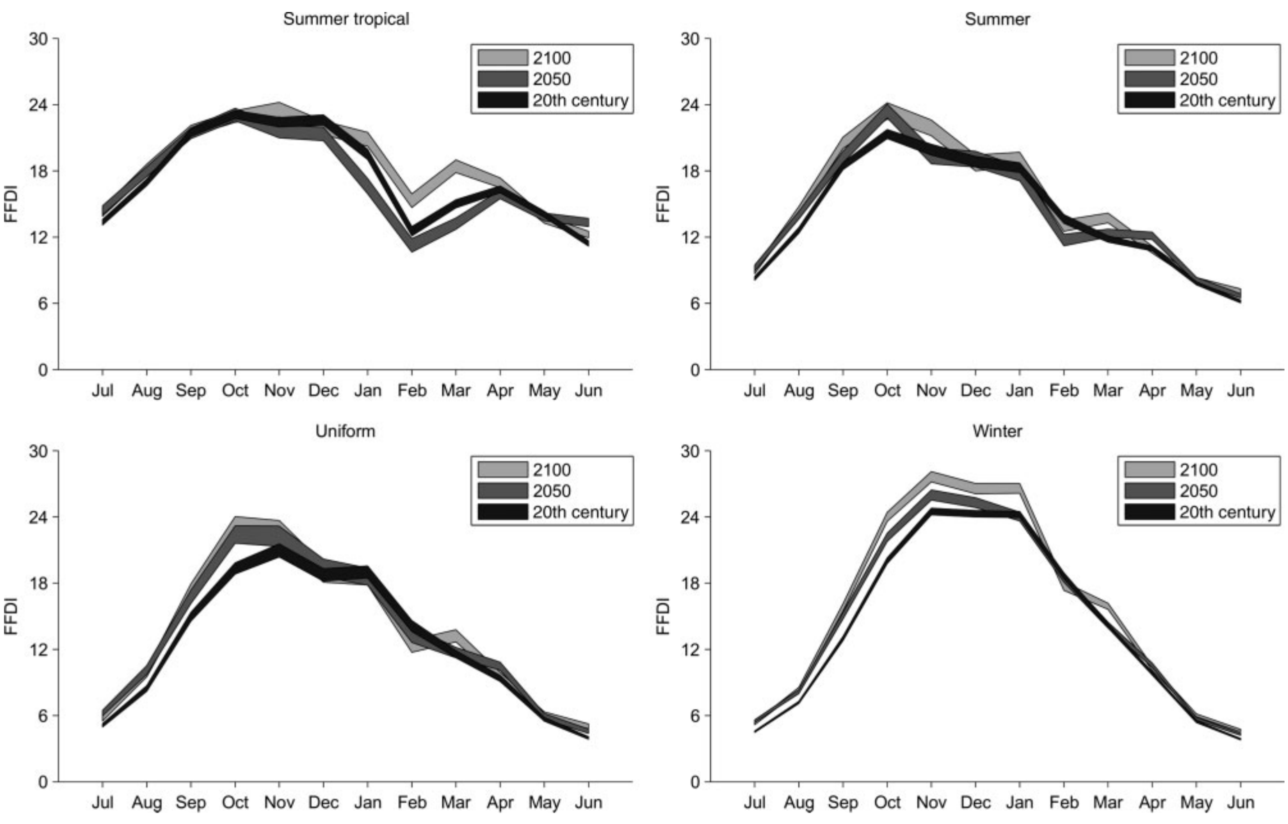

Fig. 5. As in Fig. 2 but for the MRI model.

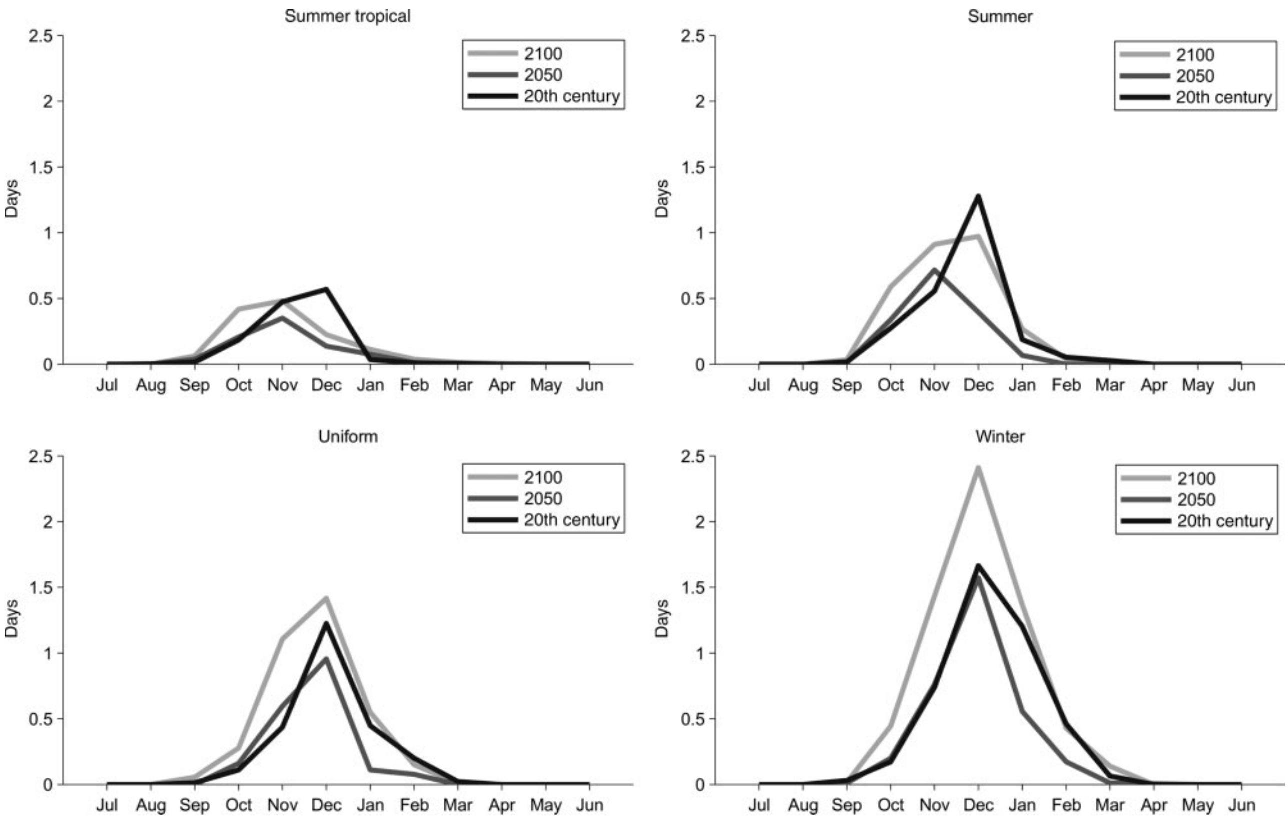

Fig. 6. Days per month with forest fire danger index (FFDI) above 40 for each scenario from the CSIRO model in each region.

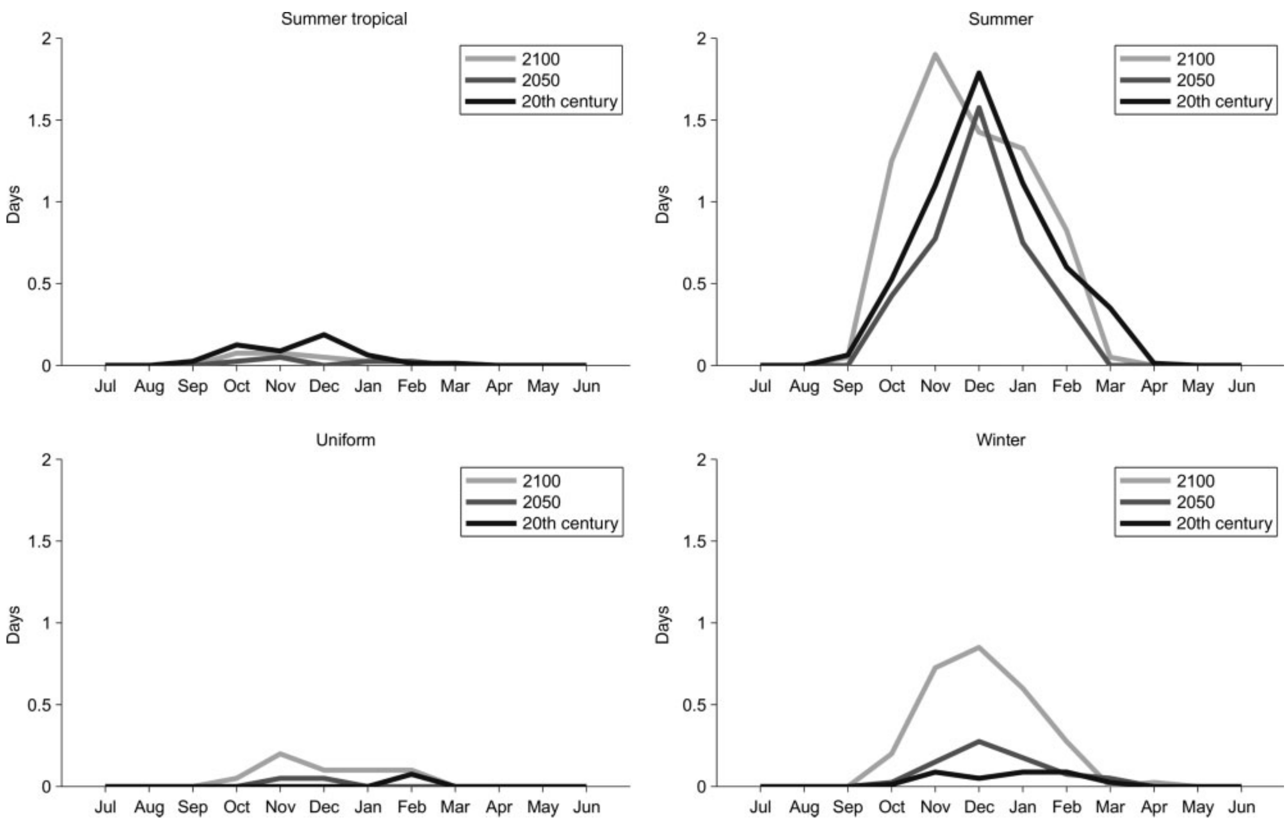

Fig. 7. As in Fig. 6 but for the IPSL model.

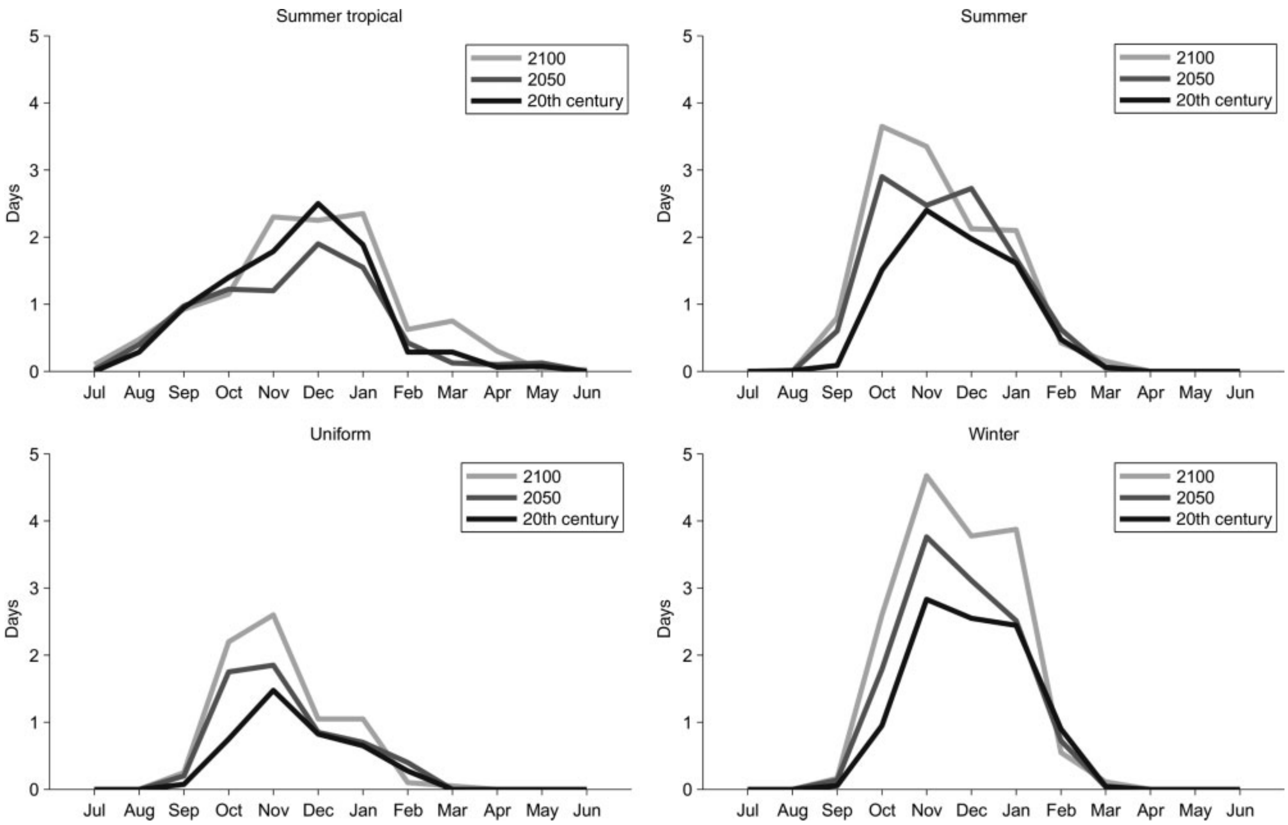

Fig. 8. As in Fig. 6 but for the MRI model.

30 depending on the region and scenario. ECHO-G (Fig. 3) monthly FFDI values peak at ~12–15, with the other two GCMs falling in between. The models contributing the least (ECHO-G; Fig. 3) and most (CSIRO; Fig. 2) amount of data have the broadest and narrowest confidence intervals respectively.

Extreme FFDI values

The number of days per month with FFDI above 40 is shown in Figs 6–8. ECHO-G results are omitted from the figures, as there were very few days over 40 in any of the ECHO-G simulations (ranging from none in the ST region to 0.4 in the SU region in October 2100). As anticipated from Figs 2–5, there is a seasonal variation in the number of days when FFDI exceeds 40.

CSIRO results are shown in Fig. 6. In the ST and SU regions, the number of days with FFDI above 40 is projected to decrease (2050) or change little (2100). However, the seasonality changes in both regions by 2100, with a clear earlier peak in ST and an earlier and longer peak in SU. Extreme FFDI is projected to decrease or remain similar to 20th century levels in the UN and WI regions by 2050 (Fig. 6), but to increase strongly by 2100 with a more intense peak and a full-month-longer period of activity. Thus, in all regions, the largest increases in days per month over 40 occur earlier in the fire season, suggesting an earlier to start to extreme fire weather.

Fig. 7 shows results for the IPSL model. Few months have days with FFDI over 40 in the ST and UN regions during any time period (Fig. 7). A decrease is projected in days above 40 in the SU region (Fig. 7) by 2050 but by 2100, a large increase over 20th century levels is projected, predominantly early in the fire season, such that the point at which the number of days of FFDI above 40 becomes non-negligible moves a full month earlier in the season. A strong increase is projected in the WI region (Fig. 7) by 2100 such that 3 to 4 months experience more than 1 day over 40 FFDI every second year. At current levels in this region, days above 40 are projected at most once every 10 years.

Results from the MRI model are shown in Fig. 8. Marked increases in days per month with FFDI above 40 are expected in all regions except ST. The WI region records the largest increases of any region in days over 40. These increases are skewed towards the early part of the fire season and are larger by 2100 than 2050.

Overall, the number of days per month with FFDI above 40 is almost always higher in 2100, and often in 2050, than in the 20th century, regardless of whether the mean monthly value follows the same trend. The risk of such days is projected to either change little or decrease in the ST region. Results are equivocal for the SU region, whereas large increases are projected in the UN and WI regions, particularly by 2100. As with mean monthly FFDI, differing magnitudes lie behind these common trends. Apart from differences in the number of days, models disagree on regional variation in extreme FFDI values. MRI (Fig. 9) and CSIRO (Fig. 7) ascribe the highest number of days per month with FFDI above 40 to the WI region, but the SU region has this trait in IPSL projections (Fig. 8). At the other end of the spectrum, the ST region has the least days per month over

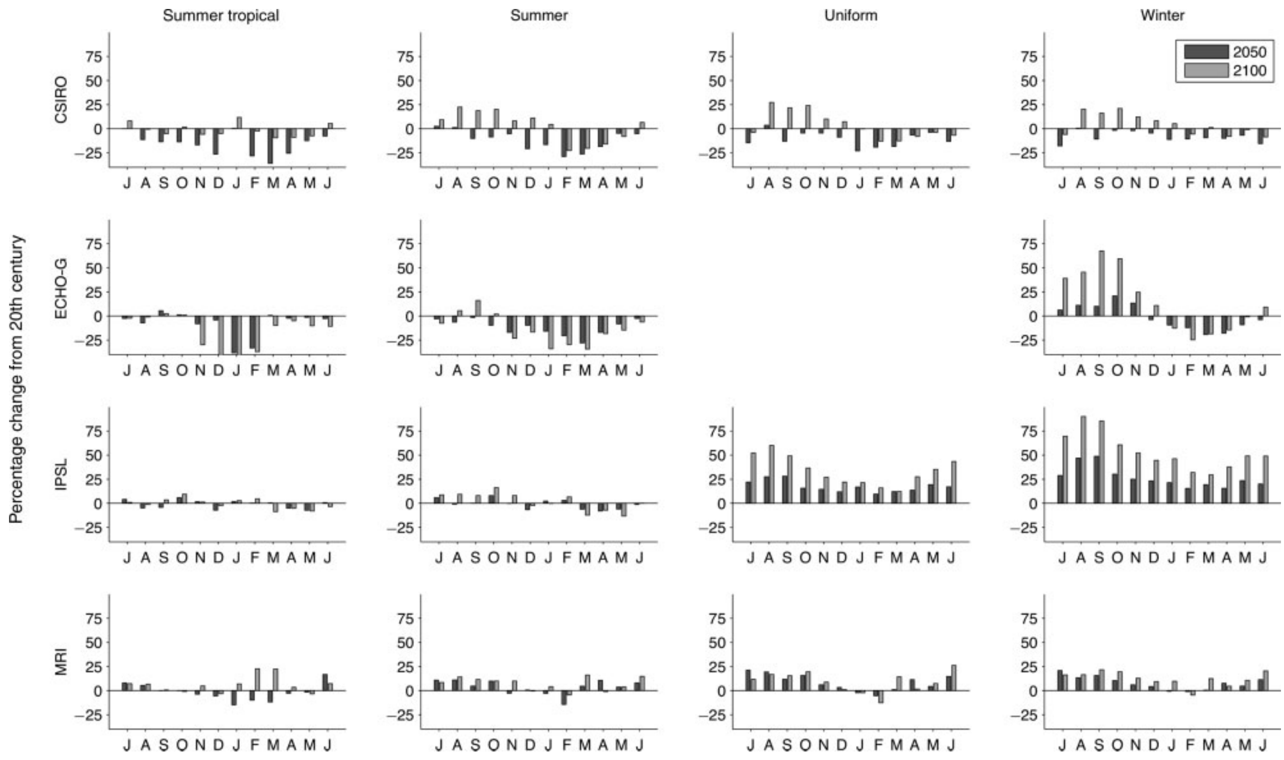

Fig. 9. Percentage change in mean monthly forest fire danger index (FFDI) by 2050 and 2100 for each region (columns) and each model (rows).

40 as projected by CSIRO, IPSL puts the ST and UN regions both at close to no days above 40, whereas MRI ranks the UN region as the least likely to have days above 40.

Fire seasonality

Percentage changes in mean monthly FFDI for each model, region and scenario are shown in Fig. 9. In the ST (first column) region, CSIRO and ECHO-G project decreases in FFDI in the peak fire months. The decreases are commonly ~25%. However, IPSL projects negligible change and MRI projects small changes of either sign. In general, therefore, the projected change in FFDI in ST is most likely a decrease (there are only isolated months with an increase) that is relatively small in magnitude. The SU region displays evidence of a shift in fire seasonality. There are increases in FFDI projected by all models early in the fire season and decreases later in the year according to CSIRO, ECHO-G and IPSL. The decrease later in the year is clear in CSIRO and ECHO-G and exceeds 25% in some months. Overall, however, changes are negligible in IPSL and MRI in terms of the magnitude of the percentage change, and the changes in SU remain inconsistent.

The UN region (third column) and WI (fourth column) regions show stronger evidence of a consistent result. In UN, CSIRO shows increases in FFDI early in the season and decreases later in the season. IPSL projects strong (10 to >50%) increases in FFDI throughout the year. MRI projects increases (~25%) early and late in the first season. In this region, there is therefore a strong indication of a more intense early fire season, which may be longer (IPSL, MRI) or merely earlier (CSIRO). Finally, in the WI region, all models project an earlier fire season, which is projected to be somewhat more intense (~25%, CSIRO, MRI) or much more intense, particularly by 2100 (50 to >75%, ECHO-G, IPSL). There is a dramatic difference in projection from the ECHO-G model (earlier and stronger peak, lower FFDI thereafter) compared with the IPSL model (much higher throughout the year).

Discussion

These results identify changes in fire weather along a roughly latitudinal gradient across eastern Australia (Fig. 10). In the tropical far north, where rainfall is summer-dominated, mean and extreme values of FFDI and the fire season length are projected to decrease by 2050. These statistics are projected to return to levels similar to those of the 21st century by 2100. A small decrease in risk from fire weather is projected for 2050 in the summer rainfall region, immediately south of the summer tropical region. This pattern is projected to reverse by 2100, with a small increase projected, as well as an earlier start to the fire season but no clear trend in duration overall. Thus, there is little change in the nature of fire weather in the northernmost regions and where changes do occur, they are unlikely to lead to significant changes in management policies designed to reduce the effect of fire.

Major increases in fire weather are projected in the southernmost regions of uniform (south-east NSW) and winter (Victoria, south-west NSW) rainfall. Projections of large-scale changes in mean and extreme FFDI are not consistent enough between models to provide unequivocal conclusions for 2050, although

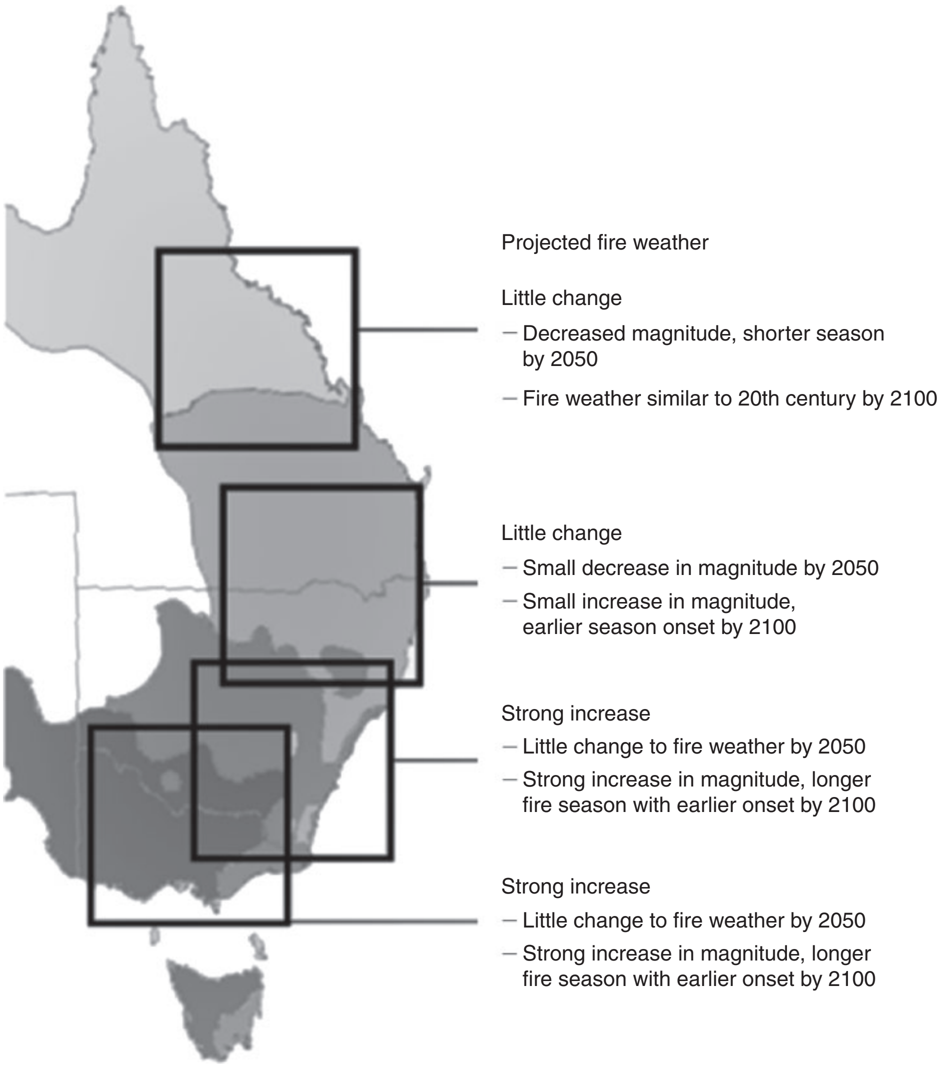

Fig. 10. Summary of effects of climate change on fire weather by 2050 and 2100 in each region.

there is some indication of an earlier fire season. However, by 2100, every model simulates both an earlier fire season and more severe fire weather. These changes are almost always large relative to the confidence bounds represented by bootstrapping. It should be noted that a value of 1 or 2 days per month with FFDI above 40 should not be interpreted as insignificant; this is a measure that predicts near-certain property losses should a fire occur. Thus the clearest and largest increases in risk from fire weather are projected in the regions where Australia's worst bushfires have occurred.

What is driving these changes in fire weather? An analysis of the variables from which FFDI is constructed shows that the biggest increases in FFDI (e.g. by 2100 in the Uniform and Winter regions) are most consistently driven by temperature increases. All models project increased temperature, regardless of region. Depending on the model, changes in humidity (IPSL, MRI) and drought factor (via reduced precipitation; CSIRO, IPSL) couple with temperature to increase FFDI in these regions. Conversely the decreases in FFDI reported here are chiefly the result of increased relative humidity. CSIRO and IPSL project increases in humidity in all regions and time-frames. The drivers of changes in fire seasonality are similar. By 2100 in the Winter region, temperature increases occur across the year but there is also a pronounced spike (dip) in drought factor (humidity) early in the season, depending on the model. Changes in wind speed contribute very little to any of the FFDI changes reported here.

These results are consistent with earlier projections and analyses that focussed on different models, different regions or different measures. For example in southeast Australia, Lucas *et al*. (2007) project more intense fire seasons, starting earlier and ending slightly later, based on projected changes in seasonal median FFDI by 2020 and 2050. In an analysis that extended beyond fire weather to the other drivers of Australian fire regimes – biomass growth, availability to burn and ignition, Bradstock (2010) concluded that future change may be limited in the tropics, but that fire activity may increase in temperate forests in the south of the country. Bradstock also suggested that increasing dryness may lead to a decrease in fire activity in dry woodlands, which occupy much of the country, particularly in between the latitudinal extremes of the tropics and the temperate south.

Although we have examined only one driver of fire regimes here, it is clear that climate change could have significant effects on fire regimes. Changes to fire regimes could have flow-on effects on biodiversity and human systems, although these effects will depend in part on whether projected changes are beyond the bounds of natural variability (which may not coincide with the model 'natural variability baseline' of 1961–2000). In the case of Australia's built environment, there is no sign yet that the annual probability of building destruction from bushfire has increased over the last century, after adjusting for changes in population, wealth and inflation (McAneney *et al*. 2009). Our results suggest that if such changes are to happen, regions of uniform and winter rainfall are the most likely locations to identify the signal.

Our results suggest that changes in the frequency of fires on an annual or fire-season basis will not be detectable (in a statistical sense) from the natural variability for at least many decades. However, it is possible that observed warming is already moving the fire season forward in ways that could be detectable. Le Goff *et al*. (2009) projected changes in monthly fire risk in eastern Canada, finding that by 2100, the fire season peak was projected to move later in the season. If the North American fire season moves later, and the Australian season moves earlier, changes in strategies to manage fire risk will be required. NSW and Victoria currently rent firefighting equipment from North America, while firefighters from both hemispheres regularly work abroad during their own off season. Thus any significant overlap in southern and northern hemisphere fire seasons would have direct effects on the sharing of firefighting resources. An earlier or longer fire season could also have implications for hazard reduction burning.

Several caveats apply to these findings. Only daily average (rather than 1500 hours) values of relative humidity and wind speed were available. Despite significant agreement between models in the regional response of fire weather to climate change, baseline differences between models mean the absolute values of FFDI vary considerably. For instance, CSIRO and ECHO-G are much 'wetter' models than IPSL and MRI, which in turn tend to be hotter. Nevertheless, bias is minimised through the use of skill selection and the direct use of GCM output (rather than adjusted historical time series) provides an estimate of the uncertainty and variability in climate that is known to exist. Uncertainties also exist about the capacity of GCMs to capture key components of the Australian climate. For example, there is a strong relationship between El Niño–Southern Oscillation and fire risk (Williams and Karoly 1999; Verdon *et al*. 2004), yet GCMs vary widely in their ability to simulate this mode of climate variability (Randall *et al*. 2007; Guilyardi *et al*. 2009).

Despite these uncertainties, our results taken in the context of earlier work point to CO_2-induced warming having the clear potential to alter fire regimes across eastern Australia. These results do not translate directly into probability of the incidence of fires, nor can they be applied to individual locations within the regions studied here. FFDI is a common proxy for fire weather, but only peripherally references fuel (through the drought factor; a standard fuel availability of $12.5\,\mathrm{t\,ha^{-1}}$ is assumed) and does not take into account ignitions, terrain or human behaviour. Nevertheless, these results are representative of the kind of changes in fire-weather risk likely to occur in these different regions under the (relatively conservative) A2 emissions scenario. A downscaled model, evaluated against historical FFDI and reanalysis datasets would address several limitations of this study and provide the next generation of high-resolution data needed for impact assessment studies.

Acknowledgements

We acknowledge the modelling groups, the Program for Climate Model Diagnosis and Intercomparison (PCMDI) and the WCRP's Working Group on Coupled Modelling (WGCM) for their roles in making available the WRCP CMIP3 multimodel dataset. Support of this dataset is provided by the Office of Science, US Department of Energy. Ross Bradstock provided invaluable comments on the manuscript, as did three anonymous reviewers. Input from colleagues is gratefully acknowledged, particularly Howard McNeil, Hugh Jones and Matt Adams.

References

Alexander LV, Arblaster JM (2009) Assessing trends in observed and modelled climate extremes over Australia in relation to future projections. *International Journal of Climatology* **29**, 417–435. doi:10.1002/JOC.1730

Australian Bureau of Meteorology (2005*a*) Australian climate zones – major classification groups (based on the Köppen classification). Available at http://www.bom.gov.au/climate/environ/other/kpn_group.shtml [Verified 28 April 2010]

Australian Bureau of Meteorology (2005*b*) Major seasonal rainfall zones of Australia. Available at http://www.bom.gov.au/jsp/ncc/climate_averages/climate-classifications/index.jsp?maptype=seasgrpb#maps [Verified 28 April 2010]

Beer T, Williams A (1995) Estimating Australian forest fire danger under conditions of doubled carbon dioxide concentrations. *Climatic Change* **29**, 169–188. doi:10.1007/BF01094015

Beeton RJS, Buckley KI, Jones GJ, Morgan D, Reichelt RE, Trewin D (2006) Australia state of the environment. Department of the Environment and Heritage, Independent report to the Australian Government Minister for the Environment and Heritage. (Canberra)

Blanchi R, Lucas C, Leonard F, Finkele K (2010) Meteorological conditions and wildfire-related houseloss in Australia. *International Journal of Wildland Fire* **19**, 914–926. doi:10.1071/WF08175

Bradstock RA (2010) A biogeographic model of fire regimes in Australia: current and future implications. *Global Ecology and Biogeography* **19**, 145–158. doi:10.1111/J.1466-8238.2009.00512.X

Bradstock RA, Gill AM (2001) Living with fire and biodiversity and the urban edge: in search of a sustainable solution to the human protection problem. *Journal of Mediterranean Ecology* **2**, 179–195.

Bradstock RA, Cohn JS, Gill AM, Bedward M, Lucas C (2009) Prediction of the probability of large fires in the Sydney region of south-eastern Australia using fire weather. *International Journal of Wildland Fire* **18**, 932–943. doi:10.1071/WF08133

Cary GJ (2002) Importance of changing climate for fire regimes in Australia. In 'Flammable Australia – the Fire Regimes and Biodiversity of a Continent'. (Eds R Bradstock, J Williams, M Gill) pp. 27–46. (Cambridge University Press: Cambridge, UK)

Cary GJ, Banks JCG (1999) Fire regime sensitivity to global climate change: an Australian perspective. In 'Biomass Burning and its Inter-Relationships with the Climate System'. (Eds J Innes, M Beniston, M Verstraete) pp. 233–246. (Kluwer: Dordrecht, the Netherlands)

Finkele K, Mills GA, Beard G, Jones DA (2006) National gridded drought factors and comparison of two soil moisture deficit formulations used in prediction of forest fire danger index in Australia. *Australian Meteorological Magazine* **55**, 183–197.

Flannigan MD, Krawchuk MA, De Groot WJ, Wotton BM, Gowman LM (2009) Implications of changing climate for global wildland fire. *International Journal of Wildland Fire* **18**, 483–507. doi:10.1071/WF08187

Griffiths D (1999) Improved formula for the drought factor in McArthur's Forest Fire Danger Meter. *Australian Forestry* **62**, 202–206.

Guilyardi E, Wittenberg A, Fedorov A, Collins M, Wang CZ, Capotondi A, Van Oldenborgh GJ, Stockdale T (2009) Understanding El Nino in ocean–atmosphere general circulation models progress and challenges. *Bulletin of the American Meteorological Society* **90**, 325–340. doi:10.1175/2008BAMS2387.1

Hasson AEA, Mills GA, Timbal B, Walsh K (2009) Assessing the impact of climate change on extreme fire weather events over south-eastern Australia. *Climate Research* **39**, 159–172. doi:10.3354/CR00817

IPCC (2007) Summary for policymakers. In 'Climate Change 2007: the Physical Science Basis. Contribution of Working Group I to the Fourth Assessment Report of the Intergovernmental Panel on Climate Change'. (Eds S Solomon, D Qin, M Manning, Z Chen, M Marquis, K Averyt, M Tignor, H Miller) pp. 1–18. (Cambridge University Press: Cambridge, UK)

Keetch JJ, Byram GM (1968) A drought index for forest fire control. USDA Forest Service, Research Paper SE-38. (Ashville, NC)

Le Goff H, Flannigan MD, Bergeron Y (2009) Potential changes in monthly fire risk in the eastern Canadian boreal forest under future climate change. *Canadian Journal of Forest Research* **39**, 2369–2380. doi:10.1139/X09-153

Le Quéré C, Raupach MR, Canadell JG, Marland G, Bopp L, Ciais P, Conway TJ, Doney SC, Feely RA, Foster P, Friedlingstein P, Gurney K, Houghton RA, House JI, Huntingford C, Levy PE, Lomas MR, Majkut J, Metzl N, Ometto JP, Peters GP, Prentice IC, Randerson JT, Running SW, Sarmiento JL, Schuster U, Sitch S, Takahashi T, Viovy N, van der Werf GR, Woodward FI (2009) Trends in the sources and sinks of carbon dioxide. *Nature Geoscience* **2**, 831–836. doi:10.1038/NGEO689

Lucas C, Hennessy K, Mills G, Bathols J (2007) Bushfire weather in southeast Australia: recent trends and projected climate change impacts. Bushfire Cooperative Research Centre and CSIRO Marine and Atmospheric Research, Consultancy Report prepared for The Climate Institute of Australia. (Melbourne)

Luke R, McArthur A (1978) 'Bushfires in Australia.' (Australian Government Publishing Service: Canberra)

McAneney J, Chen K, Pitman A (2009) 100 years of Australian bushfire property losses: is the risk significant and is it increasing? *Journal of Environmental Management* **90**, 2819–2822. doi:10.1016/J.JENVMAN.2009.03.013

Nakicenovic N, Alcamo J, Davis G, de Vries B, Fenhann J, Gaffin S, Gregory K, Grübler A, Jung T-Y, Kram T, La Rovere EL, Michaelis L, Mori S, Morita T, Pepper W, Pitcher H, Price L, Riahi K, Roehrl A, Rogner HH, Sankovski A, Schlesinger M, Shukla P, Smith S, Swart R, van Rooijen S, Victor N, Dadi Z (2000) 'IPCC Special Report on Emissions Scenarios.' (Cambridge University Press: Cambridge, UK)

Noble IR, Barry GAV, Gill AM (1980) McArthur's fire danger meters expressed as equations. *Australian Journal of Ecology* **5**, 201–203. doi:10.1111/J.1442-9993.1980.TB01243.X

Perkins SE, Pitman AJ, Holbrook NJ, McAneney J (2007) Evaluation of the AR4 climate models' simulated daily maximum temperature, minimum temperature, and precipitation over Australia using probability density functions. *Journal of Climate* **20**, 4356–4376. doi:10.1175/JCLI4253.1

Pielke RA, Cotton WR, Walko RL, Tremback CG, Lyons WA, Grasso LD, Nicholls ME, Moran MD, Wesley DA, Lee TJ, Copeland JH (1992) A comprehensive meteorological modeling system – RAMS. *Meteorology and Atmospheric Physics* **49**, 69–91. doi:10.1007/BF01025401

Pitman AJ, Narisma GT, McAneney J (2007) The impact of climate change on the risk of forest and grassland fires in Australia. *Climatic Change* **84**, 383–401. doi:10.1007/S10584-007-9243-6

Randall DA, Wood RA, Bony S, Colman R, Fichefet T, Fyfe J, Kattsov V, Pitman A, Shukla J, Srinivasan J, Stouffer RJ, Sumi A, Taylor KE (2007) Climate models and their evaluation. In 'Climate Change 2007: the Physical Science Basis. Contribution of Working Group I to the Fourth Assessment Report of the Intergovernmental Panel on Climate Change, 2007'. (Eds S Solomon, D Qin, M Manning, Z Chen, M Marquis, K Averyt, M Tignor, HL Miller) pp. 589–662. (Cambridge University Press: Cambridge, UK)

Verdon DC, Kiem AS, Franks SW (2004) Multi-decadal variability of forest fire risk – eastern Australia. *International Journal of Wildland Fire* **13**, 165–171. doi:10.1071/WF03034

Williams AAJ, Karoly DJ (1999) Extreme fire weather in Australia and the impact of the El Niño-Southern Oscillation. *Australian Meteorological Magazine* **48**, 15–22.

Williams AAJ, Karoly DJ, Tapper N (2001) The sensitivity of Australian fire danger to climate change. *Climatic Change* **49**, 171–191. doi:10.1023/A:1010706116176

Manuscript received 8 July 2010, accepted 25 October 2010

Chapter 4 Summary

Projections of fire weather from global climate models

The use of skill selected GCMs points to future changes in FFDI in eastern Australian that vary along a clear latitudinal gradient. In summer rainfall-dominated tropical northeast Australia, mean and extreme FFDI are projected to decrease or remain close to 20th century levels. In the uniform and winter rainfall regions, which occupy southeast continental Australia, FFDI is projected to increase strongly by 2100. Projections fall between these two extremes for the summer rainfall region, which lies between the uniform and summer tropical rainfall zones. Based on these changes in fire weather, the fire season is projected to start earlier in the uniform and winter rainfall regions, potentially leading to a longer overall fire season.

These and other results from global climate models point to the potential for significant increases in fire weather conditions in Australia. However, there is a strong demand from fire management agencies for finer resolution information than that available from global climate models. Such information is more suited to assessing impacts and planning adaptation at the scale at which they operate. The next chapter aims to lay the foundation for finer resolution projections by evaluating the ability of a regional climate model to accurately downscale fire weather from a global climate model.

Chapter 5 Overview

Evaluation of a regional climate model fire weather simulation

The climate system is a global phenomenon, and the global climate models developed to represent it do well at continental scales and above (Flato et al. 2013). However, it is the local and regional climate which affects our daily lives, and it is at this level that adaptation to climate change occurs. The ability of GCMs to provide information about regional variations in climate is limited by their resolution and coarse representation of important regional climate drivers such as sub-continental scale topography and offshore processes.

There is therefore a large demand, driven particularly by end users, for the conversion of information from global models to a regional level, a process known as downscaling. Dynamical downscaling with regional climate models (RCMs) overcomes many of the limitations of GCMs in providing information relevant to regional adaptation planning. Since they are built on physical principles, dynamical RCMs allow for changes in the existing relationship between weather variables or climate drivers. At the time of writing of Chapter 5, almost all existing Australian (and most global) fire weather projection studies were based on GCMs. A single study (Lucas et al., 2007) used an (atmosphere only) RCM. A clear research direction is therefore to undertake high resolution modelling of fire weather. A useful precursor to any such future modelling is an evaluation of the ability of the RCM to simulate observed fire weather conditions; this is the aim of Chapter 5.

The work reported here has been published in the peer reviewed literature and is reproduced exactly as published:

Clarke H, Evans JP, Pitman AJ (2013) Fire weather simulation skill by the Weather Research and Forecasting (WRF) model over southeast Australia from 1985 to 2009. International Journal of Wildland Fire, 22, 739-756. DOI: 10.1071/WF12048

Author contributions

I led this project. The project was conceived by Jason Evans (JE; my associate PhD supervisor), Andy Pitman and myself. JE provided the WRF data. I was jointly responsible for experimental design with JE and AP. I conducted the analysis and prepared the figures, incorporating feedback from JE and AP. I drafted the paper and revised it based on comments from JE and AP. I led the revisions following external review, preparing a response and incorporating contributions from JE and AP.

Errata

An examiner noted the following errors in the published paper:

p743 “Fig 1b” should read “Fig 1”

p753 “in the north-east of the domain” should read “in the north-west of the domain”

CSIRO PUBLISHING

International Journal of Wildland Fire **2013**, *22*, 739–756
http://dx.doi.org/10.1071/WF12048

Fire weather simulation skill by the Weather Research and Forecasting (WRF) model over south-east Australia from 1985 to 2009

Hamish Clarke[A,B,D], *Jason P. Evans*[A] *and Andrew J. Pitman*[C]

[A]Climate Change Research Centre, University of New South Wales, Sydney, NSW 2052, Australia.
[B]Climate and Atmospheric Science Branch, NSW Office of Environment and Heritage, PO Box A290, Sydney South, NSW 1232, Australia.
[C]ARC Centre of Excellence for Climate System Science, University of New South Wales, Sydney, NSW 2052, Australia.
[D]Corresponding author. Email: h.clarke@student.unsw.edu.au

Abstract. The fire weather of south-east Australia from 1985 to 2009 has been simulated using the Weather Research and Forecasting (WRF) model. The US National Oceanic and Atmospheric Administration Centers for Environmental Prediction and National Center for Atmospheric Research reanalysis supplied the lateral boundary conditions and initial conditions. The model simulated climate and the reanalysis were evaluated against station-based observations of the McArthur Forest Fire Danger Index (FFDI) using probability density function skill scores, annual cumulative FFDI and days per year with FFDI above 50. WRF simulated the main features of the FFDI distribution and its spatial variation, with an overall positive bias. Errors in average FFDI were caused mostly by errors in the ability of WRF to simulate relative humidity. In contrast, errors in extreme FFDI values were driven mainly by WRF errors in wind speed simulation. However, in both cases the quality of the observed data is difficult to ascertain. WRF run with 50-km grid spacing did not consistently improve upon the reanalysis statistics. Decreasing the grid spacing to 10 km led to fire weather that was generally closer to observations than the reanalysis across the full range of evaluation metrics used here. This suggests it is a very useful tool for modelling fire weather over the entire landscape of south-east Australia.

Additional keywords: bush fire, McArthur Forest Fire Danger Index (FFDI), model evaluation, model grid spacing, reanalysis, regional climate model (RCM), wildland fire.

Received 28 March 2012, accepted 3 January 2013, published online 13 May 2013

Introduction

In order for wildland fire to occur there must be: sufficient biomass that is dry enough to burn, the presence of ignitions and weather conditions conducive to burning. Elements of weather relevant to wildland fire risk include temperature, humidity, wind speed, atmospheric stability and the passage of wind changes (Parkyn *et al.* 2010). Fire regimes can be defined in part by the relative importance of these four drivers in limiting overall wildland fire incidence. For instance, in some ecosystems fire is limited primarily by the amount of fuel whereas in others a combination of fuel availability and ambient weather is the primary limiting factor (Archibald *et al.* 2009; Bradstock 2010).

Climate change is expected to alter global fire regimes significantly (Flannigan *et al.* 2009; Krawchuk *et al.* 2009; Bradstock 2010). Owing to the central role of coupled climate models in projecting future climate, studies of the effects of increased atmospheric carbon dioxide on wildland fire have tended to focus on fire weather, which is more directly linked to changes in the prevailing climate than are other drivers.

Global climate models model perform their task well (Randall *et al.* 2007), but their ability to provide information about regional variations in climate is limited by their coarse resolution and their representation of important regional climate drivers such as sub-continental scale topography (e.g. the Great Dividing Range) and offshore processes (e.g. the East Australian Current) (Meehl *et al.* 2007). Although the climate system is a global phenomenon, it is the local and regional climate that affects our immediate environment. Dynamical downscaling with regional climate models (RCMs) overcomes many of the limitations of global climate models in providing information relevant to regional adaptation planning (Evans *et al.* 2012*a*). They can operate at much finer spatial scales and contain additional information about drivers of regional climate including more detailed topography and improved representation of important regional land–atmosphere phenomena (Pitman *et al.*

2012) and feedback mechanisms (Evans *et al.* 2011). Because they are built on physical principles, dynamical RCMs allow for changes in the existing relationship between weather variables or climate drivers.

Given their use in downscaling fire weather projections, the ability of RCMs to simulate observed climate is of great interest. The Weather Research and Forecasting (WRF) model is an open source atmospheric simulation system that can be used as an RCM. WRF has been shown to skilfully reproduce the observed spatial patterns of surface temperature and precipitation (Evans and McCabe 2010) and the diurnal rainfall cycle (Evans and Westra 2012) from the late 20th to early 21st century in south-east Australia. The simulation described in Evans and McCabe (2010) included a positive temperature bias of ~1°C and a precipitation bias that varied in sign depending on the region and season. Mölders (2008, 2010) also examined the performance of WRF and found it to be well suited for fire weather prediction in Alaska, based on its ability to produce 1–5-day forecasts of two fire weather indices, during June 2005. Mölders (2008) found that WRF underestimated precipitation on average and slightly overestimated wind speed, but adequately captured the temporal evolution of these variables as well as temperature and relative humidity over the study period. Shimada and Ohsawa (2011) and Shimada *et al.* (2011) also reported a positive bias in wind speed from WRF, this time over Japan, in a simulation for the year 2005. WRF's ability to simulate fire weather has not yet been evaluated in Australia.

The McArthur Forest Fire Danger Index (FFDI) is a function of temperature, precipitation, relative humidity and wind speed and was derived in the late 1960s to relate weather conditions to expected fire behaviour and rate of spread (McArthur 1967; Luke and McArthur 1978). It is used operationally by weather forecasters and fire agencies in Australia to declare fire weather warnings and total fire bans, and to determine fire danger. FFDI is often used in analyses of weather conditions associated with major wildfires (e.g. Engel *et al.* 2012). The index also correlates with property loss from wildland fires (Blanchi *et al.* 2010; Bradstock and Gill 2001). There are considerable similarities between FFDI and the Canadian Forest Fire Weather Index (FWI) system: both are drawn from daily meteorological observations of temperature, wind speed, rainfall and relative humidity. The two indices differ in the vegetation used for calibration and in the FWI's greater emphasis on fuel moisture (Van Wagner 1987; Dowdy *et al.* 2010). The United States National Fire Danger Ratings System (NFDRS; Deeming *et al.* 1978) is more physically based than are the FWI and FFDI, and draws on a wider range of meteorological inputs (Mölders 2010).

Multivariate indices such as the FFDI are a useful measure of regional climate model performance. Simulating FFDI well requires a model to simulate the spatial and temporal variation of four different variables. The ability of WRF to capture extreme values of FFDI is of particular interest, as it is on these days that the largest fires are most likely and in the event of an outbreak, most difficult to control. It is important to correctly simulate the overall distribution of FFDI, as lower values are also used in determining weather conditions suitable for conducting fuel reduction burns and setting appropriate levels of community advice.

Our study evaluates the ability of WRF to simulate observed fire weather, represented by FFDI, between 1 January 1985 and 31 December 2009 over south-east Australia. This is the first study comparing observed and simulated FFDI in Australia, and it covers a substantially longer period than did previous evaluations of the model in terms of fire weather. We use reanalysis lateral boundary conditions to drive WRF, which minimises error inheritance and allows identification of positive and negative features of the RCM simulation in a reasonably controlled environment. WRF is being used to develop climate projections for south-east Australia under the New South Wales and Australian Capital Territory Regional Climate Modelling Project (NARCliM; NSW Office of Environment and Heritage 2012). This evaluation will determine whether WRF is a suitable tool to estimate the fire danger at the observation locations in this region.

Methods

Study area

Most of south-east Australia is low lying (Fig. 1*a*). The most prominent relief occurs at the Flinders Range in South Australia (between 30 and 36°S, near 139°W) and the Great Dividing Range that follows the east coast of Australia (approximately from 38°S, 146°E to 27°S, 152°E). The dotted lines in Fig. 1*a* show a 2° grid (~220 km), which approximates the grid spacing of global climate models e.g. CSIRO-MK3.0 (Gordon *et al.* 2002). At this resolution the coastline is distorted and features such as the Flinders and Great Dividing Ranges tend to be smoothed and poorly represented. In Australia, these topographic features have considerable influence on the regional scale hydrometeorology, representing a clear boundary between the drier semiarid interior and the wetter coastal fringe. Inadequate representation of complex mountainous terrain is likely to lead to omission of their characteristic features: rapid and systematic changes in climatic parameters such as precipitation and temperature, enhanced direct runoff and erosion and systematic variation of other environmental (e.g. soil types) and climatic (e.g. radiation) factors (Christensen *et al.* 2007).

There is an approximately latitudinal gradient in fire seasonality over south-east Australia, beginning in spring in the northern part of the domain and shifting to mid to late summer in the southernmost regions. Vegetation ranges from subtropical rainforests in the north-east to the forested Great Dividing Range including alpine heathlands in the southern Alps, through dry forests and rangelands of the mid-west to the dry plains of the north-west. Along with vegetation patterns, rainfall seasonality is a primary driver of existing fire regime patterns in the study area (Russell-Smith *et al.* 2007). Russell-Smith *et al.* (2007) modelled the relationship between satellite-derived fire incidence data from 1997 to 2005 and a range of biophysical variables, finding rainfall seasonality to be the dominant influence, followed by vegetation (i.e. fuel) structure.

Observational data

The observational data used in this study are based on the high quality historical FFDI dataset described by Lucas (2010*a*). FFDI is derived from standard weather observations of air temperature, relative humidity, 10-min averaged wind speed

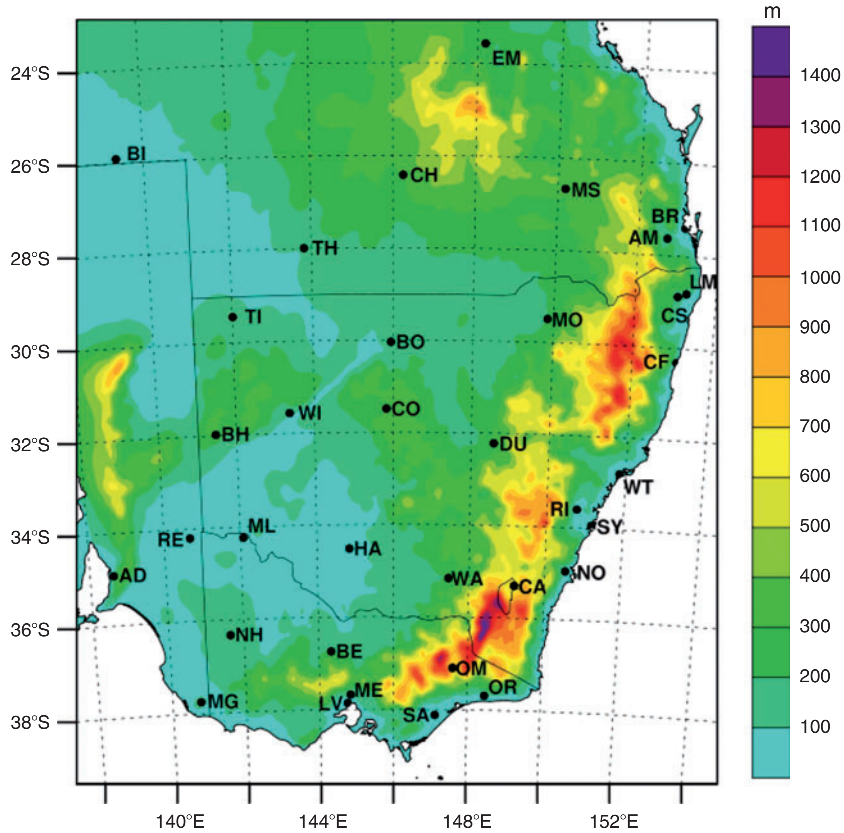

Fig. 1. Map of study area showing elevation and the location of weather stations. See Table 1 for key to station names.

and rainfall to estimate the fire weather conditions. FFDI is given by Noble *et al.* (1980) as:

$$\mathrm{FFDI} = 2 \times \exp(0.987 \times \ln(DF) - 0.0345 \times H + 0.0338 \times T + 0.0234 \times V - 0.45) \tag{1}$$

where DF is the drought factor, T is the temperature (°C), V the wind speed (km h^{-1}) and H the relative humidity (%). In the formulation used here, FFDI is based on maximum daily temperature, and wind speed and relative humidity measured at 1500 hours local time. The drought factor is an empirical estimate of the state of the fuel and is calculated following the methodology described in Griffiths (1999). This uses the Keetch-Byram Drought Index (Keetch and Byram 1968) as its input for soil moisture deficit, based on total daily rainfall collected at 0900 hours local time.

FFDI is widely used across Australia by weather forecasters and fire managers. The fire danger rating scale divides FFDI into a series of threshold values with associated descriptions: 0–11 (low–moderate), 12–24 (high), 25–49 (very high), 50–74 (severe), 75–99 (extreme) and 100+ (catastrophic). FFDI ignores local variations in fuel amounts and types, as well as the slope of the terrain. These factors have a significant influence on the fire behaviour. FFDI is therefore primarily a tool for understanding weather- and climate-related aspects of fire risk. The FFDI also has a similarly derived counterpart, the Grassland Fire Danger Index (GFDI), which is designed to be applied to large areas of grassland that are subject to fire, e.g. central and northern Australia. GFDI is not evaluated here, being problematic as a result of uncertainties in the amounts of historical grassland curing. In any case, future climate projections show considerable overlap in the behaviour of the GFDI and FFDI (Hennessy *et al.* 2005).

Lucas (2010*a*) describes inhomogeneities in wind speed data that in some cases have a large effect on the FFDI. These inhomogeneities arise from the changing local environment of the wind measurement as well as the changing instrumentation used to record wind speeds. The inhomogeneities are most evident in rural stations and before the 1990s, and as a general rule the mean of past wind speed measurements is lower than those measured with contemporary anemometers. Lucas (2010*a*) proposes a methodology for correcting these data that is applicable to the statistics of the FFDI distribution, rather than individual observations. The methodology breaks down at the extreme upper ends of the FFDI distribution, typically above the 90th percentile. In order to retain data with daily resolution we used uncorrected data. This leads to an underestimate of average FFDI values by ~5% for the period of this study (corrected and uncorrected data supplied by Chris Lucas, Australian Weather and Climate Research, Bureau of Meteorology).

Table 1. Location of stations, distance from stations to centre of NNRP, WRF 50 km (W50) and WRF 10 km (W10) grid cells, and summary of missing data for each station

Station (abbreviation)	Station location (°)		Distance from grid cell centre (to nearest kilometre)			Total days missing (years missing >90 days)
	Latitude	Longitude	NNRP	W50	W10	
Adelaide (AD)	−34.92	138.62	37	71[A]	1	16
Amberley (AM)	−27.63	152.71	82	7	3	259
Bendigo (BE)	−36.74	144.33	45	8	2	57
Birdsville (BI)	−25.90	139.35	64	28	6	652 (1997)
Bourke (BO)	−30.04	145.95	64	15	7	561 (1998)
Brisbane (BR)	−27.39	153.13	66	18	5	7
Broken Hill (BH)	−31.98	141.47	101	25	5	708 (1985, 1991)
Canberra (CA)	−35.30	149.20	73	20	3	16
Casino (CS)	−28.88	153.05	99	25	5	1012 (1985–86)
Charleville (CH)	−26.42	146.25	79	15	5	27
Cobar (CO)	−31.49	145.83	40	29	7	80
Coffs Harbour (CF)	−30.31	153.12	106	23	5	18
Dubbo (DU)	−32.22	148.58	98	17	3	298
Emerald (EM)	−23.57	148.18	27	19	5	159
Hay (HA)	−34.52	144.85	91	15	5	441 (1991)
Laverton (LV)	−37.86	144.76	87	31	5	21
Lismore (LM)	−28.81	153.26	92	10	4	680 (1986–87)
Melbourne (ME)	−37.68	144.84	73	12	5	19
Mildura (ML)	−34.23	142.08	107	31	3	10
Miles (MS)	−26.66	150.18	107	14	5	530 (1987)
Moree (MO)	−29.49	149.85	15	13	2	24
Mount Gambier (MG)	−37.75	140.77	69	31	3	8
Nhill (NH)	−36.33	141.64	118	11	1	104
Nowra (NO)	−34.95	150.54	59	9	5	246
Omeo (OM)	−37.10	147.60	47	20	4	1021 (1986, 2002, 2009)
Orbost (OR)	−37.69	148.47	68	12	2	47
Renmark (RE)	−34.20	140.68	97	21	2	173 (1988)
Richmond (RI)	−33.60	150.78	78	19	3	29
Sale (SA)	−38.12	147.13	128	10	3	101
Sydney (SY)	−33.94	151.17	94	17	3	6
Thargomindah (TH)	−27.99	143.82	68	32	4	345
Tibooburra (TI)	−29.44	142.01	48	7	7	131
Wagga (WA)	−35.16	147.46	61	33	6	13
Wilcannia (WI)	−31.56	143.37	84	25	4	1057 (1985, 1988–92, 1996)
Williamtown (WT)	−32.79	151.84	60	28	6	9

[A]The grid cell closest to the coordinates of the station at Adelaide occurred in a cell flagged as sea; the next closest land grid cell was picked.

Model data

The WRF modelling system is developed collaboratively by several agencies and the research community. In this study the Advanced Research WRF (ARW) version 3 is used (Skamarock *et al.* 2008). WRF was run from 1 November 1984 to 31 December 2009, excluding the first two months which were discarded as model spin-up. The model timestep is 1 min. Model top pressure is 50 hPa. The monthly atmospheric carbon dioxide concentration changed monthly from measurements at Baring Head, New Zealand (Evans and McCabe 2010). Sea surface temperatures are continuously updated and deep soil moisture varies dynamically throughout the simulation according to the physics embodied in the Noah land surface model. The following physics schemes were used: WRF single moment 5-class microphysics scheme; the rapid radiative transfer model (RRTM) longwave radiation scheme; the Dudhia shortwave radiation scheme; Monin-Obukhov surface layer similarity; Noah land-surface scheme; Yonsei University boundary layer scheme; Kain-Fritsch cumulus physics scheme and Rayleigh damping in the upper 5 km of the atmosphere. The model has 30 vertical levels spaced closer together in the planetary boundary layer (both domains). The physics schemes used here were chosen as a compromise between schemes that have been found to perform well in other studies (Evans and McCabe 2010; Evans *et al.* 2012*b*), represent the required physical processes and are computationally efficient enough to perform long simulations.

Two domains are used with one-way nesting. The parent and nested domain have respective horizontal grid spacings of 50 and 10 km. The two simulations are referred to as WRF_{50} and WRF_{10}. The lateral boundary conditions of the parent domain are provided by 6-hourly National Centers for Environmental Prediction (NCEP) and National Center for Atmospheric Research (NCAR) reanalysis project data (NNRP; Kalnay *et al.* 1996) at a grid spacing of 250 km. By using as many observations as possible, NNRP produces an estimate of the

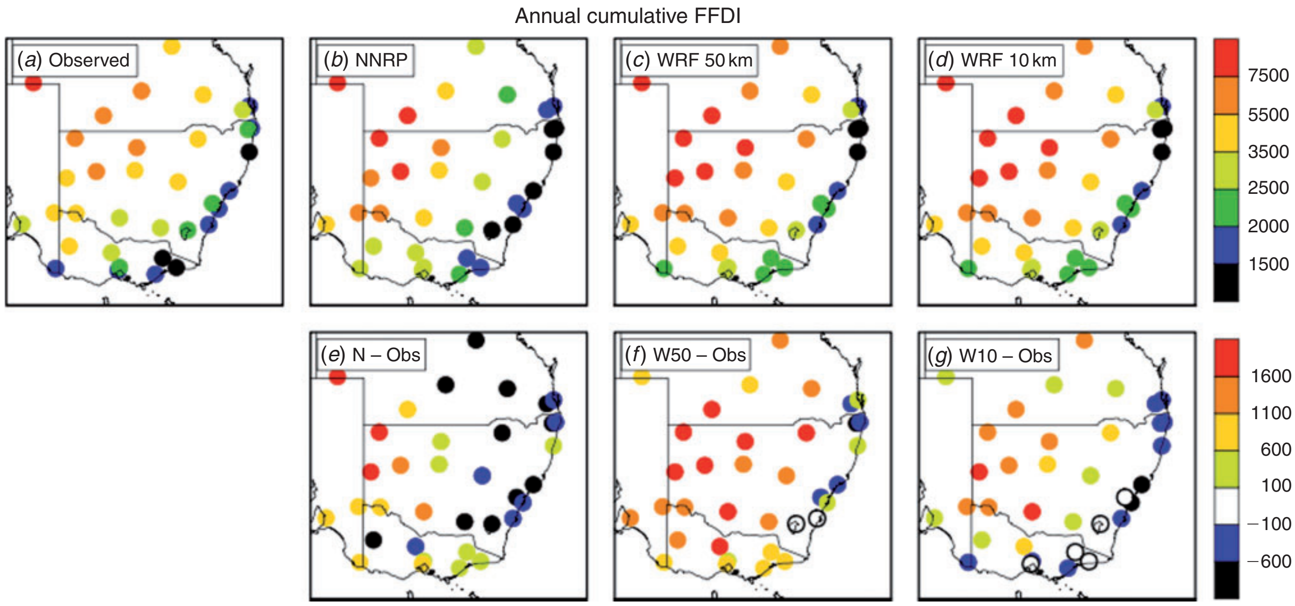

Fig. 2. Mean annual cumulative FFDI (1985–2009). Top row shows absolute values: (*a*) Observed, (*b*) NNRP, (*c*) WRF 50 km, (*d*) WRF 10 km. Second row shows error values: (*e*) NNRP – Observed, (*f*) WRF 50 km – Observed, (*g*) WRF 10 km – Observed. Bin sizes are nonlinear and have been chosen to maximise representation in each bin. Owing to their proximity, there is overlap between the markers for Laverton and Melbourne, Sydney and Richmond, Casino and Lismore, and Brisbane and Amberley.

state of the atmosphere that is as close to reality as possible. The regional climate produced by the WRF simulation driven by the NNRP reanalysis has been extensively evaluated on time scales ranging from diurnal to inter-annual (Evans and McCabe 2010; Evans and Westra 2012). This simulation was found to be a good representation of the observed regional climate. The outermost six horizontal layers of both nests were discarded from the analysis to minimise lateral boundary effects, resulting in the domain areas shown in Fig. 1*b*.

Analysis

All weather stations from Lucas (2010*a*) that fell within both WRF nests were used for the analysis; 35 in total. FFDI at each station was compared with FFDI at the closest WRF grid cell over land. Comparisons with the closest NNRP grid cell were also made. In several cases the same NNRP grid cell was compared with multiple stations. It is preferable to use grid-based observations to evaluate model output, which is generally taken to represent area averaged rather than point processes (Osborn and Hulme 1998). Moreover, the larger the model grid cell, the less likely it is that weather at any given point in the landscape will be representative of the entire grid cell; this is particularly the case for 250-km NNRP grid cells. However, no grid-based FFDI observations are available for this time period and in any case such observations are also subject to limitations, such as representativeness and sensitivity of interpolation techniques to changes in network density (Klein Tank *et al.* 2009; King *et al.* 2012). The location of each station and its distance from the centre of the closest WRF grid cell are shown respectively in Fig. 1*b* and Table 1. All stations are missing some observational data (Table 1).

The variables chosen to summarise and evaluate the fire weather climate were:

1. Annual cumulative FFDI (ΣFFDI) – calculated as the sum of all daily FFDI values over the entire year (e.g. Beer and Williams 1995). It provides a useful metric to compare relative levels of fire weather danger over long time periods or different spatial areas. ΣFFDI is calculated as the average over the period 1985–2009.
2. Days per year over 50 – this variable is indicative of extreme conditions. The largest, most intense wildfires are more likely to happen on these days and any fires that do occur are unlikely to be controllable. It has also been found that 90% of property loss from major fires in Australia occurred during times when FFDI was above 50 (Blanchi *et al.* 2010). Days per year over 50 is calculated over the same time period as ΣFFDI. Although there is great interest in FFDI categories above 50 (namely 75 and 100) the sample size at many stations is too small to draw robust conclusions.
3. Skill score for FFDI and underlying variables – also known as the overlap statistic of the probability density function (PDF). It is calculated by taking the area under the curve defined by the minimum of the modelled and observed PDFs. Expressed in terms of the empirical bins used:

$$\text{Skill score} = \sum_{1}^{n} \min(Z_m, Z_o) \qquad (2)$$

where n is the number of bins used to calculate the PDF, Z_m is the relative frequency of values in a given bin from the model and Z_o is the relative frequency of values in a given bin from the observations. Skill score ranges from zero to one, with zero indicating no overlap and one indicating identical

Table 2. Annual cumulative FFDI and days per year with FFDI over 50 from observations (Obs), NNRP, WRF 50 km (W50) and WRF 10 km (W10)

Station	Annual cumulative FFDI				Days per year over 50			
	Obs	NNRP	W50	W10	Obs	NNRP	W50	W10
Adelaide	2779	3507	4305	3069	1.7	0.2	0.8	0.1
Amberley	3197	1640	3046	2688	1.7	0.0	0.7	1.0
Bendigo	2812	2641	4444	3487	1.8	0.2	2.4	3.2
Birdsville	9352	12213	10383	9765	29.8	68.8	27.1	19.4
Bourke	5735	6320	7589	7048	6.8	5.0	13.9	13.6
Brisbane	1855	1640	1976	1289	0.7	0.0	0.2	0.1
Broken Hill	4432	6733	8115	7324	2.4	3.8	13.4	13.8
Canberra	2417	1351	2513	2362	1.1	0.0	0.2	0.6
Casino	2305	1309	1278	1970	1.9	0.0	0.0	0.7
Charleville	6396	4854	7453	6762	7.7	2.4	8.7	6.6
Cobar	5035	5330	6564	5725	5.4	3.0	7.2	7.0
Coffs Harbour	1167	1309	1492	693	0.2	0.0	0.0	0.0
Dubbo	3577	3450	4785	4038	2.7	1.0	1.9	2.4
Emerald	4584	2900	6023	5705	1.4	0.3	2.2	2.3
Hay	3350	4554	6258	5552	1.0	3.4	6.9	8.6
Laverton	1945	2641	2550	1854	1.7	0.2	0.3	0.9
Lismore	1728	1309	1278	1142	0.3	0.0	0.0	0.2
Melbourne	2361	2641	2550	2094	3.3	0.2	0.3	1.0
Mildura	5284	6268	6821	6532	8.4	7.0	7.5	12.7
Miles	4103	2458	5266	4582	0.6	0.0	1.9	1.8
Moree	4198	2613	5801	5020	3.2	0.0	3.6	3.7
Mount Gambier	1847	2606	2457	1502	1.8	0.0	0.1	0.1
Nhill	3677	2861	5114	4098	4.6	0.3	3.0	3.8
Nowra	1762	1351	1721	1442	1.0	0.0	0.1	0.2
Omeo	1395	1599	2164	1390	0.0	0.0	0.0	0.0
Orbost	1043	1599	2005	1039	0.2	0.0	0.0	0.0
Renmark	5304	6313	6640	6719	10.2	7.1	6.3	14.2
Richmond	2469	1525	2272	2462	1.7	0.0	0.2	1.1
Sale	1679	2259	2326	1530	0.6	0.1	0.1	0.2
Sydney	1897	1525	2216	1293	1.4	0.0	0.0	0.1
Thargomindah	7238	8023	8971	8393	15.3	15.8	24.2	19.8
Tibooburra	7339	8963	9095	8506	18.0	23.8	18.4	17.7
Wagga	3461	2359	4608	3578	4.9	0.0	2.9	2.9
Wilcannia	6408	7720	8200	7559	11.6	11.0	15.2	16.2
Williamtown	1914	1076	1619	1184	1.6	0.0	0.1	0.2

Table 3. Station-averaged values for bias and root mean square error (RMSE) in annual cumulative FFDI (ΣFFDI) and days per year with FFDI over 50, and skill score for FFDI, drought factor (*DF*), temperature (*T*), wind speed (*V*) and relative humidity (*H*)

		NNRP	WRF 50 km	WRF 10 km
ΣFFDI	Bias	40	967	381
	RMSE	1118	1348	909
Days over 50	Bias	−0.11	0.38	0.55
	RMSE	7.08	3.27	3.64
Skill score	FFDI	85.7	85.4	91.2
	DF	81.8	88.9	92.0
	T	85.4	91.6	92.7
	V	65.0	74.1	74.2
	H	79.0	79.8	84.9

PDFs. We multiplied by 100 to simplify visual interpretation. This metric is useful as it is quite robust to sampling errors or random errors in the observations and it measures more than just the mean: simulation of an entire PDF demonstrates an ability to simulate values at the tails of the distribution as well as at the centre. However, skill scores do not indicate the sign of bias, and are increasingly insensitive to errors as values become rarer (Perkins *et al.* 2007).

Bias and root mean square error (RMSE) were calculated for annual cumulative FFDI and days per year with FFDI over 50 at each station. In order to investigate potential sources of WRF error, FFDI is also recalculated after replacing WRF values with observed values for the variables underlying FFDI. One limitation of this approach is that the variables are not independent, particularly in the case of relative humidity and temperature, so changing one without changing the other(s) may lead to physical inconsistencies. Proportional error is defined here as: the absolute value of (WRF – Observed) ÷ Observed. The effect of substituting observed data is labelled Improvement, defined as:

$$(|\mathrm{WRF} - \mathrm{Observed}| - |WRF_s - \mathrm{Observed}|) \div |\mathrm{WRF} - \mathrm{Observed}| \quad (3)$$

where WRF_S is WRF with one variable substituted with either observed drought factor (*DF*), maximum temperature (*T*), wind

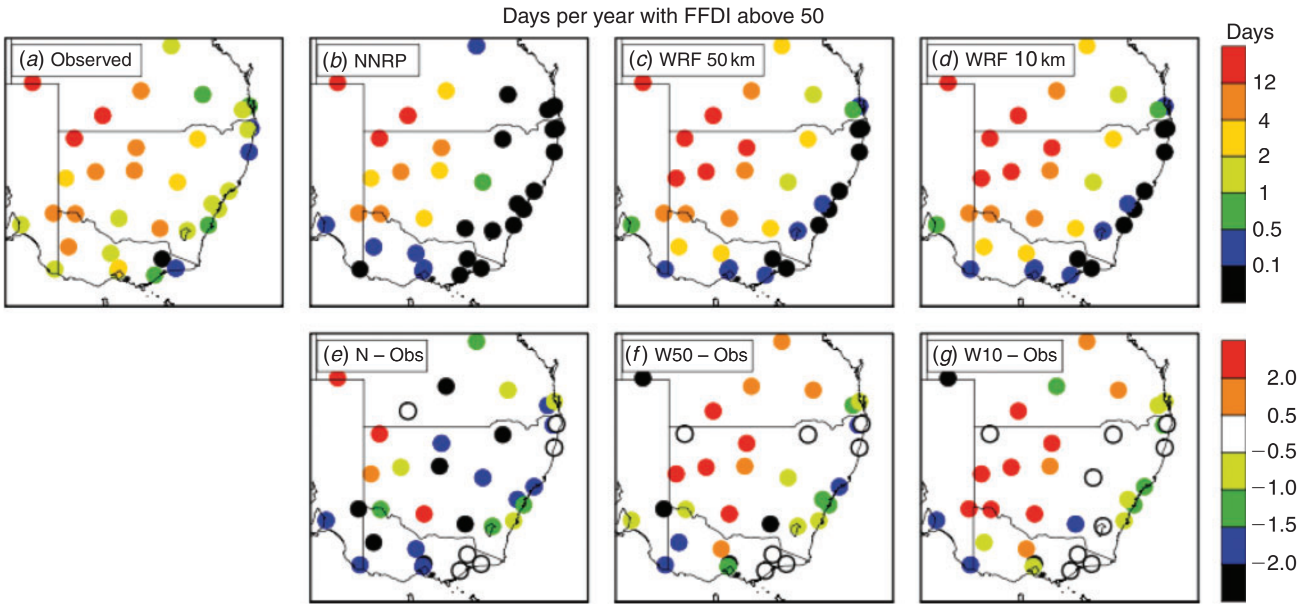

Fig. 3. Mean days per year with FFDI above 50 (1985–2009). Top row shows absolute values: (*a*) Observed, (*b*) NNRP, (*c*) WRF 50 km, (*d*) WRF 10 km. Second row shows error values: (*e*) NNRP – Observed, (*f*) WRF 50 km – Observed, (*g*) WRF 10 km – Observed. Bin sizes are nonlinear and have been chosen to maximise representation in each bin. Owing to their proximity, there is overlap between the markers for Laverton and Melbourne, Sydney and Richmond, Casino and Lismore, and Brisbane and Amberley.

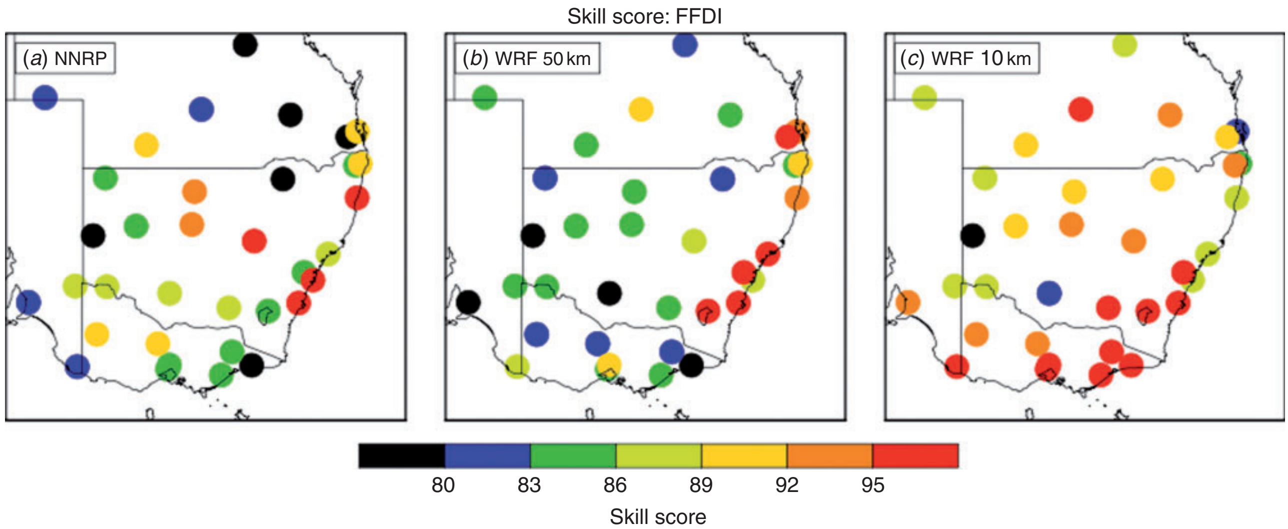

Fig. 4. FFDI skill score: (*a*) NNRP, (*b*) WRF 50 km, (*c*) WRF 10 km. Owing to their proximity, there is overlap between the markers for Laverton and Melbourne, Sydney and Richmond, Casino and Lismore, and Brisbane and Amberley.

speed (W) or relative humidity (H). A negative value of Improvement implies that model accuracy has deteriorated with substitution relative to the original model value. Generally, Improvement behaves as follows:

$$\text{As } |WRF_s - \text{Observed}| \to 0, \text{ Improvement} \to 1$$

$$\text{As } |\text{WRF} - \text{Observed}| \to 0, \text{ Improvement} \to -\infty$$

$$\text{As } |WRF_s - \text{Observed}| \to |\text{WRF} - \text{Observed}|, \text{ Improvement} \to 0$$

$$\text{For } |\text{WRF} - \text{Observed}| \gg |WRF_s - \text{Observed}|, \text{ Improvement} \to 1$$

Results

Annual cumulative FFDI

Fig. 2 and Table 2 show ΣFFDI. The observed data (Fig. 2*a*) ranged from just over 1000 to over 8000 with a strong gradient from low values near the coast to very high values inland. Modelled ΣFFDI and error are shown for NNRP (Fig. 2*b*, *e*), WRF_{50} (Fig. 2*c*, *f*) and WRF_{10} (Fig. 2*d*, *g*). Although NNRP captures well the overall coastal–inland gradient (Fig. 2*b*), it significantly underestimates ΣFFDI for much of eastern Australia (Fig. 2*e*). Indeed, Fig. 2*e* shows much of the region dominated by errors exceeding 600. WRF_{50} also underestimates

Table 4. FFDI skill scores for the NNRP, WRF 50 km (W50) and WRF 10 km (W10)

Station	FFDI skill score		
	NNRP	W50	W10
Adelaide	81	76	93
Amberley	72	96	91
Bendigo	91	80	92
Birdsville	82	86	88
Bourke	92	84	90
Brisbane	90	94	81
Broken Hill	76	68	75
Canberra	85	95	97
Casino	85	83	95
Charleville	82	89	95
Cobar	94	85	93
Coffs Harbour	96	92	86
Dubbo	97	86	94
Emerald	71	82	87
Hay	88	72	80
Laverton	84	85	99
Lismore	92	90	86
Melbourne	85	89	97
Mildura	89	83	89
Miles	73	85	94
Moree	78	81	89
Mount Gambier	82	86	96
Nhill	90	82	94
Nowra	96	96	95
Omeo	83	83	97
Orbost	79	75	98
Renmark	87	83	86
Richmond	86	97	99
Sale	85	83	97
Sydney	95	87	87
Thargomindah	89	85	90
Tibooburra	85	83	88
Wagga	88	85	97
Wilcannia	85	84	90
Williamtown	87	97	88

ΣFFDI along areas of the east coast, but more frequently overestimates FFDI, particularly in inland areas and along the south coast (Fig. 2*f*). Relative to those for NNRP, the simulated errors are considerably smaller. Fig. 2*c* shows that WRF_{10} also captures extremely well the basic gradient in ΣFFDI from the coast towards the inland. Five sites, located in the south-east, are within ±100, but elsewhere along both the east and south coast WRF_{10} tends to underestimate ΣFFDI. As with WRF_{50}, WRF_{10} also overestimates ΣFFDI inland, but the bias is generally smaller than with WRF_{50} and NNRP. The observed values of ΣFFDI are positively correlated with the absolute error for NNRP ((correlation coefficient (r) of 0.64, $P < 0.001$ from t statistic)), WRF_{50} ($r = 0.50$, $P < 0.001$) and WRF_{10} ($r = 0.42$, $P = 0.01$). However, there was no correlation between observations and proportional error for NNRP ($r = -0.20$, $P = 0.24$), WRF_{50} ($r = -0.24$, $P = 0.41$) or WRF_{10} ($r = -0.05$, $P = 0.77$).

The station-averaged bias for ΣFFDI for NNRP is relatively low at 40, compared with 967 for WRF_{50} and and 381 for WRF_{10} (Table 3). However, this masks a range of large positive and negative biases in NNRP, as shown by the RMSE (1118). WRF_{10} has the lowest RMSE (909) and WRF_{50} the highest (1348).

Days per year with FFDI above 50

Fig. 3 and Table 2 show days per year with FFDI above 50. As expected based on the results for the ΣFFDI, the number of days where FFDI exceeds 50 also shows a strong gradient from the coast to inland (Fig. 3*a*). Near the coast, the observations point mainly to 0.5–2 days per year with FFDI exceeding 50, with this increasing to more than 12 inland. NNRP captures some of the gradient, but consistently underestimates values along the east and south-east coasts, and seriously overestimates the value at Birdsville (Fig. 3*b*). WRF_{50} and WRF_{10} capture well the overall pattern of the observations (Fig. 3*c*, *d*). The difference between WRF_{50} and the observations (Fig. 3*f*) shows seven stations where the model is within ±0.5 days per year. Although WRF_{50} tends to underestimate this measure near the coast, the overall simulation appears close to the observations. A similar result is apparent for WRF_{10}; there are nine stations within ±0.5 days per year of the observations, elsewhere the model tends to be closer to the observations than for WRF_{50}. Both WRF simulations yield more overestimates of days per year over 50 than did NNRP. The observed values of days per year with FFDI over 50 are positively correlated with the absolute error for NNRP ($r = 0.77$, $P < 0.001$) and WRF_{10} ($r = 0.52$, $P < 0.001$), but not WRF_{50} ($r = 0.27$, $P = 0.12$). Proportional error is correlated with observed values for NNRP ($r = -0.34$, $P = 0.05$), but not for WRF_{50} ($r = -0.29$, $P = 0.09$) or WRF_{10} ($r = -0.22$, $P = 0.21$).

NNRP has a slight negative bias on average across all stations (−0.11; Table 3) in the simulation of the number of days where FFDI exceeds 50. On average WRF has a positive bias (0.38 for WRF_{50} and 0.55 for WRF_{10}). As with annual cumulative FFDI, the low mean bias of NNRP relative to WRF masks one particularly large positive bias (Birdsville, 39) and a range of negative biases, such that the RMSE for NNRP is 7.08, compared with 3.27 for WRF_{50} and 3.64 for WRF_{10}.

FFDI skill score

To assess the models more generally, skill scores were calculated based on the overlap of the PDF (Fig. 4 and Table 4). Sample PDFs are shown for two stations for which WRF_{10} had high skill scores (Fig. 5; see Supplementary material Fig. S1 for WRF_{50} and Fig. S2 for NNRP). Fig. 5 also shows the insensitivity of skill score to errors in rare values (see Methods). The station-averaged skill scores were 85.7 for NNRP, 85.4 for WRF_{50} and 91.2 for WRF_{10}. Although WRF_{50} and NNRP display similar performance overall, WRF_{50} (Fig. 4*b*) has two fewer stations in the lowest skill score bin than does NNRP (Fig. 4*a*), and one more in the highest bin. In contrast, WRF_{10} (Fig. 4*c*) clearly captures the observed PDF of FFDI better than does either NNRP or WRF_{50}. Compared to WRF_{10}, WRF_{50} does relatively poorly along the southern coast (<85) and in inland areas this remains <90. WRF_{50} does capture the observations along the east coast very well in most cases. WRF_{10} shows a significant improvement over WRF_{50} (Fig. 4*c*). WRF_{10} skill scores along the south coast increase to >95. There is a small reduction in skill scores along parts of the east coast. The major improvement is further inland where the skill score improves by 5–10 over

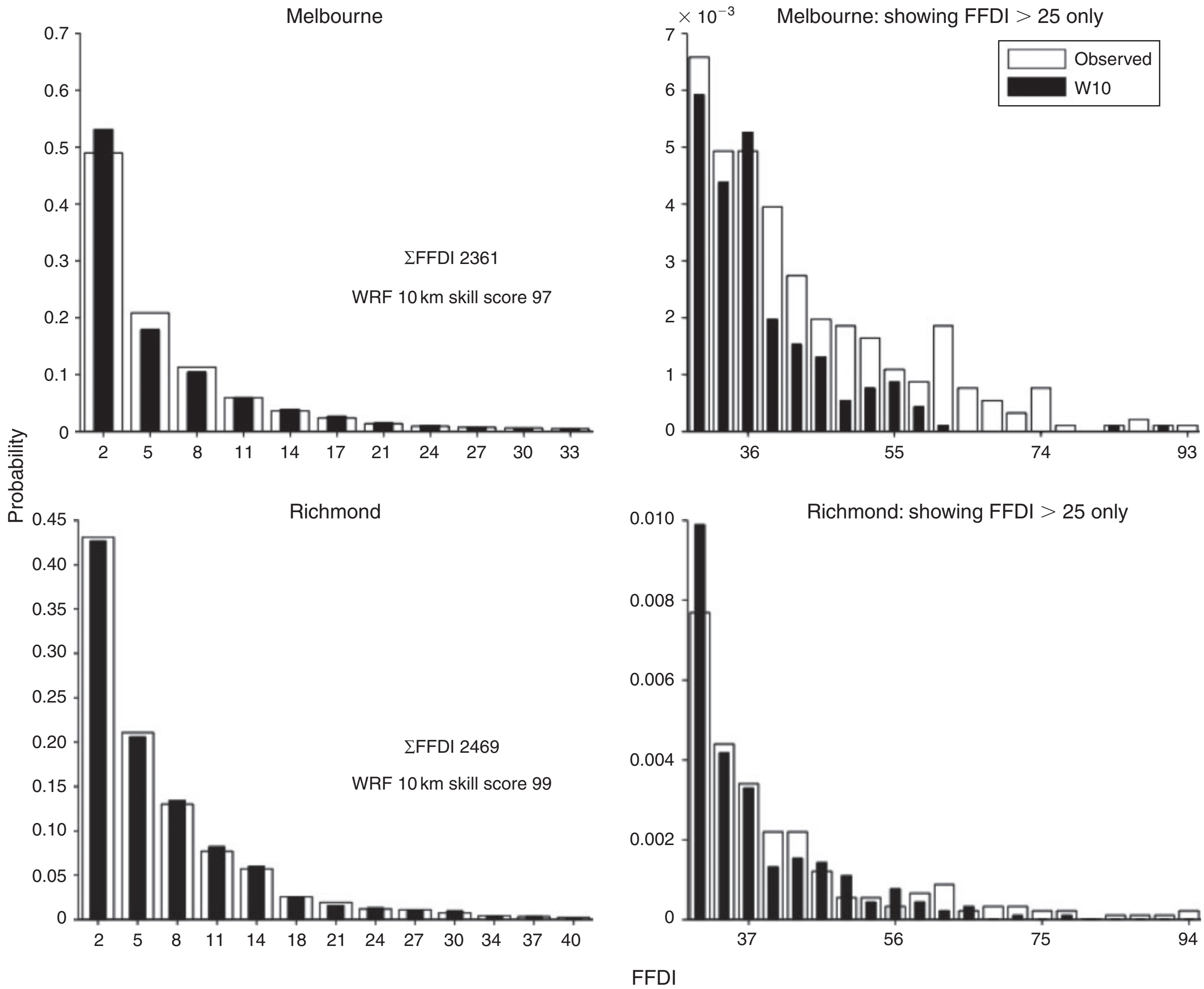

Fig. 5. Probability density functions (PDFs) of FFDI at two stations for which WRF 10 km has a high skill score. Right hand side excludes values below 25, showing relative insensitivity of skill score to errors in rare values.

WRF_{50} such that only one station has a skill score <80 in contrast to 4 in WRF_{50}.

What causes WRF errors in average and extreme FFDI?

The Improvement metric (see Methods) demonstrates which variables contribute to the errors in the WRF-derived FFDI values. Table 5 shows the results for ΣFFDI for both WRF_{50} and WRF_{10}, with stations ranked by proportional error. Where the proportional error is <0.05 (that is, WRF is within 5% of the observations) we have not colour coded the outcomes on the grounds that WRF is likely within observational error without implementing any corrections using the observations. Table 5 shows that substituting drought factor or temperature does not lead to significant improvements in WRF_{50}. The main effect is caused by replacing WRF's simulated relative humidity with the observed humidity, suggesting that there is a systematic difference between the WRF_{50} and observed humidity that strongly affects the derived FFDI. A similar result is shown for WRF_{10}. Although substituting each of *DF*, *T* and *V* does contribute improvements, the only systematic substitution that has a large effect is humidity. Table 6 shows the equivalent result for FFDI days over 50. In this case, it is not the substitution of humidity that contributes most to an improvement of the simulated FFDI, rather it is the substitution of wind speed.

Tables 5 and 6 demonstrate that different components of the FFDI contribute to different measures of WRF's ability to simulate FFDI. The ΣFFDI errors in WRF_{50} and WRF_{10} are largely determined by differences between the observed and simulated relative humidity. The errors in simulating days over 50 are largely determined by differences between the observed and simulated wind speed. Tables 5 and 6 also show stations where substituting observed values of each quantity degrades the WRF-derived FFDI. This is counterintuitive but is likely related to a physical consistency in WRF between the simulation of each variable, which leads to an accurate simulation of FFDI in many stations. Removing one of these variables and replacing it with an observed quantity causes physical inconsistencies,

Table 5. Effect of substituting in each of the observed variables on WRF error in annual cumulative FFDI

Stations are arranged in reverse order of proportional error. See Methods for definition of improvement. Dark grey shading shows improvement >0.7, grey shows improvement between 0.3 and 0.7, no shading shows improvement between −0.3 and 0.3 and light grey shading shows improvement below −0.3 (i.e. an increase in error). Stations where WRF_{10}-modelled FFDI is within 5% of the observed value have been italicised. Absolute error is shown for reference

Station	Proportional error	Absolute error	Improvement (WRF 50 km + observed)				Improvement (WRF 10 km + observed)			
			DF	*T*	*V*	*H*	*DF*	*T*	*V*	*H*
Hay	0.66	−2203	0.25	−0.11	0.07	0.49	−0.5	−0.96	−1.5	0.48
Broken Hill	0.65	−2892	−0.29	0.14	0.39	0.63	0.59	0.56	0.17	0.82
Coffs Harbour	0.41	474	0.15	0.02	−0.02	0.61	−0.09	−0.17	−0.15	0.54
Williamtown	0.38	730	−0.16	−0.24	−0.36	0.84	−0.35	−0.95	−1.41	−0.32
Lismore	0.34	586	−0.12	−0.03	0.16	0.74	−0.21	−0.14	0.24	0.73
Sydney	0.32	605	−1.24	−1.19	−1.57	0.1	0.32	0.37	0.41	0.92
Brisbane	0.31	567	0.09	0.04	0.16	0.69	0.05	−0.06	0.27	0.65
Renmark	0.27	−1416	−2.19	−2.83	−1.74	0.46	−1.29	−2.01	−1.24	0.97
Bendigo	0.24	−675	0.38	0.26	0.21	0.56	0.82	0.78	0.42	0.73
Emerald	0.24	−1121	−0.02	−0.03	−0.07	0.62	−0.37	−0.47	−0.3	0.8
Mildura	0.24	−1248	−0.08	−0.08	0.27	0.58	−0.41	−0.35	0.41	0.54
Bourke	0.23	−1313	−0.31	−0.4	−1.21	0.83	0.4	0.36	0.53	0.87
Moree	0.2	−822	−0.02	−0.1	−0.29	0.94	−0.27	−0.48	−0.82	0.71
Mount Gambier	0.19	345	−0.12	−0.06	−0.19	0.95	−0.15	−0.18	−0.09	0.95
Nowra	0.18	321	0.08	−0.01	0.34	0.58	0.04	−0.07	0.4	0.51
Wilcannia	0.18	−1151	−0.36	−0.16	−0.6	0.99	−0.53	0.32	−1.69	−0.06
Amberley	0.16	509	0.69	0.51	0.22	0.85	0.43	0.4	0.23	0.91
Thargomindah	0.16	−1155	−1.19	−0.64	−2.25	0.75	0.92	0.59	0.53	0.26
Tibooburra	0.16	−1167	0.08	0.04	−0.27	0.82	0.01	−0.03	−0.05	0.68
Casino	0.15	336	−0.12	−0.13	0.06	0.71	−0.3	−0.55	0.02	0.76
Cobar	0.14	−690	0.2	0.03	−0.21	0.71	0.18	−0.11	−0.4	0.79
Dubbo	0.13	−461	−0.12	−0.06	−1.04	0.95	0.58	0.62	0.94	0.59
Miles	0.12	−480	0.27	−0.06	−0.15	0.64	−0.14	−0.54	−0.21	0.53
Melbourne	0.11	267	−5.6	−1.39	−5.33	−2.46	0.67	0.42	0.88	0.68
Nhill	0.11	−421	−0.2	−0.07	−0.13	0.66	−42	−37	−17	−8.15
Adelaide	0.1	−289	−0.07	−0.06	−0.11	0.67	−58	−46	−43	−36
Sale	0.09	149	−0.04	−0.09	−0.16	0.89	−0.05	−0.09	0.09	0.71
Charleville	0.06	−366	0.94	0.92	0.92	0.97	−19	−27	−16	−14
Laverton	0.05	91	0.14	−0.06	−0.35	0.28	0.88	0.89	−0.45	0.87
Birdsville	0.04	−413	*−0.53*	*−0.3*	*−2.39*	*0.36*	*0.46*	*0.33*	*0.77*	*0.41*
Wagga	0.03	−117	*−0.07*	*−0.07*	*0.28*	*0.59*	*−0.16*	*−0.19*	*0.35*	*0.59*
Canberra	0.02	55	*−0.01*	*0*	*0.08*	*0.69*	*−0.08*	*−0.16*	*0.15*	*0.69*
Omeo	0	6	*0.16*	*−0.07*	*−0.16*	*0.69*	*−1.23*	*−1.55*	*−2.12*	*0.97*
Orbost	0	3	*−0.01*	*−0.08*	*−0.11*	*0.92*	*−0.16*	*−0.23*	*−0.11*	*0.97*
Richmond	0	7	*0.5*	*0.49*	*0.19*	*0.4*	*0.24*	*0.26*	*0.56*	*0.63*

which degrades the model's performance in the resulting metric. In some cases, however, a markedly decreased improvement arises when relatively large positive and negative biases in multiple variables balance each other out. At Moree for example, WRF_{50} simulates 3.6 days per year with an FFDI above 50, compared with 3.2 actually observed. Substituting observed wind speed and relative humidity changes the respective WRF_{50} value to 5.6 and 1.7, because negative and positive biases in extreme values of these variables no longer cancel each other out.

What causes WRF errors in FFDI skill score?

To explore the causes of remaining weaknesses in WRF's capacity to capture the overall distribution of FFDI we explored the performance of the model in simulating each of its component variables using the PDF-based skill score. Fig. 6*a* shows that WRF_{50} captures well the drought factor across the region with most stations exceeding 80. Fig. 6*b* shows the WRF_{50} simulation of temperature. The model is outstanding over all regions and it is unlikely that remaining errors are associated with weaknesses in simulating FFDI. Fig. 6*c* shows the wind speed and Fig. 6*d* shows humidity. Clearly, for both wind and humidity WRF_{50} simulates the distribution poorly compared with the drought factor or temperature. Along the east coast and inland wind speed is captured with a skill score frequently below 73. A similar result is clear for relative humidity, although it is simulated slightly better than wind by WRF_{50}. Interestingly, although the station-averaged FFDI skill scores for WRF_{50} and NNRP are almost identical, WRF_{50} has a higher station-averaged skill score than does NNRP for each variable (Table 3): drought factor (88.9 *v.* 81.8), temperature (91.6 *v.* 85.4), wind speed (74.1 *v.* 65.0) and relative humidity (79.8 *v.* 79.0). It follows that to some extent, the WRF_{50} errors reinforce each other, the NNRP errors cancel each other out, or both.

Table 6. Effect of substituting in each of the observed variables on WRF error in days per year with FFDI over 50

Stations are arranged in reverse order of proportional error. See Methods for definition of improvement. Dark grey shading shows improvement >0.7, grey shows improvement between 0.3 and 0.7, no shading shows improvement between −0.3 and 0.3 and light grey shading shows improvement below −0.3 (i.e. an increase in error). Stations where WRF_{10} modelled FFDI is within 5% of the observed value have been italicised. Absolute error is shown for reference. inf, infinity

Station	Proportional error	Absolute error	Improvement (WRF 50 km + observed)				Improvement (WRF 10 km + observed)			
			DF	*T*	*V*	*H*	*DF*	*T*	*V*	*H*
Hay	7.60	−7.6	0.2	0.18	0.66	0.91	0.08	0.16	0.78	0.59
Broken Hill	4.67	−11.4	0.23	0.23	0.27	0.98	0.15	−0.06	0.71	0.69
Miles	1.93	−1.16	0.51	0.27	0.58	0.71	0.35	0.13	0.98	0.9
Bourke	1.01	−6.84	0.05	0.26	0.33	0.93	−0.12	0.12	0.84	0.77
Coffs Harbour	1.00	0.24	0	0	0.2	−0.2	0	0	0.17	0
Sydney	0.94	1.32	0	0.03	0.43	0.06	0	−0.03	0.67	−0.06
Mount Gambier	0.93	1.6	0	0.02	0.79	0.07	0	0.02	0.23	0.16
Adelaide	0.93	1.72	−0.36	0.55	0.83	0.19	0.02	0.1	0.65	0
Brisbane	0.88	0.6	0.15	0.15	0.16	0.46	0.33	0.07	0.8	0.2
Williamtown	0.88	1.44	0	0	0.28	0.1	−0.03	0	0.19	0.08
Orbost	0.80	0.16	0	0	0.2	0.2	0.25	0	0.5	0
Nowra	0.79	0.76	−0.05	0	0.24	0.1	0.05	0.05	0.49	0.11
Bendigo	0.74	−1.36	0.47	0.91	−2.11	−0.75	0.3	0.44	0.55	0.73
Melbourne	0.71	2.32	0	−0.03	0.72	0.07	0.03	−0.02	0.71	0.09
Casino	0.65	1.24	0	0	0.27	−0.02	−0.03	0.1	0.64	−0.33
Sale	0.64	0.36	−0.18	−0.18	0.98	0.46	−0.22	0	0.9	0.12
Emerald	0.58	−0.84	0.04	−0.11	−0.9	0.37	0	0	−0.07	0.5
Mildura	0.50	−4.24	−1.59	−1.9	−4.48	−4.12	0.26	0.36	0.3	0.75
Laverton	0.48	0.8	0.03	−0.03	0.98	−0.03	0.4	−0.1	0.8	−0.3
Amberley	0.44	0.76	0	−0.03	0.38	0.09	0	0.11	0.84	0.29
Canberra	0.43	0.48	−0.18	0.05	0.55	−0.14	−0.08	0.17	0.5	−0.42
Wagga	0.41	2	−0.31	−0.06	0.46	−0.39	0.06	−0.02	0.74	−0.02
Wilcannia	0.40	−4.6	0.25	−0.18	−1.82	−0.51	−0.01	−0.21	−0.05	0.61
Renmark	0.39	−4	−0.16	−0.05	0.3	−0.89	0.13	0.17	0.56	0.75
Birdsville	0.35	10.48	−0.04	0.7	−3.08	−3.74	0.01	0.52	0.55	−0.54
Richmond	0.33	0.56	−0.05	0.03	0.54	0.14	0.14	0	0.79	−0.28
Thargomindah	0.29	0.08	0.18	0.06	0.58	0.96	0.08	−0.16	0.94	0.98
Lismore	0.29	−4.48	0	0	0.17	−0.17	−0.5	−0.49	0.53	−1.42
Cobar	0.28	−1.52	0.1	−0.21	0.72	0.83	−0.55	−0.47	0.39	0.29
Nhill	0.17	0.76	−0.71	−0.25	−0.5	−1.09	0.42	0.44	0.42	0.05
Moree	0.15	−0.48	−0.68	−0.18	−4.97	−2.79	0.92	0.91	−1.27	−0.75
Charleville	0.14	1.04	0.9	0.98	−0.35	0.1	0.19	−0.12	−0.37	−0.42
Dubbo	0.10	0.28	0.16	0.22	−1.42	−1.57	−0.43	0.18	−3.39	−4
Tibooburra	0.02	0.32	*−0.22*	*0.95*	*−17.12*	*−15.36*	*−0.41*	*−3.14*	*−0.82*	*−10.19*
Omeo[A]	n/a	n/a	*n/a*	*−inf*	*−inf*	*n/a*	*0*	*−1.05*	*−1.24*	*1*

[A]The observed value at Omeo is 0, so proportional error cannot be calculated.

The improvement in skill score in capturing the drought factor using WRF_{10} is only clear at several stations in the southern part of the domain (Fig. 7*a*). Elsewhere, the improvements in WRF_{10} are incremental, but no station is captured with a skill score of less than 85. In effect, the drought factor is simulated very well in WRF_{50} and because of this only a handful of stations are improved in WRF_{10}. Similarly, there is incremental improvement in simulating temperature (Fig. 7*b*). Indeed, at no station is either temperature or drought factor captured with a skill score of <80 and in most cases values exceed 90. Weaker performance for WRF_{10} is apparent for wind speed, with almost identical results to WRF_{50} (Figs 6*c*, 7*c*). In contrast, humidity is improved considerably in WRF_{10} such that there are only five stations with skill scores <80 in WRF_{10}, in contrast to 17 in WRF_{50}. And although there are only four stations over 90 in WRF_{50}, there are eight in WRF_{10}.

WRF_{50} and WRF_{10} have very similar RMSE values overall for drought factor (station-averaged RMSE 2.6 and 2.5); individual station data not shown) and temperature (2.3 and 2.2). In contrast, WRF_{10} clearly improves overall on WRF_{50} in terms of wind speed (8.1 compared with 10.6) and relative humidity (13.0 compared with 18.7).

Summarising the skill score difference between WRF_{50} *and* WRF_{10}

The differences between WRF_{50} and WRF_{10} in simulating the distribution of each variable are summarised in Fig. 8. Points above the $y=x$ line indicate better skill score in WRF_{10}, whereas

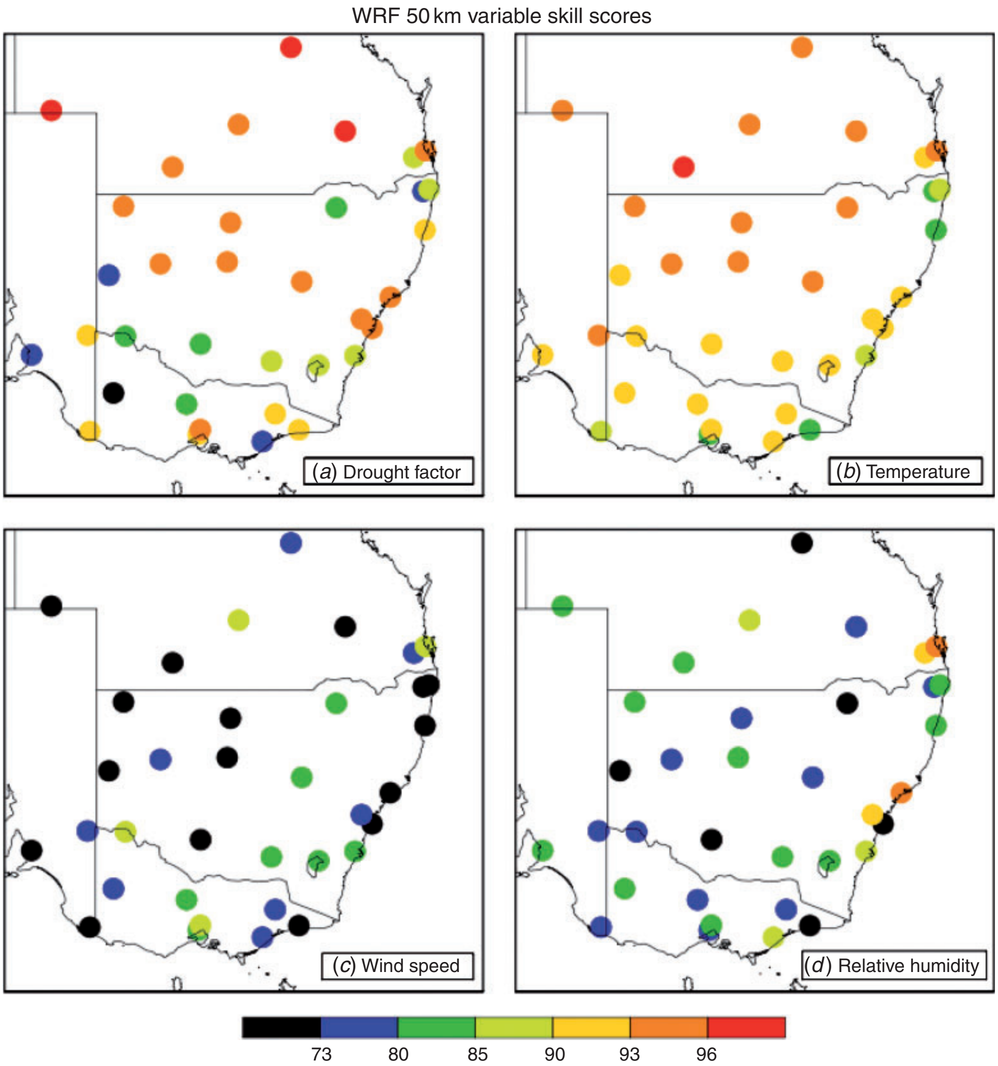

Fig. 6. WRF 50 km variable skill score: (*a*) drought factor, (*b*) temperature, (*c*) wind speed, (*d*) relative humidity. Bin sizes are nonlinear and have been chosen to maximise representation in each bin. Owing to their proximity, there is overlap between the markers for Laverton and Melbourne, Sydney and Richmond, Casino and Lismore, and Brisbane and Amberley.

points below the line indicate better skill score in WRF_{50}. For FFDI (Fig. 8*a*), WRF_{10} outperforms WRF_{50} in most cases, usually by a small margin but sometimes by over 10 points. There are, however, five stations at which WRF_{50} records higher skill scores than does WRF_{10}. These stations are Amberley, Brisbane, Lismore, Coffs Harbour and Williamtown; all are found along the middle to upper eastern seaboard. Skill scores for drought factor (Fig. 8*b*) cluster more closely to the line $y = x$ than for FFDI, but there remain several stations at which WRF_{10} perform considerably better than does WRF_{50}. Little is gained by moving from 50- to 10-km grid spacing when simulating the distribution of maximum temperature (Fig. 8*c*) or wind speed (Fig. 8*d*). Skill scores for both variables are fairly tightly and evenly clustered around the line $y = x$. In contrast, the pattern of relative humidity skill scores is quite similar to FFDI (Fig. 8*e*). There is a clear and often large improvement in humidity skill score when moving from 50- to 10-km grid spacing, but there are also five stations – the same as for FFDI – where WRF_{10} performs worse than does WRF_{50}. In summary, decreasing WRF grid spacing typically leads to either an improvement or no change in skill score. At a few stations, however, WRF's simulation accuracy actually degrades when grid spacing is decreased.

Discussion and conclusions

This study provides strong evidence for the first time of a regional climate model's capacity to simulate fire weather over multiple decades. WRF was evaluated over a period of 25 years, covering a much broader range of weather conditions than had previous studies, which assessed periods of days to weeks. At both 10- and 50-km grid spacings WRF is able to capture large spatial gradients in average and extreme FFDI, as well as

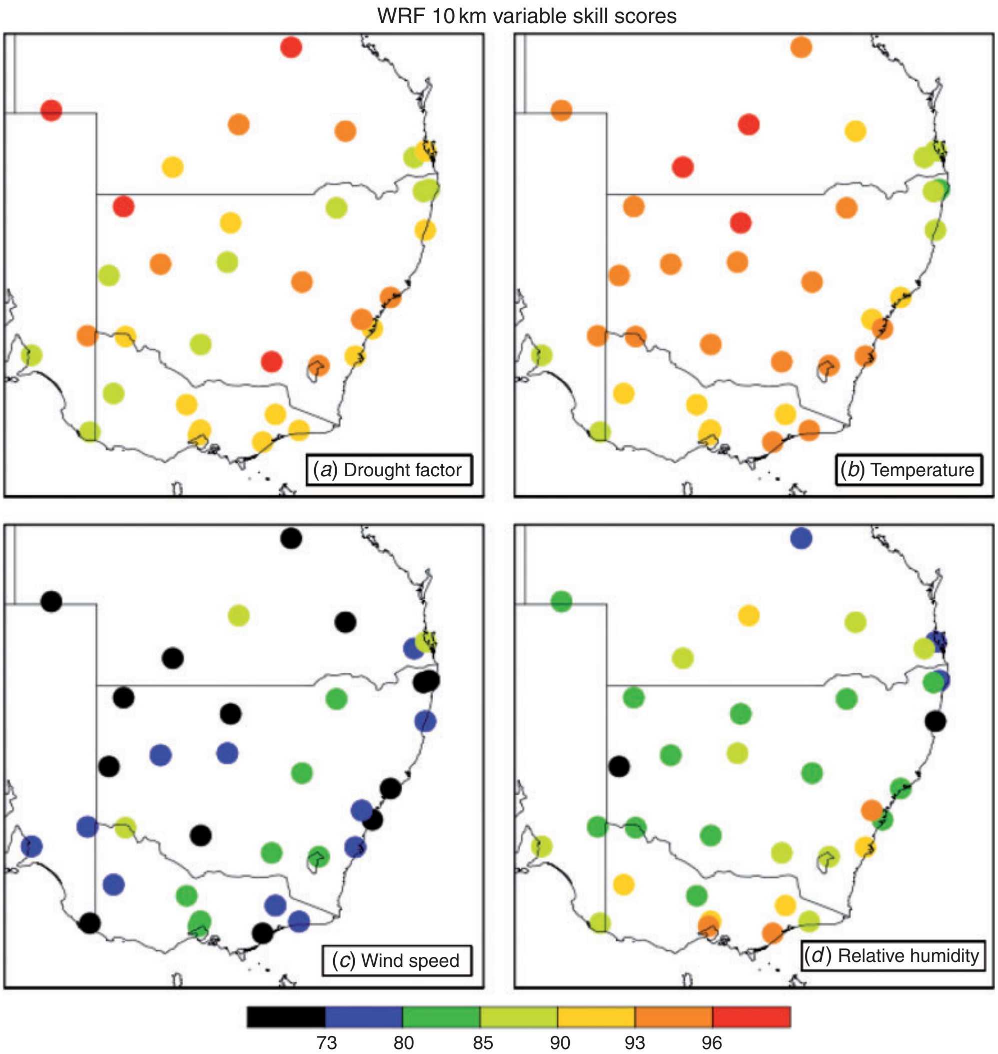

Fig. 7. WRF 10 km variable skill score: (*a*) drought factor, (*b*) temperature, (*c*) wind speed, (*d*) relative humidity. Bin sizes are nonlinear and have been chosen to maximise representation in each bin. Owing to their proximity, there is overlap between the markers for Laverton and Melbourne, Sydney and Richmond, Casino and Lismore, and Brisbane and Amberley.

reproduce the overall distribution of FFDI. The major biases in WRF are underestimates of FFDI along the east coast and overestimates at hot and arid inland locations. These overestimates apply more to average than extreme FFDI values and are mitigated partly by the known underestimation of observed average FFDI values (see Methods).

There are several sources of errors in the WRF simulations. The boundary conditions (NNRP) and deficiencies in the representation of physical processes in the model both contribute to the errors. The fact that the NNRP has similar spatial patterns of error indicates these boundary conditions are a dominant source of error. The biases in temperature and precipitation found by Evans and McCabe (2010) influence results here, but only negligibly so compared with the other two variables that comprise FFDI. Based on the improvement scores from substituting in observed variables to recalculate FFDI, relative humidity is the largest driver of errors in annual cumulative FFDI, whereas wind speed has the most influence on errors in extreme FFDI values. Given that FFDI is more sensitive to changes in wind speed than it is to changes in the other variables (Dowdy *et al.* 2010) and that FFDI is an exponential function, the influence of WRF errors in wind speed will be disproportionately high at the upper extremes of the distribution. Conversely, relative humidity is very low on the highest FFDI days, so errors must be proportionately larger to have an equivalent effect on FFDI. Our results do, however, demonstrate the value of separately examining measures of central tendency (in this case the annual cumulative FFDI) and measure of extreme values (days per year with FFDI above 50).

It is noteworthy that where the observations are more consistent (temperature and drought factor, which is derived from precipitation) WRF performs very well. As noted by Evans and McCabe (2010), WRF improves almost all temperature and

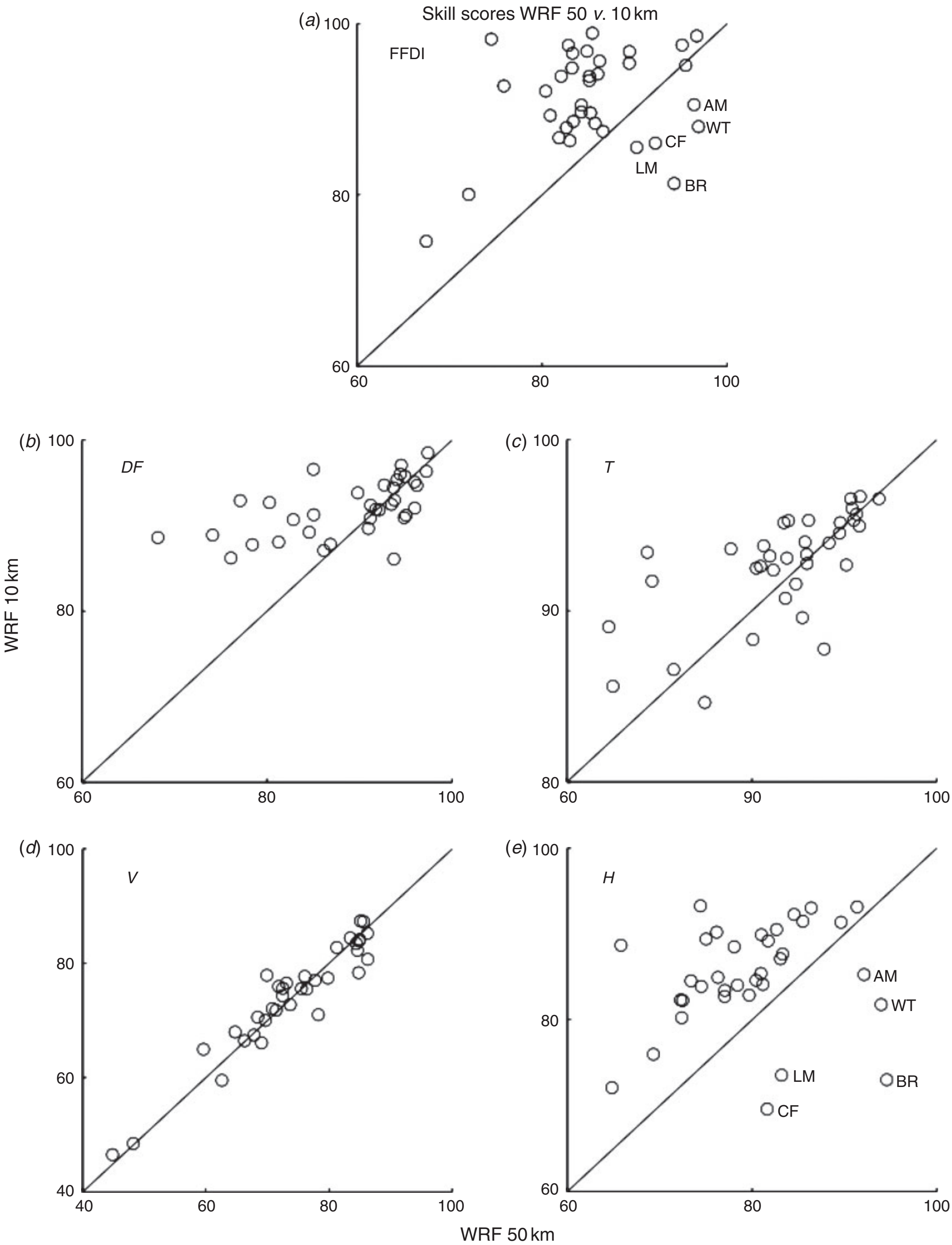

Fig. 8. Skill score scatterplots for WRF 50 km *v.* WRF 10 km: (*a*) FFDI, (*b*) drought factor, (*c*) temperature, (*d*) wind speed, (*e*) relative humidity. Stations at which WRF 50 km clearly outperforms WRF 10 km in FFDI and relative humidity are marked. See Table 1 for key to station names.

precipitation statistics relative to those derived from the NNRP reanalysis data, which supplied the lateral boundary conditions for their and our study. However, for wind speed and relative humidity, for which inhomogeneity in observational datasets is a greater issue than for temperature and rainfall (Jakob 2010; Lucas 2010*b*), there are larger differences between the model and the observations. A significant fraction of these errors are likely associated with model error, but some fraction is very

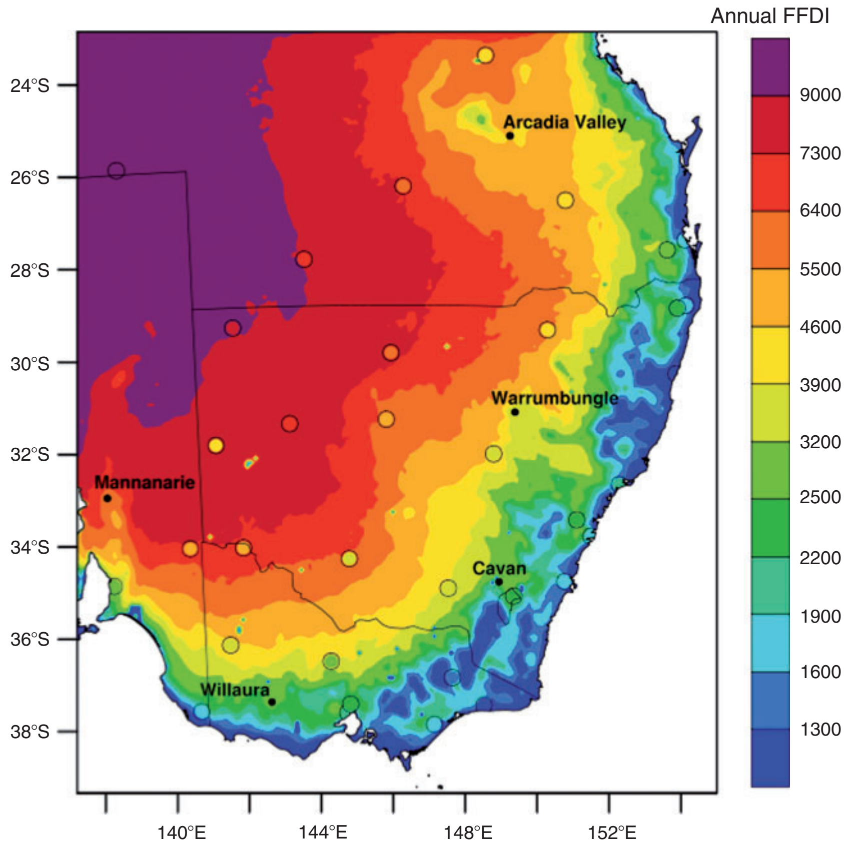

Fig. 9. WRF 10 km map of mean annual cumulative FFDI (1985–2009). Markers show observed values. Small black markers show examples of places where days per year with FFDI over 50 differs substantially from the surrounding area.

probably observational errors. We cannot determine the relative fractions, but an exploration of how well WRF captures wind and relative humidity at those stations that are particularly reliable would be worthwhile.

The performance of WRF run at 50-km grid spacing, with respect to the NNRP reanalysis dataset that provided the lateral boundary conditions to drive the WRF simulations, depends on the measure used. Owing to the introduction of a positive bias overall in the WRF simulation, NNRP averages smaller errors in annual cumulative FFDI. WRF performs better than NNRP for extreme values and simulates the overall distribution of each of the variables underlying FFDI better than does NNRP. WRF also better captures lower values (in average and extreme FFDI). In contrast, WRF run at 10-km grid spacing represents a clear improvement over NNRP and in most cases WRF at 50 km, especially in the south-east corner of continental Australia. The two WRF simulations perform similarly with respect to extreme FFDI values, with much smaller errors in variance than for NNRP; WRF at 10 km also improves upon NNRP in simulating variation in average values. At a small number of locations along the east coast WRF performance actually degrades with finer grid spacing. This is likely because of introduced deficiencies in simulating relative humidity at these locations. Any errors in wind speed simulation internal to WRF are essentially unaffected by decreasing the grid spacing of the model from 50 to 10 km. The improvement of WRF at finer grid spacing appears unrelated to its greater proximity to weather stations; there is no correlation between error and distance from model grid cell centre for either WRF at 10 km or WRF at 50 km grid spacing (data not shown). Whether the improvement in model performance warrants the additional computational resources required for high-resolution model runs depends on the location and the needs of users of the data.

An advantage of high resolution climate models over station-based meteorological datasets is their comprehensive spatial coverage. WRF can be used to generate estimates of FFDI risk across the entire landscape rather than just at station locations, which may provide novel information to fire managers. Figs 9 and 10 respectively show WRF maps of average annual cumulative FFDI and average days per year with FFDI above 50. The maps also show the observed values at each station for reference. For both metrics the areas of largest fire weather risk are found in the north-east of the domain, which is dominated by grassland and desert, rather than forest. There is a clear gradient of increasing risk from the coast inwards, which is stronger in the south-west than along the east coast. The full landscape coverage of regional climate models such as WRF can provide important information that a sparse station network cannot. For example, Warrumbungle (31.3°S, 149.1°E) is surrounded by areas with between 1.5 and 6.5 days per year of FFDI above 50,

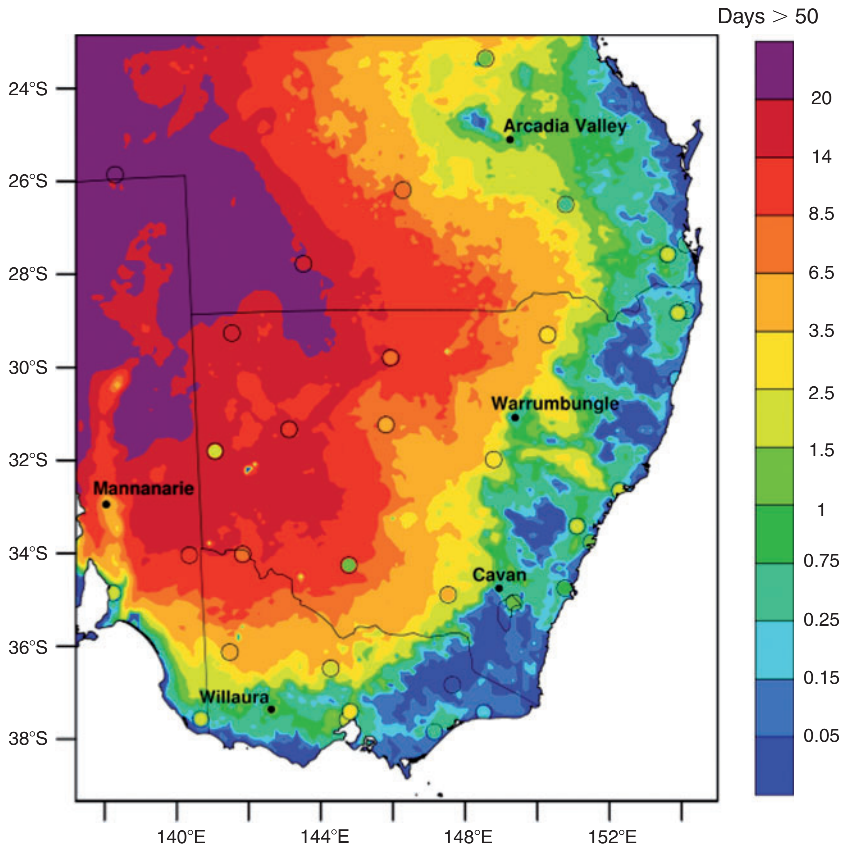

Fig. 10. WRF 10 km map of mean days per year with FFDI over 50 (1985–2009). Markers show observed values. Small black markers show examples of places where FFDI differs substantially from the surrounding area.

whereas much of it records less than 1 day per year (Fig. 10). Conversely, Willaura (37.6°S, 142.7°E) records approximately double the number of days above 50 than in much of the surrounding area. Cavan, Mannanarie and Arcadia Valley are other towns with extreme FFDI values that are considerably different to their surrounds. When taken into account with other wildfire risk factors, these differences in fire weather conditions have the potential to influence a range of decisions in fire management, including prioritisation of prescribed burns and guidelines for housing construction and setback distances between buildings and vegetation.

WRF simulates observed FFDI quite well and does this despite the additional constraint of matching grid-based values with point-based observations. WRF run with 50-km grid spacing does not consistently outperform the reanalysis data, improving in some areas but not in others. The fire weather derived from WRF with 10-km grid spacing is generally closer to observations than the reanalysis across the full range of evaluation metrics used here. This suggests it is a very useful tool for modelling fire weather over the entire landscape of south-east Australia. The evaluation of WRF against multi-decadal observations also provides a useful reference for any future projections of FFDI derived from WRF. Further studies evaluating RCMs against long-term observational datasets will provide more opportunities to judge the relative merit of this simulation.

Acknowledgements

This work was supported by a grant to H. Clarke from the NSW and Commonwealth Governments under the Natural Disaster Resilience Program. Chris Lucas provided the FFDI dataset used for this study and also helpful comments on the manuscript. This work has been partially funded by the Australian Research Council as part of the Discovery Project DP0772665 and by the ARC Centre of Excellence for Climate System Science (CE110001028). We also acknowledge support from the NSW Environmental Trust (RM08603). The simulations were supported by the NCI National Facility via the provision of computing resources.

References

Archibald S, Roy DP, Van Wilgen BW, Scholes RJ (2009) What limits fire? An examination of drivers of burnt area in southern Africa. *Global Change Biology* **15**, 613–630. doi:10.1111/J.1365-2486.2008.01754.X

Beer T, Williams A (1995) Estimating Australian forest fire danger under conditions of doubled carbon dioxide concentrations. *Climatic Change* **29**, 169–188. doi:10.1007/BF01094015

Blanchi R, Lucas C, Leonard F, Finkele K (2010) Meteorological conditions and wildfire-related house loss in Australia. *International Journal of Wildland Fire* **19**, 914–926. doi:10.1071/WF08175

Bradstock RA (2010) A biogeographic model of fire regimes in Australia: current and future implications. *Global Ecology and Biogeography* **19**, 145–158. doi:10.1111/J.1466-8238.2009.00512.X

Bradstock RA, Gill AM (2001) Living with fire and biodiversity and the urban edge: in search of a sustainable solution to the human protection problem. *Journal of Mediterranean Ecology* **2**, 179–195.

Christensen JH, Hewitson B, Busuioc A, Chen A, Gao X, Held I, Jones R, Kolli RK, Kwon W-T, Laprise R, Magaña Rueda V, Mearns L, Menéndez CG, Räisänen J, Rinke A, Sarr A, Whetton P (2007) Regional Climate Projections. In 'Climate Change 2007: The Physical Science Basis. Contribution of Working Group I to the Fourth Assessment Report of the Intergovernmental Panel on Climate Change'. (Eds S Solomon, D Qin, M Manning, Z Chen, M Marquis, KB Averyt, M Tignor, HL Miller) pp. 847–940. (Cambridge University Press: Cambridge, UK)

Deeming JE, Burgan RE, Cohen JE (1977) The National Fire-Danger Rating System: basic equations. USDA Forest Service, Intermountain Forest and Range Experiment Station, General Technical Report INT-39. (Ogden, UT)

Dowdy AJ, Mills GA, Finkele K, de Groot W (2010) Index sensitivity analysis applied to the Canadian Forest Fire Weather Index and the McArthur Forest Fire Danger Index. *Meteorological Applications* **17**, 298–312.

Engel CB, Lane TP, Reeder MJ, Rezny M (2012) The meteorology of Black Saturday. *Quarterly Journal of the Royal Meteorological Society* [Published online early 25 June 2012]. doi:10.1002/QJ.1986

Evans JP, McCabe MF (2010) Regional climate simulation over Australia's Murray–Darling basin: a multi-temporal assessment. *Journal of Geophysical Research* **115**, D14114. doi:10.1029/2010JD013816

Evans JP, Westra S (2012) Investigating the mechanisms of diurnal rainfall variability using a regional climate model. *Journal of Climate*. doi:10.1175/JCLI-D-11-00616.1

Evans JP, Pitman AJ, Cruz FT (2011) Coupled atmosphere and land surface dynamics over southeast Australia: a review, analysis and identification of future research priorities. *International Journal of Climatology* **31**, 1758–1772. doi:10.1002/JOC.2206

Evans JP, McGregor JL, McGuffie K (2012*a*) Future Regional Climates. In 'The Future of the World's Climate'. (Eds A Henderson-Sellers, K McGuffie) pp. 223–252. (Elsevier: Oxford, UK)

Evans JP, Ekstrom M, Ji F (2012*b*) Evaluating the performance of a WRF physics ensemble over south-east Australia. *Climate Dynamics* **39**, 1241–1258. doi:10.1007/S00382-011-1244-5

Flannigan MD, Krawchuk MA, De Groot WJ, Wotton BM, Gowman LM (2009) Implications of changing climate for global wildland fire. *International Journal of Wildland Fire* **18**, 483–507. doi:10.1071/WF08187

Gordon HB, Rotstayn LD, McGregor J, Dix MR, Kowalczyk EA, Farrell SPO, Waterman LJ, Hirst AC, Wilson SG, Collier MA, Watterson IG, Elliott TI (2002) The CSIRO Mk3 climate system model. CSIRO Atmospheric Research, Technical Report 60. (Melbourne)

Griffiths D (1999) Improved formula for the drought factor in McArthur's Forest Fire Danger Meter. *Australian Forestry* **62**, 202–206.

Hennessy K, Lucas C, Nicholls N, Bathols J, Suppiah R, Ricketts J (2005) Climate change impacts on fire-weather in south-east Australia. CSIRO and Bureau of Meteorology, Consultancy report for the New South Wales Greenhouse Office, Victorian Department of Sustainability and Environment, ACT Government, Tasmanian Department of Primary Industries, Water and Environment and the Australian Greenhouse Office. (Melbourne)

Jakob D (2010) Challenges in developing a high-quality surface wind-speed data-set for Australia. *Australian Meteorological and Oceanographic Journal* **60**, 227–236.

Kalnay E, Kanamitsu M, Kistler R, Collins W, Deaven D, Gandin L, Iredell M, Saha S, White G, Woollen J, Zhu Y, Leetmaa A, Reynolds R, Chelliah M, Ebisuzaki W, Higgins W, Janowiak J, Mo KC, Ropelewski C, Wang J, Jenne R, Joseph D (1996) The NCEP/ NCAR 40-year reanalysis project. *Bulletin of the American Meteorological Society* **77**, 437–471. doi:10.1175/1520-0477(1996)077<0437:TNYRP>2.0.CO;2

Keetch JJ, Byram GM (1968) A drought index for forest fire control. USDA Forest Service, Southeastern Forest Experiment Station, Research Paper SE-38. (Ashville, NC)

King A, Alexander L, Donat M (2012) The efficacy of using gridded data to examine extreme rainfall characteristics: a case study for Australia. *International Journal of Climatology* [Published online early 11 September 2012]. doi:10.1002/JOC.3588

Klein Tank AMG, Zwiers FW, Zhang X (2009) Guidelines on analysis of extremes in a changing climate in support of informed decisions for adaptation. World Meteorological Organization, WCDMP-72, WMO-TD/Number 1500. (Geneva Switzerland)

Krawchuk MA, Moritz MA, Parisien M, Van Dorn J, Hayhoe K (2009) Global pyrogeography: the current and future distribution of wildfire. *PLoS ONE* **4**(4), e5102. doi:10.1371/JOURNAL.PONE.0005102

Lucas C (2010*a*) On developing a historical fire weather data-set for Australia. *Australian Meteorological and Oceanographic Journal* **60**, 1–14.

Lucas C (2010*b*) A high-quality historical humidity database for Australia. CSIRO and Bureau of Meteorology, CAWCR Technical Report Number 24. (Melbourne)

Luke R, McArthur A (1978) 'Bush Fires in Australia.' (Australian Government Publishing Service: Canberra)

McArthur (1967) Fire behaviour in eucalypt forest. Commonwealth of Australia Timber Bureau, Leaflet 107. (Canberra)

Meehl GA, Stocker TF, Collins WD, Friedlingstein P, Gaye AT, Gregory JM, Kitoh A, Knutti R, Murphy JM, Noda A, Raper SCB, Watterson IG, Weaver AJ, Zhao Z-C (2007) Global climate projections. In 'Climate Change 2007: the Physical Science Basis. Contribution of Working Group I to the Fourth Assessment Report of the Intergovernmental Panel on Climate Change'. (Eds Solomon S, Qin D, Manning M, Chen Z, Marquis M, Averyt KB, Tignor M, Miller HL) pp. 589–662. (Cambridge University Press: Cambridge, UK)

Mölders N (2008) Suitability of the Weather Research and Forecasting (WRF) Model to predict the June 2005 fire weather for Interior Alaska. *Weather and Forecasting* **23**(5), 953–973. doi:10.1175/2008WAF2007062.1

Mölders N (2010) Comparison of Canadian Forest Fire Danger Rating System and National Fire Danger Rating System fire indices derived from Weather Research and Forecasting (WRF) model data for the June 2005 Interior Alaska wildfires. *Atmospheric Research* **95**(2–3), 290–306. doi:10.1016/J.ATMOSRES.2009.03.010

Noble IR, Barry GAV, Gill AM (1980) McArthur's fire danger meters expressed as equations. *Australian Journal of Ecology* **5**, 201–203. doi:10.1111/J.1442-9993.1980.TB01243.X

NSW Office of Environment and Heritage (2012) Improving regional climate projections. Available at http://www.environment.nsw.gov.au/research/Regionalclimate.htm [Verified 28 August 2012]

Osborn TJ, Hulme M (1998) Evaluation of the European daily precipitation characteristics from the Atmospheric Model Intercomparison Project. *International Journal of Climatology* **18**, 505–522. doi:10.1002/(SICI)1097-0088(199804)18:5<505::AID-JOC263>3.0.CO;2-7

Parkyn K, Yeo C, Bannister T (2010) Meteorological Lessons Learned from 'Black Saturday', the 7 February 2009 Victorian Fires. Victoria Regional Office, Bureau of Meteorology. (Melbourne)

Perkins SE, Pitman AJ, Holbrook NJ, McAneney J (2007) Evaluation of the AR4 Climate Models' simulated daily maximum temperature, minimum temperature, and precipitation over Australia using probability density functions. *Journal of Climate* **20**, 4356–4376. doi:10.1175/JCLI4253.1

Pitman AJ, Arneth A, Ganzeveld L (2012) Regionalizing global climate models. *International Journal of Climatology* **32**, 321–337. doi:10.1002/JOC.2279

Randall DA, Wood RA, Bony S, Coleman R, Fichefet T, Fyfe J, Kattsov V, Pitman A, Shukla J, Srinivasan J, Stouffer RJ, Sumi A, Taylor KE (2007) Climate models and their evaluation. In 'Climate Change 2007: the Physical Science Basis. Contribution of Working Group I to the Fourth Assessment Report of the Intergovernmental Panel on Climate Change'. (Eds Solomon S, Qin D, Manning M, Chen Z, Marquis M, Averyt KB, Tignor M, Miller HL) pp. 589–662. (Cambridge University Press: Cambridge, UK)

Russell-Smith J, Yates CP, Whitehead PJ, Smith R, Craig R, Allan GE, Thackway R, Frakes I, Cridland S, Meyer MCP, Gill AM (2007) Bushfires 'down under': patterns and implications of contemporary Australian landscape burning. *International Journal of Wildland Fire* **16**, 361–377. doi:10.1071/WF07018

Shimada S, Ohsawa T (2011) Accuracy and characteristics of offshore wind speeds simulated by WRF. *Scientific Online Letters on the Atmosphere* **7**, 21–24. doi:10.2151/SOLA.2011-006

Shimada S, Ohsawa T, Chikaoka S, Kozai K (2011) Accuracy of the wind speed profile in the lower PBL as simulated by the WRF model. *Scientific Online Letters on the Atmosphere* **7**, 109–112. doi:10.2151/SOLA.2011-028

Skamarock WC, Klemp JB, Dudhia J, Gill DO, Barker DM, Duda MG, Huang X-Y, Wang W, Powers JG (2008) A description of the advanced research WRF version 3. National Center for Atmospheric Research, NCAR Technical Note. (Boulder, CO)

Van Wagner CE (1987) Development and structure of the Canadian Forest Fire Weather Index System. Canadian Forestry Service, Technical Report 35. (Ottawa, ON)

doi:10.1071/WF12048_AC

Supplementary material

Fire weather simulation skill by the Weather Research and Forecasting (WRF) model over south-east Australia from 1985 to 2009

Hamish Clarke[A,B,D], *Jason P. Evans*[A], *Andrew J. Pitman*[C]

[A]Climate Change Research Centre, University of New South Wales, Sydney, NSW 2052, Australia

[B]Climate and Atmospheric Science Branch, NSW Office of Environment and Heritage, Sydney, NSW, Australia.

[C]ARC Centre of Excellence for Climate System Science, University of New South Wales, Sydney, NSW 2052, Australia.

[D]Corresponding author. Email: h.clarke@student.unsw.edu.au

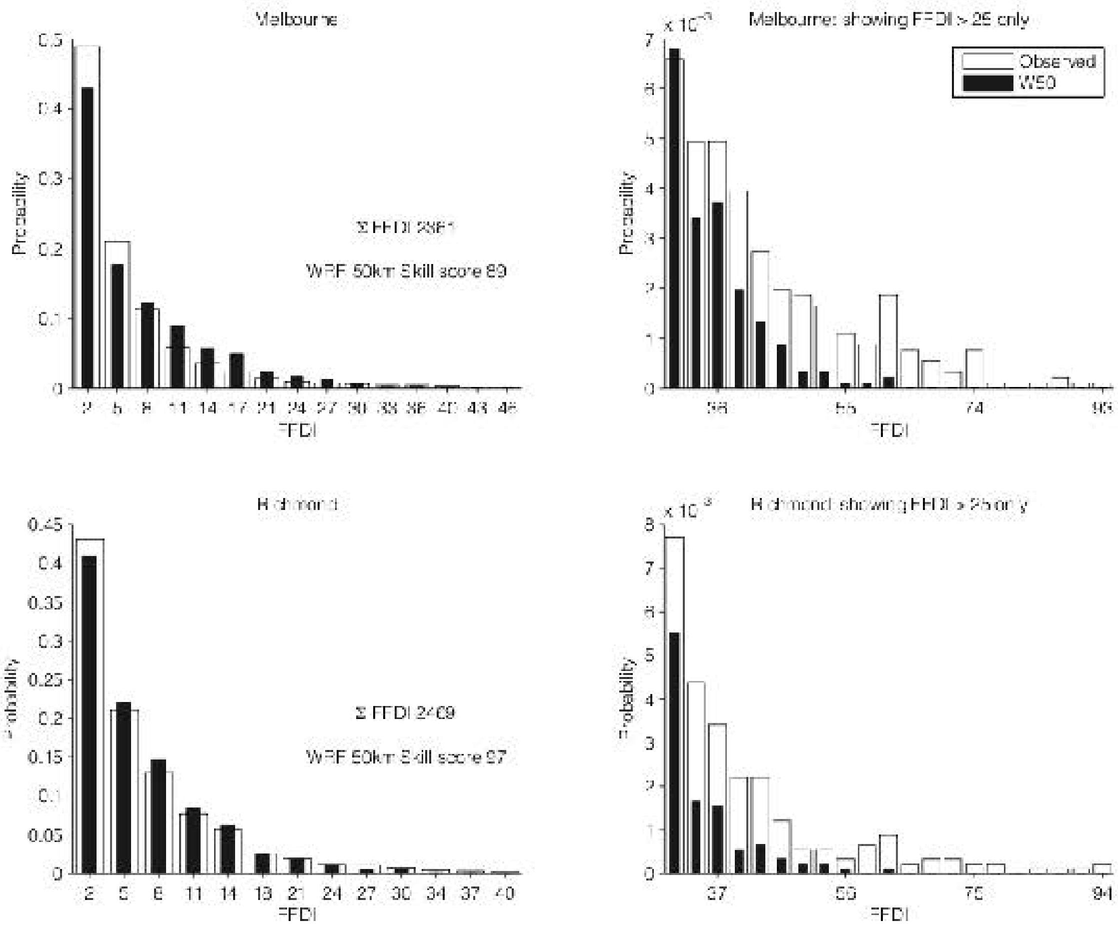

Fig. S1. Same as Fig. 5, but with WRF 50 km instead of WRF 10 km.

doi:10.1071/WF12048_AC

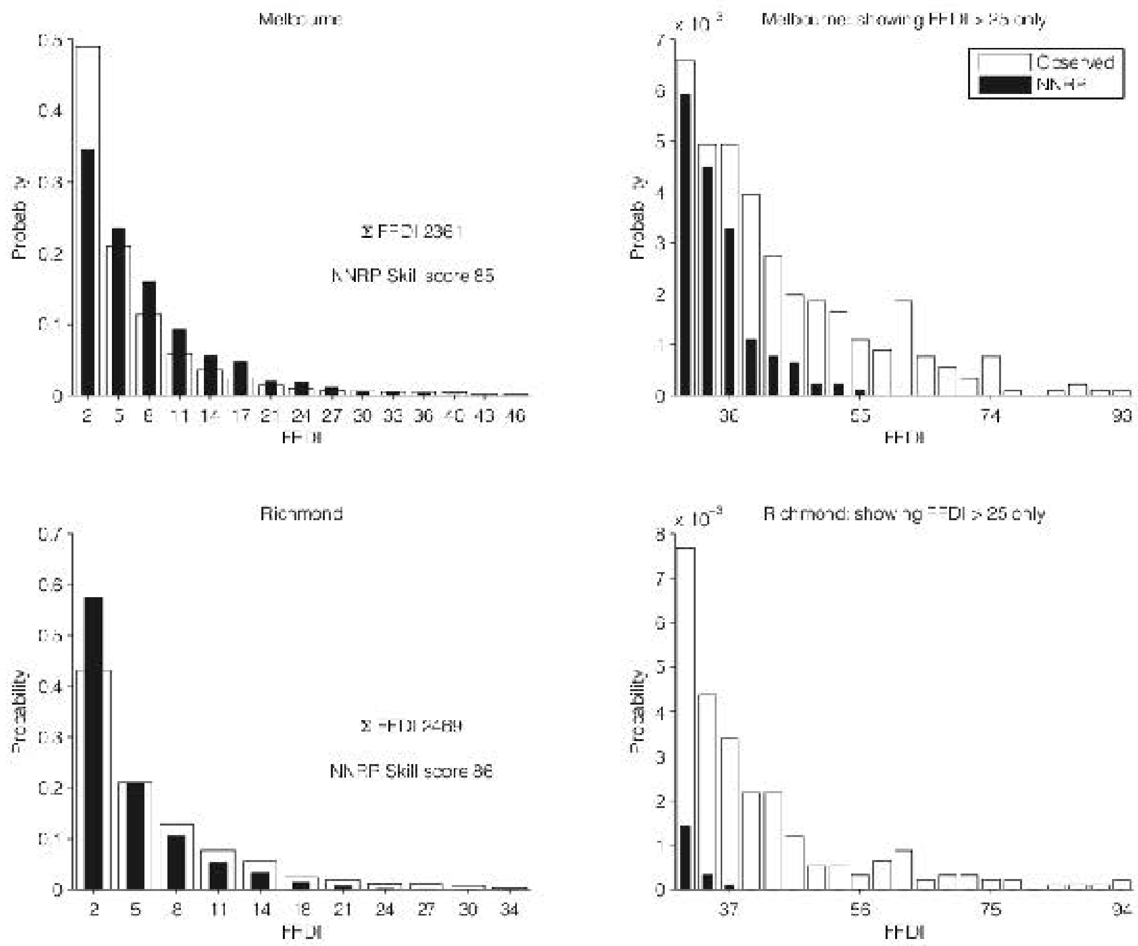

Fig.S2. Same as Fig. 5, but with NNRP instead of WRF 10 km.

Chapter 5 Summary

Evaluation of a regional climate model fire weather simulation

The evaluation of WRF against multidecadal station-based observations of FFDI suggests it is a very useful tool for modelling fire weather over southeast Australia. WRF simulated the main features of the FFDI distribution and its spatial variation, with an overall positive bias. Errors in WRF simulating mean FFDI conditions appear connected with errors in simulating relative humidity. In contrast, errors in simulating extreme FFDI conditions are more linked with errors in wind simulation. Improving the resolution of WRF from 50 km to 10 km generally improved model performance. A fuller evaluation of WRF's skill in simulating FFDI would be facilitated by an improved observational FFDI data-set. Ideally this would be grid-based, and would incorporate longer term and higher quality records than those available at the time of writing Chapter 5.

Based on the evidence presented in Chapter 5, WRF is well placed to add value to GCM projections of fire weather in Australia. A different way of adding further value to projections of future bushfire risk is to expand the analysis from fire weather conditions to include one of the other major drivers of bushfire incidence: fuel load, fuel moisture or ignitions. Chapter 6 aims to lay the foundation for such an expansion, by developing a model capable of projecting changes in bushfire fuel load.

Chapter 6 Overview

Simulation of fuel load with a land surface model

The previous chapters dealt with a single major driver of bushfire risk: fire weather conditions. Chapter 6 lays the foundations for a broader evaluation of future bushfire risk by examining a second major driver, fuel load. The meteorological variables required for assessing future changes in fire weather conditions are generally directly available as output from global and regional climate models. In contrast, simulating changes in biomass growth or fuel load requires a significant transformation of climate model data. Climate models used in CMIP5 do not simulate fuel load and this is not a variable reported in simulations assessed by the IPCC's Fifth Assessment Report. Simulating fuel loads is complicated by the need to factor in the potential response of vegetation to changes in both climate and atmospheric CO_2 concentration.

The work described in Chapter 6 aims to address this challenge by exploring the use of net primary production (NPP) as a fuel load proxy. NPP is routinely simulated by land surface models (LSMs), which incorporate impacts of both climate and atmospheric CO_2. The land surface model used here is CABLE (Community Atmosphere Biosphere Land Exchange), which has an advantage over other process-based estimates of fuel load, as it provides the lower boundary conditions for the Australian Community Climate and Earth System Simulator (ACCESS), the Australian GCM used in numerical weather prediction and global intercomparisons.

The following study has been submitted to a peer reviewed journal and is reproduced as submitted:

Clarke H, Pitman AJ, Kala J, Carouge C, Haverd V (submitted) Multidecadal wildfire fuel load over Australia simulated with a land surface model. International Journal of Wildland Fire.

Author contributions

I led this project. The project was conceived over a long period of time through discussions between Andy Pitman (AP; my PhD supervisor), Vanessa Haverd (VH) and myself. The experimental design was led by myself and AP, incorporating substantial contributions from Jatin Kala (JK), Claire Carouge (CC) and VH. BIOS2 data was supplied by VH. I led the modelling, with regular input from JK and CC. I led the analysis and prepared the figures, incorporating comments from all other coauthors. I drafted the manuscript and incorporated comments from the other coauthors.

Title: Multidecadal wildfire fuel load over Australia simulated with a land surface model

Hamish Clarke[1,2,4] , Andrew J. Pitman[1], Jatin Kala[1], Claire Carouge[1], Vanessa Haverd[3]

[1]ARC Centre of Excellence for Climate System Science and Climate Change Research Centre, University of New South Wales, Sydney, 2052, Australia

[2]Climate and Atmospheric Science Branch, NSW Office of Environment and Heritage, PO Box 3720, Parramatta, 2150, Australia

[3]CSIRO Marine and Atmospheric Research, GPO Box 664, Canberra, 2601, Australia

For submission to International Journal of Wildland Fire

19th January, 2015

Suggested Running Head: Fuel load from a land surface model

Additional keywords: CABLE, wildland fire, bushfire, Net Primary Production

Summary: We model recent fuel load over Australia using a land surface model. By using productivity as a surrogate for load, the model incorporates influences of both climate and carbon dioxide fertilisation on fuel load, paving the way for better estimates of future load in Australia.

[4]h.clarke@student.unsw.edu.au

Abstract

This study explores the use of net primary production as a proxy for wildfire fuel load using a process-based land surface model. Fuel load is simulated over the Australian continent from 1980 to 2008 and ranges from 304 to 417 g C m^{-2} annually in temperate areas of Australia, 67 to 101 g C m^{-2} in grassland regions and 175 to 263 g C m^{-2} in subtropical areas. Annual fuel load anomalies were robust to variation in key model parameters and no simulations showed any statistically significant trend. We compared the relative contributions of fire weather and fuel load to variability in mean fire rate of spread in temperate regions, finding that most interannual variability is driven by fire weather rather than load. We show that net primary productivity can be used as a proxy to estimate fuel load, and that combining this simple proxy with a process-based model of net primary production allows a range of experiments to be conducted, including estimates of future changes in load. Although our results are specific to CABLE, the broad methodology could to applied to other land surface models.

Introduction

Net primary productivity (NPP), the net flux of carbon from the atmosphere into green plants, is a key ecosystem parameter, representing plant growth and biogeochemical cycling (Ito 2011). NPP has been equated to litter production (Matthews 1997) and been found to be approximately linearly correlated to standing biomass (Kindermann et al., 2008). In the wildfire context, these links provide a rationale for the use of NPP as a proxy for vegetation biomass i.e. fuel (Hely et al., 2004; Roberts et al., 2008; Moritz et al., 2012;). Plant biomass in turn exerts a major influence on wildfire incidence, fire behaviour, burning emissions and the carbon cycle (Archibald et al., 2009; Bradstock et al., 2010). The term fuel load is more commonly used than biomass when discussing the influence of vegetation on wildfire risk, but the two are not necessarily synonymous. In forests, for example, fuel load is often defined as a subset of biomass: surface litter (the foliage and twigs found on the forest floor), and possibly also near surface and elevated fuels, ladder fuels, canopy fuels and coarse woody debris (Watson 2009). Alternative classifications emphasise different fuel class sizes, which ignite and burn at different rates (Deeming et al., 1977). Whatever the definition, if NPP can be related to fuel load then it can be used as a surrogate in modelling it.

There is already evidence of changes in NPP over time, raising questions of whether there have been associated changes in fuel load. At a global level there is high confidence in increases in terrestrial NPP relative to the preindustrial era, but less agreement about trends over recent decades (Settele et al., 2014). Satellite observations over Australia from 1981 to 2006 show that nondeciduous perennial vegetation types have increased by 21% (Donohue et al. 2009). Deciduous, annual and ephemeral vegetation types decreased by 7% over the same period, although the result was not statistically significant. In a modelling study constrained by multiple observation types, NPP over Australia between 1990 and 2011 was found to be higher than almost every other 22-year period since 1900 (Haverd et al. 2013b). High continental NPP values were due to high NPP in the Tropics, Savanna and Desert, and were partially offset by below-median NPP in Mediterranean, Cool Temperate and Warm Temperate regions. A common factor of these modelled increases (decreases) in NPP was above (below) average rainfall in the area. The same study showed that rising CO_2 increased continental NPP by 13% compared with steady preindustrial forcing.

There are many methods available for modelling fuel load and NPP, both empirical and process-based. Process-based approaches to fuel load dynamics are incorporated in several major classes of models, including dynamical global vegetation models (DGVMs), landscape fire succession models and biogeochemical models. DGVMs in particular are widely used to model ecosystem process feedbacks and climate change impacts on terrestrial vegetation (Sitch et al., 2008; Scheiter and Higgins, 2009). While these models may not use NPP as a fuel load proxy per se, they allocate NPP into multiple load or litter pools based on the balance of litterfall and decomposition (e.g. Wang et al. 2010, Keane et al. 2011). Litterfall is typically linked to phenology and primary productivity, while decomposition is determined by a combination of heat and moisture. Although process-based approaches contain a range of biases and uncertainties (e.g. Sitch et al., 2008; Quillet et al., 2010; Ito 2011; Kelley et al., 2013), a key advantage is that they can incorporate the effects of both climate and carbon dioxide fertilisation on vegetation growth, which remains a key uncertainty in the response of terrestrial ecosystems to climate change (Donohue et al., 2013; Settele et al., 2014).

Land surface models (LSM) provide a process-based alternative to the models listed above. The major Australian LSM is the Community Atmosphere Biosphere Land Exchange (CABLE; Wang et al. 2011) model, a sophisticated LSM that simulates fluxes of heat, water and carbon. CABLE has been extensively evaluated (Abramowitz et al. 2008, Wang et al. 2011) and has been used at site-specific (Abramowitz et al. 2007), regional (Cruz et al. 2010), and global (Pitman et al. 2011, Zhang et al. 2011, Lorenz et al. 2014) scales. Critically, CABLE also provides the lower boundary condition for the Australian Community Climate and Earth System Simulator (ACCESS) coupled climate model used in numerical weather prediction (NWP) and global intercomparisons (Kowalczyk et al. 2013). The use of CABLE in this context provides an advantage over other process-based models that provide explicit measures of fuel load but are not routinely used for NWP or in Intergovernmental Panel on Climate Change (IPCC) assessments.

The goal of our study is to represent fuel load in CABLE, which, when operated within the ACCESS coupled model, will provide valuable data on current and future changes in fuel load. Three specific objectives are: 1) to determine a relationship between NPP and fuel load using available data, 2) to use this relationship in CABLE to model recent fuel load in Australia on a climatological timescale and 3) to estimate the uncertainty in simulated load by varying key model parameters.

Materials and methods

Our study has two parts (Figure 1). Part A aims to derive the relationship between fuel load and NPP. In the absence of observations of both quantities at a sufficiently long time-scale and over a range of ecosystem/vegetation types, the next best source of fuel load and NPP data is from an ecosystems model, ideally one that has been constrained using observations. The routine use of CABLE in Australia, including coupled to ACCESS and regional climate models, provides our rationale for part B of our study, which aims to simulate fuel load in CABLE by using the relationship derived in Part A.

Part A – Linking fuel load with NPP in BIOS2

BIOS2 model description

BIOS2 is a system for modelling the coupled energy, water and carbon balances of the Australian continent at fine spatial (0.05°) and temporal (hourly) resolutions (Haverd et al. 2013a). BIOS2 is limited to the Australian continent and was not designed to be coupled to the global ACCESS model. BIOS2 is partly based on the land surface model CABLE, but with some important differences (see Part B for a description of CABLE). Instead of using CABLE's default soil process and carbon modules, BIOS2 uses the SLI soil model (Haverd and Cuntz, 2010) and the CASA-CNP biogeochemical model (Wang et al. 2010). CASA-CNP allocates the carbon cycling through the terrestrial ecosystem into plant, litter and soil pools. There are three litter pools: metabolic (easily broken down), structural (resistant) and coarse woody debris. BIOS2 does not include fire so its litter pools should be considered potential, rather than realised, fuel load.

BIOS2 was run from 1990 to 2011 using meteorological forcing from the Bureau of Meteorology's Australian Water Availability Project data set (AWAP) (Grant et al. 2008, Jones et al. 2009). BIOS2 simulations were constrained by observations of many variables including streamflow, evapotranspiration, net ecosystem production and litterfall. BIOS2 has been evaluated against a number of point-based observations of quantities related to fuel load (Haverd et al. 2013a). When compared with 49 long-term above-ground fine litter observations across different climate zones (Barrett 2001), BIOS2 has an r^2 of only 0.1 and a RMSE of 315 g C m^{-2}. BIOS2 is better at predicting litterfall ($r^2 = 0.36$), above-ground biomass ($r^2 = 0.58$) and a proxy for gross primary productivity derived from net ecosystem production ($r^2 = 0.80$). Despite these biases, the use of observational constraints along with the best available gridded observations for Australia i.e. AWAP, means the simulations by BIOS2 are likely the best available estimates of quantities such as fuel load that are not measured often enough or over a large enough sample, to provide a direct observational data set.

We define fuel load as fine litter, the sum of metabolic and structural litter pools (e.g. Wang et al. 2010, Haverd et al. 2013a). Fires typically ignite in fuels found on the surface, and fine litter is widely used as a measure of fuel load in Australia. BIOS2 divides vegetation cover in each grid cell into persistent (mostly woody) and recurrent (mostly grassy) fractions based on partitioning of remotely sensed estimates of the fraction of photosynthetic absorbed radiation (fPAR; Haverd et al. 2013a). Figure 2 shows the mean annual fine litter from BIOS for a) woody and b) grassy fractions. This is consistent with the expected distribution, namely that woody fine litter is mostly along the southwest and southeast coast and in Tasmania, where most of the evergreen broadleaf forests are found. Grassy fine litter is mostly within the agricultural regions of the southwest and southeast wheat belts and parts of the northern tropical savannas.

To obtain the relationship between NPP and fuel load for BIOS2 we used the Pearson product-moment correlation coefficient on annual NPP and fine litter for the period 1990 to 2011. We also compared BIOS2's fine litter values with NPP values in the preceding year i.e. lag-1 correlation, on the grounds that it should be on the order of one seasonal cycle before NPP is translated into fine litter load. Given the strong correlation and lack of evidence for a non-linear relationship (Supplementary Figure 1), fine litter was related to NPP using ordinary least squares linear regression, with NPP taken as the independent variable. A linear model was calculated for each model grid cell with a significant ($p < 0.05$) lag-1 correlation.

To understand regional variation in model output, we use a modified Köppen climate classification, which separates Australia into 6 mostly-contiguous and climatically similar regions (Figure 3; Stern et al. 1999). The major Köppen zones are: equatorial, tropical, subtropical, desert, grassland and temperate. A linear model was also developed for each of these climate zones. Although one of the climate zones is called 'grassland', there is no separation of woody and grassy fractions in this or any other climate zone in our analysis; in all cases the combined pools are used.

Part B – Simulating fuel load and fuel load uncertainty in CABLE

<u>The CABLE model description</u>

CABLE is a land surface model designed to simulate fluxes of energy, water, and carbon at the land surface and can be run fully coupled to an atmospheric model within a global or regional climate model ('online', e.g. Hirsch et al. 2014), or as an 'offline' model with prescribed meteorology (e.g. Kala et al. 2014). CABLE is a key part of the Australian Community Climate Earth System Simulator (ACCESS; see http://www.accessimulator.org.au), a fully coupled earth system science model and contributor to the Fifth Assessment Report (AR5) of the IPCC. The version used in this study is CABLEv1.4b.

In CABLEv1.4b, the one-layered, two-leaf canopy radiation module of Wang and Leuning (1998) is used for sunlit and shaded leaves and the canopy micrometeorology module of Raupach (1994) is used for computing surface roughness length, zero-plane displacement height, and aerodynamic resistance. The model also consists of a surface flux module to compute the sensible and latent heat flux from the canopy and soil, the ground heat flux, as well as net photosynthesis. A soil module is used for the transfer of heat and water within the soil and snow, and an ecosystem carbon module based on Dickinson et al. (1998) is used for the terrestrial carbon cycle. A detailed description of CABLE is provided by Wang et al. (2011). CABLE, like most LSMs, uses plant functional types (PFTs), as opposed to the partitioning of cells between recurrent and persistent vegetation as BIOS2 does. Our implementation of CABLE uses fixed PFTs derived from the International Geosphere–Biosphere Programme (IGBP) land-use classification map.

Simulations

CABLEv1.4b was used within the National Aeronautics and Space Administration Land Information System version 6.1 (LIS-6.1; Kumar et al. 2006, 2008), a flexible software platform designed as a land surface modeling and hydrological data assimilation system. A grid resolution of 0.25° was utilized, covering continental Australia (including Tasmania). The model was forced with meteorological data sourced from the Modern-Era Retrospective Analysis for Research and Applications (MERRA) reanalysis (Rienecker et al. 2011) at 3-hourly intervals from 1980 to 2008. The forcing variables included incoming longwave and shortwave radiation, air temperature, specific humidity, surface pressure, wind speed, and precipitation. The MERRA reanalysis was bias corrected for precipitation following Decker et al. (2013) using the AWAP gridded precipitation dataset. Monthly carbon dioxide concentrations were prescribed using measurements from Baring Head, New Zealand (Keeling et al. 2005). We omitted the first year of CABLE output as a spin-up period. Soil moisture initialisation can take longer than one year in drier environments but these are not the focus of our study.

To estimate uncertainty in NPP from CABLE, and hence fuel load, we carried out a series of sensitivity experiments using the upper, lower and middle estimates of three vegetation parameters that influence NPP (Supplementary Table 1). We refer to the set of simulations resulting from these structurally distinct instances of CABLE as an ensemble. Globally, the most important parameters in CABLE affecting gross primary production (GPP), and therefore affecting NPP, are the maximum carboxylation rate (v_{cmax}, the maximum ribulose-1,5-bisphosphate carboxylation rate of the leaves at the canopy top at a leaf temperature of 25°C) and Leaf Area Index (LAI, the total one-sided surface area of leaf per ground surface area; Lu et al., 2013). v_{cmax} partially determines the rate of photosynthesis and hence GPP and thereby NPP and is estimated as a function of leaf nitrogen per unit leaf area. LAI affects photosynthesis directly-in the ecosystem carbon module, where it also affects GPP and to a lesser extent autotrophic respiration. Finally, we varied the rooting depth (r). NPP is partially dependent on soil moisture since transpiration cannot occur in the absence of water. Varying r changes the amount of water available for transpiration and photosynthesis and therefore, GPP and NPP. Root depths are not well known and therefore r remains a parameter that is uncertain but important.

We prescribe LAI using the maximum, mean and minimum ensemble members from Kala et al. (2014). These are drawn from a 15-member ensemble, based on the Moderate Resolution Imaging Spectroradiometer (MODIS) LAI product and gridded temperature and precipitation observations, and designed to examine the influence of realistic interannual variations in LAI on the surface energy and carbon balance in CABLE. We derive upper and lower estimates of v_{cmax} values from Kattge et al. (2009), but since their values did not match the default CABLE values for each plant functional type exactly, we varied the CABLE values by the ratio of standard deviation to mean values as shown in Table 3 of Kattge et al. (2009). Upper and lower estimates for r were derived by varying default values by the standard deviation of the default r values for all plant functional types (0.015). We use the key 1 = low, 2 = default

(v_{cmax}, r) or mean (LAI), 3 = high to describe our experiments. For example, L3V1R2 is the ensemble member with a high LAI parameter value, a low v_{cmax} parameter value and the default r value.

To frame changes in fuel load linked with NPP with changes in meteorological forcing we examined the relative impact of load and weather in forested areas using rate of spread of fire (McArthur 1967). The rate of spread (R, in km h^{-1}) is defined as

$$R = 0.0012 \times F \times L$$

where F is the McArthur Forest Fire Danger Index (FFDI) and L is load in t ha^{-1}. FFDI is defined as

$$F = 2 \times \exp(-0.45 + 0.987\log D + 0.0345H + 0.0338T + 0.0234U)$$

where D is a drought factor (0–10), H is the relative humidity (%), T is the air temperature (°C) and U is the wind speed at 10 m in the open (km h^{-1}) (Noble et al. 1980).

This provides a simple way of comparing the impact of changes in load and fire weather conditions. We restrict our analysis to the temperate region, which contains the forest types in which this rate of spread function was calibrated. Because fuel load is not a significant driver of the rate of spread of grass fires, compared to fuel moisture and weather (Cheney et al. 1998, Sharples and McRae 2013), we make no comparison of the relative influence of load and weather on grassland fire rate of spread.

Results

Part A – Linking fuel load with NPP in BIOS2

The correlation between fine litter and NPP from BIOS2 in the same year was not significant in most of southern and central Australia (data not shown). In contrast, the lag-1 correlation between fine litter and NPP was statistically significant ($p < 0.05$) for most of Australia, with most correlation coefficients ranging from 0.6 to 0.95 (Figure 4, areas marked in white are not statistically significant). The lag-1 correlation is weakest, and sometimes not significant, in northern Australia, as well as some regions of southern central Australia. The areas with a poor lag-1 correlation correspond closely to areas where the lag-0 correlation (i.e. between fine litter and NPP in the same year) is significant and/or greater than the lag-1 correlation. Lag-1 correlations were significant in each climate zone (Table 1) and were greater than those between fine litter and NPP in the same year. The lag-1 correlation was greatest in the subtropical, temperate and grassland climate zones and lowest in the equatorial zone.

The generally strong and significant lag-1 correlation between NPP and fine litter obtained from BIOS2 forms the basis for using this correlation to derive fuel load from NPP in CABLE. Although correlations are significant for the desert, tropical and equatorial regions as a whole, we omit these regions from our analysis because a large fraction of individual grid cells found in the tropical and equatorial regions have a low correlation or none at all, and in the desert zone the overall litter and NPP amounts are small.

Part B – Simulating fuel load and fuel load uncertainty in CABLE

The boxplot in Figure 5 shows the mean daily NPP from of all 27 CABLE ensemble members obtained by perturbing LAI, v_{cmax} and r. The median NPP is 1.10 g C m^{-2} d^{-1}, while the lowest (0.70 g C m^{-2} d^{-1}) and highest (1.51 g C m^{-2} d^{-1}) ensemble NPP values differ by a factor of about two. The lowest (highest) values correspond to the ensemble members with all three parameters at their low (high) values. Figure 5 also shows the change in NPP that results from varying a single parameter. NPP is much more sensitive to the prescribed changes in LAI and v_{cmax} than r, with v_{cmax} having a slightly larger effect than LAI. Lower LAI and v_{cmax} parameter values lead to a slightly larger departure from the default than high values. The largest variations in NPP result from changes in more than one parameter i.e. high values of both LAI and v_{cmax} lead to higher NPP than either parameter alone. Although it is not the focus of this study, ensemble results provide evidence for interacting, rather than additive, effects between vegetation parameters.

Figure 6 shows fine litter from CABLE based on the linear model for each grid cell, developed using BIOS2 as was described in Part A. The spatial pattern of average fine litter is very similar between the lowest, median and highest ensemble members. Fine litter is highest in the southwest and southeast, including Tasmania, and along the coastal strip extending from the southeast up to far northeast Australia. Litter is relatively low in inland areas. The prescription of LAI strongly influences the spatial distribution of fine litter, both within and between ensembles. Changes resulting from increasing parameter values are most noticeable in those regions where fine litter is already high.

Mean fine litter from CABLE averaged by climate zone is shown in Figure 7. Load is highest in the temperate zone (ensemble range 304 to 417 g C m^{-2}) , followed by the equatorial (186 to 268 g C m^{-2}), subtropical (175 to 263 g C m^{-2}) and tropical (167 to 248 g C m^{-2}) zones. Load in grasslands (67 to 101 g C m^{-2}) is substantially lower and lowest in the desert climate zone (32 to 47 g C m^{-2}). Error bars in Figure 7 show the standard deviation (calculated on the zone-averaged timeseries), which is proportional to fine litter amount. This can also be seen in Figure 8, which shows the annual time series in mean fine litter anomaly across all 27 ensembles, for the temperate (Figure 8a), grassland (Figure 8b) and subtropical (Figure 8c) zones. The temperate zone displays the most interannual variability, followed by subtropical and grassland areas.

There is a considerable degree of coherence (i.e. robustness to parameter variation) amongst ensemble members in the sequence of fine litter anomalies, in terms of both direction and magnitude of change. The ensemble range in fine litter anomaly is proportional to the mean absolute anomaly, such that the greater the deviation from mean values, the greater the spread in ensemble values. This effect is strongest in grassland areas ($r^2 = 0.89$, $p = 0.000$), followed by subtropical areas ($r^2 = 0.82$, $p = 0.000$) and then temperate areas ($r^2 = 0.74$, $p = 0.000$). There is no significant trend for any ensemble members within the temperate, grassland or tropical zones ($p<0.05$). At a significance level of 0.1, three ensemble members in the subtropical zone display an increasing trend: L3V1R1 ($p = 0.07$), L3V1R2 ($p = 0.07$), L3V1R3 ($p = 0.09$). A high value of LAI and a low value of v_{cmax} are common to these three positive trends at a weaker significance level.

BIOS2 fine litter is lower than that simulated by CABLE over the same period, with the greatest difference in the temperate (60 g C m^{-2} d^{-1}) and subtropical (33 g C m^{-2} d^{-1}) regions and lowest in the grassland region (7 g C m^{-2} d^{-1}).

Figure 9 shows the sensitivity of fire rate of spread to fuel load and fire weather conditions in the temperate zone. Rate of spread calculated from annually varying fine litter and FFDI fluctuates between about 0.06 and 0.19 km h^{-1}. For any given year, rate of spread has an uncertainty of between 0.02 and 0.04 km h^{-1}, due to uncertainty in fine litter from the CABLE sensitivity ensemble. Rate of spread closely tracks interannual variation in mean annual FFDI, as shown by the overlapping curves showing rate of spread calculated from both varying and constant fine litter. In contrast, holding FFDI constant at its annual mean value results in a rate of spread with far less interannual variation, reflecting the lower variation in fine litter, even taking into account the wide range of ensemble litter values. There is no significant trend in rate of spread over the period of the simulation (ensemble p values between 0.25 and 0.85).

Discussion

We have developed a model of fuel load that combines the physical rigour and consistency of a land surface model with a simple empirical relationship between productivity in one year and load in the next. The link between fine litter and NPP is derived from the observationally constrained ecosystem model BIOS2, and is statistically significant for both most individual grid cells and area averages in temperate, grassland and subtropical areas of Australia. The relationship is far weaker in tropical and equatorial regions, and northern Australia in general. Much of the affected areas are grassy rather than woody, where the time between plant growth (i.e. primary productivity) and availability for burning as litter is much shorter. However, there are other regions of grassy vegetation, particularly in southern Australia, where the litter is significantly correlated to the previous year's, but not the same year's NPP. Given these weaknesses, and the overall low litter and NPP amounts in desert regions, we focus on the temperate, grassland and subtropical zones. Tradeoffs in model applicability such as these are unsurprising given the simplicity of our approach and the complexities of Australian fire seasonality and fuel dynamics (Russell-Smith et al. 2007, Murphy et al. 2012).

There is considerable interannual variation in simulated load, but little indication of a trend over the study period of 1980 to 2008. Variation of model parameter values within the overall parameter space does not strongly influence trends in NPP and load, although absolute values of these quantities were sensitive to variations in the maximum carboxylation rate and LAI. 3 of the 81 total ensemble members recorded a weakly significant ($p<0.10$) increasing trend in load. A common feature of each of these was a high value of leaf area index combined with low value of the maximum carboxylation rate parameter, a result we plan to explore further in the future.

We compared the relative influence of load and fire weather conditions on fire behaviour in the temperate region, using a simple formulation of rate of spread (Figure 9). Even accounting for the wide range of load estimates arising from the sensitivity ensemble, the rate of spread is far more sensitive to variation in FFDI than changes in fuel amount. Although we underestimate maximum potential fuel load by using mean annual values, the same statistic is applied to FFDI. Moreover, while mean load may be close to representative of actual load when a wildfire takes place, mean annual FFDI may be an order of magnitude below that experienced during major wildfires. Given that significant increases in FFDI have been projected for this part of the world (Clarke et al. 2011, Fox-Hughes et al. 2014), this suggests that future changes in load are not likely to be an important contributor to fire rate of spread in temperate regions, except where these changes are exceptionally high. However, these findings also reflect the construction of the rate of spread function and do not imply that fire weather is or will become more important the load in determining fire behaviour or other measures of fire risk. Regional variation in fire regimes is strongly linked to differences in the relative importance of load, fuel availability, weather conditions and ignitions in limiting overall wildfire incidence (Bradstock et al., 2010).

Since the link between fine litter and NPP is simple, our model cannot account for mechanistic changes in litterfall and litter decomposition, the two processes that translate primary productivity into fuel load amount. However, the model of NPP in CABLE is mechanistic and is sensitive to changes in climate forcing and atmospheric carbon dioxide concentration. There is thus the potential to incorporate major influences on the evolution of a key driver of fuel load. This contrasts with the negative exponential model (Jenny et al., 1949; Olson et al., 1963), which assumes a fixed fuel load amount at equilibrium. This widely used, empirical model has been modified in the past to show variation about a steady state value, but, in comparison to our modeling approach, this is not typically tied to drivers of litter amount. Conversely, unlike the negative exponential model, our model does not account for disturbance (i.e. fire) and post-fire recovery of load. Such a feature could be added to the model, for instance by periodically setting NPP close to zero to represent the incidence of wildfire, with the existing observations of fuel load accumulation serving as a test of model performance.

Our model is vulnerable to biases and weaknesses in CABLE and BIOS2. Despite significant differences, these models are not entirely independent because BIOS2 is based on a modified version of CABLE. The relatively poor performance of BIOS2 in simulating one set of litter observations is concerning, but other related quantities are modeled more skillfully and any litter simulation should be interpreted in light of the disparate nature of litter observations (Keane et al., 2012), which do not share a common methodology and are subject to large errors from fine scale heterogeneity (Haverd et al. 2013a). CASA-CNP, the biogeochemical model within BIOS2, has been run with a much coarser grid than BIOS2 (220 km compared to ~5 km for BIOS2) and found to agree well with previous global estimates of total fine litter production and total fine litter pool size (Wang et al. 2010). Ultimately, rigorous evaluation of our model, BIOS2 and other landscape-scale models of load over Australia, would benefit from the development of a long term, high quality, gridded observational dataset of fuel load.

There are several other aspects of our model which may limit its applicability. As mentioned above, we have so far only examined annual mean values, rather than seasonal or finer time scale variation in load, including extremes. Other definitions of fuel load are possible (e.g. Migliavacca et al. (2013) include coarse woody debris) and the model does not address fuel strata or structure, which can be more important to aspects of fire behaviour than overall fuel mass (Cheney et al. 1992, Gould et al. 2007, Hines et al. 2010, Zylstra 2011). At 25 km horizontal resolution, the model is too coarsely grained to address detailed variation in vegetation and corresponding implications for fire management.

However, our aim is not to provide fuel estimates for detailed fire behaviour modelling at specific locations. Our aim is to investigate the response of wildfire fuel load to climate and atmospheric carbon dioxide concentration at a regional to continental scale. Using this model we will drive CABLE with output from dynamically downscaled climate model projections (Evans et al. 2014), combining estimates of fuel load with projections of changes in fire weather conditions to investigate the trajectories of weather and load in contributing to overall wildfire risk. Finally, although our methodology can be used in other land surface models, its application in CABLE has important implications for research capacity in Australia. CABLE is a community model, with users in weather forecasting, climate change projections, water resources management, carbon management and accounting, environmental information and accounting and integrated assessment (Law et al. 2012).

Acknowledgements

We thank Ying Ping Wang and Bernard Pak for help with CABLE parameter selection. This study was supported by the Australian Research Council Centre of Excellence for Climate System Science grant CE110001028. The computational modeling was supported by the NCI National Facility at the ANU, Australia.

References

Abramowitz G, Pitman AJ, Gupta H, Kowalczyk E, Wang Y (2007) Systematic bias in land surface models. *Journal of Hydrometeorology* **8**, 989–1001. doi:10.1175/JHM628.1.

Abramowitz G, Leuning R, Clark M, Pitman AJ (2008). Evaluating the performance of land surface models. *Journal of Climate* **21**, 5468–5481. doi:10.1175/2008JCLI2378.1.

Archibald S, Roy DP, van Wilgen BW, Scholes RJ (2009) What limits fire? An examination of drivers of burnt area in Southern Africa. *Global Change Biology* **15**, 613–630.

Barrett DJ (2001). NPP Multi-Biome: VAST Calibration Data. Oak Ridge National Laboratory Distributed Active Archive Centre. (Oak Ridge, TN)

Bradstock, R (2010). A biogeographic model of fire regimes in Australia: current and future implications. *Global Ecology and Biogeography* **19,** 145-158.

Cheney NP, Gould JS, Knight I (1992) A Prescribed Burning Guide for Young Regrowth Forest of Silvertop Ash. Forestry Commission of New South Wales, Research Paper No. 16. (Sydney, NSW)

Cheney NP, Gould JS, Catchpole WR (1998) Prediction of fire spread in grasslands. *International Journal of Wildland Fire* **8**, 1-13.

Clarke H, Smith PL, Pitman AJ (2011) Regional signatures of future fire weather over eastern Australia from global climate models. *International Journal of Wildland Fire* **20**, 550-562.

Cruz FT, Pitman AJ, Wang Y (2010). Can the stomatal response to higher atmospheric carbon dioxide explain the unusual temperatures during the 2002 Murray–Darling Basin drought. *Journal of Geophysical Research* **115**, D02101, doi:10.1029/2009JD012767.

Decker M, Pitman AJ, Evans JP (2013) Groundwater constraints on simulated transpiration variability over south- eastern Australian forests. *Journal of Hydrometeorology* **14**, 543–559. doi:10.1175/JHM-D-12-058.1.

Deeming JE, Burgan RE, Cohen JE. 1977. The National Fire-Danger Rating System – 1978. USDA Forest Service, Intermountain Forest and Range Experiment Station. General Technical Report INT-39. (Ogden, UT)

Dickinson RE, Shaikh M, Bryant R, Graumlich L (1998) Interactive canopies for a climate model. *Journal of Climate* **11**, 2823–2836. doi:10.1175/1520-0442(1998)011,2823:ICFACM.2.0.CO;2.

Donohue RJ, McVicar TR, Roderick ML (2009) Climate- related trends in Australian vegetation cover as inferred from satellite observations, 1981–2006. *Global Change Biology* **15**, 1025– 1039.

Donohue RJ, Roderick ML, McVicar TR, Farquhar GD (2013). Impact of CO_2 fertilization on maximum foliage cover across the globe's arid, warm environments. *Geophysical Research Letters* **40**, 3031-3035.

Evans JP, Ji F, Lee C, Smith P, Argueso D, Fita L (2014). Design of a regional climate modeling projection ensemble experiment – NARCliM. *Geoscientific Model Development* **7**, 621-629. doi:10.5194/gmd-7-621-2014

Fox-Hughes P, Harris RMB, Lee G, Grose MR, Bindoff NL (2014) Future fire danger climatology for Tasmania, Australia, using a dynamically downscaled regional climate model. *International Journal of Wildland Fire* doi:10.1071/WF13126

Gould JS, McCaw WL, Cheney NP, Ellis PF, Knight IK, Sullivan AL (2007a) 'Project Vesta. Fire in Dry Eucalypt Forest: Fuel Structure, Fuel Dynamics and Fire Behaviour.' (Ensis–CSIRO: Canberra, ACT; and WA Department of Environment and Conservation: Perth)

Grant I, Jones D, Wang W, Fawcett R, Barratt D (2008) Meteorological and remotely sensed datasets for hydrological modelling: A contribution to the Australian Water Availability Project, Catchment-scale Hydrological Modelling & Data Assimilation (CAHMDA-3) International Workshop on Hydrological Prediction: Modelling, Observation and Data Assimilation. (Melbourne, VIC).

Haverd V, Cuntz M (2010) Soil-Litter-Iso A one-dimensional model for coupled transport of heat, water and stable isotopes in soil with a litter layer and root extraction. *Journal of Hydrology* **388**, 438–455.

Haverd V, Raupach MR, Briggs PR, Canadell JG, Isaac P, Pickett-Heaps C, Roxburgh SH, van Gorsel E, Viscarra Rossel RA, Wang Z (2013a). Multiple observation types reduce uncertainty in Australia's terrestrial carbon and water cycles. *Biogeosciences* **10**, 2011-2040.

Haverd V, Raupach MR, Briggs PR, Canadell JG, Davis SJ, Law RM, Meyer CP, Peters GP, Pickett-Heaps C, Sherman B (2013b) The Australian terrestrial carbon budget. *Biogeosciences* **10**, 851-869.

Hély C, Caylor KK, Dowty P, Swap RJ, Shugart HH (2004). SAFARI 2000 Modeled Fuel Load in Southern Africa, 1999-2000. Data set. Available on-line [http://daac.ornl.gov/] from Oak Ridge National Laboratory Distributed Active Archive Center. (Oak Ridge, TN)

Hines F, Tolhurst KG, Wilson AAG, McCarthy GJ (2010). Overall Fuel Hazard Assessment Guide. Fourth edition. Department of Sustainability and Environment, Fire and Adaptive Management Report No. 82. (Melbourne, VIC).

Hirsch AL, Pitman AJ, Seneviratne SI, Evans JP, Haverd V (2014) Summertime maximum and minimum temperature coupling asymmetry over Australia determined using WRF. *Geophysical Research Letters* 10.1002/2013GL059055

Houldcroft C J, Grey WMF, Barnsley M, Taylor SM, Los SO, North PRJ (2009). New vegetation albedo parameters and global fields of soil background albedo derived from MODIS for use in a climate model. *Journal of Hydrometeorology* **10**, 183–198. doi:10.1175/2008JHM1021.1.

Ito, A (2011). A historical meta-analysis of global terrestrial net primary productivity: are estimates converging? *Global Change Biology* **17**, 3161-3175.

Jenny H, Gessel SP, Bingham FT (1949). Comparative study of decomposition rates of organic matter in temperate and tropical regions. *Soil Science* **68**, 419-432.

Jones, D, Wang W, Fawcett R (2009) High-quality spatial climate data-sets for Australia. *Australian Meteorological Magazine* **58**, 233–248.

Kala J, Decker M, Exbrayat J-F, Pitman AJ, Carouge C, Evans JP, Abramowitz G (2014) Influence of Leaf Area Index Prescriptions on Simulations of Heat, Moisture, and Carbon Fluxes. *Journal of Hydrometeorology* **15**, 489-503.

Kattge J, Knorr W, Raddatz T, Wirth C (2009) Quantifying photosynthetic capacity and its relationship to leaf nitrogen content for global-scale terrestrial biosphere models, *Global Change Biology* **15**, 976–991, doi:10.1111/j.1365-2486.2008.01744.x.

Keane RE, Loehman RA, Holsinger LM (2011). The FireBGCv2 landscape fire and succession model: a research simulation platform for exploring fire and vegetation dynamics. General Technical Report RMRS-GTR-255. USDA Forest Service, Rocky Mountain Research Station. (Fort Collins, CO)

Keane RE (2012). Describing wildland surface fuel loading for fire management: a review of approaches, methods and systems. *International Journal of Wildland Fire* **22**, 51-62. http://dx.doi.org/10.1071/WF11139

Keeling CD, Piper SC, Bacastow RB, Wahlen M, Whorf TP, Heimann M, Meijer HA (2005) Atmospheric CO_2 and $^{13}CO_2$ exchange with the terrestrial biosphere and oceans from 1978 to 2000: Observations and carbon cycle implications. In 'A History of Atmospheric CO2 and Its Effects on Plants, Animals, and Ecosystems'. (Eds JR Ehleringer, TE Cerling, MD Dearing) pp. 83-113. (Springer Verlag: New York)

Kelley DI, Prentice IC, Harrison SP, Wang H, Simard M, Fisher JB, Willis KO (2013) A comprehensive benchmarking system for evaluating global vegetation models. *Biogeosciences* **10**, 3313–3340. doi:10.5194/bg-10-3313-2013, 2013.

Kindermann GE, McAllum I, Fritz S, Obersteiner M (2008) A global forest growing stock, biomass and carbon map based on FAO statistics. *Silva Fennica* **42**, 387–396

Kowalczyk EA, Stevens L, Law RM, Dix M, Wang YP, Harman I, Haynes K, Srbinovsky J, Pak B (2013) The land surface model component of ACCESS: description and impact on the simulated surface climatology. *Australian Meteorological and Oceanographic Journal* **63**, 65–82.

Kumar SV, Peters-Lidard CD, Tian Y, Houser PR, Geiger J, Olden S, Lighty L, Eastman JL, Doty B, Dirmeyer P, Adams J, Mitchell K, Wood EF, Sheffield J (2006) Land Information System - An Interoperable Framework for High Resolution Land Surface Modeling. *Environmental Modelling and Software* **21**, 1402-1415.

Kumar SV, Peters-Lidard CD, Eastman JL, Tao W-K (2008) An integrated high-resolution hydrometeorological modeling testbed using LIS and WRF. *Environmental Modelling and Software* **23**, 169–181, doi:10.1016/j.envsoft.2007.05.012.

Law RM, Raupach MR, Abramowitz G, Dharssi I, Haverd V, Pitman AJ, Renzullo L, Van Dijk A, Wang Y-P (2012) The Community Atmosphere Biosphere Land Exchange (CABLE) model Roadmap for 2012-2017. CAWCR Technical Report No. 57 (CSIRO: Melbourne)

Lorenz R, Pitman AJ, Donat MG, AL Hirsch, Kala J, Kowalczyk EA, Law RM, Srbinovsky J (2014) Representation of climate extreme indices in the coupled atmosphere-land surface model ACCESS1.3b. *Geoscientific Model Development* **7**, 545–567. doi: 10.5194/gmd-7-545-2014.

Lu X, Wang Y-P, Ziehn T, Dai Y (2013) An efficient method for global parameter sensitivity analysis and its applications to the Australian community land surface model (CABLE). *Agricultural and Forest Meteorology* **182–183**, 292–303. doi:10.1016/ j.agrformet.2013.04.003.

Maathew E (1997) Global litter production, pools, and turnover times: Estimates from measurement data and regression models. *Journal of Geophysical Research* **102,** 18771-18800.

McArthur AG (1967). Fire behaviour in eucalypt forests. Forestry and Timber Bureau, Number 107. (Commonwealth Department of National Development: Canberra, ACT)

Migliavacca M, Dosio A, Camia A, Hobourg R, Houston-Durrant T, Kaiser JW, Khabarov N, Krasovskii AA, Marcolla B, San Miguel-Ayanz J, Ward DS, Cescatti A (2013) Modeling biomass burning and related carbon emissions during the 21st century in Europe. *Journal of Geophysical Research: Biogeosciences* **118**(4), 1732– 1747.

Moritz MA, Parisien M-A, Batllori E, Krawchuk ME, Van Dorn J, Ganz DJ, Hayhoe, K (2012) Climate change and disruptions to global fire activity. *Ecosphere* **3**, Article 49.

Murphy BP, Bradstock RA, Boer MM, Carter J, Cary GJ, Cochrane MA, Fensham RJ, Russell-Smith J, Williamson GJ, Bowman DMJS (2012) Fire regimes of Australia: a pyrogeographic model system. *Journal of Biogeography* **40**, 1048-1058. doi:10.1111/jbi.12065

Noble IR, Barry GAV, Gill AM (1980) McArthur's fire danger meters expressed as equations. *Australian Journal of Ecology* **5**, 201 – 203.

Olson JS (1963) Energy storage and the balance of producers and decomposers in ecological systems. *Ecology* **44**, 322-331.

Pitman AJ, Avila FB, Abramowitz G, Wang YP, Phipps SJ, de Noblet-Ducoudre N (2011) Importance of background climate in determining impact of land–cover change on regional climate. *Nature Climate Change* **1**, 472–475. doi:10.1038/ nclimate1294.

Quillet A, Peng C, Garneau M (2010) Toward dynamic global vegetation models for simulating vegetation-climate interactions and feedbacks: recent developments, limitations, and future challenges, *Environmental Reviews* **18**, 333–353.

Raupach MR (1994) Simplified expressions for vegetation roughness length and zero-plane displacement as functions of canopy height and area index. *Boundary-Layer Meteorology* **71**, 211– 216. doi:10.1007/BF00709229.

Rienecker MM, Suarez MJ, Gelaro R, Todling R, Bacmeister J, Liu E, Bosilovich MG, Schubert SD, Takacs L, Kim G-K, Bloom S, Chen J, Collins D, Conaty A, da Silva A, et al. (2011) MERRA - NASA's Modern-Era Retrospective Analysis for Research and Applications. *Journal of Climate* **24**, 3624-3648. doi:10.1175/JCLI-D-11-00015.1

Roberts G, Wooster MJ, Lagoudakis E (2008) Annual and diurnal African biomass burning temporl dynamics. *Biogeosciences Discussions* **5**, 3623-3663.

Russell-Smith J, Yates CP, Whitehead PJ, Smith R, Craig R, Allan GE, Thackway R, Frakes I, Cridland S, Meyer MCP, Gill AM (2007). Bushfires 'down under': patterns and implications of contemporary Australian landscape burning. *International Journal of Wildland Fire* **16**, 361–377. doi:10.1071/WF07018

Scheiter, S. & Higgins, S. I. Impacts of climate change on the vegetation of Africa: an adaptive dynamic vegetation modelling approach. Glob. Change Biol. 15, 2224–2246 (2009).

Settele J, Scholes R, Betts R, Bunn S, Leadley P, Nepstad D, Overpeck JT, Taboada MA (2014) Terrestrial and inland water systems. In 'Climate Change 2014: Impacts, Adaptation, and Vulnerability. Part A: Global and Sectoral Aspects. Contribution of Working Group II to the Fifth Assessment Report of the Intergovernmental Panel on Climate Change'. (Eds CB Field, VR Barros, DJ Dokken, KJ Mach, MD Mastrandrea, TE Bilir, M Chatterjee, KL Ebi, YO Estrada, RC Genova, B Girma, ES Kissel, AN Levy, S MacCracken, PR Mastrandrea, LL White) pp. 271-359. (Cambridge University Press: Cambridge, UK)

Sharples JJ, McRae RHD (2013) A fire spread index for grassland fuels. 20th International Congress on Modelling and Simulation, Adelaide, Australia, 1–6 December 2013.

Sitch S, Huntingford C, Gedney N et al (2008) Evaluation of the terrestrial carbon cycle, future plant geography and climate-carbon cycle feedbacks using five Dynamic Global Vegetation Models (DGVMs). *Global Change Biology* **14**(9), 2015–2039.

Stern H, de Hoedt G, Ernst J (1999) Objective classification of Australian climates. *Australian Meteorological Magazaine* **49**, 87-96.

Wang Y-P, Leuning R (1998) A two-leaf model for canopy conductance, photosynthesis and partitioning of available energy I: Model description and comparison with a multi-layered model. *Agricultural and Forest Meteorology* **91**, 89–111. doi:10.1016/ S0168-1923(98)00061-6.

Wang YP, Law RM, Pak B (2010) A global model of carbon, nitrogen and phos- phorus cycles for the terrestrial biosphere. *Biogeosciences* **7**, 2261–2282.

Wang YP, Kowalczyk E, Leuning R, Abramowitz G, Raupach MR, Pak B, van Gorsel E, Luhar A (2011). Diagnosing errors in a land surface model (CABLE) in the time and frequency domains. *Journal of Geophysical Research* **116**, G01034. doi:10.1029/2010JG001385.

Watson PJ (2009) Understanding Bushfire Fuels. A Report for the NSW Rural Fire Service. Centre for the Environmental Risk Management of Bushfires, University of Wollongong. (Wollongong, NSW)

Zhang Q, Wang YP, Pitman AJ, Dai JY (2011) Limitations of nitrogen and phosphorous on the terrestrial carbon uptake in the 20th century. *Geophysical Research Letters* **38**, L22701. doi:10.1029/2011GL049244.

Zylstra, P. 2011. Forest Flammability. Modelling and Managing a Complex System. PhD thesis, University of New South Wales, Australian Defence Force Academy.

List of Figures

lines show rate of spread calculated using default ensemble members, dotted lines show the lowest and highest ensemble members.

Supplementary Figure 1 Scatterplots of mean annual NPP and fine litter in each climate zone. Fine litter from same year as NPP is shown on left hand side, fine litter from the year following NPP is shown on the right hand side.

List of Tables

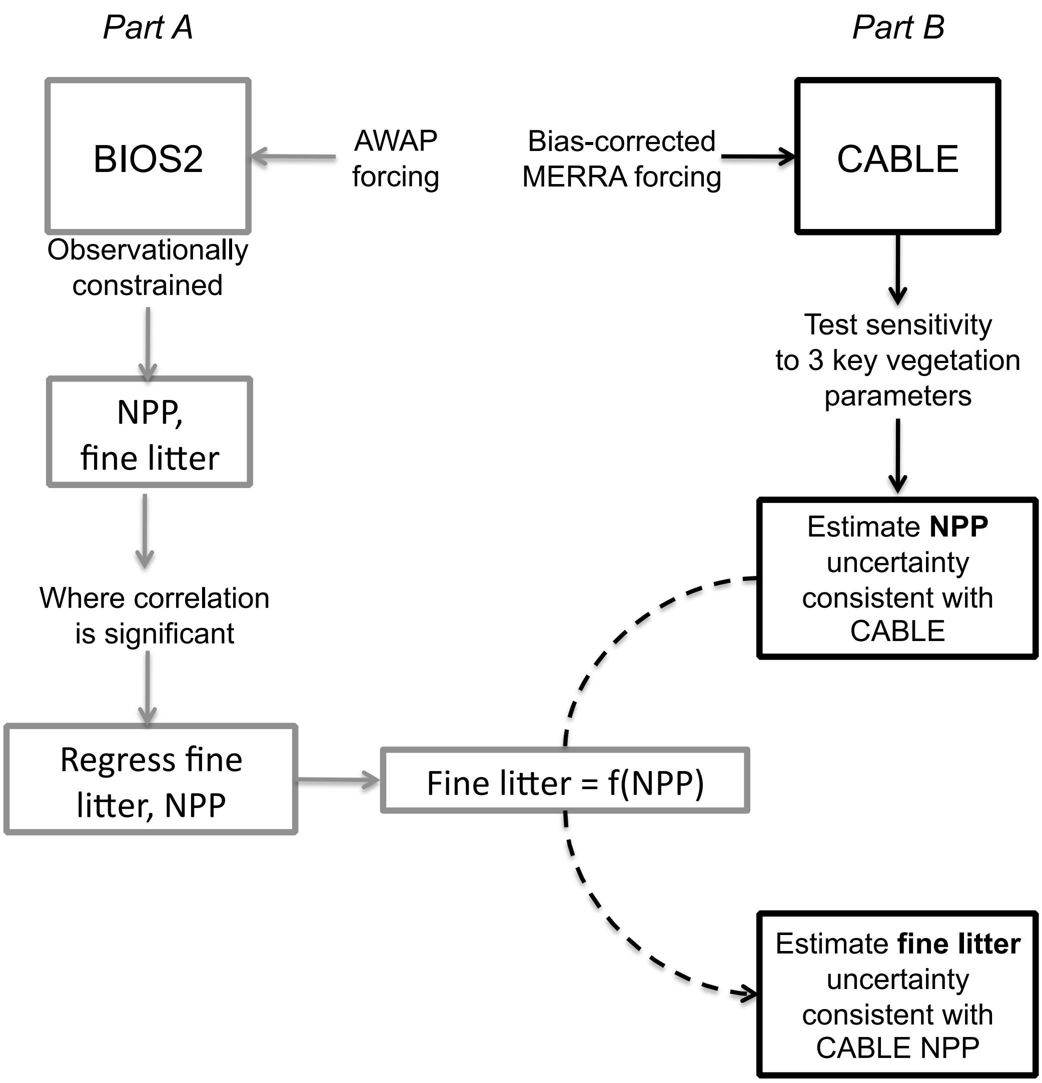

Figure 1 Part A aims to derive the relationship between fuel load and NPP. BIOS2 includes a biogeochemical model that includes NPP and fine litter pools, and is constrained by multiple observational datasets. Unlike BIOS2, CABLE is routinely used coupled to ACCESS and regional climate models. Hence, Part B aims to simulate fuel load in CABLE by using the relationship derived in Part A. Uncertainty in CABLE estimation of fuel load is addressed by varying three key vegetation parameters.

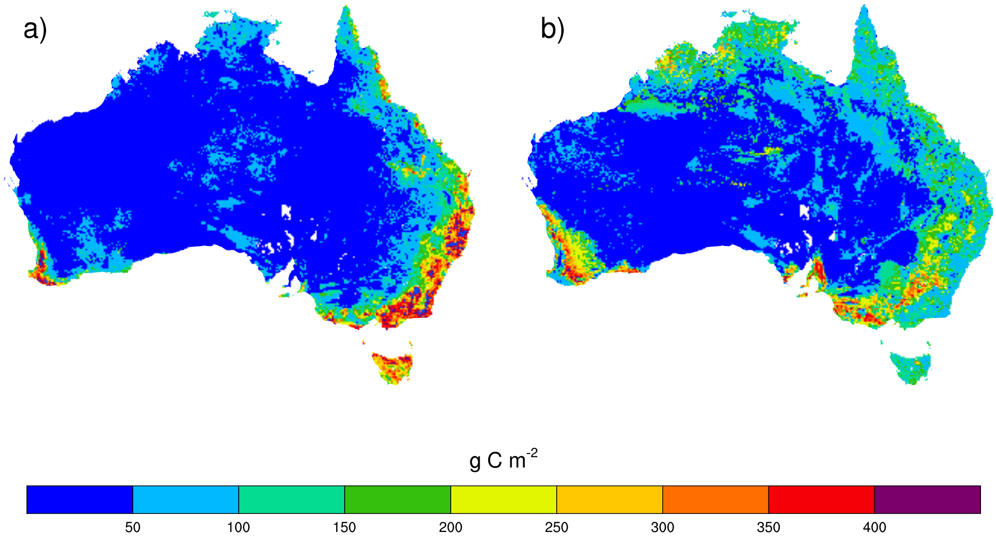

Figure 2 Mean annual fine litter in BIOS2 (1990-2011) for a) woody and b) grassy vegetation.

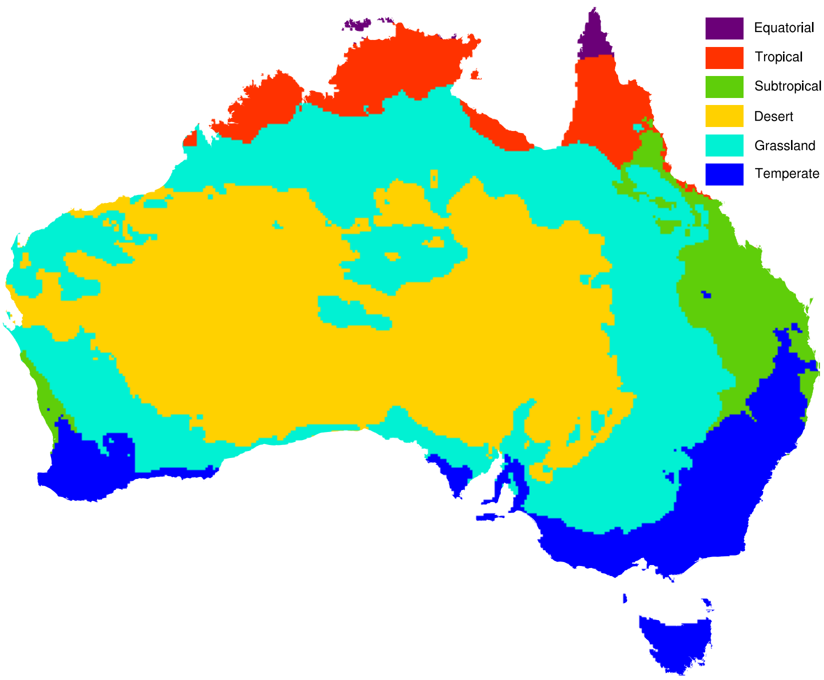

Figure 3 Köppen classification major climate zones.

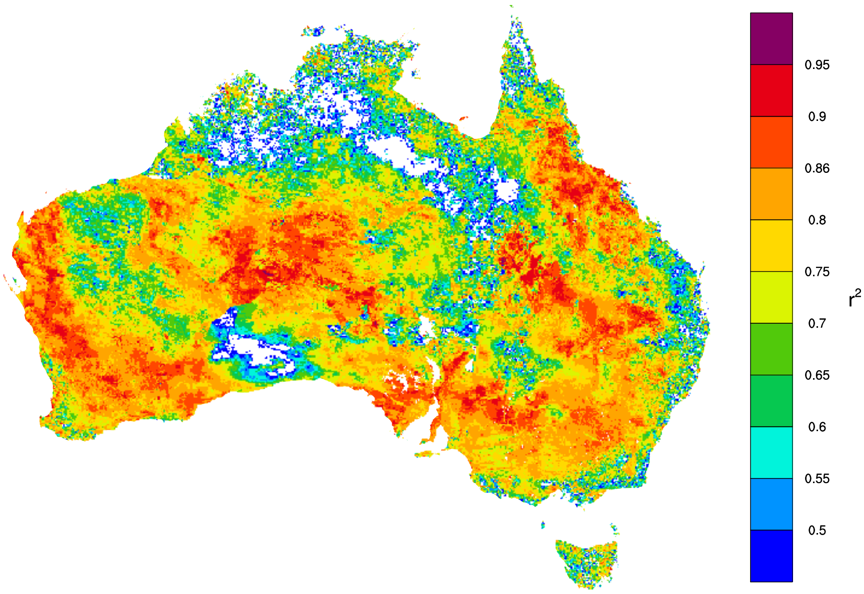

Figure 4 Lag-1 correlation between annual fine litter and the previous year's NPP in BIOS2. White areas indicate no significant correlation ($p<0.05$).

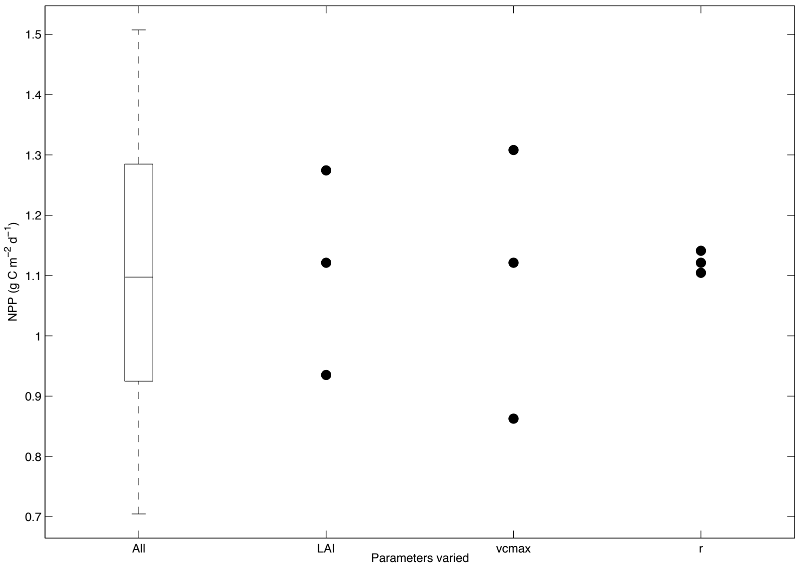

Figure 5 Summary of ensemble continental mean annual NPP from CABLE. Boxplot whiskers show the range of all 27 simulations, box shows the quartiles. The black dots show continental mean annual NPP where a single parameter is varied: v_{cmax}, LAI and r. The central dot in each of these columns shows NPP with default parameter values.

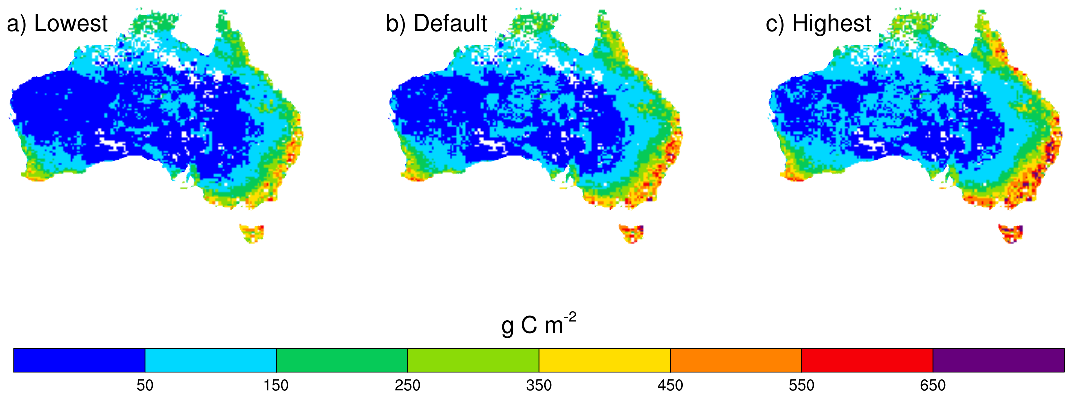

Figure 6 Mean annual fine litter from CABLE for the a) lowest, b) default and c) highest ensemble members.

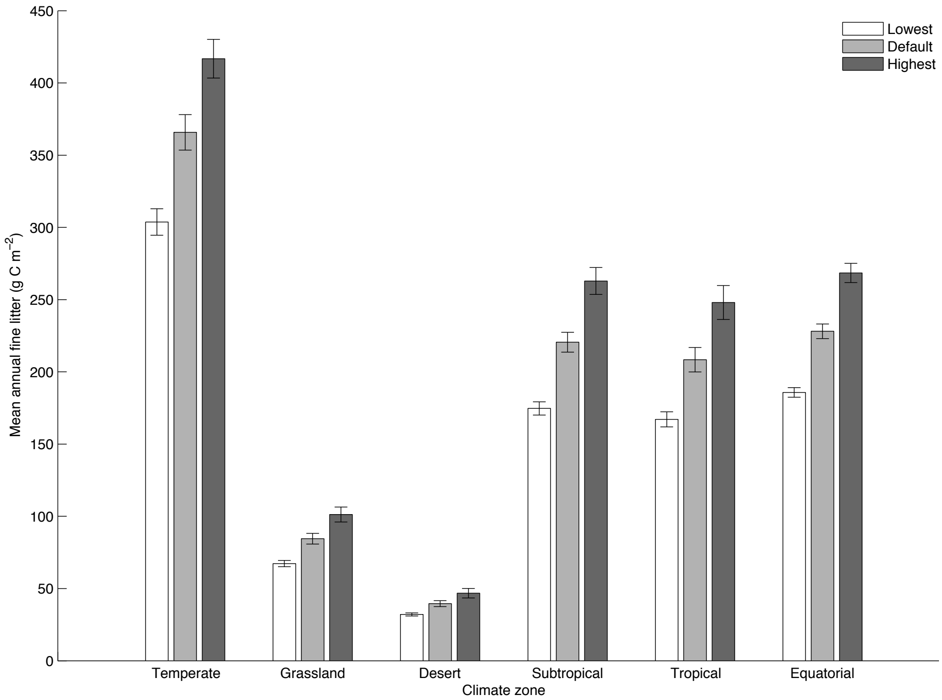

Figure 7 Mean annual fine litter from CABLE by climate zone from the lowest, default and highest ensemble members. Error bars show standard deviation.

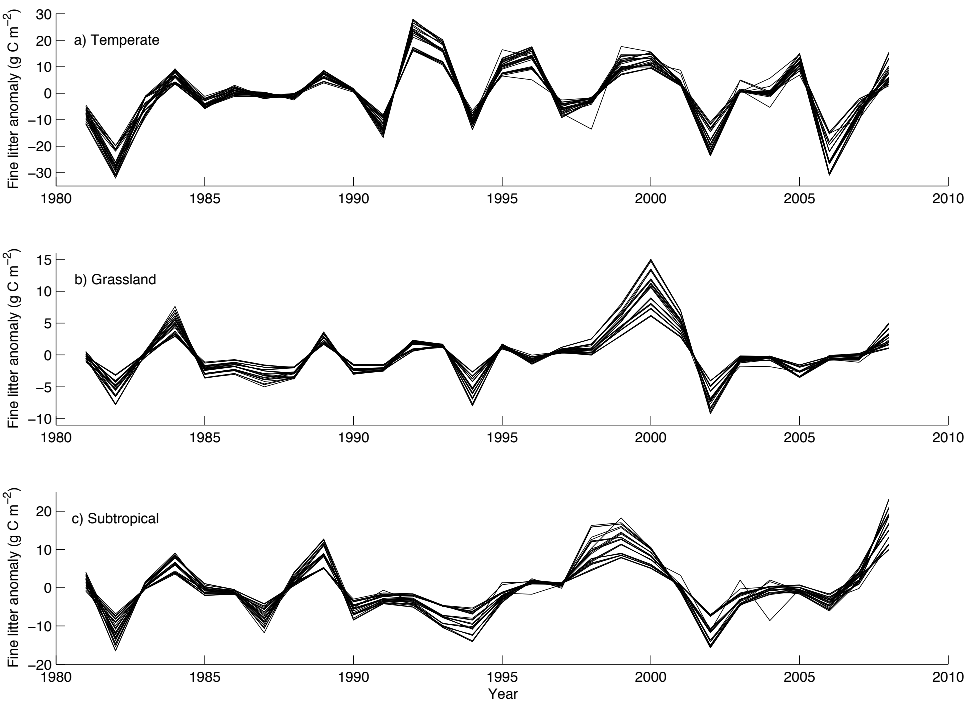

Figure 8 Ensemble annual fine litter anomaly from CABLE for the a) temperate, b) grassland and c) subtropical climate zones. Each ensemble member is a separate line.

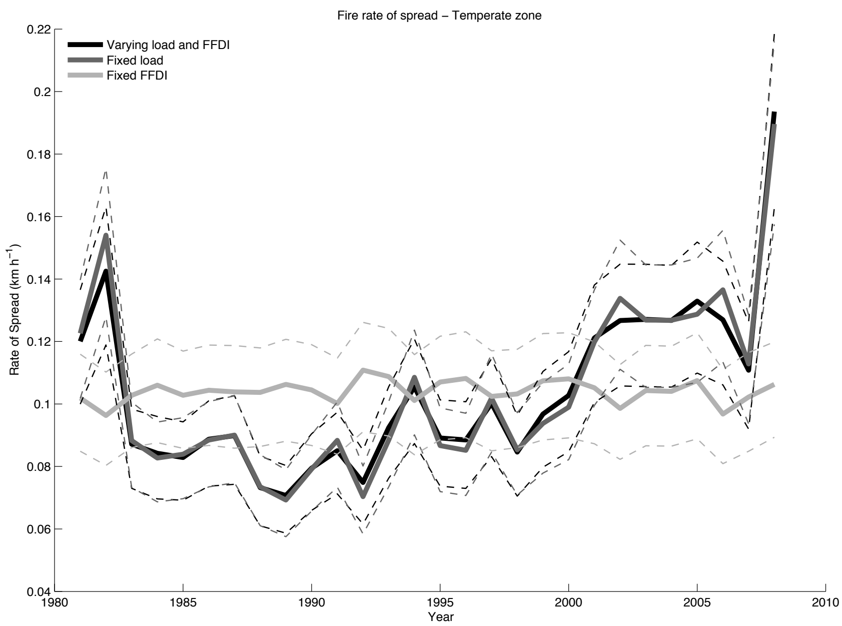

Figure 8 Ensemble annual fine litter anomaly from CABLE for the a) temperate, b) grassland and c) subtropical climate zones. Each ensemble member is a separate line.

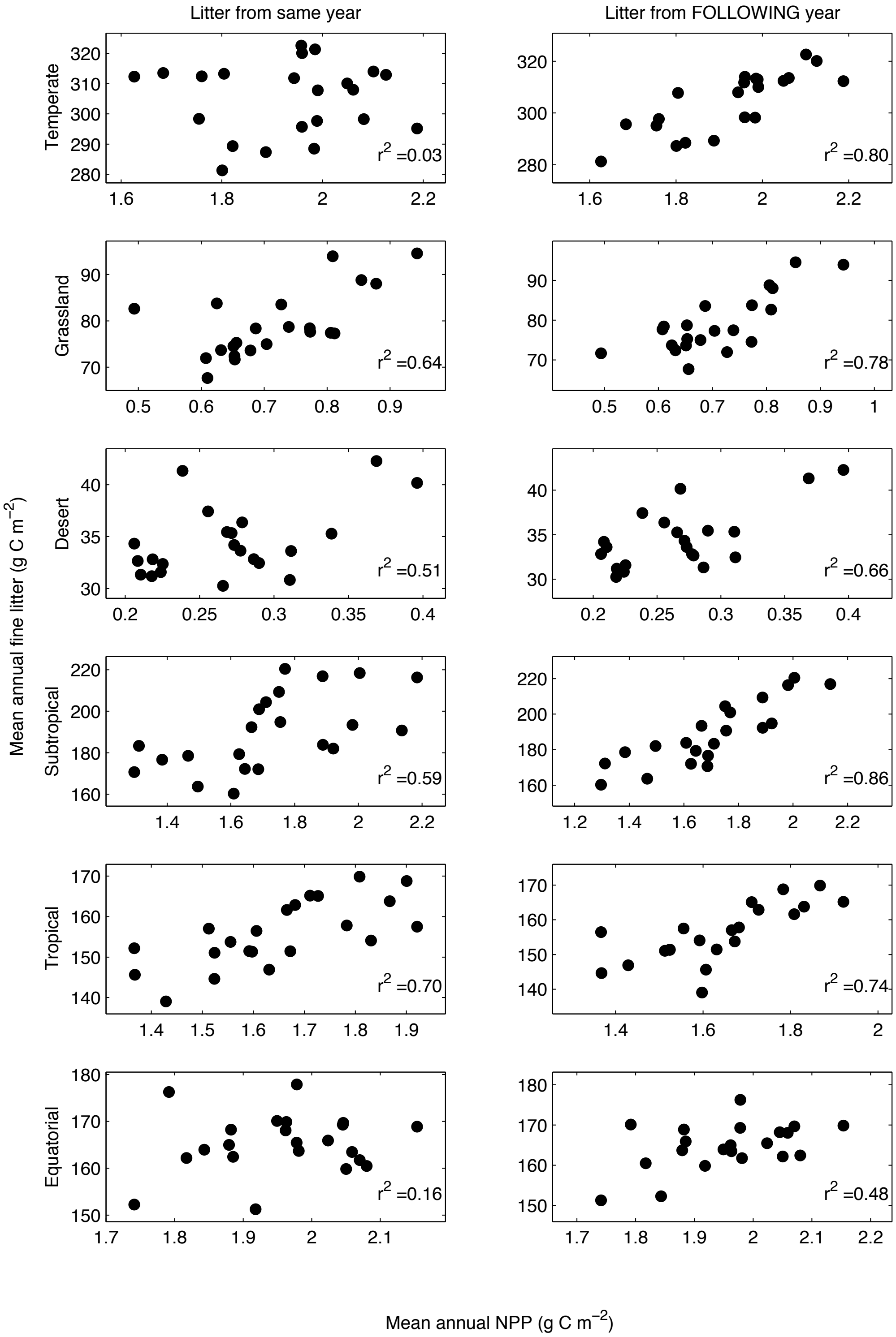

Supplementary Figure 1 Scatterplots of mean annual NPP and fine litter in each climate zone. Fine litter from same year as NPP is shown on left hand side, fine litter from the year following NPP is shown on the right hand side.

Table 1. Lag-1 correlation between fine litter and NPP by climate zone

Climate zone	**r^2 (p value)**
Temperate	0.80 (0.00)
Grassland	0.78 (0.00)
Desert	0.66 (0.00)
Subtropical	0.86 (0.00)
Tropical	0.74 (0.00)
Equatorial	0.48 (0.03)

Supplementary Table 1. Parameter values used in sensitivity ensemble

IGBP Vegetation Name	v_{cmax} (mol m^{-2} s^{-1})	r
Evergreen Needleleaf	$6.52 \pm 2.35 \times 10^{-5}$	0.943 ± 0.015
Evergreen Broadleaf	$6.50 \pm 2.34 \times 10^{-5}$	0.962 ± 0.015
Deciduous Needleleaf	$7.00 \pm 2.52 \times 10^{-5}$	0.966 ± 0.015
Deciduous Broadleaf	$8.50 \pm 3.06 \times 10^{-5}$	0.961 ± 0.015
Mixed Forest	$8.00 \pm 2.88 \times 10^{-5}$	0.966 ± 0.015
Closed Shrub	$2.00 \pm 0.72 \times 10^{-5}$	0.914 ± 0.015
Open Shrub	$2.00 \pm 0.72 \times 10^{-5}$	0.964 ± 0.015
Woody Savanna	$1.00 \pm 0.36 \times 10^{-5}$	0.972 ± 0.015
Savanna	$2.00 \pm 0.72 \times 10^{-5}$	0.943 ± 0.015
Grassland	$1.00 \pm 0.36 \times 10^{-5}$	0.943 ± 0.015
Wetland	$5.00 \pm 1.80 \times 10^{-5}$	0.961 ± 0.015
Cropland	$8.00 \pm 2.88 \times 10^{-5}$	0.961 ± 0.015
Urban	$1.00 \pm 0.36 \times 10^{-6}$	0.961 ± 0.015
Cropland & Natural Mosaic	$8.00 \pm 2.88 \times 10^{-5}$	0.961 ± 0.015
Ice	$1.70 \pm 0.61 \times 10^{-5}$	0.961 ± 0.015
Barren	$1.70 \pm 0.61 \times 10^{-5}$	0.975 ± 0.015
Land Ice	$1.70 \pm 0.61 \times 10^{-5}$	0.975 ± 0.015

Chapter 6 Summary

Simulation of fuel load with a land surface model

The model of fuel load developed in Chapter 6 is based on a simple relationship between net primary productivity and fine litter. This relationship is derived from a process-based carbon, water and energy modelling framework that incorporates observations of a broad range of variables. It therefore likely represents our best estimate of values such as load across the landscape. The model was run over Australia from 1980 to 2008, with uncertainty represented by variation in three key model parameters. No trend in load was detected over the period of simulation, regardless of parameter variation.

Through its link with a mechanistic representation of NPP, this model allows for the influence of both climate and atmospheric CO_2 on fuel load. This serves as the foundation for the experiments in Chapter 7, which aim to quantify the response of fuel load to future climate change in Australia, and their relative importance compared to changes in fire weather conditions.

Chapter 7 Overview

Downscaled projections of fuel load and fire weather

The work described in Chapters 3 to 6 lays the groundwork for the study presented in Chapter 7. Fire weather in Australia has been undergoing pronounced changes over recent decades; changes that are projected by global climate models to continue under scenarios of future climate change. A tool for converting these global projections into fine scaled, physically consistent regional information has been shown to capture key aspects of the observed distribution of fire weather conditions in southeast Australia. A separate tool has been developed for simulating the evolution of bushfire fuel load, combining a simple model of load as a function of net primary productivity (NPP), with a process-based model of NPP that accounts for influences of both climate and atmospheric CO_2 on terrestrial vegetation.

Chapter 7 aims to build on the above by developing the first fine scaled (50 km) continental assessment of the impact of future climate change on two key drivers of fire risk in Australia, fire weather and fuel load, taking into account the interplay between rising CO_2 levels and vegetation growth.

The following study has been submitted to a peer reviewed journal and is reproduced as submitted:

Clarke H, Pitman AJ, Kala J, Carouge C, Haverd V, Evans JP (submitted) An investigation of future fuel load and fire weather in Australia. Climatic Change.

Author contributions

I led this project. The project was the culmination of several years of planning and discussion, building on multiple previous papers. The study was chiefly conceived by myself and Andy Pitman (AP; my PhD supervisor) The experimental design was led by myself, incorporating substantial contributions from AP, Jatin Kala (JK) and Jason Evans (JE). I led the modelling, with input from JK and Claire Carouge (CC). I led the analysis and prepared the figures, incorporating comments from all other coauthors. I drafted the manuscript and incorporated comments from all other coauthors.

An investigation of future fuel load and fire weather in Australia

Hamish Clarke[1,2], Andrew J. Pitman[1], Jatin Kala[1], Claire Carouge[1], Vanessa Haverd[3] and Jason P. Evans[1]

[1] ARC Centre of Excellence for Climate System Science and Climate Change Research Centre, University of New South Wales, Sydney, 2052, Australia

[2]Climate and Atmospheric Science Branch, NSW Office of Environment and Heritage, PO Box 3720, Parramatta, Australia

[3]CSIRO Marine and Atmospheric Research, GPO Box 664, Canberra 2601, Australia

For submission to Climatic Change

January 21, 2015

Address for correspondence

Hamish Clarke

Climate Change Research Centre, University of New South Wales, Sydney, 2052, Australia

Ph. +61 2 9375 7075, h.clarke@student.unsw.edu.au

Key words

Climate change, wildland fire, bushfire, CABLE, WRF

Abstract

A continental assessment of the impact of future climate change on two key drivers of fire risk in Australia, fire weather and fuel load, is presented. Fire weather conditions are represented by the McArthur Forest Fire Danger Index (FFDI), calculated from a 12-member regional climate model ensemble. Fuel load is derived from net primary production, simulated using a land surface model forced by the same regional climate model ensemble. Mean annual fine litter is projected to increase across all ensemble members, by 56 to 78 g C m^{-2} in temperate areas, 13 to 25 g C m^{-2} in grassland areas and 33 to 53 g C m^{-2} in subtropical areas. Ensemble changes in annual cumulative FFDI vary widely, from 57 to 550 in temperate areas, -186 to 1372 in grassland areas and -231 to 907 in subtropical areas. The largest increases in fuel load and fire weather are projected to occur in spring. Rate of fire spread, a function of both fire weather and fuel load, increases in temperate areas by 0.02 to 0.07 km h^{-1} on average annually. Failing to take into account changes in both fuel load and fire weather leads to underestimates of fire rate of spread. These results suggest that FFDI projections will not be robust if only a single simulation is used. Our methods can be applied to other regions to estimate future fuel load, when this information is not directly available from climate model outputs.

1 Introduction

Wildfires occur with sufficient and continuous plant biomass (fuel), fuel dry enough to burn, weather conducive to fire spread and an ignition source (Archibald et al. 2009; Bradstock 2010). How climate change affects fire weather has commonly been examined using indices designed to relate surface weather conditions to wildfire risk, such as the Canadian Forest Fire Weather Index system (FWI; van Wagner 1987) and the Australian McArthur Forest Fire Danger Index (FFDI; McArthur 1967; Luke and McArthur 1978). Since both are widely used in fire management and can be calculated from standard climate model output, numerous studies have projected changes in FWI and FFDI (e.g. Williams et al. 2001; Bedia et al. 2013; Fox-Hughes et al. 2014; Lehtonen et al. 2014). Other elements of fire weather that have been related to climate change include atmospheric stability (Luo et al. 2013), synoptic patterns (Hasson et al. 2009; Grose et al. 2014) and modes of climate variability (Cai et al. 2009). By relating observed weather patterns to fire incidence or burned area, projected changes in weather have also been used as a proxy for the presence of fire and its impacts (e.g. Mori and Johnson 2013).

In contrast to the direct use of meteorological variables for fire weather, predicting changes in biomass growth or fuel load requires a significant transformation of climate model data. The task is complicated by the need to include the potential response of vegetation to increasing carbon dioxide (CO_2), in addition to climate (Donohue et al. 2013). There are multiple approaches to examining how climate change affects wildfire fuel loads. Statistical relationships have been developed between current vegetation patterns and meteorological variables (Matthews et al. 2012; Thomas et al. 2014; Williamson et al. 2014). These relationships allow vegetation changes to be derived from projected changes in meteorological variables, but do not account for CO_2 effects. Process-based approaches to fuel load and vegetation include dynamic global vegetation models (DGVMs), landscape fire succession models and biogeochemical models. These models may represent direct influences on fuel amount, such as litterfall, decomposition and fire incidence, as well as indirect causes like phenology, primary productivity, heat and moisture. Process-based models can incorporate fertilisation effects of CO_2 on plant growth (e.g. Jiang et al. 2013).

Quantitative, integrated assessments of the impact of climate change on multiple fire drivers are relatively rare (Pechony and Shindell 2010; Kloster et al. 2012; Loepfe et al. 2012; Eliseev et al. 2014). In Australia, Bradstock (2010) provides a qualitative assessment based on case studies of five fire regimes drawing on quantitative and qualitative data. Bradstock concludes that increasing temperatures and dryness may lead to divergent impacts on fire activity across Australia, with potential increases in temperate forests, but decreases in areas where fires are currently limited by fuel amount rather than fire weather conditions. The impact of climate change on multiple wildfire drivers in forested and grassland regions of southeast Australia was estimated by King et al. (2011, 2012). Both studies examined potential changes in fire weather and fuel load, but only the grassland study included fuel moisture (curing) as well as fertilisation effects of $CO_{2,}$ via a process-based grassland and water-balance model. Each study projected increases in fire weather conditions and overall decreases in fuel load, which translated to increases in fire incidence and area burned in forests, but minimal changes in fire risk in grasslands.

Our study aims to provide the first quantitative, landscape-scale assessment of the impact of projected changes in climate and CO_2 on fuel load and fire weather focused on Australia. Fire weather projections are derived from a regional climate model, which is then used to force a land surface model from which fuel load is estimated, following Clarke et al. (submitted; see Section 2.4), incorporating both direct and indirect effects of elevated atmospheric CO_2. Variation in Regional Climate Models (RCMs) and their forcing Global Climate Models (GCMs) is a major source of uncertainty in climate impact projections (Lung et al. 2013). We aim to improve the robustness of these projections through the use of a 12-member ensemble, selected for both its skill in representing the regional climate as well as the independence of individual ensemble members

(Evans et al. 2014). By accounting for uncertainty in GCMs and RCMs, and by including CO_2 fertilisation and its impact on fuel load, we provide a more complete estimate of future changes in key aspects of wildfire risk.

2 Materials and Methods

Our study uses a combination of new and pre-existing regional climate and land surface model simulations (Figure 1).

2.1 Regional climate model simulations

Future climate projections used the Weather Research and Forecasting (WRF) modelling system (Skamarock et al. 2008), which has been extensively evaluated and shown to perform well in terms of regional Australian climate (Evans and McCabe 2010, 2013) and fire weather (Clarke et al. 2013). The simulations used in this study are drawn from the NSW and ACT Regional Climate Modelling (NARCliM) project (Evans et al. 2014).

NARCliM uses the Advanced Research WRF (ARW) version 3.3. Four GCMs are downscaled using three configurations of WRF resulting in a 12 member ensemble (Figure 1). A three step GCM selection process was used. First, a large set drawn from the 3rd Coupled Model Intercomparison Project (CMIP3; Meehl et al. 2007) was evaluated in order to remove the worst performing models. Second, better performing models were ranked according to their independence (Bishop and Abramowitz 2013). Last, GCMs were placed within the future change space and the most independent models that span that space were chosen. A similar process was used to select RCMs. A large set consisting of different physical parameterisations was evaluated in order to remove the worst performing RCMs. From the better performing models, a subset was chosen such that each chosen RCM is as independent as possible from the other RCMs. Although partial bias correction of FFDI is possible (Fox-Hughes et al. 2014), we opt to maintain physical consistency in model dynamics and instead address model bias via ensemble design and reporting of modelled changes, rather than absolute values.

GCMs are downscaled in two time slices 1990–2008 (‘present’) and 2060–2078 (‘future’). For future projections the SRES A2 emissions scenario is used (IPCC 2000). RCMs were run at 50 km resolution over the CORDEX AustralAsia region (Giorgi et al. 2009).

2.2 Land surface model simulations

Fuel load projections are developed from the Community Atmosphere-Biosphere Land Exchange (CABLE, version 2.0) land surface model, which is designed to simulate fluxes of energy, water, and carbon at the land surface (Wang et al. 2011). CABLE has been extensively tested against observational data (Abramowitz et al. 2008; Wang et al. 2011). CABLE can be run with prescribed meteorology (e.g. Kala et al. 2014), or coupled in a global or regional climate model. CABLE is a key part of the Australian Community Climate Earth System Simulator (ACCESS; see http://www.accessimulator.org.au), a fully coupled earth system science model and contributor to the Fifth Assessment Report of the Intergovernmental Panel on Climate Change (IPCC).

CABLE was used within the National Aeronautics and Space Administration Land Information System version 6.1 (LIS-6.1; Kumar et al. 2008) at a grid resolution of 25 km. 12 offline simulations were run, each forced with meteorological data from one of the 12 regional climate model ensemble members described above (Figure 1). The emissions scenarios used in WRF (i.e. present day and SRES A2) were also used with CABLE. Leaf Area Index (LAI) is prescribed for the present and future using the mean of a 15 member monthly LAI ensemble based on the Moderate Resolution Imaging Spectroradiometer (MODIS) LAI product and gridded observations of temperature and precipitation (Kala et al. 2014).

2.3 Fire weather estimation

Following Noble et al. (1980), FFDI is computed as

$$\mathrm{FFDI} = 2 \times \exp(0.987 \times \ln(\mathrm{DF}) - 0.0345 \times H + 0.0338 \times T + 0.0234 \times V - 0.45) \quad (1)$$

where DF is the drought factor, T is the temperature (°C), V the wind speed (km h^{-1}) and H the relative humidity (%). The drought factor is an estimate of fuel dryness (Griffiths 1999) and is computed using the Keetch-Byram Drought Index (Keetch and Byram 1968) based on total daily rainfall. Daily FFDI was calculated from the 12 member regional climate model ensemble.

2.4 Fuel load estimation

Fuel load is calculated from net primary productivity (NPP) following Clarke et al. (submitted). NPP is used as a fuel load proxy since it represents the rate of production of vegetation. NPP has been equated to litter production (Matthews 1997) and is strongly correlated with biomass (Kindermann et al. 2008).

The relationship between fuel load and NPP is derived from the BIOS2 modelling environment, which simulates both quantities (Figure 1; Haverd et al. 2013). BIOS2 simulates the energy, water and carbon balances of the Australian continent at fine spatial (0.05°, ~5 km) and temporal (hourly) resolution. BIOS2 has similarities with CABLE v1.4, but the soil and carbon modules are replaced by the SLI soil model (Haverd and Cuntz 2010) and the CASA-CNP biogeochemical model (Wang et al. 2010). CASA-CNP allocates the carbon cycling through the terrestrial ecosystem into plant, litter and soil pools. BIOS2 was run from 1990 to 2011 using meteorological forcing from the Bureau of Meteorology's Australian Water Availability Project data set (AWAP) (Jones et al. 2009). The BIOS2 simulations were constrained by observations of streamflow, evapotranspiration, net ecosystem production and litterfall. The use of observational constraints along with the best available gridded observations for Australia (AWAP) means the simulations by BIOS2 are likely the best available estimates of fuel load in the absence of high quality, long term, landscape-scale observations.

The Pearson product-moment correlation coefficient was used to calculate the relationship between annual NPP and fuel load in BIOS2 for the period 1990 to 2011. Fuel load was defined as the fine litter pool; the sum of the metabolic and structural litter pools in CASA-CNP (Wang et al. 2010). Where the correlation between NPP and fine litter was significant ($p < 0.05$), fine litter was related to NPP using ordinary least squares linear regression. Although there is no physical reason why this relationship should be strictly linear, the correlation was generally high with no clear evidence for a non-linear relationship. Since the link between fine litter and NPP is statistical, this model cannot account for mechanistic changes in litterfall and litter decomposition, the two processes that mediate the translation of primary productivity into fuel load. However, the model of NPP in CABLE is mechanistic and is sensitive to changes in climate forcing and CO_2 concentration.

To understand regional variations the same methods were applied to model output aggregated into climate zones. A modified Köppen climate classification was used, which separates Australia into 6 mostly contiguous and climatically similar regions (Figure 2; Stern et al. 1999). The major Köppen zones are: equatorial, tropical, subtropical, desert, grassland and temperate. The lag-1 correlations were significant ($p < 0.05$) for all 6 climate zones with the highest correlations in the subtropical ($r^2 = 0.86$), temperate ($r^2 = 0.80$) and grassland ($r^2 = 0.78$) climate zones.

The linear models (Clarke et al. submitted) for each climate zone and each model grid cell were then applied to the present study, allowing fuel load to be calculated from NPP simulated by the 12 member land surface model ensemble (Figure 1). We focus on the temperate, grassland and subtropical zones because of the high correlation between NPP and load in these regions.

2.5 Analysis

To frame changes in fuel load with changes in meteorological forcing we examined the rate of spread of fire (R, in km h^{-1}, McArthur 1967):

$R = 0.0012 \times F \times L$	(2)

where F is the FFDI and L is load in t ha^{-1}. This provides a simple way of comparing the impact of changes in load and fire weather conditions. We restrict our analysis of rate of spread to the temperate region that contains the forest types used in the calibration of R.

3 Results

Figure 3a shows the simulated spread in continental mean annual fine litter depending on choice of GCM and RCM, and how the fine litter changes between the present and future. Mean continental fine litter is projected to increase substantially by 2060-2078 in all model simulations, such that the lowest future ensemble member (154 g C m^{-2}) is higher than the highest present ensemble member (151 g C m^{-2}). Increases in continental fine litter are projected for every ensemble member, with increases ranging from 17 to 26 g C m^{-2} (11% to 20%). Figure 3 also shows those models simulating the lower (higher) values of fine litter in the present remain the lower (higher) models in the future. Further, RCM3 consistently simulates the highest litter amounts, illustrating the importance of RCM physics settings.

Figure 3b shows results for continental mean annual cumulative FFDI. While substantial increases are projected by some ensemble members, the results are strongly model dependent in contrast to Figure 3a. Ensemble members driven by CCCMA3.1 and MIROC3.2 show little change and occasionally small decreases. Ensemble members driven by the other two GCMs project larger increases in FFDI. The projected change in continental mean annual cumulative FFDI from all ensemble members ranges from a decrease of 109 to an increase of 1275. Overall there is an increase in the ensemble mean FFDI from 5274 to 5816 (10%). Selecting only ECHAM5 and CSIRO-Mk3.0, the range of increases is 10 to 23%, while selecting only CCCMA3.1 and MIROC3.2 gives a range of -2 to 15% (excluding outlier MIROC3.2/RCM3 gives a range of -2 to 2%). This highlights the dangers of using single GCMs for estimating future changes in FFDI; the choice of model strongly influences the sign and magnitude of the overall change. The consistent placement of RCM3 at lower end of ensemble simulated FFDI (in contrast to its placement at the upper end of litter estimates in Figure 3) further demonstrates the importance of RCM physics settings.

Figure 4 shows the change in mean annual fine litter from CABLE based on the linear model for each grid cell, developed using BIOS2 (see Figure 1). The ensemble members representing the least (4a) and most (4b) change are shown, selected by taking the continental average of all grid point change values for each ensemble member and then ranking these from lowest to highest. The overall pattern of change in each of the 12 ensemble members is very similar, with all models showing increases in fine litter in the southeast and northeast of Australia, particularly along the coast (Online Resource 1). Overall, our results consistently show increasing fine litter in the future.

Figure 4 also shows the change in annual cumulative FFDI at each grid cell. The overall pattern of change in all 12 ensemble members is strongly divergent, with ensemble members forming two groups, some with substantial increases and others with modest decreases (Online Resource 2). In the lowest ensemble member (4c), little change in FFDI is projected across the continent. The highest ensemble member (4d) projects increases ranging from 200 to 600 in the southeast and extending along the coast to the northeast, to over 1800 over parts of northwest Australia. Again, this highlights the dangers of using single GCMs for estimating future FFDI since the choice of model determines the sign and magnitude of the overall change. The overall spatial pattern of change in FFDI is most strongly dictated by GCM, with RCMs modulating the magnitude of these changes (Online Resource 2).

Figure 5a-c shows the projected change in mean monthly fine litter values in temperate, grassland and subtropical climate zones (actual values in Online Resource 3). Increases in fine litter are projected every month in all three zones, and the highest increases are projected to occur in mid to late spring. In the subtropical zone, and to a lesser extent the temperate zone, there is clear separation between the lowest future ensemble member and the highest present member (Online Resource 4). The increase in fine litter across all regions by 2060-2078 from each ensemble member gives us confidence in the robustness of this result.

In contrast to the fuel load results, monthly values of mean daily FFDI show both decreases and increases in all three zones (Figure 5d-f; actual values in Online Resource 3). However, the magnitude of increases in FFDI is much greater than that of decreases. As with fine litter, in all three climate zones the largest projected increases in FFDI are projected to occur in mid to late spring (October and November). In contrast to litter, however, there is considerable overlap between the lowest future ensemble member and the highest present member in all three zones (Online Resource 4).

Mean fire rate of spread in the temperate zone (Figure 6a) shows considerable overlap between the ensemble values for present (0.13 to 0.19 km h^{-1}) and future rate of spread (0.17 to 0.25 km h^{-1}). Despite this overlap, there is a clear trend towards increasing rate of spread in every ensemble member, with the projected increase ranging from 0.02 to 0.07 km h^{-1}. The second two boxplots in Figure 6a show the change in rate of spread from changes in only FFDI and only load, respectively. Rate of spread increases, but not as much as when both future FFDI and future load are used. Calculating rate of spread using only projected changes in FFDI results in a change of between 0 and 0.04 km h^{-1}, compared to more consistent increases of ~0.02 km h^{-1} for all ensemble members when calculating the rate of spread using only projected changes in load.

Figure 6b shows the change in mean monthly rate of spread in the temperate zone (actual values in Online Resource 5). Changes are similar across model ensemble members, with the largest increases projected during spring and summer. The difference is that the smallest values projected by minimum ensemble members, which occur in winter and late autumn, are actually (relatively small) decreases in rate of spread. In contrast, the multimodel mean and maximum ensemble members project increases in rate of spread throughout the year. The minimum ensemble members also project increases in rate of spread to peak in early summer, compared to a late spring peak for the multimodel mean and maximum ensemble members. In all simulations the rate of spread therefore increases in spring, summer and early autumn, with the maximum increase occurring in late spring or early summer.

4 Discussion

Our results suggest that changes in climate and CO_2 will increase fuel load in both forested and grassland areas of Australia by the latter part of the 21st century. In contrast, changes in fire weather are more uncertain and model-dependent. The high end of ensemble projections represents substantial increases in fire weather conditions, while the lower end represents little change. These results suggest that FFDI projections are strongly dependent on the choice of GCM and the physics settings of the RCM. Across all ensemble members, the biggest increases in fire weather conditions are projected to occur in late spring, suggesting a longer fire season. In combination these findings suggest that fire risk in temperate areas, based on fire rate of spread, will increase and that failing to account for both weather and load leads to underestimates in this risk. These changes would have implications for fire management agencies’ scheduling of prescribed burning.

These fire weather projections, particular in temperate areas, are in broad agreement with a range of previous studies which have projected increased wildfire risk from weather (Cai et al. 2009; Hasson et al. 2009; Clarke et al. 2011; Matthews et al. 2012; Fox-Hughes et al. 2014). These studies project a tendency towards a longer fire season, via intensified fire weather conditions early in the fire season. In contrast to significant increases at the upper end of the ensemble, projections at the lower end suggest little change by 2070 or decreases in fire weather consistent with Flannigan et al. (2009) and Clarke et al. (2011). The decreases tend to be of a smaller magnitude than corresponding increases in fire weather conditions. Note also that our study focuses on measures of average, rather than extreme, fire weather conditions. Changes at the upper end of the FFDI distribution, when fires that occur are most difficult to control, are likely to be even higher that those at the centre of the distribution, based on both modelling (e.g. Clarke et al. 2011) and observational (Clarke et al. 2012) studies. Similar provisos apply to our use of average, rather than extreme, fire rate of spread.

Our findings of uniform and widespread increases in fuel load under climate change differ from several previous assessments for Australia. King et al. (2012) projected mostly decreases in grassy fuel load in southeast Australia, with CO_2 fertilisation insufficient to compensate for changing temperature and rainfall. Matthews et al. (2012) and Penman and York (2010) projected decreases in forest fuel load at two forested sites in southeast Australia, although the decreases reported by Penman and York (2010) were not considered significantly different to present values. Neither of these studies factored in CO_2 fertilization. However, the scenarios used by King et al. (2012), Penman and York (2010) and Matthews et al. (2012) all utilised GCMs which project an overall decrease in rainfall. These differ from our ensemble which was designed to account for uncertainty by selecting GCMs that projected both increases and decreases in rainfall.

Improving certainty in regional rainfall projections may not clarify all vegetation trends, due to differences in the response of major vegetation types to precipitation (Thomas et al. 2014; Gibson et al. 2014). The complex relationships observed between climate and vegetation type contrast with the near uniform changes in vegetation amount projected in our study. A possible reason is the strong CO_2 fertilisation effect in ours and other land surface models. In one study of the response of vegetation to a range of climate scenarios, CO_2 fertilisation was found to be the major cause of modelled increases in gross primary productivity (NPP plus autotrophic respiration), well in excess of rainfall or temperature and regardless of climate zone (Raupach et al. 2013). Process-based models could benefit from incorporation of empirical findings and the emergence of high quality, landscape-scale fuel load observations.

In conclusion, we have provided the first landscape-scale assessment of the combined effects of climate change and increasing CO_2 on fuel load levels and fire weather conditions in Australia. Our results suggest that wildfire risk will be increased under climate change in temperate, grassland and subtropical climate zones, due to the combined effects of increased fuel load and either stable or increasing fire weather. However, these results contrast with other studies projecting decreases in fuel load under climate change in Australia, possibly related to our selection of GCMs that spanned a range of possible climate futures. While work is required to understand the reasons for these differences and refine of our simple fuel load model, a better understanding of long-term changes in fire risk over Australia will benefit from more accurate predictions of regional-scale rainfall.

Acknowledgements

This study was supported by the ARC Centre of Excellence for Climate System Science (CE110001028) and by the NCI National Facility at the Australian National University, Australia. Regional climate data have been provided by the New South Wales and Australian Capital Territory Regional Climate Model (NARCLiM) project funded by NSW Government Office of Environment and Heritage, University of New South Wales Climate Change Research Centre, ACT Government

Environment and Sustainable Development Directorate and other project partners. Jason Evans was funded by the ARC Future Fellowship FT110100576.

Figure captions

Fig 1 Summary of methodology. FFDI is calculated from a regional climate model ensemble spanning present (1990-2008) and future (2060-2078) periods. The same ensemble supplies the meteorological forcing to CABLE, yielding NPP. Based on the relationship between fine litter and NPP in BIOS2, fine litter is calculated from NPP in CABLE.

Fig 2 Köppen classification major climate zones

Fig 3 Ensemble mean annual continental (a) fine litter and (b) cumulative FFDI for present and future periods. Whiskers show the ensemble range, box shows the quartiles. Individual GCM/RCM combinations are represented by marker (GCM) and colour (RCM).

Fig 4 Change in mean annual (a) fine litter and (b) cumulative FFDI from the lowest and highest ensemble members, calculated from the average of all grid cell changes

Fig 5 Change in mean monthly (a) fine litter load and (b) FFDI in temperate, grassland and subtropical climate zones. Unbroken line shows multimodel mean, dotted lines show ensemble minimum and maximum values.

Fig 6 a) Ensemble mean fire rate of spread in the temperate climate zone, calculated using combinations of present and future FFDI and load. Whiskers show the ensemble range, box shows the quartiles. b) Change in mean monthly fire rate of spread in the temperate climate zone. Unbroken line shows multimodel mean, dotted lines show ensemble minimum and maximum values.

Electronic supplementary material (ESM) captions

ESM 1 Change in mean annual fine litter from each ensemble member

ESM 2 Change in mean annual cumulative FFDI from each ensemble member

ESM 3 Present and future mean monthly fine litter (a-c) and FFDI (d-f) in temperate, grassland and subtropical climate zones. Unbroken line shows multimodel mean, dotted lines show ensemble minimum and maximum values.

ESM 4 Ensemble mean annual fine litter (a-c) and cumulative FFDI (d-f) for present and future periods in temperate, grassland and subtropical climate zones. Whiskers show the range of all 12 simulations, box shows the quartiles.

ESM 5 Present and future mean monthly rate of spread in the temperate climate zone. Unbroken line shows multimodel mean, dotted lines show ensemble minimum and maximum values.

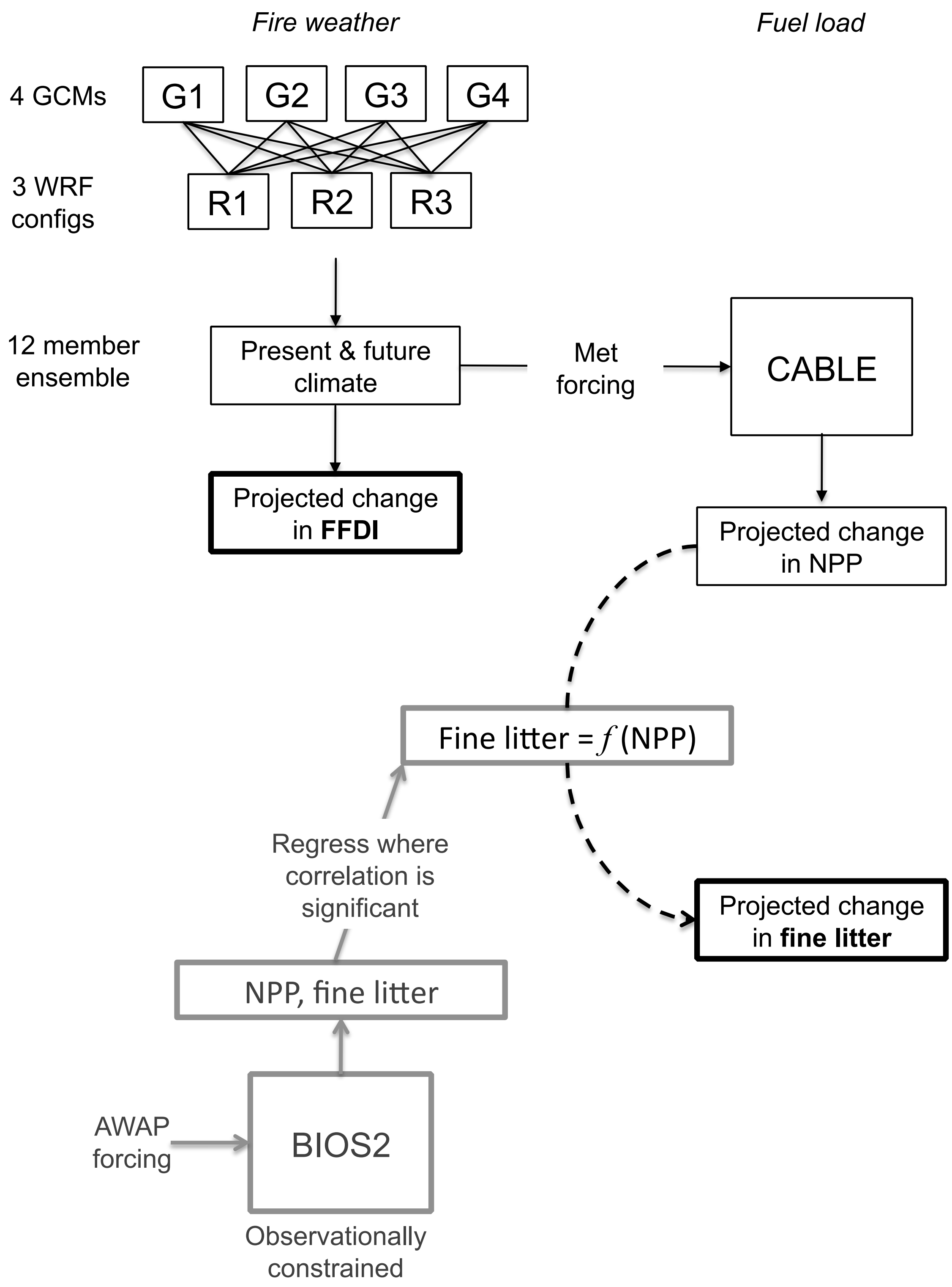

Fig 1 Summary of methodology. FFDI is calculated from a regional climate model ensemble spanning present (1990-2008) and future (2060-2078) periods. The same ensemble supplies the meteorological forcing to CABLE, yielding NPP. Based on the relationship between fine litter and NPP in BIOS2, fine litter is calculated from NPP in CABLE.

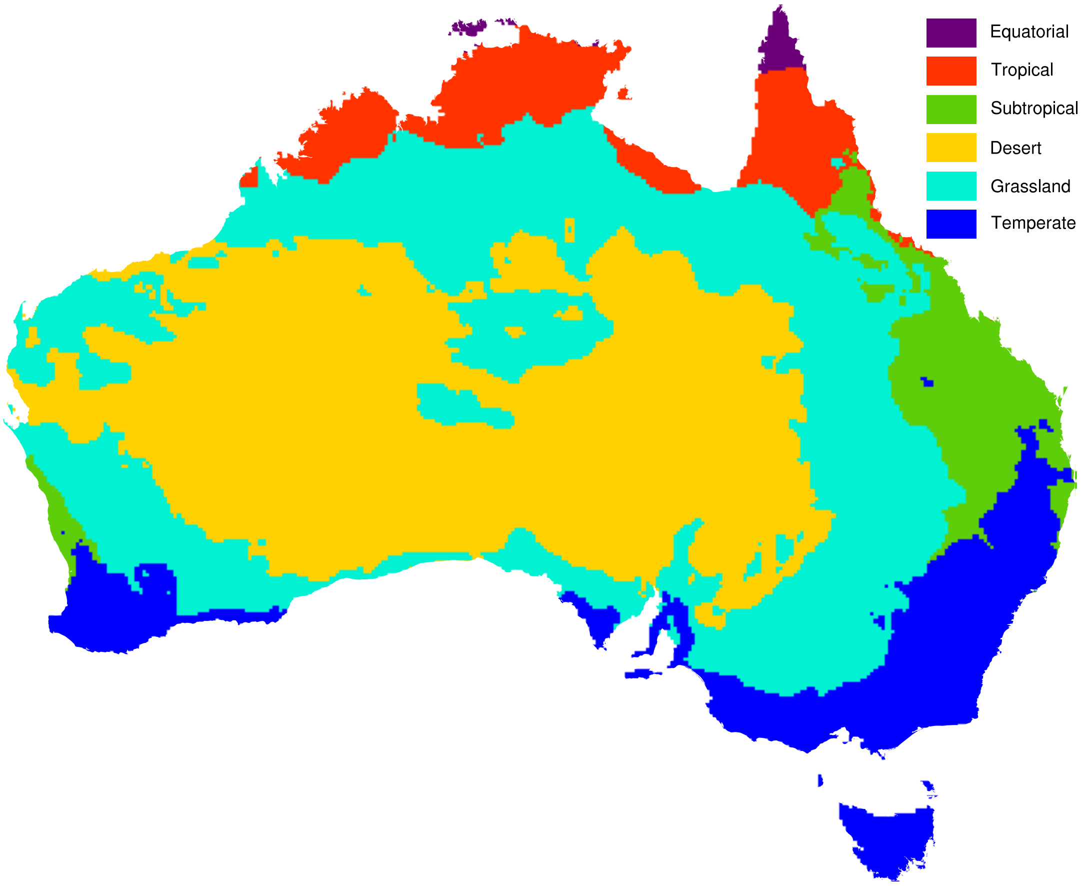

Fig 2 Köppen classification major climate zones

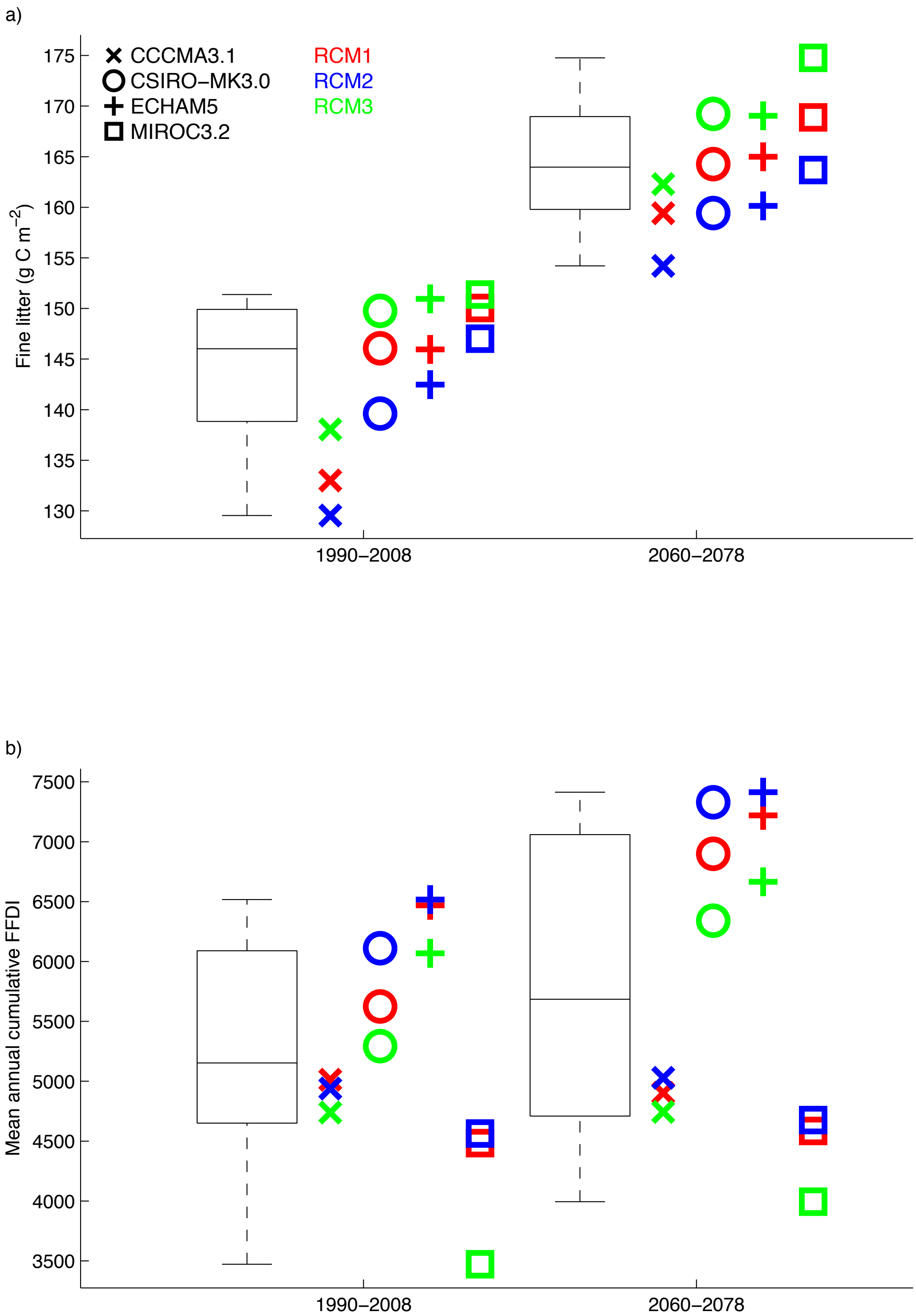

Fig 3 Ensemble mean annual continental (a) fine litter and (b) cumulative FFDI for present and future periods. Whiskers show the ensemble range, box shows the quartiles. Individual GCM/RCM combinations are represented by marker (GCM) and colour (RCM).

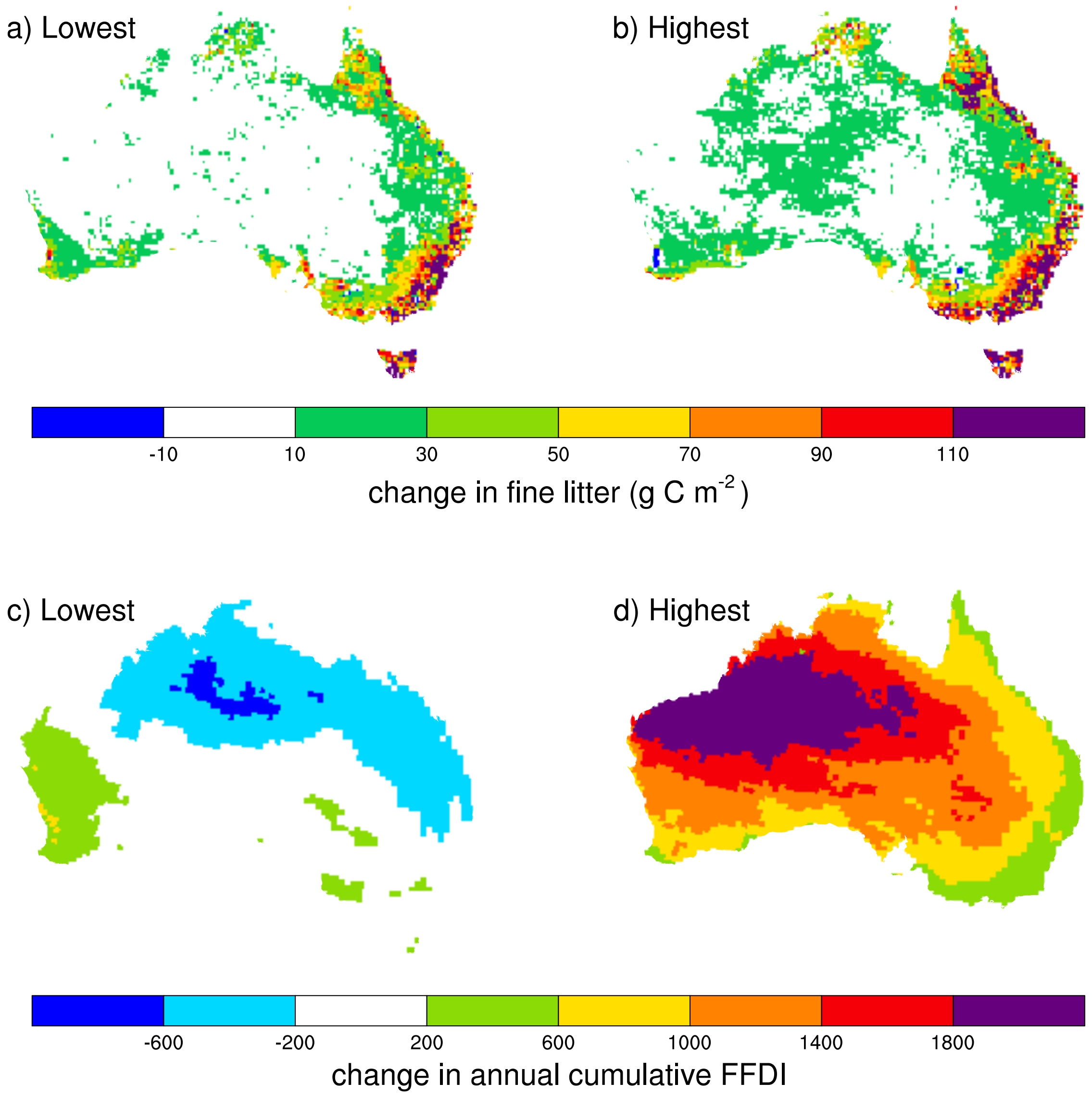

Fig 4 Change in mean annual (a) fine litter and (b) cumulative FFDI from the lowest and highest ensemble members, calculated from the average of all grid cell changes

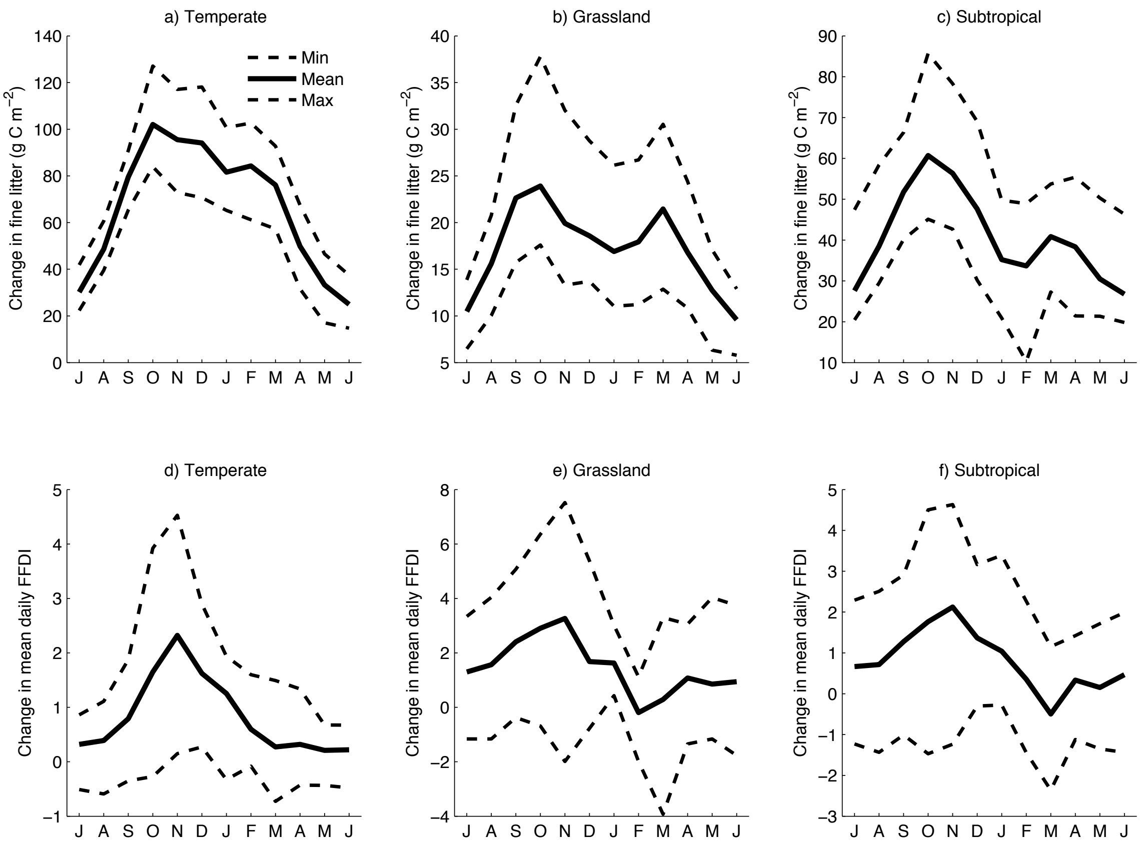

Fig 5 Change in mean monthly (a) fine litter load and (b) FFDI in temperate, grassland and subtropical climate zones. Unbroken line shows multimodel mean, dotted lines show ensemble minimum and maximum values.

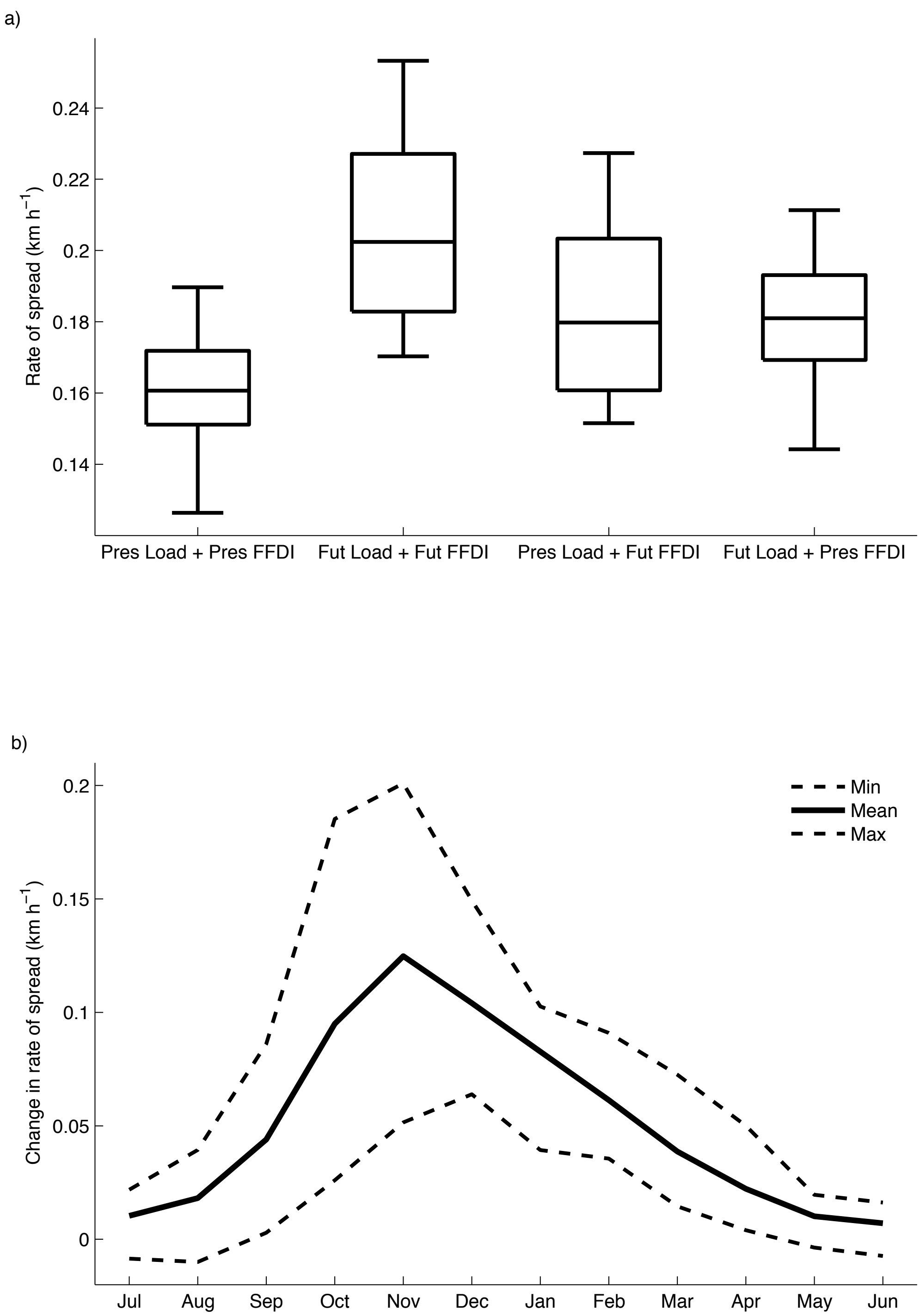

Fig 6 a) Ensemble mean fire rate of spread in the temperate climate zone, calculated using combinations of present and future FFDI and load. Whiskers show the ensemble range, box shows the quartiles. b) Change in mean monthly fire rate of spread in the temperate climate zone. Unbroken line shows multimodel mean, dotted lines show ensemble minimum and maximum values.

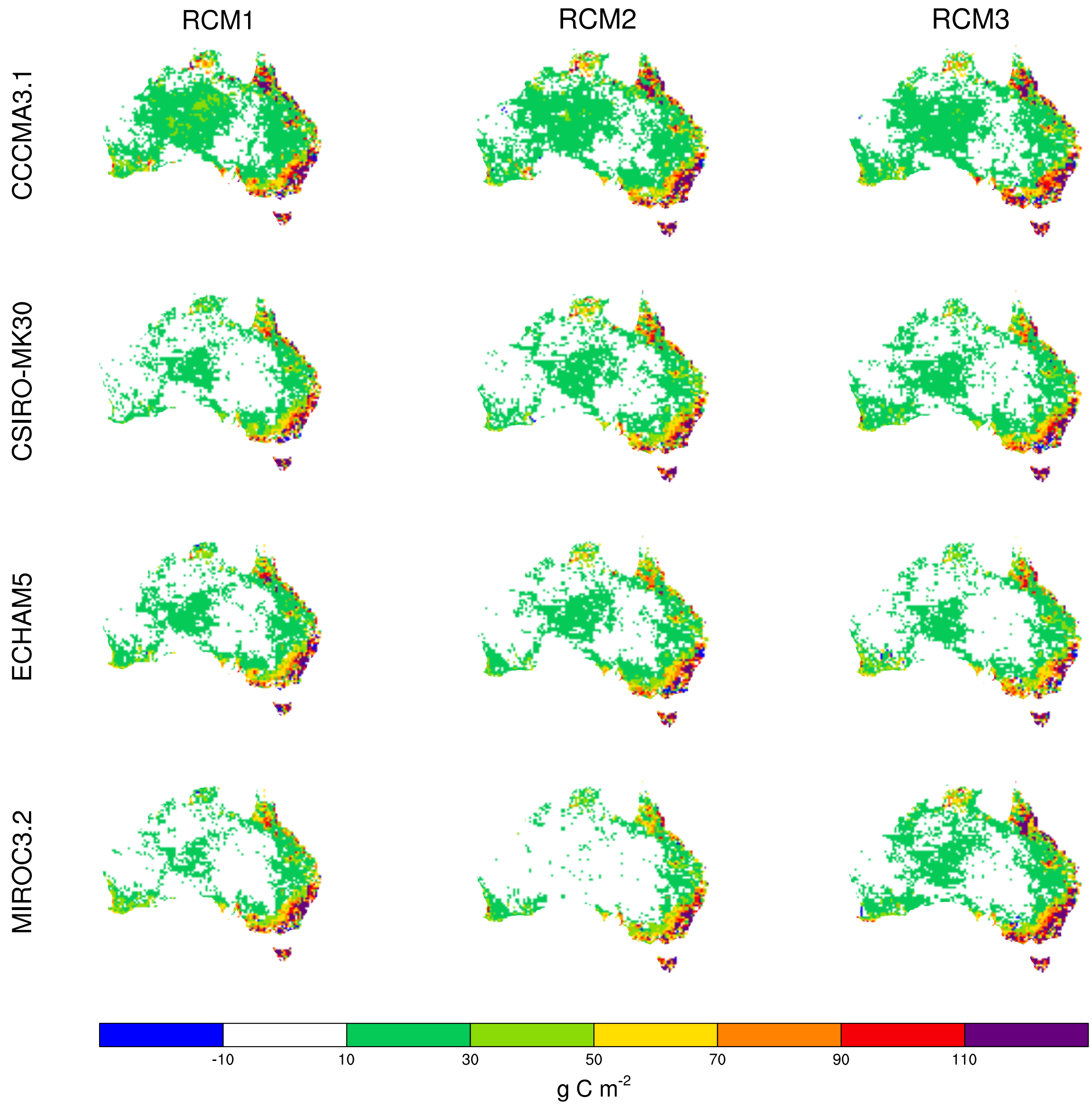

ESM 1 Change in mean annual fine litter from each ensemble member

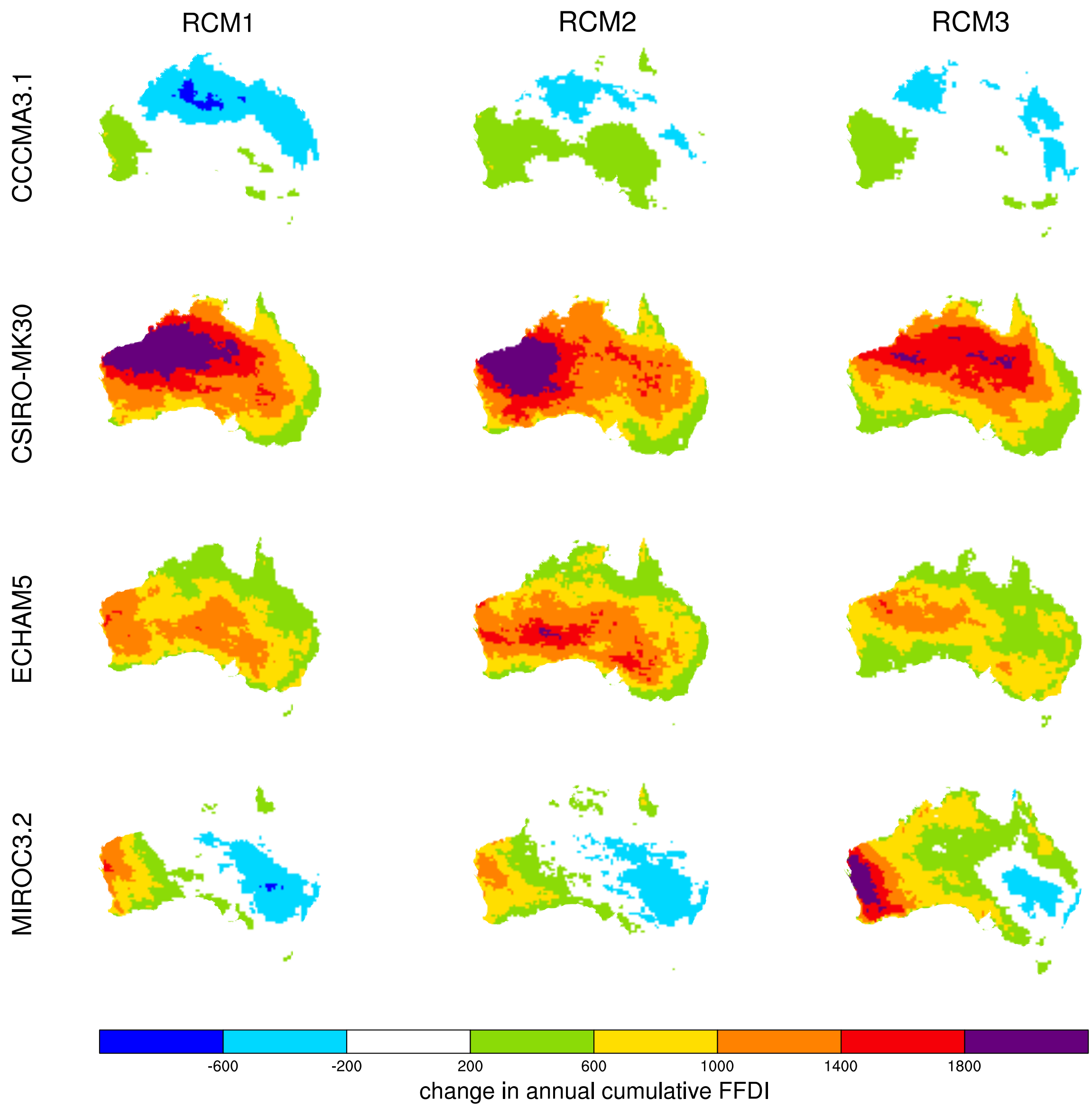

ESM 2 Change in mean annual cumulative FFDI from each ensemble member

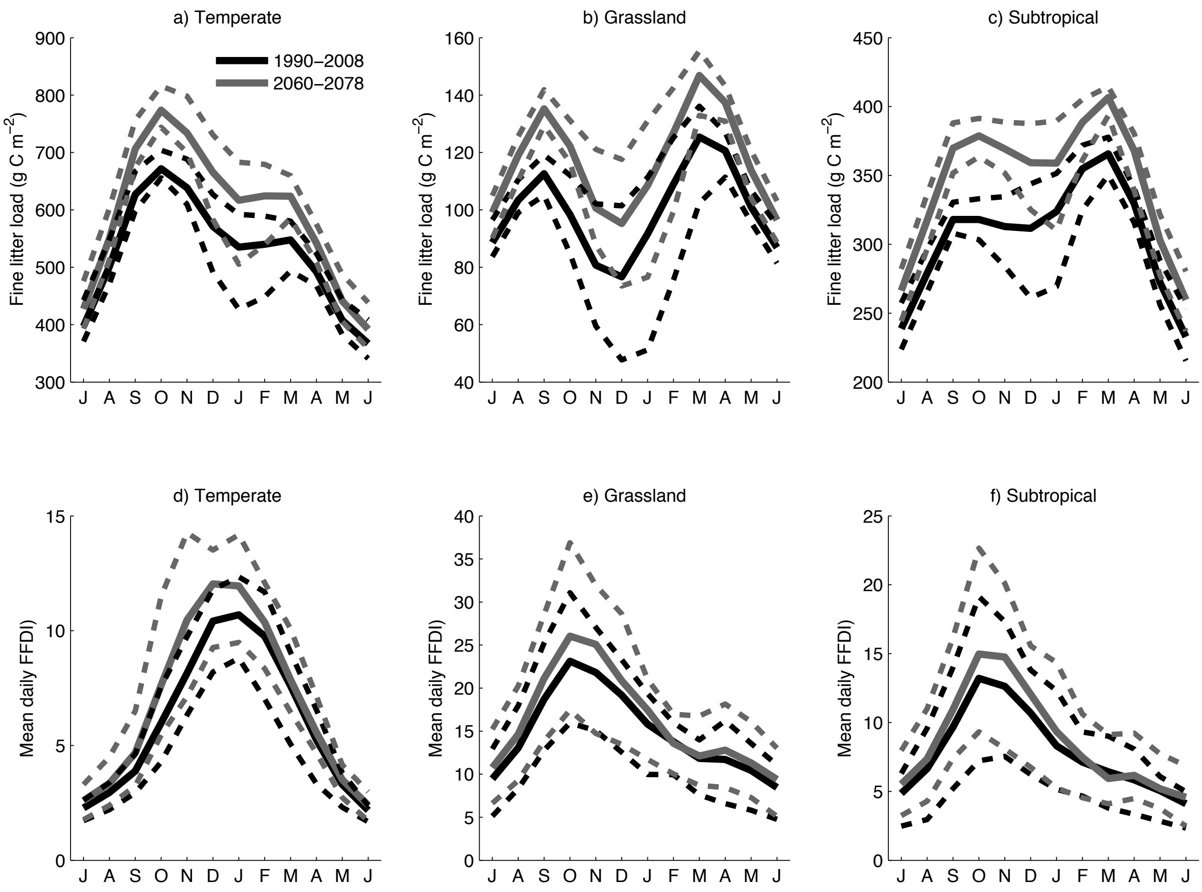

ESM 3 Present and future mean monthly fine litter (a-c) and FFDI (d-f) in temperate, grassland and subtropical climate zones. Unbroken line shows multimodel mean, dotted lines show ensemble minimum and maximum values.

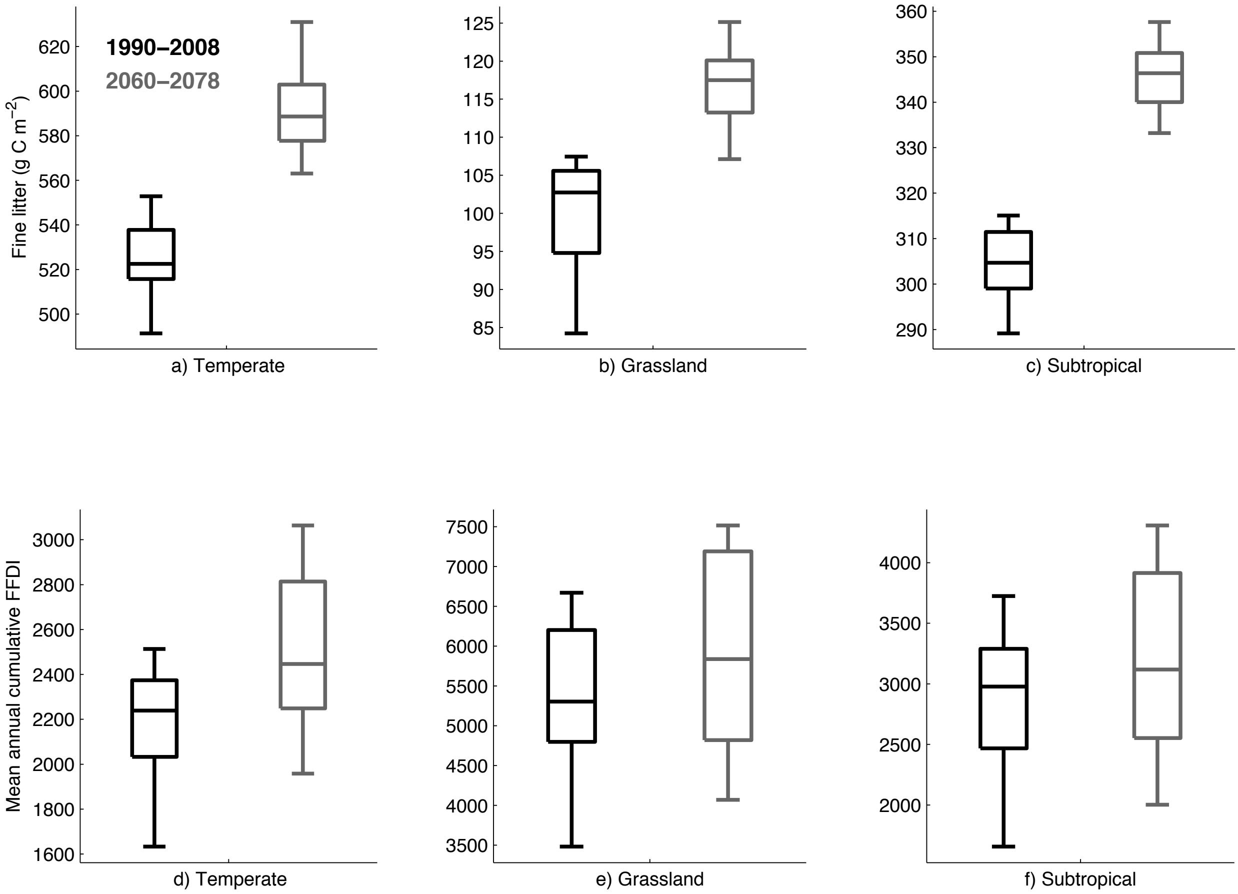

ESM 4 Ensemble mean annual fine litter (a-c) and cumulative FFDI (d-f) for present and future periods in temperate, grassland and subtropical climate zones. Whiskers show the range of all 12 simulations, box shows the quartiles.

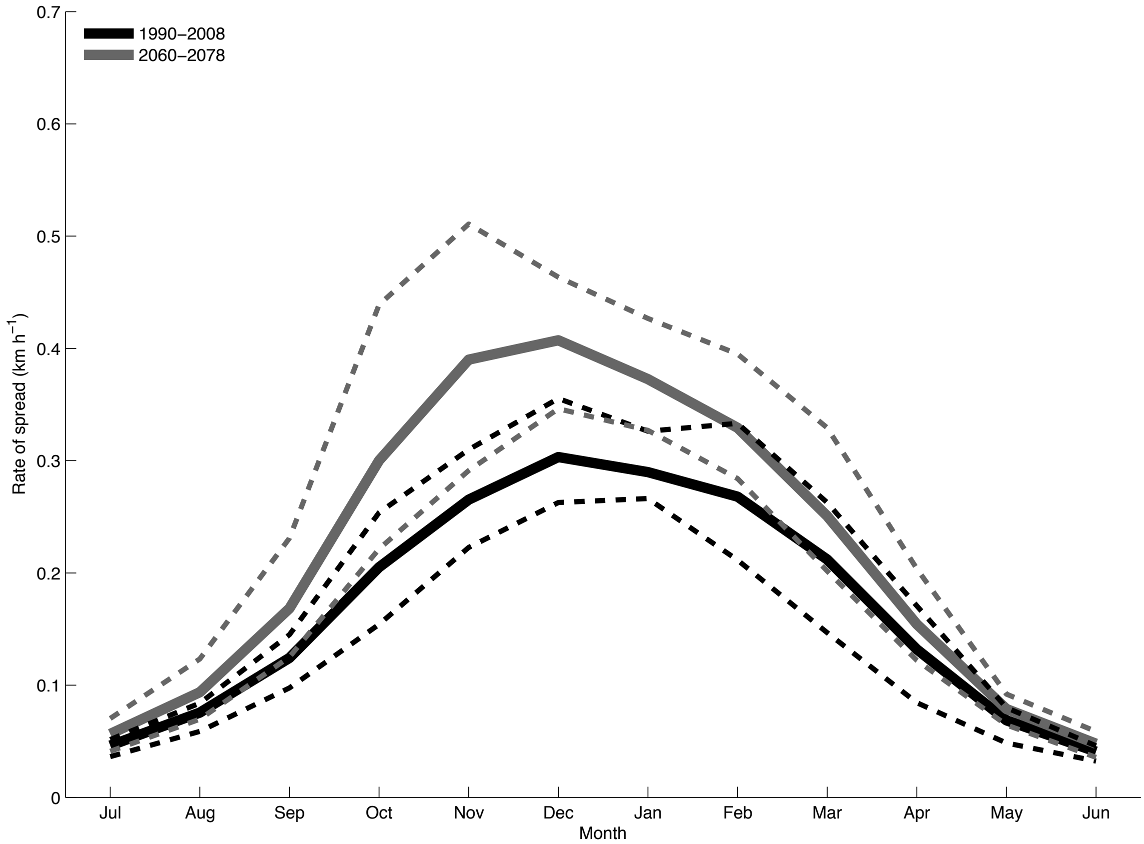

ESM 5 Present and future mean monthly rate of spread in the temperate climate zone. Unbroken line shows multimodel mean, dotted lines show ensemble minimum and maximum values.

Chapter 7 Summary

Downscaled projections of fuel load and fire weather

The study described in Chapter 7 suggests that climate change will bring increases in bushfire risk throughout much of Australia due to changes in fuel load and fire weather conditions. Fuel load is projected to increase substantially across both forested and grassy landscapes by the late 21^{st} century. None of the ensemble members projected a decrease in mean fuel load amounts for the broadscale climate zones analysed. Fire weather projections are much more sensitive to the choice of model, with roughly half the ensemble projecting significant increases, and the other half projecting little change, including minor decreases. Across both fuel load and fire weather, the largest projected increases occur in spring, suggesting a lengthening of the existing fire season.

This study, along with those described in Chapters 3-6, suggests some robust conclusions that can be drawn about the impacts of climate change on bushfire risk, as well as a number of important caveats. These are discussed in Chapter 8 in the context of the broader literature and the four research questions which guide this thesis.

Chapter 8

Discussion

This thesis aims to improve the understanding of the potential impacts of climate change in Australia on two of the four 'switches' of bushfire, fire weather and fuel load (the other two switches are fuel dryness and ignitions; Archibald et al. 2009; Bradstock 2010). These switches are represented by two measures, one well established and the other novel. Fire weather conditions are represented by the FFDI, widely used in fire management, forecasting of fire danger and research (FFDI includes a measure of the third switch, fuel dryness, but it is not explicitly examined here). In contrast, fuel load projections are based on a simple model of fuel load as a function of NPP, developed specifically for this purpose. Climate change impacts on fire weather and fuel load are derived from climate model simulations and, in the case of load, land surface model simulations. These numerical experiments are supplemented by a study of fire weather observations, providing a baseline against which the projections can be interpreted. The overarching aim of the thesis is addressed through four research questions, discussed here in order (8.1-8.4). The chapter concludes with uncertainties, caveats and issues of scope (8.5).

8.1 Are there significant trends in average or extreme fire weather within the observational record?

Chapter 3 provides strong evidence that fire weather conditions in Australia have changed over the observational record. These changes are widespread – occurring at about half of all sites in the network and in all states and territories – and are all increases, pointing to increases in both fire weather magnitude and fire season length. A changing climate poses a challenge to one of the key steps of climate change impact science – establishing a baseline against which to measure future change[1]. It is of course still possible to calculate standard climatological values such as annual and seasonal means, but these values are less representative of the climate over a given period when there is a significant trend.

Although trends in observations of meteorological variables such as temperature and rainfall have received considerable attention (Hartmann et al. 2013; Australian Bureau of Meteorology

[1] The baseline could be in climate, or it in some aspect of a fire regime e.g. burned area.

and CSIRO 2014), there are few other studies of trends in fire weather indices globally. A study of historical FFDI at four sites in South Africa found significant positive trends at all four locations (Kraaij et al. 2013). Long term trends have been assessed for a range of fire weather metrics in alpine regions of Europe, with changes detected at multiple locations and most of these increases (Wastl et al. 2012). A small number (2 out of 25) of stations recorded decreases in some fire danger metrics, but most of these were not statistically significant. At the upper ends of the distribution, indicating extreme conditions, all changes detected were increases. Strong increases in fire weather, particularly in the last two decades, were detected at five stations in the northern Sierra Nevada region of the U.S. (Collins et al. 2014). Positive trends in the FWI have been found across southern and eastern Europe, although these findings are based on reanalyses, rather than meteorological observations (Venäläinen et al. 2014; see Chapter 2 for more information on reanalysis). Venäläinen et al. (2014) found positive trends in a reanalysis covering the period 1980 to 2012, but no obvious trends for a separate reanalysis for the period 1960 to 1999. As with Australia, the changes in fire weather detected in these studies occurred against a backdrop of large interannual variability. This variability is likely to remain a strong feature of fire weather conditions and may produce periods of no trend or even deceases in fire weather in spite of overall increasing trends, as has been shown for global temperatures (Easterling and Wehner 2009).

Results from Chapter 3 and the international studies cited above suggest that increases in fire weather conditions are greater at the upper ends of the distribution. However, in Chapter 3, a relatively conservative extreme value was adopted (90^{th} percentile FFDI). For example, bushfire impacts on property (Blanchi et al. 2010) and life (Blanchi et al. 2014) are dominated by events occurring on days with FFDI values above 100. Values near 100 are at the very uppermost of the FFDI distribution in many parts of Australia, having occurred only once during the entire 38 year record. Inhomogeneities in the variables making up FFDI (particularly wind) are an obstacle to analyses of extremes, limiting the effective duration and spatial coverage of extreme values. However, over time more stations will have longer and higher quality records.

Chapter 3 does not present a detailed investigation into the drivers of observed fire weather trends, including their regional and seasonal variation. Such drivers might go beyond the individual variables comprising FFDI (temperature, relative humidity, precipitation, wind speed) to include local meteorological effects (Sharples et al. 2010), dynamics (Peace et al. 2012), synoptic patterns (Skinner et al. 2002; Girardin et al. 2004; Mills 2005a, 2005b; Mills 2008a, 2008b) and teleconnections (Williams and Karoly 1999; Verdon et al. 2004; Lucas 2005; Le Goff et al. 2007; Cai et al. 2009). A benefit of establishing relationships between any of these phenomena and local fire weather is that they can then be used as proxies for fire weather in climate change impact studies (e.g. Cai et al. 2009; Hasson et al. 2009). A related issue is the attribution of observed changes in fire weather conditions in the formal sense of climate change detection and attribution (D&A; Stone et al. 2009; Stott et al. 2010). There have been some attempts to provide quantitative links between human-induced climate change and fire activity (Piñol et al. 1998; Gillett et al. 2004; Kasischke and Turetsky 2006; Westerling et al. 2006) but none of these focused explicitly on fire weather metrics. Attributing changes in FFDI is complicated by the fact that it is calculated from multiple variables, not all of which are independent (e.g. temperature and relative humidity). Nevertheless, growth in the number of D&A studies adds confidence in the possibility of such a task (Herring et al. 2014).

In short, evidence from multiple studies points to increasing trends in fire weather during the observational record. Research presented in this thesis, representing a systematic examination of fire weather in Australia, also identifies clear and statistically significant increasing trends in average and extreme fire weather.

8.2 How is fire weather projected to change in different rainfall seasonality regions by skill-selected global climate models?

The major way in which the fire weather projections developed in Chapter 4 build upon earlier studies is through the use of an ensemble of skill-selected GCMs. The aim of this is to sample uncertainty while minimising biases arising from poorly performing models. The objective design of model ensembles according to skill or other means follows on from the use of ensembles. The general premise is that any individual climate model simulation will represent just one of many possible pathways of the climate system. Therefore, to evaluate uncertainties due to differences in model formulation and the initial conditions, it is necessary to carry out simulations with multiple models, or multiple simulations using the same model (Flato et al. 2013). The publication of the Intergovernmental Panel on Climate Change's (IPCC's) Fourth Assessment Report (IPCC 2007) coincided with the release of a large associated archive of GCM output under the auspices of CMIP3 (Meehl et al. 2007a). Conducting climate change impact studies based on an ensemble of multiple GCMs became much easier with the availability of this dataset of consistently produced climate model output. Prior to 2011, when Chapter 4 was published, only a very small number of fire weather projections used more than 2 GCMs; exceptions include pioneers Flannigan and Van Wagner (1991; 3 GCMs), Stocks et al. (1998; 4 GCMs), Malevsky-Malevich et al. (2008; 6 GCMs) and Hasson et al. (2009; 10 GCMs). Hasson et al. (2009) was the only Australian study, focusing on southeast Australia.

Of course, there have been and continue to be pragmatic reasons for using a limited number of models in climate impact studies. Models may be chosen because researchers have personal experience with, or links to the modelling group behind, a given GCM, or because output from multiple models is not available, or not available for all required variables and time resolutions (Evans et al. 2014). For example, in selecting four GCMs used in Chapter 4, daily data for all variables required to compute FFDI were not available from the model ranked first by Perkins et al. (2007), so the fifth ranked GCM was used instead. Even where model data is available, the computational resources required to process large ensembles can be significant, especially when used in combination with other experimental treatments (e.g. Tarancón et al. 2014). A common multiplier of model results is the use of multiple SRES emissions scenarios (Nakicenovic et al. 2000) or RCPs (Moss et al. 2010), which aim to address uncertainty in the future evolution of GHG emissions. This thesis does not attempt to sample uncertainty in emissions scenarios, using a single emissions scenario in Chapters 4 and 7. However, the scenario selected in Chapter 4 (A2) was the closest one to global emissions trends at the time (Le Quéré et al. 2009) and emissions continue to track the high end of emissions scenarios (Friedlingstein et al. 2014), giving confidence in the choice of this over lower emissions pathways.

Whether 2 or 10 GCMs are used, the assumption is generally that while models differ in their formulation, each member of the ensemble provides an independent and equally likely estimate of future climate change, and that results should thus be weighted equally (Abramowitz 2010). However, there is now a wealth of information on just how well different models simulate different aspects of the climate system (Randall et al. 2007; Flato et al. 2013). It is thus possible to weight models by performance[2], select those that perform best, or remove those that perform worst – noting, however, that any selection methodology is likely to reveal different 'best' models, depending on the variable and metric chosen, as well as the region of evaluation (Perkins et al. 2007). At the time of the design of the study in Chapter 4, Perkins et al. (2007) had recently published an evaluation of GCMs' ability to simulate the Australian climate, based on PDFs of temperature and rainfall. To the author's knowledge, Chapter 4 presents the first projections of climate change impacts on fire weather conditions using multiple GCMs selected with a peer-reviewed methodology. A subsequent example is Litschert et al. (2012), who develop a model of burned area in the Southern Rockies Ecoregion of the U.S. Litschert et al. (2012) select two GCMs from an ensemble of 16, evaluated by Dominguez et al. (2010) for their ability to simulate modes of climate variability important to fire regimes in the region.

There are other methods for addressing biases in climate models, including the use of scaled observations rather than direct climate model output (e.g. Lucas et al. 2007; Amatulli et al. 2013; Lehtonen et al. 2014) and the adjustment of model output to match observations (e.g. Fox-Hughes et al. 2014). However, the correction of model output carries with it the risk of

[2] The use of independence and spanning future change space as model selection criteria will be addressed under question 4, below.

invalidating a key strength of climate models, namely their adherence to a range of physical laws describing the behaviour of the climate system (Ehret et al. 2012). Some correction of biases may be necessary to carry out certain climate change impact applications, but it should be made clear that the increase in fidelity to observations may be accompanied by a corresponding decrease in fidelity to physical principles, such as the relationship between variables or the consistency of spatiotemporal fields. Without these clarifications, bias correction may only bring results closer to reality to the extent that changing the stickers on a Rubik's cube brings it closer to a solution.

A second feature of Chapter 4 that builds upon previous GCM-based fire weather studies is its grouping of results by a key driver of Australian fire regimes, rainfall seasonality (Russell-Smith et al. 2007; Bradstock 2010; Murphy et al. 2012). The great majority of fire weather projections using GCMs do not group results along biophysical boundaries; rather they are applied over an entire region of interest (and perhaps interpolated or summarised in the form of contours or area averages) or to individual sites corresponding to locations with historical fire weather records. While such an approach does not preclude the subsequent grouping of results by different categories, this task is generally left to the user (or literature reviewer). Using direct model output also avoids the assumption, made in Chapter 4, that GCMs faithfully reproduce observed patterns of rainfall seasonality. Nevertheless, grouping of GCM output into biophysically relevant categories is common in studies of the impact of climate change on other aspects of fire regimes, such as fire activity (Vázquez de la Cueva et al. 2012; Moritz et al. 2012; Girardin et al. 2013; Migliavacca et al. 2013; Mori and Johnson 2013; Yue et al. 2013). Boulanger et al. (2013) even make groupings the focus of their research, objectively deriving zones with homogenous fire regimes in Canada for use in climate projections and to highlight otherwise hidden aspects of fire regimes under prevailing classifications.

The point of grouping model output by regions of rainfall seasonality is to help interpret and use the results, which is a major aim of all climate change impact studies. Indeed, even though GCMs are designed to simulate the global climate, they are often used for specific regions (North America, boreal forests, the Mediterranean, southeast Australia) rather than global analyses (see Moritz et al. 2012 for an exception). This clearly points to the fact that it is at the local and regional level at which the impacts of climate change are felt, and at which adaptation takes place. It is this factor that has driven another trend in climate research, the increasing downscaling of GCM output. This use of RCMs to downscale will be addressed below, but despite the push towards downscaling, global climate models remain critical to climate change impact studies. They provide the boundary conditions needed to run RCMs and the raw data required by statistical downscaling, and are still widely used without downscaling. Future fire weather projections will therefore benefit from further development and evaluation of GCMs.

In summary, research presented in this thesis uses an ensemble of skill-selected GCMs to project future fire weather in eastern Australia by regions of rainfall seasonality, a key driver of variation in Australian fire regimes. The use of these methods builds upon earlier studies to deliver a clearer picture of the broad patterns of fire weather conditions expected in Australia under climate change. In the summer rainfall-dominated, tropical northeast, fire weather is projected to decrease or remain close to 20th century levels. In the uniform and winter rainfall areas of the southeast, strong increases in fire weather magnitude and duration are projected.

8.3 Can a simple model of fuel load be developed for use in the Australian land surface model, that accounts for both climate and atmospheric CO_2 effects on vegetation growth?

Chapter 6 demonstrates that NPP can be used as a proxy to model fuel load, based on a strong linear relationship between annual NPP and the subsequent year's load in large areas of Australia, including temperate, grassland and subtropical climate zones. The use of NPP as a proxy allows load to be modelled using the process-based land surface model CABLE, which incorporates effects of climate and CO_2 fertilisation on plant growth. The use of NPP as a proxy for load in CABLE allows a range of offline and coupled experiments on the sensitivity of fuel load to changing environmental conditions.

The skill and scope of this model should be placed in the context of existing process-based and empirical[3] options for modelling the impact of climate change on fuel load (Tables 8.1 and 8.2). CABLE has some advantages over other approaches. Firstly, CABLE is the standard land surface model for the Australian global climate model, ACCESS. This provides direct and easy access to a range of past and potential future experiments linked to a climate model that has been designed for the Australian context, and that is routinely used for numerical weather prediction and global climate projection intercomparisons. While DGVMs are regularly forced with climate model output ('offline'), the coupling of DGVMs to GCMs ('online') has not generally been standard, although this is changing (Flato et al. 2014). Secondly, by emphasising interactions between the land surface and the atmosphere, CABLE provides an alternative framework with which to potentially reduce one of the major uncertainties around climate change and vegetation, namely the response of productivity to climate change (Settele et al.

[3] This dichotomy is somewhat misleading. Empirical models assume a process underlying the correlative link, while process-based models rely heavily on, and generally include some, empirical information (Adams et al. 2013).

Table 8.1 Major approaches to modelling response of fuel load to climate change – general features.

Model type	Model (example)	Aim	Spatial resolution	Vegetation resolution	Fuel load representation
Process-based	Dynamic global vegetation model (Bonan et al. 2003)	Ecosystem processes esp. climate and vegetation interactions	Regional to global	Plant functional types	Small number of pools e.g. litter, coarse woody debris
Process-based	Land surface model[1] (Wang et al. 2011)	Land surface and atmosphere interactions esp. water, energy and carbon fluxes	Regional to global	Plant functional types	By proxy e.g. NPP
Process-based	Biogeochemical model (Wang et al. 2010)	Cycling of carbon, other elements through earth system	Regional to global	Plant functional types	Small number of pools e.g. metabolic litter, structural litter, coarse woody debris
Process-based	Landscape fire succession model (Keane et al. 2011)	Climate, fuel and fire interactions	Local to regional	Species to plant functional types	Single to large number of pools e.g. surface fuels, canopy fuels
Empirical	Statistical-correlative modelling (Thomas et al. 2014)	Link load[2] with variable available from climate model	Point to global	Species to plant functional types	Varies e.g. temperature, precipitation

[1] The approach taken in this thesis is highlighted in grey

[2] Indirect correlative models have also been developed, linking meteorological variables to a proxy for load e.g. NPP (Batllori et al. 2013)

Table 8.2 Major approaches to modelling response of fuel load to climate change – mechanisms.

Model type	Model (see Table 8.1 for examples)	Key processes affecting load	Incorporation of climate change impacts	Allows for CO_2 fertilisation?
Process-based	Dynamic global vegetation model	Primary: litterfall, decomposition, disturbance. Secondary: primary productivity, heat, moisture	Forced by climate model output, coupling to climate model	Yes
Process-based	Land surface model[1]	Primary: primary productivity, carbon flow between vegetation and soil	Forced by climate model output, coupling to climate model	Yes
Process-based	Biogeochemical model	Primary: litterfall, decomposition Secondary: primary productivity, heat, moisture, nutrient limitation	Forced by climate model output, coupling to climate model	Yes
Process-based	Landscape fire succession model	Varies[2] e.g. gap model, state and transition model, fuel accumulation model; includes disturbance	Forced by climate model output (generally temperature and precipitation only)	Generally no
Empirical	Statistical-correlative modelling	Function of environmental variables e.g. temperature, precipitation	Forced by climate model output	No

[1] The approach taken in this thesis is highlighted in grey

[2] Some components of landscape fire succession models can be used as fuel load models in their own right e.g. gap models, state and transition models. See also the growth and yield model, with origins in forestry (Hurteau et al. 2014a) and the tree demography and landscape structure model (Haverd et al. 2013c).

2014). Clearly, however, CABLE is a complement to, rather than a substitute for, existing approaches to capturing the relationship between fuel load and climate change (e.g. King et al. 2012). In the same way that model ensembles can reduce uncertainty in climate projections, adopting a portfolio of modelling approaches can reduce uncertainty in the modelled phenomenon (e.g. Ito 2011).

Process-based and empirical approaches to fuel load modelling will improve through evaluation and the incorporation of new findings. For instance, evidence from observational and modelling studies of litter and litter decomposition suggests the strong possibility of interacting effects between climate, CO_2, species composition (vegetation, macrofauna, microbes) and litter quality (Rouifed et al. 2010; Boyero et al. 2011; Ferreira and Chauvet 2011; Brovkin et al. 2012; Ott et al. 2012; Saura-Mas et al. 2012). Empirical studies of the existing relationship between climate and major fuel types (Bowman et al. 2014b; Gibson et al. 2014; Thomas et al. 2014) suggest a more nuanced response than the broad shifts (e.g. away from grasslands and towards forests) projected by DGVMs (Scheiter and Higgins 2009; Jiang et al. 2011; Jiang et al. 2013).

The model developed in Chapter 6 does not presently include disturbance, nor is it based on detailed measures of current land cover. As a result the fuel load modelled should be considered potential, rather than realised fuel load. However, this points to a much broader issue in modelling the impacts of climate change on bushfire and other complex systems: the presence of interactions and feedbacks. In spite of the presence of a large body of relatively reductionist research on bushfires and climate change, the potential for interactions and feedbacks has been widely recognised (e.g. Cary et al. 2012; Gill et al. 2013; Clark et al. 2014; Hurteau et al. 2014a, 2014c; Mitchell et al. 2014). This thesis has assumed that changes in fire weather or fuel load will lead to changes in bushfire risk, depending on their significance to local fire regimes. However, fire is just as often a cause as it is an effect. Changes in fire regimes will likely have a range of direct and indirect effects on these same fire regimes in ways not modelled in the original study. For instance, it is commonly projected that climate change could lead to a doubling or more in fire weather conditions or area burned in some areas (Guyette et al. 2014; Hurteau et al. 2014b; Stavros et al. 2014). However, if large and severe fires act to reduce available fuel for future fires, this could act as a negative feedback, potentially limiting their overall frequency and extent (e.g. Heon et al. 2014). Conversely, it is likely that suppression has had some influence on historical fires, which form the basis of correlative models used in projections (Turco et al. 2014). If increases in fire weather conditions are large enough to overwhelm humans' ability to suppress them and lead to increases in the number of uncontrollable fires (de Groot et al. 2013b), then projections of future fire based on correlative models may be underestimates. The following is a small sample of impacts of fire with potential for feedback effects including and up to transition to entirely different fire regimes (Zinck et al. 2011; Batllori et al. 2013; Pausas and Keeley 2014)

- the age of vegetation and fuel load (Raymond and McKenzie 2012; Taylor et al. 2014) and overall biomass carbon stock (Keith et al. 2014)
- litter properties (Papanikolaou et al. 2010; Aponte et al. 2014; Toberman et al. 2014)
- soil properties, hydrology and water supply (Dunbar et al. 2012; Bladon et al. 2014)
- a wide range of impacts on animals and plants – for instance on weeds and invasive species vis-à-vis fuel load – beyond that explored by DGVMs (Driscoll et al. 2010; Vivian et al. 2010; Banks et al. 2014; Dolanc et al. 2014)
- GHG emissions (Keith et al. 2014; Loehman et al. 2014)
- fire management including prescribed burning (Bradstock et al. 2012; Tarancón et al. 2014) and land management (Gibbons et al. 2012)
- a range of social and health impacts, e.g. land use (Bryant and Westerling 2014), smoke (Price et al. 2012), national park visitation (Duffield et al. 2013) and employment (Nielsen-Pincus et al. 2014)

Chapter 6 does not present an evaluation of the simple fuel load model developed in it. The high quality, long term, gridded observational datasets available for climate model validation[4], stand in stark contrast to the lack of similar fuel load observational datasets. Still, there are a number of options for evaluating fuel load models. Watson (2012) provides a useful synthesis of a range of fuel load observations in NSW, including many sites beyond the initial dataset used to validate BIOS2 (Haverd et al. 2013a). Site-based observations are not an ideal test for grid-based models – they may not be representative of the entire model grid-cell with which they are being compared, and there have been considerable differences in fuel assessment methodologies over the years (Watson 2009; Keane 2012). Nevertheless, these represent the longest running and most diverse source of fuel load observations and will give some indication of model bias. In contrast, vegetation-formation based estimates of load developed by Watson (2012) are more or less spatially continuous, having been generalised from multiple point-based observations for a range of vegetation types found in NSW, including rainforests, dry and wet sclerophyll forests and grassy woodlands.

[4] More for temperature and precipitation than other meteorological variables.

There are a number of remotely sensed products of a spatial scale suitable for process-based fuel load model evaluation. LiDAR measurements have been empirically related to various spatial properties of fuel, including density and amount (Clark et al. 2009; Bolton et al. 2013). They have also been used as close to pure observations (see Keane et al.'s (2001) discussion of direct versus indirect mapping using remote sensing). Passive microwave remote sensing of vegetation optical depth (VOD), which reflects vegetation water content, has been used as a proxy for terrestrial aboveground (living) biomass (Liu et al. 2011; Liu et al. 2013). The normalized difference vegetation index (NDVI) derived from remote sensing has been used to estimate fuel amount as well as the curing of herbaceous vegetation (Chafer 2007; Turner et al. 2011). Finally, remotely sensed estimates of NPP have been used to estimate fuel load (Hély et al. 2003; Roberts et al. 2008). It would be ironic, but not physically inconsistent, if these NPP-based load values[5] were to serve as observations for the validation of model of load derived from NPP.

The research presented in Chapter 6 does not attempt to isolate the effects of rising CO_2 on the load during the twentieth century. One study has found that Australian continental NPP between 1990 and 2011 was 13% higher than it would have been in the absence of anthropogenic CO_2 (Haverd et al. 2013b). Isolating CO_2 effects on NPP has of course more than historical relevance, given the increasing trajectory of global atmospheric CO_2 emissions. The use of this model to project future load is described in Chapter 7 and addressed below. A separate issue relates to the length of the simulation presented in Chapter 6. At 28 years, it is longer than any other historical fuel load simulation focused on Australia that author is aware of, but longer reanalysis datasets are available. For instance, the NNRP dataset (Kalnay et al. 1996) begins in 1948 and would allow for a considerably extended simulation of load, making it easier to investigate interdecadal variability and spatial and temporal trends.

To sum up, this thesis presents research which demonstrates that in an observationally constrained ecosystem model, fuel load expressed as a simple linear function of the previous year's NPP explains most of the variation in annual fuel load over large regions of Australia, particularly in temperate, grassland and subtropical regions. The Australian land surface model CABLE incorporates both climate and atmospheric CO_2 into its simulation of NPP and can therefore be used to simulate fuel load under changing climate and CO_2, based on this simple relationship. As presently formulated, there is most confidence in the model's ability to simulate variation in fuel load at coarse temporal scales (annually) and over large climate regions. At a fine spatial scale, the model performs strongly in some areas and weakly in others. Improving

[5] Themselves based on empirical relationships between observable quantities, such as greenness, and NPP.

the temporal resolution and accuracy of the model, through model evaluation and the incorporation of more realistic mechanisms, will improve its overall applicability.

8.4 How are fire weather and fuel load projected to change at a relatively fine scale (50 km) by an ensemble of global and regional climate models, selected to span the possible future climate change space?

Chapter 7 presents the first continental, relatively fine scaled projections of the impact of climate change on both fire weather and fuel load. These projections suggest an increase in bushfire risk in temperate, grassland and subtropical areas of Australia due to climate change, driven by increasing fuel load, increasing or stable fire weather and a lengthened fire season. If these changes were to occur, they would likely have impacts across the country's fire regimes. However, projections of increasing fuel load are potentially more significant in grassland regions, where fire incidence tends to be load-limited, while increases in fire weather conditions may be more significant in forested areas, where fire incidence is limited more by weather conditions that dry fuel out enough for it to burn (Bradstock 2010; King et al. 2013).

The study relies on the fuel load model developed in Chapter 6 (discussed above) and the ability of WRF to simulate FFDI, which is demonstrated for southeast Australia in Chapter 5. With respect to fire weather, WRF is yet to be evaluated over the rest of Australia, including parts of the climate zones used in Chapter 7. The simulations used in Chapter 7 are part of a larger RCM dataset that includes a three member reanalysis-driven ensemble, which provides additional model data to evaluate against observations (Evans et al. 2014). Moreover, the reanalysis dates back to 1950. A small number of stations in the observational network also go back to around this time (Lucas 2010), raising the prospect of testing the ability of WRF to capture long term variation in FFDI. Work is underway to develop a gridded FFDI product (M. Boer, K Braganza, pers. comm.), which would provide a more appropriate test of WRF's performance and facilitate bias correction of WRF output beyond individual stations. Chapter 5 does not investigate the reasons for the WRF biases identified (e.g. a tendency towards positive bias inland and negative bias on the coastline), nor for differences in WRF performance at different model resolution. Evans and McCabe (2013) found that mountainous and coastline areas are generally simulated better at 10 km resolution than 50 km resolution, and that coarser resolution RCM simulations can actually mask errors in the driving GCM, which are revealed by finer resolution simulations.

As noted, the need for regionally useful climate change information has led to increased downscaling of global climate models for fire weather projections (and other measures of bushfire risk). Two major avenues for converting GCM output to a finer scale are dynamical regional climate models (RCMs; Mearns et al. 2003) and statistical downscaling (Wilby et al. 2004). This thesis focuses on RCMs, but the two have different strengths and weaknesses and importantly, they are not mutually exclusive. The use of RCMs in climate change research on bushfires goes surprisingly far back, with two studies published in 2001 that used an RCM to explore changes in fire weather conditions in the west (Amiro et al. 2001) and boreal forest (Flannigan et al. 2001) of Canada. In Australia, the atmosphere-only RCM, CCAM, was used to project changes in FFDI in southeast Australia in 2005 (Hennessy et al. 2005). There has been a strong increase in the number of studies since then, facilitated by model development and the availability of large GCM output archives, as well as increased expertise amongst scientists in using these models. In 2013 and 2014 alone, there were at least 13 fire weather projection studies using RCMs, spanning the Mediterranean, Europe, North America, Australia and China.

The increasing use of RCMs has benefited from the development of several regional climate projection ensembles, including PRUDENCE (Christensen et al. 2007), ENSEMBLES (van der Linden and Mitchell 2009), and NARCCAP (Mearns et al. 2012). Chapter 7 employs an ensemble selected not just for its skill in representing climate, but for two other important attributes: model independence and spanning a range of possible futures. The issue of model independence relates to the treatment of ensemble members as equally likely projections of future climate. As an example, if an ensemble of three models contains two that are very similar, and one that is quite different, it would be misleading to consider each one an equally likely representation of a possible future climate. The ensemble used in Chapter 7 draws on the work of Bishop and Abramowitz (2013), who provide a means for defining model independence based on covariance in model errors. The author is not aware of any other fire projection studies that use an ensemble of climate model simulations selected for independence.

The use of ensembles that span a range of possible future climates is more common (Jiang et al. 2011; Lung et al. 2013; Hurteau et al. 2014b; Mann et al. 2014). The selection of a subset of models that spans the range of a large ensemble reduces the complexity and computational cost of the study, while retaining critical information about the extremes of possible change. It is therefore an acknowledgement that climate projection studies are undertaken to inform policy and management decisions, with the assumption that users will be interested in not just average projections, but also ‘best’ and ‘worst’ case scenarios. All studies the author is aware of use temperature and precipitation as their criteria for defining the span of possible change (e.g. warm and wet vs. hot and dry) but other options are possible and will depend on the needs of the users. The growing use of objectively designed model ensembles has led some to refer to an unweighted collection of models, not long ago something of a gold standard in climate research, as a Poor Man's Ensemble (Cane et al. 2013).

As discussed above, the fire weather projections presented in Chapter 7 are drawn from a larger RCM dataset. This dataset includes a 12 member ensemble, using the same GCMs and RCMs as Chapter 7, but at 10 km horizontal resolution. While 50 km can be considered fine scale in terms of GCM resolution, these higher resolution simulations provide an opportunity to examine finer scale variation in future fire weather and further compare the effect of model resolution on model performance. The increased resolution comes at a cost in spatial coverage, with the 10 km resolution ensemble available only over southeast Australia, rather than all of Australia. The 10 km dataset also includes bias-corrected temperature and precipitation data, which raises the prospect of comparing what would be a partially corrected (but physically inconsistent) FFDI against uncorrected FFDI, in terms of both projections as well as ability to simulate observed fire weather (see Fox-Hughes et al. 2014 for an example from Tasmania).

In conclusion, this thesis presents projections of fire weather and fuel load under climate change in Australia from a global and regional climate member ensemble, selected for model skill and independence, as well as to span the range of possible climate change futures. Fuel load is projected to increase strongly across Australia by all ensemble members. In contrast, projections of fire weather conditions are highly sensitive to the choice of model, with two of four GCMs suggesting little change in FFDI, including small decreases, and the other two suggesting strong increases in FFDI. All ensemble members project the largest increases in fire weather to occur in spring, suggesting a longer fire season overall.

8.5 Caveats, uncertainties and scope

There are of course major uncertainties inherent in these conclusions. Uncertainty in fire weather projections is closely linked to uncertainty in the global climate model forcings used, although it is notable that the magnitude of projected increases is far larger than that of decreases. This contrasts with fuel load, which is consistently projected to increase, likely linked to the CO_2 fertilisation effect. Uncertainty in projected load is strongly related to the model of load as a function of NPP itself, developed in this thesis. The rationale for linking these two variables is sound, but the implementation is simple, temporally coarse (based on annual values) and is unable to represent changes in the drivers of litter amount, litterfall and litter decomposition. As a result, fuel load projections should be considered indicative of potential broadscale vegetation responses to changed climate and increased CO_2, rather than prescriptive of detailed changes in vegetation amount feeding into fire behaviour models.

Another limitation is the ability of the models used in Chapters 3 to 7, particularly WRF, to accurately simulate FFDI. In a similar vein, thesis results are limited by CABLE's ability to simulate NPP and carbon fluxes more generally. Reducing uncertainty in the response of vegetation to increased atmospheric CO_2 is a major research challenge. Another caveat applicable across this thesis is that uncertainty in the trajectory of global GHG emissions is not sampled. All projections use a single emissions scenario, A2, a choice supported by evidence showing that global emissions continue to track at the upper end of the various IPCC scenarios. Finally, the models used here are relatively fine in spatial scale with regard to global climate models, but relatively coarse compared to some other models (e.g. landscape fire succession models). Although they can be run at higher resolution than used here, they are not generally designed to simulate very fine (e.g. below 1 km) variation in fuels, weather and fire behaviour. That said, by providing a robust link to mechanisms of climate change, the approach used in this thesis still yields insights about the relationship between climate, weather and fuel load that will be useful to decision making and adaptation planning.

The results in this thesis should also be interpreted in light of a number of important factors beyond scope. The thesis takes the four switches of fire framework, focusing on the drivers of bushfire incidence, rather than patterns of fire behaviour and impacts of fire. Within this framework, the thesis focuses on fire weather and fuel load, omitting ignitions and treating fuel moisture only indirectly, as a component of the fire weather index used. In using FFDI to represent fire weather conditions, some pertinent aspects of fire weather are not addressed: wind direction and wind changes, upper atmospheric properties, and more broadly synoptic features, teleconnections and other drivers of fire weather. Moreover, FFDI as a measure of fire danger and behaviour is subject to its own strengths and weaknesses (Zylstra 2011). FFDI's weaknesses are most obvious in predominantly grassland areas, where results should be interpreted with caution. Although it behaves similarly to its counterpart, the Grassland Fire Danger Index, FFDI does not place as a great an emphasis on wind speed or explicitly account for the distinctive curing of herbaceous vegetation. As mentioned above, given the spatial scale of the climate and land surface models used in this thesis, exploring the mechanisms responsible for fine variation in fuels, fire behaviour and local weather are beyond the scope of this research. Also out of scope are the wide range of potential interactions and feedbacks between these projections and human and natural systems, including fire regimes themselves.

In spite of these caveats and uncertainties, a number of conclusions can be reached about the research presented in this thesis. These are discussed in Chapter 9, which also addresses future work and the broader context of this research.

Chapter 9

Conclusion

This thesis aims to develop improved projections of the impact of climate change on bushfire weather conditions and fuel load, via four specific research questions:

1. Are there significant trends in average or extreme fire weather within the observational record?
2. How is fire weather projected to change in different rainfall seasonality regions by skill-selected global climate models?
3. Can a simple model of fuel load be developed for use in the Australian land surface model, that accounts for both climate and atmospheric CO_2 effects on vegetation growth?
4. How are fire weather and fuel load projected to change at a fine scale (50 km) by an ensemble of global and regional climate models, selected to span the possible future climate change space?

The first aim is addressed through the first Australia-wide analysis of a high quality fire weather dataset (Chapter 3), which reveals an increasing trend in mean and extreme fire weather at around half of all stations, and no decreasing trends. The analysis also suggests that the fire season in Australia has been lengthening since 1973. This analysis was published by Clarke et al. (2013a).

The second aim is addressed through the use of a four member ensemble of skill selected global climate models to project fire weather under climate change over eastern Australia (Chapter 4). Fire weather is projected to increase strongly in regions of uniform and winter dominated rainfall in southeast Australia. In contrast, little change or even decreases are projected in summer dominated rainfall regions in the north. This analysis was published by Clarke et al. (2011).

The third aim is addressed by using net primary productivity, a measure of the rate of vegetation growth, as a proxy for fuel load (Chapter 6). A strong relationship is found between net primary productivity and fuel load in an observation-constrained ecosystem model; this relationship is applied to a sensitivity ensemble of land surface model simulations from 1980 and 2008 over Australia, incorporating the effects of both climate and atmospheric carbon dioxide on vegetation. This analysis has been submitted to a journal for publication.

The fourth and final aim of the thesis is addressed by running an ensemble of regional climate model and land surface models to predict fire weather and fuel load respectively (Chapter 7). The study builds on previous work in the thesis, particularly the fuel load model developed in Chapter 6 and an evaluation of a regional climate model's ability to simulate fire weather in southeast Australia presented in Chapter 5. The ensemble is derived from a mixture of global and regional climate models selected for their skill in simulating Australia's climate, their independence as models, and their ability to span the range of predicted climate change in Australia. Strong increases in fuel load are projected in temperate, grassland and subtropical regions of Australia, likely driven by increases in carbon dioxide fertilisation. Fire weather projections are more contingent on the climate forcing, which spans both drying and wetting futures, but tend towards a lengthening of the fire season and much larger increases in fire weather than decreases. The regional climate model evaluation was published by Clarke et al. (2013b). The fire weather and fuel load projections have been submitted to a journal for publication.

In summary, this thesis provides strong evidence that climate change will have significant impacts on fire weather and fuel load in Australia. These findings are broadly consistent with a large body of international research on climate change impacts on bushfire, namely that there is the potential for large increases in fire risk, partly compensated for by little change or even decreases in some areas. One of the strengths of the 'four switches of fire' framework is its idea of a limiting switch. Considering which of the switches limits overall fire incidence in a given area is particularly useful when interpreting climate change impact studies. Thus increases in fire weather conditions or fuel load are unlikely to lead to corresponding increases in fire risk everywhere. Increases in fire weather conditions are likely to be particularly significant in forests in the southeast and southwest of Australia, where load is typically plentiful but does not often dry out enough to support fire (Bradstock 2010). In contrast, increases in fuel load may be more significant in arid environments, where hot, dry conditions do not lead to frequent fire because of insufficient rain in preceding months to allow fuel buildup.

There are important caveats to these results, including uncertainty in the future regional response of rainfall to climate change, limitations to the simple fuel load model developed in Chapter 6, some weaknesses in the ability of climate models to accurately simulate fire weather and the response of vegetation to changing climate and atmospheric CO_2. Despite these uncertainties, there is little doubt that climate change poses a clear challenge to fire managers[1]. Nor should this challenge be considered a purely long-term one, given that changes in fire weather conditions have already been observed in many areas across Australia since the early 1970s. Society and fire managers must plan for changes and reduce systemic vulnerability in fire risk. One tool for achieving this is the framework of robust decision making, which shares some features of the objective design of climate model ensembles (Weaver et al. 2013). Rather than focus exclusively on narrowing the bounds of uncertainty to some arbitrarily narrow window, this framework emphasises the need for managers and modellers to understand the current bounds of uncertainty and how robust their systems are to it. A related, and somewhat difficult question for climate and fire modellers, is the likelihood of their results being used by decision makers (Tang and Dessai 2012). There is a clear need for an improved understanding of the links between science, policy and management, a topic that extends well beyond the scope of this thesis.

Apart from the potential for more and larger fires, the changes projected here are likely to have implications for the use of prescribed burning, which is a major risk management activity in NSW and elsewhere (OEH 2012; Penman et al. 2011). Prescribed burning is generally undertaken in shoulder seasons, which stand to be redefined by changes in fire weather (Flannigan et al. 2013). How will prescribed burn windows change? More evidence is required of the fire weather conditions currently prevailing during prescribed burns. Developing a climatology of such conditions would be a useful first step to evaluating potential changes in prescribed burning windows.

Other areas for future research include:

- exploring observed trends at greater extremes in the FFDI distribution than those analysed here;
- exploring in greater detail the absolute and relative amount of observed changes in FFDI;
- investigating the drivers of observed changes in fire weather, including a formal detection and attribution study;
- evaluating WRF fire weather simulations, and reasons for biases, over a longer time period and greater spatial domain;

[1] Spare a thought for fire managers, who need to consider not just the vast and varying effects of climate change, but other potential disruptors such as invasive plant species and socioeconomic and policy changes (Pausas and Keeley 2014).

- conducting finer scale projections of fire weather over southeast Australia using WRF;
- evaluating the fuel load model against observations (even though these themselves are subject to uncertainties);
- investigating additional methods of determining forest fire rate of spread (e.g. Cheney et al. 2012);
- running coupled land surface model-regional climate model simulations to dynamically explore past and future fuel load and fire weather pathways, with a focus on the relative importance of carbon dioxide fertilisation in determining the overall response of vegetation to climate change;
- a broader examination of the likely impacts of the changes projected here on fire regimes and human and natural systems.

Humanity has had considerable notice of its potential to alter our earth's climate system (Le Treut et al. 2007), from Arrhenius' seminal climate prediction in the century before last, to Keeling's discovery of rising atmospheric CO_2 in the 1950s, to the formation of the IPCC in the late 1980s and the Rio Earth Summit in the early 1990s. Despite this, global temperatures and GHG emissions continue to rise and no agreement has been reached on a global mechanism to deeply cut emissions. In this context, the task of understanding potential impacts of unmitigated climate change on human and natural systems takes on extra significance. That is the aim of this thesis, for the coupled natural and human system of bushfires. The studies presented here provide robust evidence of potential climate change impacts on two key drivers of bushfire risk, fire weather and fuel load. They add to a growing body of evidence that bushfire risk could increase strongly in some areas, but remain stable or even decrease moderately in others. The resolution of major uncertainties in these responses is likely to take years of research across disciplinary boundaries. But work to understand the sensitivity of fire management to these potential impacts can, and should, begin immediately.

Chapter 10

Bibliography

Abramowitz G, Pitman AJ, Gupta G, Kowalczyk E, Wang Y (2007) Systematic bias in land surface models. Journal of Hydrometeorology 8:989–1001

Abramowitz G, Leuning R, Clark M, Pitman AJ (2008) Evaluating the performance of land surface models. Journal of Climate 21:5468-5481

Abramowitz G (2010) Model independence in multi-model ensemble prediction. Australian Meteorological and Oceanographic Journal 59:3-6

Adams HD, Williams AP, Xu C, Rauscher SA, Jiang X, McDowell NG (2013) Empirical and process-based approaches to climate-induced forest mortality models. Frontiers in Plant Science 4:1-5

Alexander LV, Arblaster JM (2009) Assessing Trends in Observed and Modelled Climate Extremes Over Australia in Relation to Future Projections. International Journal of Climatology 29:417-435

Amatulli G, Camia A, San-Miguel-Ayanz J (2013) Estimating future burned areas under changing climate in the EU-Mediterranean countries, Science of the Total Environment 450-451:209-22

Amiro BD, Stocks BJ, Alexander ME, Flannigan MD, Wotton BM (2001) Fire, climate change, carbon and fuel management in the Canadian boreal forest. International Journal of Wildland Fire 10:405-413

Andrys J, Lyons T, Kala J (2014) Multi-decadal Evaluation of WRF Downscaling Capabilities Over Western Australia in Simulating Rainfall and Temperature Extremes. Journal of Applied Meteorology and Climatology doi:10.1175/JAMC-D-14-0212.1 in press.

Aponte C, Tolhurst KG, Bennett LT (2014) Repeated prescribed fires decrease stocks and change attributes of coarse woody debris in a temperate eucalypt forest. Ecological Applications 24(5):976-989

Archibald S, Roy DP, van Wilgen BW, Scholes RJ (2009) What limits fire? An examination of drivers of burnt area in Southern Africa. Global Change Biology 15:613-630

Australian Bureau of Meteorology (2005a) Australian climate zones - major classification groups (based on the Köppen classification). http://www.bom.gov.au/climate/environ/other/kpn_group.shtml. Accessed 28 April 2010

Australian Bureau of Meteorology (2005b) Major seasonal rainfall zones of Australia. http://www.bom.gov.au/jsp/ncc/climate_averages/climate-classifications/index.jsp?maptype=seasgrpb#maps. Accessed 28 April 2010

Australian Bureau of Meteorology and CSIRO (2014) State of the Climate 2014. http://www.bom.gov.au/state-of-the-climate/. Accessed 30 October 2014

Avila FB, Pitman AJ, Donat MG, Alexander LV, Abramowitz G (2012) Climate model simulated changes in temperature extremes due to land cover change. Journal of Geophysical Research 117:D04108

Bala G, Krishna S, Narayanappa D, Cao L, Caldeira K, Nemani R (2013) An estimate of equilibrium sensitivity of global terrestrial carbon cycle using NCAR CCSM4. Climate Dynamics 40:1671-1686

Banks SC, Cary GJ, Smith AL, Davies ID, Driscoll DA, Gill AM, Lindenmayer DB, Peakall R (2014) How does ecological disturbance influence genetic diversity? Trends in Ecology and Evolution 28(11):670-679

Barrett DJ (2001) NPP Multi-Biome: VAST Calibration Data. Oak Ridge National Laboratory Distributed Active Archive Centre, Oak Ridge, Tennessee, USA

Barton CVM, Ellsworth DS, Medlyn BE, Duursma RA, Tissue DT, Adams MA, Eamus D, Conroy JP, McMurtrie RE, Parsby J, Linder S (2010) Whole-tree chambers for elevated atmospheric CO2 experimentation and tree scale flux measurements in south-eastern Australia: The Hawkesbury Forest Experiment. Agricultural and Forest Meteorology 150:941-951

Bates BC, Hope P, Ryan B, Smith I, Charles S (2008) Key findings from the Indian Ocean Climate Initiative and their impact on policy development in Australia. Climatic Change 89(3-4):339-354

Batllori E, Parisien M-A, Krawchuk MA, Moritz MA (2013) Climate change-induced shifts in fire for Mediterranean ecosystems. Global Ecology and Biogeography 22:1118-1129

Bedia J, Herrera S, San Martin D, Koutsias N, Gutierrez JM (2013) Robust projections of Fire Weather Index in the Mediterranean using statistical downscaling. Climatic Change 120:229-247

Beer T, Williams A (1995) Estimating Australian forest fire danger under conditions of doubled carbon dioxide concentrations. Climatic Change 29:169-188

Beeton RJS, Buckley KI, Jones GJ, Morgan D, Reichelt RE, Trewin D (2006) Australia State of the Environment. Department of the Environment and Heritage, Canberra

Birk EM, Bridges RG (1989) Recurrent fires and fuel accumulation in even-aged Blackbutt (Eucalyptus pilularis) forests. Forest Ecology and Management 29:59-79

Bishop CH, Abramowitz G (2013) Climate model dependence and the replicate Earth paradigm, Climate Dynamics 41:885-900

Bistinas I, Oom D, Sá ACL, Harrison SP, Prentice IC, Pereira JMC (2013) Relationships between Human Population Density and Burned Area at Continental and Global Scales. PLoS ONE 8:e81188

Bladon KD, Emelko MB, Silins U, Stone M (2014) Wildfire and the future of water supply. Environmental Science and Technology 48:8936-8943

Blanchi R, Lucas C, Leonard F, Finkele K (2010) Meteorological conditions and wildfire-related house loss in Australia. International Journal of Wildland Fire 19:914-926

Blanchi R, Leonard J, Haynes K, Opie K, James M, de Oliveira FD (2014) Environmental circusmtances surrounding bushfire fatalities in Australia 1901-2011. Environmental Science and Policy 37:192-203

Bolton DK, Coops NC, Wulder MA (2013) Measuring forest structure along productivity gradients in the Canadian boreal with small-footprint Lidar. Environmental Monitoring and Assessment 185:6617-6634

Bonan GB, Levis S, Sitch S, Vertenstein M, Oleson KW (2003) A dynamic global vegetation model for use with climate models: concepts and description of simulated vegetation dynamics. Global Change Biology 9:1543-1566

Boulanger Y, Gauthier S, Gray DR, Le Goff H, Lefort P, Morissette J (2013) Fire regime zonation under current and future climate over eastern Canada. Ecological Applications 23(4):904-923

Bowman DMJS, Balch JK, Artaxo P, Bond WJ, Carlson JM, Cochrane MA, D'antonio CM, Defries RS, Doyle JC, Harrison SP, Johnston FH, Keeley JE, Krawchuk MA, Kull CA, Marston BJ, Moritz MA, Prentice IC, Roos CI, Scott AC, Swetnam TW, Van Der Werf GR, Pyne SJ (2009) Fire in the Earth System. Science 324:481-484

Bowman DMJS, Balch J, Artaxo P, Bond WJ, Cochran MA, D'Antonio CM, Defries R, Johnston FH, Keeley JE, Krawchuk ME, Kull CA, Mack M, Moritz MA, Pyne S, Roos CI, Scott AC, Sodhi NS and Swetnam TW (2011) The human dimension of fire regimes on Earth. Journal of Biogeography 38:2223-2236

Bowman DMJS, O'Brien JA, Goldammer JG (2013) Pyrogeography and the Global Quest for Sustainable Fire Management. Annual Review of Environment and Resources 38:57-80

Bowman DMJS, Murphy BP, Williamson GJ, Cochrane MA (2014a) Pyrogeographic models, feedbacks and the future of global fire regimes. Global Ecology and Biogeography 23:821-824

Bowman DMJS, Williamson GJ, Keenan RJ, Prior LD (2014b) A warmer world will reduce tree growth in evergreen broadleaf forests: evidence from Australian temperate and subtropical eucalypt forests. Global Ecology and Biogeography 23:925-934

Boyero L, Pearson RG, Gessner MO, Barmuta LA, Ferreira V, Graca MAS, Dudgeon D, Boulton AJ, Callisto M, Chauvet E, Helson JE, Bruder A, Albarino RJ, Yule CM, Arunachalam M, Davies JN, Figueroa R, Flecker AS, Ramirez A, Death RG, Iwata T, Mathooko JM, Mathuriau C, Goncalves Jr JF, Moretti MS, Jinggut T, Lamothe S, M'Erimba C, Ratnarajah L, Schindler MH, Castela J, Buria LM, Cornejo A, Villanueva VD, West DC (2011) A global experiment suggests climate warming will not accelerate litter decomposition in streams but might reduce carbon sequestration. Ecology Letters 14:289-294

Bradstock RA, Gill AM (2001) Living with fire and biodiversity and the urban edge: in search of a sustainable solution to the human protection problem. Journal of Mediterranean Ecology 2:179-195

Bradstock RA, Cohn JS, Gill AM, Bedward M, Lucas C (2009) Prediction of the probability of large fires in the Sydney region of south-eastern Australia using fire weather. International Journal of Wildland Fire 18 932-943

Bradstock RA (2010) A biogeographic model of fire regimes in Australia: current and future implications. Global Ecology and Biogeography 19 145-158

Bradstock RA, Hammill K, Collins L, Price O (2010) Effects of weather, fuel and terrain on fire severity in topographically diverse landscapes of south-eastern Australia. Landscape Ecology 25:607-619

Bradstock RA, Boer MM, Cary GJ, Price OF, Williams RJ, Barrett D, Cook G, Gill AM, Hutley LBW, Keith H, Maier SW, Meyer M, Roxburgh SH, Russell-Smith J (2012) Modelling the potential for prescribed burning to mitigate carbon emissions from wildfires in fire-prone forests of Australia. International Journal of Wildland Fire 21:629-639

Brovkin V, van Bodegom PM, Kleinen T, Wirth C, Cornwell WK, Cornelissen, JHC, Kattge J (2012) Plant-driven variation in decomposition rates improves projections of global litter stock distribution, Biogeosciences 9:565-576

Bryant BP, Westerling AL (2014) Scenarios for future wildfire risk in California: links between changing demography, land use, climate, and wildfire. Environmetrics 25:454-471

Cai W, Cowan T, Raupach M (2009) Positive Indian Ocean Dipole events precondition southeast Australia bushfires. Geophysical Research Letters 36:L19710

Cane D, Wastl C, Barbarino S, Renier LA, Schunk C, Menzel A (2013) Projection of fire potential to future climate scenarios in the Alpine area: some methodological considerations. Climatic Change 119:733-746

Cary GJ, Banks JCG (1999) Fire Regime Sensitivity to Global Climate Change: an Australian Perspective. In: Innes J, Beniston M, Verstraete M (eds). Biomass Burning and Its Inter-Relationships With the Climate System. Kluwer, USA, pp 233-246

Cary GJ (2002) Importance of a changing climate for fire regimes in Australia. In: Bradstock RA, Williams JE, Gill AM (eds). Flammable Australia: the fire regimes and biodiversity of a continent. Cambridge University Press, Cambridge, pp 26-46

Cary GJ, Bradstock RA, Gill AM, Williams RJ (2012) Global change and fire regimes in Australia. In: Bradstock RA, Gill AM, Williams RJ (eds). Flammable Australia: Fire Regimes, Biodiversity and Ecosystems in a Changing World. CSIRO Publishing, Collingwood, Victoria, pp 149-169

Chafer CJ (2007) Using Satellite Imagery to Estimate Landscape Fuel Loads in a Diverse Eucalypt Environment on the Central Coast of New South Wales, Australia. Sydney Catchment Authority, Sydney, Australia

Cheney NP, Gould JS, McCaw WL, Anderson WR (2012) Predicting fire behaviour in dry eucalypt forest in southern Australia. Forest Ecology and Management 280:120-131

Cheney NP, Gould JS, Knight I (1992) A Prescribed Burning Guide for Young Regrowth Forest of Silvertop Ash. Forestry Commission of New South Wales, Research Paper No. 16, Sydney, Australia

Cheney NP, Gould JS, Catchpole WR (1998) Prediction of fire spread in grasslands. International Journal of Wildland Fire 8:1-13

Christensen J, Carter T, Rummukainen M, Amanatidis G (2007) Evaluating the performance and utility of regional climate models: the PRUDENCE project (2007) Climatic Change 81:1-6

Christensen JH, Hewitson B, Busuioc A, Chen A, Gao X, Held I, Jones R, Kolli RK, Kwon W-T, Laprise R, Magaña Rueda V, Mearns L, Menéndez CG, Räisänen J, Rinke A, Sarr A, Whetton P (2007) Regional Climate Projections. In: Solomon S, Qin D, Manning M, Chen Z, Marquis M, Averyt KB, Tignor M, Miller HL (eds). Climate Change 2007: The Physical Science Basis. Contribution of Working Group I to the Fourth Assessment Report of the Intergovernmental Panel on Climate Change. Cambridge University Press, Cambridge, United Kingdom, pp 847-940

Clark KL, Skowronski N, Hom J, Duveneck M, Pan Y, Van Tuyl S, Cole J, Patterson M, Maurer S (2009) Decision support tools to improve the effectiveness of hazardous fuel reduction treatments in the New Jersey Pine Barrens. International Journal of Wildland Fire 18:268-277

Clark KL, Skowronski N, Renninger H, Scheller R (2014) Climate change and fire management in the mid-Atlantic region. Forest Ecology and Management 327:306-315

Clarke HC, Smith PL, Pitman AJ (2011) Regional signatures of future fire weather over Eastern Australia from Global Climate Models. International Journal of Wildland Fire 20:550-562

Clarke H, Lucas C, Smith P (2013a) Changes in Australian fire weather between 1973 and 2010. International Journal of Climatology 33:931-944

Clarke H, Evans JP, Pitman AJ (2013b) Fire weather simulation skill by the Weather Research and Forecasting (WRF) model over south-east Australia from 1985 to 2009. International Journal of Wildland Fire 22:739-756

Collins M, SI A, Cai W, Ganachaud A, Guilyardi E, Jin FF, Jochum M, Lengaigne M, Power S, Timmermann A, Cecchi G, Wittenberg A (2010) The impact of global warming on the tropical Pacific ocean and El Niño. Nature Geoscience 3(6):391-397

Collins BM (2014) Fire weather and large fire potential in the northern Sierra Nevada. Agricultural and Forest Meteorology 189-190:30-35

Crimmins MA (2006) Synoptic Climatology of Extreme Fire Weather Conditions across the Southwest United States. International Journal of Climatology 26:1001-1016

Crutzen PJ (2002) Geology of mankind. Nature 415(6867):23

Cruz FT, Pitman AJ, Wang Y (2010) Can the stomatal response to higher atmospheric carbon dioxide explain the unusual temperatures during the 2002 Murray-Darling Basin drought. Journal of Geophysical Research 115:D02101

CSIRO, Australian Bureau of Meteorology (2010) State of the Climate. http://www.bom.gov.au/inside/eiab/State-of-climate-2010-updated.pdf. Accessed December 1 2011

CSIRO (2011) McArthur Mk 5 Forest Fire Danger Meter. http://www.csiro.au/Outcomes/Safeguarding-Australia/Mk5ForestfireDangerMeter.aspx. Accessed December 17 2014

de Groot WJ, Flannigan MD, Cantin AS (2013) Climate change impacts on future boreal fire regimes. Forest Ecology and Management 294:35-44

de Kauwe MG, Kala J, Lin Y-S, Pitman AJ, Medlyn B, Duursma R, Abramowitz G, Wang Y-P (submitted) A test of an optimal stomatal conductance scheme within the CABLE Land Surface Model. Geoscientific Model Development.

Decker M, Pitman AJ, Evans JP (2013) Groundwater constraints on simulated transpiration variability over southeastern Australian forests. Journal of Hydrometeorology 14:543-559

Deeming JE, Burgan RE, Cohen JE (1977) The National Fire-Danger Rating System - 1978. General Technical Report INT39, USDA Forest Service Intermountain Forest and Range Experiment Station, Ogden, Utah

Dickinson RE, Shaikh M, Bryant R, Graumlich L (1998) Interactive canopies for a climate model. Journal of Climate 11:2823-2836

Dolanc CR, Safford HD, Dobrowski SZ, Thorne JH (2014) Twentieth century shifts in abundance and composition of vegetation types of the Sierra Nevada, CA, US. Applied Vegetation Science 17:442-455

Dominguez F, Cañon J, Valdéz J (2010) IPCC-AR4 climate simulations for the Southwestern US: the importance of future ENSO projections. Climatic Change 99:499-514

Donohue RJ, Roderick ML, McVicar TR, Farquhar GD (2013) Impact of CO2 fertilization on maximum foliage cover across the globe’s arid, warm environments. Geophysical Research Letters 40:3031-3035

Dovers S, Cary GJ, Lindenmayer D (2004) Fire research and policy priorities: insights from the 2003 national fire forum. Australian Journal of Emergency Management 19:76-84

Dowdy AJ, Mills GA, Finkele K, de Groot W (2010) Index sensitivity analysis applied to the Canadian Forest Fire Weather Index and the McArthur Forest Fire Danger Index. Meteorological Applications 17:298-312

Driscoll DA, Lindenmayer DB, Bennett AF, Bode M, Bradstock RA, Cary GJ, Clarke MF, Dexter N, Fensham R, Friend G, Gill M, James S, Kay G, Keith DA, MacGregor C, Russell-Smith J, Salt D, Watson JEM, Williams RJ, York A (2010) Fire management for biodiversity conservation: key research questions and our capacity to answer them. Biological Conservation 143:1928-1939

Duffield JW, Neher CJ, Patterson DA, Deskins AM (2013) Effects of wildfire on national park visitation and the regional economy: a natural experiment in the Northern Rockies. International Journal of Wildland Fire 22:1155-1166

Dunbar J, Eichorst SA, Gallegos-Graves LV, Silva S, Xie G, Hengartner NW, Evans RD, Hungate BA, Jackson RB, Megonigal JP, Schadt CW, Vilgalys R, Zak DR, Kuske CR (2012) Common bacterial responses in six ecosystems exposed to 10 years of elevated atmospheric carbon dioxide. Environmental Microbiology 14(5):1145-1158

Easterling DR, Peterson TC (1995) A new method for detecting undocumented discontinuities in climatological time series. International Journal of Climatology 15:369-377

Easterling DR, Wehner MF (2009) Is the climate warming or cooling? Geophysical Research Letters 36:L08706

Edwards GP, Allan GE, Brock C, Duguid A, Gabrys K, Vaarzon-Morel P (2008) Fire and its management in central Australia. The Rangeland Journal 30:109-121

Ehret U, Zehe E, Wulfmeyer V, Warrach-Sagi K, Liebert J (2012) Should we apply bias correction to global and regional climate model data? Hydrology and Earth System Sciences 16:3391-3404

Eliseev AV, Mokhov II, Chernokulsky AV (2014) An ensemble approach to simulate CO2 emissions from natural fires. Biogeosciences 11:3205-3223

Engel CB, Lane TP, Reeder MJ, Rezny M (2012) The meteorology of Black Saturday. Quarterly Journal of the Royal Meteorological Society 139:585-599

Evans JP, McCabe MF (2010) Regional climate simulation over Australia's Murray-Darling basin: A multi-temporal assessment. Journal of Geophysical Research 115:D14114

Evans JP, McGregor JL, McGuffie K (2012a) Future Regional Climates. In: Henderson-Sellers A, McGuffie K (eds). The Future Of The World's Climate. Elsevier, Oxford, UK, pp 223-252

Evans JP, Ekstrom M, Ji F (2012b) Evaluating the performance of a WRF physics ensemble over south-east Australia. Climate Dynamics 39:1241-1258

Evans JP, Westra S (2012) Investigating the Mechanisms of Diurnal Rainfall Variability Using a Regional Climate Model. Journal of Climate 25(20):7232-7247

Evans JP, McCabe MF (2013) Effect of model resolution on a regional climate model simulation over southeast Australia. Climate Research 56(2):131-145

Evans JP, Ji F, Lee C, Smith P, Argueso D, Fita L (2014) Design of a regional climate modeling projection ensemble experiment - NARCliM. Geoscientific Model Development 7:621-629

Macias Fauria M, Michaletz ST, Johnson EA (2011) Predicting climate change effects on wildfires requires linking processes across scales. WIREs Climate Change 2(1):99-112

Ferreira V, Chauvet E (2011) Future increase in temperature more than decrease in litter quality can affect microbial litter decomposition in streams. Oecologia 167:279-291

Finkele K, Mills GA, Beard G, Jones DA (2006) National Gridded Drought Factors and Comparison of Two Soil Moisture Deficit Formulations Used in Prediction of Forest Fire Danger Index in Australia. Australian Meteorological Magazine 55:183-197

Flannigan MD, Van Wagner CE (1991) Climate Change and Wildfire in Canada. Canadian Journal of Forest Research 21:66-72

Flannigan MD, Campbell I, Wotton M, Carcaillet C, Richard P, Bergeron Y (2001) Future fire in Canada's boreal forest: paleoecology results and general circulation model - regional climate model simulations. Canadian Journal of Forest Research 31:854-864

Flannigan MD, Krawchuk MA, De Groot WJ, Wotton BM, Gowman LM (2009) Implications of Changing Climate for Global Wildland Fire. International Journal of Wildland Fire 18:483-507

Flannigan MD, Cantin AS, de Groot WJ, Wotton M, Newbery A, Gowman LM (2013) Global wildland fire season severity in the 21st century. Forest Ecology and Management 294:54-61

Flato G, Marotzke J, Abiodun B, Braconnot P, Chou SC, Collins W, Cox P, Driouech F, Emori S, Eyring V, Forest C, Gleckler P, Guilyardi E, Jakob C, Kattsov V, Reason C, Rummukainen M (2013) Evaluation of Climate Models In: Stocker TF, Qin D, Plattner G-K, Tignor M, Allen SK, Boschung J, Nauels A, Xia Y, Bex V, Midgley PM (eds). Climate Change 2013: The Physical Science Basis Contribution of Working Group I to the Fifth Assessment Report of the Intergovernmental Panel on Climate Change. Cambridge University Press, Cambridge, United Kingdom and New York, NY, USA

Folland CK, Parker DE, Colman AW, Washington R (1999) Large scale modes of ocean surface temperatures since the late nineteenth century. In: Navarra A (ed). Beyond El Niño: Decadal and interdecadal Climate Variability. Springer-Verlag, Netherlands

Fox-Hughes P (2011) Impact of more frequent observations on the understanding of tasmanian fire danger. Journal of Applied Meteorology 50:1617-1626

Fox-Hughes P, Harris RMB, Lee G, Grose MR, Bindoff NL (2014) Future fire danger climatology for Tasmania, Australia, using a dynamically downscaled regional climate model. International Journal of Wildland Fire. doi:10.1071/WF13126

Friedlingstein P, Andrew RM, Rogelj J, Peters GP, Canadell JG, Knutti R, Luderer G, Raupach MR, Schaeffer M, van Vuuren DP, Le Quéré C (2014) Persistent growth of CO2 emissions and implications for reaching climate targets. Nature Geoscience 7(10):709-715

Gibbons P, Van Bommel L, Gill AM, Cary GJ, Driscoll DA, Bradstock RA, Knight E, Moritz MA, Stephens SL, Lindenmayer DB (2012) Land management practices associated with house loss in wildfires. PLoS ONE 7:e29212

Gibson RK, Bradstock RA, Penman TD, Keith DA, Driscoll DA (2014) Changing dominance of key plant species across a Mediterranean climate region: implications for fuel types and future fire regimes. Plant Ecology 215:83-95

Gill AM (1975) Fire and the Australian flora: a review. Australian Forestry 38:4-25

Gill AM, Stephens SL, Cary GJ (2013) The worldwide "wildfire" problem. Ecological Applications 23:438-454

Gillett NP, Weaver AJ, Zwiers FW, Flannigan MD (2004) Detecting the effect of climate change on Canadian forest fires. Geophysical Research Letters 31:L18211

Giorgi F, Jones C, Asrar GR (2009) Addressing climate information needs at the regional level: the CORDEX framework, WMO Bulletin 58:175-183

Girardin MP, Tardif J, Flannigan MD, Wotton BM, Bergeron Y (2004) Trends and periodicities in the Canadian drought code and their relationships with atmospheric circulation for the southern Canadian boreal forest. Canadian Journal of Forest Research 34:103-119

Girardin MP, Ali AA, Carcaillet C, Blarquez O, Hély C, Terrier A, Genries A, Bergeron Y (2013) Vegetation limits the impact of a warm climate on boreal wildfires. New Phytologist 199(4):1001-1011

Goldammer JG, Price C (1998) Potential impacts of climate change on fire regimes in the tropics based on MAGICC and a GISS GCM-derived lightning model. Climatic Change 39:273-296

Gordon HB, Rotstayn LD, McGregor J, Dix MR, Kowalczyk EA, Farrell SPO, Waterman LJ, Hirst AC, Wilson SG, Collier MA, Watterson IG, Elliott TI (2002) The CSIRO Mk3 climate system model. CSIRO Atmospheric Research, Technical Report 60, Aspendale, Melbourne

Gould JS, McCaw WL, Cheney NP, Ellis PF, Knight IK, Sullivan AL (2007) Project Vesta - Fire in Dry Eucalypt Forest: Fuel Structure, Fuel Dynamics and Fire Behaviour. Ensis-CSIRO, Canberra, and Department of Environment and Conservation, Perth

Grant I, Jones D, Wang W, Fawcett R, Barratt D (2008) Meteorological and remotely sensed datasets for hydrological modelling: A contribution to the Australian Water Availability

Project. Catchment-scale Hydrological Modelling & Data Assimilation (CAHMDA-3) International Workshop on Hydrological Prediction: Modelling, Observation and Data Assimilation, Melbourne

Griffiths D (1999) Improved formula for the drought factor in McArthur's Forest Fire Danger Meter. Australian Forestry 62:202-206

Grose M, Fox-Hughes P, Harris RMB, Bindoff N (2014) Changes to the drivers of fire weather with a warming climate - a case study of southeast Tasmania. Climatic Change doi:10.1007/S10584-014-1070-Y

Guilyardi E, Wittenberg A, Fedorov A, Collins M, Wang C, Capotondi A, van Oldenborgh GJ, Stockdale T (2009) Understanding El Niño in ocean-atmosphere general circulation models: Progress and challenges. Bulletin of the American Meteorological Society 90:325-340

Guyette RP, Stambaugh MC, Dey DC, Muzika RM (2012) Estimating fire frequency with the chemistry and climate. Ecosystems 15:322-335

Guyette RP, Thompson FR, Whittier J, Stambaugh MC, Dey DC (2014) Future Fire Probability Modeling with Climate Change Data and Physical Chemistry. Forest Science 60(5):862-870

Haines DA (1988) A lower atmospheric severity index for wildland fires. National Weather Digest 13:23-27

Hartmann DL, Klein Tank AMG, Rusticucci M, Alexander LV, Brönnimann S, Charabi Y, Dentener FJ, Dlugokencky EJ, Easterling DR, Kaplan A, Soden BJ, Thorne PW, Wild M, Zhai PM (2013) Observations: Atmosphere and Surface In: Stocker TF, Qin D, Plattner G-K, Tignor M, Allen SK, Boschung J, Nauels A, Xia Y, Bex V, Midgley PM (eds). Climate Change 2013: The Physical Science Basis Contribution of Working Group I to the Fifth Assessment Report of the Intergovernmental Panel on Climate Change. Cambridge University Press, Cambridge, United Kingdom and New York, NY, USA

Hasson AEA, Mills GA, Timbal B, Walsh K (2009) Assessing the Impact of Climate Change on Extreme Fire Weather Events Over Southeastern Australia. Climate Research 39:159-172

Haverd V, Cuntz M (2010) Soil-Litter-Iso A one-dimensional model for coupled transport of heat, water and stable isotopes in soil with a litter layer and root extraction. Journal of Hydrology 388:438-455

Haverd V, Raupach MR, Briggs PR, Canadell JG, Isaac P, Pickett-Heaps C, Roxburgh SH, van Gorsel E, Viscarra Rossel RA, Wang Z (2013a) Multiple observation types reduce uncertainty in Australia's terrestrial carbon and water cycles. Biogeosciences 10:2011-2040

Haverd V, Raupach MR, Briggs PR, Canadell JG, Davis SJ, Law RM, Meyer CP, Peters GP, Pickett-Heaps C, Sherman B (2013b) The Australian terrestrial carbon budget. Biogeosciences 10:851-869

Haverd V, Smith B, Cook GD, Briggs PR, Nieradzik L, Roxburgh SH, A Liedloff, C P Meyer, J G Canadell (2013c) A stand-alone tree demography and landscape structure module for Earth system models. Geophysical Research Letters 40:5234-5239

Hély C, Dowty PR, Alleaume S, Caylor K, Korontzi S, Swap RJ, Shugart HH, Justice CO (2003) Regional fuel load for two climatically contrasting years in southern Africa. Journal of Geophysical Research 108:8475

Hendon HH, Thompson DWJ, Wheeler M (2007) Australian rainfall and surface temperature variation associated with the Southern Hemisphere Annular Mode. Journal of Climate 20:2452-2467

Hennessy K, Lucas C, Nicholls N, Bathols J, Suppiah R, Ricketts J (2005) Climate change impacts on fire-weather in south-east Australia. CSIRO and Bureau of Meteorology, Victoria

Heon J, Arseneault D, Parisien M-A (2014) Resistance of the boreal forest to high burn rates. Proceedings of the National Academy of Sciences 111(38):13888-13893

Herring SC, Hoerling MP, Peterson TC, Stott PA (Eds) (2014) Explaining Extreme Events of 2013 from a Climate Perspective. Bulletin of the American Meteorological Society 95(9):S1-S96

Hessl AE (2011) Pathways for climate change effects on fire: models, data, and uncertainties. Progress in Physical Geography 35:393-407

Hines F, Tolhurst KG, Wilson AAG, McCarthy GJ (2010) Overall Fuel Hazard Assessment Guide, 4th edn. Department of Sustainability and Environment, Fire and Adaptive Management Report No. 82, Melbourne, Victoria, Australia

Hirsch AL, Pitman AJ, Seneviratne SI, Evans JP, Haverd V (2014) Summertime maximum and minimum temperature coupling asymmetry over Australia determined using WRF. Geophysical Research Letters 41:1546-1552

Houldcroft CJ, Grey WMF, Barnsley M, Taylor CM, Los SO, North PRJ (2009) New vegetation albedo parameters and global fields of soil background albedo derived from MODIS for use in a climate model. Journal of Hydrometeorology 10:183-198

Hurteau MD, Robards TA, Stevens D, Saah D, North M, Koch GW (2014a) Modeling climate and fuel reduction impacts on mixed-conifer forest carbon stocks in the Sierra Nevada, California. Forest Ecology and Management 315:30-42

Hurteau MD, Westerling AL, Wiedinmyer C, Bryant BP (2014b) Projected effects of climate and development on California wildfire emissions through 2100. Environmental Science and Technology 48(4):2298-2304

Hurteau MD, Bradford JB, Fulé PZ, Taylor AH, Martin KL (2014c) Climate change, fire management, and ecological services in the Southwestern US. Forest Ecology and Management 327:280-289

IPCC (2007) Summary for Policymakers. In: Solomon S, Qin D, Manning M, Chen Z, Marquis M, Averyt K, Tignor M, Miller H (eds). Climate Change 2007: The Physical Science Basis. Contribution of Working Group I to the Fourth Assessment Report of the Intergovernmental Panel on Climate Change. Cambridge University Press, Cambridge, United Kingdom and New York, NY, USA, pp. 1-18

IPCC (2013): Summary for Policymakers. In: Stocker TF, Qin D, Plattner G-K, Tignor M, Allen SK, Boschung J, Nauels A, Xia Y, Bex V, Midgley PM (eds). Climate Change 2013: The Physical Science Basis. Contribution of Working Group I to the Fifth Assessment Report of the Intergovernmental Panel on Climate Change. Cambridge University Press, Cambridge, United Kingdom and New York, NY, USA

Ito A (2011) A historical meta-analysis of global terrestrial net primary productivity: are estimates converging? Global Change Biology 17:3161-3175

Jakob D (2010) Challenges in developing a high-quality surface wind-speed data-set for Australia. Australian Meteorological and Oceanographic Journal 60:227-236

Jenny H, Gessel SP, Bingham FT (1949) Comparative study of decomposition rates of organic matter in temperate and tropical regions. Soil Science 68:419-432

Jiang D, Zhang Y, Lang X (2011) Vegetation feedback under future global warming. Theoretical and Applied Climatology 106:211-227

Jiang X, Rauscher SA, Ringler TD, Lawrence DM, Williams AP, Allen CD, Steiner AL, Cai DM, McDowell NG (2013) Projected future changes in vegetation in western North America in the twenty-first century. Journal of Climate 26:3672-3687

Johnston F, Henderson SB, Chen Y, Randerson JT, Marlier M, Defries RS, Kinney P, Bowman DM, Brauer M (2012) Estimated global mortality attributable to smoke from landscape fires. Environmental Health Perspectives 120(5):695-701

Johnston F, Bowman DMJS (2013) Bushfire Smoke: An exemplar of coupled natural and human systems. Geographical Research 52:45-54

Jones D, Wang W, Fawcett R (2009) High-quality spatial climate data-sets for Australia. Australian Meteorological Magazine 58:233-248

Jones T, Woolf M, Cechet RP, French I (2012) Quantitative bushfire risk assessment framework for severe and extreme fires. Australian Meteorological and Oceanographic Journal 62:171-178

Kala J, Decker M, Exbrayat J-F, Pitman AJ, Carouge C, Evans JP, Abramowitz G (2014) Influence of Leaf Area Index Prescriptions on Simulations of Heat, Moisture, and Carbon Fluxes. Journal of Hydrometeorology 15:489-503

Kalnay E, Kanamitsu M, Kistler R, Collins W, Deaven D, Gandin L, Iredell M, Saha GS, White JW, Zhu Y, Leetmaa A, Reynolds B, Chelliah M, Ebisuwaki W, Higgins W, Janowiak J, Mo KC, Ropelewski C, Wang J, Jenne R, Joseph D (1996) The NCEP/ NCAR 40-year reanalysis project. Bulletin of the American Meteorological Society 77:437-471

Kalnay E (2003) Atmospheric modeling, data assimilation and predictability. Cambridge University Press, Cambridge, United Kingdom.

Karnosky DF (2003) Impacts of elevated atmospheric CO_2 on forest trees and forest ecosystems: knowledge gaps. Environment International 29:161-169

Kasischke ES, Turetsky MR (2006) Recent changes in the fire regime across the North American boreal region - spatial and temporal patterns of burning across Canada and Alaska. Geophysical Research Letters 33:L09703

Kattge J, Knorr W, Raddatz T, Wirth C (2009) Quantifying photosynthetic capacity and its relationship to leaf nitrogen content for global-scale terrestrial biosphere models. Global Change Biology 15:976-991

Keane RE, Burgan R, van Wagtendonk J (2001) Mapping wildland fuels for fire management across multiple scales: integrating remote sensing, GIS, and biophysical modelling. International Journal of Wildland Fire 10:301-319

Keane RE, Loehman RA, Holsinger LM (2011) The FireBGCv2 landscape fire and succession model: a research simulation platform for exploring fire and vegetation dynamics. USDA Forest Service, Rocky Mountain Research Station, General Technical Report RMRS-GTR-255, Fort Collins, Colorado, USA

Keane RE (2012) Describing wildland surface fuel loading for fire management: a review of approaches, methods and systems. International Journal of Wildland Fire 22:51-62

Keane RE, Cary GJ, Flannigan MD, Parsons RA, Davies ID, King KJ, Lif C, Bradstock RA, Gill AM (2013) Exploring the role of fire, succession, climate and weather on landscape dynamics using comparative modelling. Ecological Modelling 266:172-186

Keeling CD, Piper SC, Bacastow RB, Wahlen M, Whorf TP, Heimann M, Meijer HA (2005) Atmospheric CO_2 and $^{13}CO_2$ exchange with the terrestrial biosphere and oceans from 1978 to 2000: Observations and carbon cycle implications. In: Ehleringer JR, Cerling TE, Dearing MD (eds). A History of Atmospheric CO2 and Its Effects on Plants, Animals, and Ecosystems. Springer Verlag, New York

Keetch JJ, Byram GM (1968) A drought index for forest fire control. USDA Forest Service, Research Paper SE-38, Ashville, NC

Keith H, Lindenmayer DB, Mackey BG, Blair D, Carter L, McBurney L, Okada S, Konishi-Nagano T (2014) Accounting for Biomass Carbon Stock Change Due to Wildfire in Temperate Forest Landscapes in Australia. PLOS One 9(9):e107126

Kindermann GE, McAllum I, Fritz S, Obersteiner M (2008) A global forest growing stock, biomass and carbon map based on FAO statistics. Silva Fennica 42:387–396

King KJ, de Ligt RM, Cary GJ (2011) Fire and carbon dynamics under climate change in south eastern Australia: insights from FullCAM and FIRESCAPE modelling. International Journal of Wildland Fire 20:563-577

King KJ, Cary GJ, Gill AM, Moore AD (2012) Implications of changing climate and atmospheric CO_2 for grassland fire in south-east Australia: insights using the GRAZPLAN grassland simulation model. International Journal of Wildland Fire 21:695-708

King KJ, Cary GJ, Bradstock RA, Marsden-Smedley JB (2013) Contrasting fire responses to climate and management: insights from two Australian ecosystems. Global Change Biology 19:1223-1235

Klein Tank AMG, Zwiers FW, Zhang X (2009.) Guidelines on analysis of extremes in a changing climate in support of informed decisions for adaptation. World Meteorological Organisation, WCDMP-72, WMO-TD/No.1500, Switzerland

Kloster S, Mahowald N, Randerson J, Lawrence P (2012) The impacts of climate, land use, and demography on fires during the 21st century simulated by CLM-CN. Biogeosciences 9:509-525

Knorr W, Lehsten V, Arneth A (2012) Determinants and predictability of global wildfire emissions. Atmospheric Chemistry and Physics 12:6845-6861

Knorr W, Kaminski T, Arneth A, Weber U (2014) Impact of human population density on fire frequency at the global scale. Biogeosciences 11:1085-1102

Kowalczyk EA, Stevens L, Law RM, Dix M, Wang YP, Harman I, Haynes K, Srbinovsky J, Pak B (2013) The land surface model component of ACCESS: description and impact on the simulated surface climatology. Australian Meteorological and Oceanographic Journal 63:65-82

Kraaij T, Cowling RM, van Wilgen BW (2013) Lightning and fire weather in eastern coastal fynbos shrublands: seasonality and long-term trends. International Journal of Wildland Fire 22:288-295

Krause A, Kloster S, Wilkenskjeld S, Paeth H (2014) The sensitivity of global wildfires to simulated past, present, and future lightning frequency. Journal of Geophysical Research: Biogeosciences 119:312-322

Krawchuk MA, Cumming SG, Flannigan MD (2009) Predicted changes in fire weather suggest increases in lightning fire initiation and future area burned in the mixedwood boreal forest. Climatic Change 92:83-97

Krawchuk MA, Moritz MA, Parisien M, Van Dorn J, Hayhoe K (2009) Global pyrogeography: the current and future distribution of wildfire. PLoS ONE 4(4):e5102

Krebs P, Pezzatti GB, Mazzoleni S, Talbot LM, Conedera M (2010) Fire regime: history and definition of a key concept in disturbance ecology. Theory in Biosciences 129:53-69

Kumar SV, Peters-Lidard CD, Tian Y, Houser PR, Geiger J, Olden S, Lighty L, Eastman JL, Doty B, Dirmeyer P, Adams J, Mitchell K, Wood EF, Sheffield J (2006) Land Information System - An Interoperable Framework for High Resolution Land Surface Modeling. Environmental Modelling and Software 21:1402-1415

Kumar SV, Peters-Lidard CD, Eastman JL, Tao W-K (2008) An integrated high-resolution hydrometeorological modeling testbed using LIS and WRF. Environmental Modelling and Software 23:169-181

Law RM, Raupach MR, Abramowitz G, Dharssi I, Haverd V, Pitman AJ, Renzullo L, Van Dijk A, Wang Y-P (2012) The Community Atmosphere Biosphere Land Exchange (CABLE) model Roadmap for 2012-2017. CAWCR, Technical Report No. 57, Victoria

Le Goff H, Flannigan MD, Bergeron Y, Girardin MP (2007) Historical fire regime shifts related to climate teleconnections in the Waswanipi area, central Quebec, Canada. International Journal of Wildland Fire 16(5):607-618

Le Goff H, Flannigan MD, Bergeron Y (2009) Potential Changes in Monthly Fire Risk in the Eastern Canadian Boreal Forest Under Future Climate Change. Canadian Journal of Forest Research-Revue Canadienne De Recherche Forestiere 39:2369-2380

Le Quere C, Raupach MR, Canadell JG, Marland G, Bopp L, Ciais P, Conway TJ, Doney SC, Feely RA, Foster P, Friedlingstein P, Gurney K, Houghton RA, House JI, Huntingford C, Levy PE, Lomas MR, Majkut J, Metzl N, Ometto JP, Peters GP, Prentice IC, Randerson JT, Running SW, Sarmiento JL, Schuster U, Sitch S, Takahashi T, Viovy N, van der Werf GR, Woodward FI (2009) Trends in the sources and sinks of carbon dioxide. Nature Geoscience 2:831-836

Le Treut H, Somerville R, Cubasch U, Ding Y, Mauritzen C, Mokssit A, Peterson T, Prather M (2007) Historical Overview of Climate Change. In: Solomon S, Qin D, Manning M, Chen Z, Marquis M, Averyt KB, Tignor M, Miller HL (eds). Climate Change 2007: The Physical Science Basis. Contribution of Working Group I to the Fourth Assessment Report of the Intergovernmental Panel on Climate Change. Cambridge University Press, Cambridge, United Kingdom and New York, NY, USA

Lehtonen I, Ruosteenoja K, Venäläinen A, Gregow H (2014) The projected 21st century forest fire risk in Finland under different greenhouse gas scenarios. Boreal Environment Research 19:127-139

Litschert SE, Brown TC, Theobald DM (2012) Historic and future extent of wildfires in the Southern Rockies Ecoregion, USA. Forest Ecology and Management 269:124-133

Liu YY, de Jeu RAM, McCabe MF, Evans JP, van Dijk AIJM (2011) Global long-term passive microwave satellite-based retrievals of vegetation optical depth. Geophysical Research Letters 38:L18402

Liu YY, van Dijk AIJM, McCabe MF, Evans JP, de Jeu RAM (2013) Global vegetation biomass change (1988-2008) and attribution to environmental and human drivers. Global Ecology and Biogeography 22:692-705

Loehman RA, Reinhardt E, Riley KL (2014) Wildland fire emissions, carbon, and climate: seeing the forest and the trees - A cross-scale assessment of wildfire and carbon dynamics in fire-prone, forested ecosystems. Forest Ecology and Management 317:9-19

Loepfe L, Martinez-Vilalta J, Piñol J (2012) Management alternatives to offset climate change effects on Mediterranean fire regimes in NE Spain. Climatic Change 115:693-707

Long M (2006) A climatology of extreme fire weather days in Victoria. Australian Meteorological Magazine 55:3-18

Lorenz R, Pitman AJ, Donat MG, Hirsch AL, Kala J, Kowalczyk EA, Law RM, Srbinovsky J (2014) Representation of climate extreme indices in the coupled atmosphere-land surface model ACCESS1.3b. Geoscientific Model Development 7:545-567

Lu X, Wang Y-P, Ziehn T, Dai Y (2013) An efficient method for global parameter sensitivity analysis and its applications to the Australian community land surface model (CABLE). Agricultural and Forest Meteorology 182-183:292-303

Lucas C (2005) Fire climates of Australia: Past, present and future. Proceedings, 6th Symposium on Fire and Forest Meteorology, Canmore, Alberta, Canada

Lucas C, Hennessy K, Mills G, Bathols J (2007) Bushfire weather in southeast Australia: recent trends and projected climate change impacts. Bushfire Cooperative Research Centre, Victoria

Lucas C (2010) On developing a historical fire weather data-set for Australia. Australian Meteorological and Oceanographic Journal 60:1-14

Luke R, McArthur A (1978) Bushfires in Australia. Australian Government Publishing Service, Canberra

Lung T, Dosio A, Becker W, Lavalle C, Bouwer LM (2013) Assessing the influence of climate model uncertainty on EU-wide climate change impact indicators. Climatic Change 120:211-227

Luo L, Tang Y, Zhong S, Bian X, Heilman WE (2013) Will Future Climate Favor More Erratic Wildfires in the Western United States? Journal of Applied Meteorology and Climatology 52:2410-2417

Malevsky-Malevich SP, Molkentin EK, Nadyozhina ED, Shklyarevich OB (2008) An assessment of potential change in wildfire activity in the Russian boreal forest zone induced by climate warming during the twenty-first century. Climatic Change 86:463-474

Mann ML, Berck P, Moritz M, Batllori E, Baldwin JG, Gately C, Cameron DR (2014) Modeling residential development in California from 2000-2050: Integrating wildfire risk, wildland and agricultural encroachment. Land Use Policy 41:438-452

Marlon J, Bartlein P, Carcaillet C, Gavin DG, Harrison SP, Higuera PE, Joos F, Power MJ, Prentice CI (2008) Climate and human influences on global biomass burning over the past two millennia. Nature Geoscience 1:697-701

Matthew E (1997) Global litter production, pools, and turnover times: Estimates from measurement data and regression models. Journal of Geophysical Research 102:18771-18800

Matthews S, Nguyen K, McGregor J (2011) Modelling fuel moisture under climate change. International Journal of Climate Change Strategies and Management 3:6-15

Matthews S, Sullivan AL, Watson P, Williams RJ (2012) Climate change, fuel and fire behaviour in a eucalypt forest. Global Change Biology 18:3212-3223

McAneney J, Chen K, Pitman A (2009) 100-years of Australian bushfire property losses: Is the risk significant and is it increasing? Journal of Environmental Management 90:2819-2822

McArthur AG (1967) Fire behaviour in eucalypt forests. Forestry and Timber Bureau, Leaflet 107, Canberra, ACT, Australia

McCaw L, Mills G, Sullivan A, Hurley R, Ellis P, Matthews S, Plucinski M, Pippen B, Boura J (2009) Fire behaviour investigation. In: Victorian 2009 Bushfire Research Response Final Report. Bushfire CRC, Victoria.

McGuffie K, Henderson-Sellers A (1987) A Climate Modelling Primer. John Wiley & Sons, New York

McVicar TR, Van Niel TG, Li LT, Roderick ML, Rayner DP, Ricciardulli L, Donohue RJ (2008) Wind speed climatology and trends for Australia, 1975-2006: Capturing the stilling phenomenon and comparison with near-surface reanalysis output. Geophysical Research Letters 35:L20403

Mearns LO, Giorgi F, Whetton P, Pabon D, Hulme M, Lal M (2003) Guidelines for Use of Climate Scenarios Developed from Regional Climate Model Experiments. IPCC Data Distribution Centre, Switzerland

Mearns LO, Arritt R, Biner S, Bukovsky MS, McGinnis S, Sain S, Caya D, Correia Jr J, Flory D, Gutowski W, Takle ES, Jones R, Leung R, Moufouma-Okia W, McDaniel L, Nunes AMB, Qian Y, Roads J, Sloan L, Snyder, M (2012) The North American Regional Climate Change Assessment Program Overview of Phase I results. Bulletin of the American Meteorological Society 93:1337- 1362

Medvigy D, Wofsy SC, Munger JW, Moorcroft PR (2010) Responses of terrestrial ecosystems and carbon budgets to current and future environmental variability. Proceedings of the National Academy of Sciences of the United States of America 107(18):8275-9280

Meehl GA, Covey C, Delworth T, Latif M, McAvaney B, Mitchell JF, Stouffer RJ, Taylor KE (2007a) The WCRP CMIP3 multimodel dataset: a new era in climate change research. Bulletin of the American Meteorological Society 88:1383-1394

Meehl GA, Stocker TF, Collins WD, Friedlingstein P, Gaye AT, Gregory JM, Kitoh A, Knutti R, Murphy JM, Noda A, Raper SCB, Watterson IG, Weaver AJ, Zhao Z-C (2007b) Global climate projections. In: Solomon S, Qin D, Manning M, Chen Z, Marquis M, Averyt KB, Tignor M, Miller HL (eds). Climate change 2007: the physical science basis. Contribution of Working Group I to the Fourth Assessment Report of the Intergovernmental Panel on Climate Change. Cambridge University Press, Cambridge, UK, pp 589-662

Mercer GN, Gill AM, Weber RO (1995) A flexible, non-deterministic, litter accumulation model. Proceedings of the Australian Bushfire Conference, Hobart, Tasmania, Australia.

Meyer CP, Cook GD, Reisen F, Smith TEL, Tattaris M, Russell-Smith J, Maier SW, Yates CP, Wooster MJ (2012) Direct measurements of the seasonality of emission factors from savanna fires in northern Australia. Journal of Geophysical Research 117:D20305

Migliavacca M, Dosio A, Camia A, Hobourg R, Houston-Durrant T, Kaiser JW, Khabarov N, Krasovskii AA, Marcolla B, San Miguel-Ayanz J, Ward DS, Cescatti A (2013) Modeling biomass burning and related carbon emissions during the 21st century in Europe. Journal of Geophysical Research: Biogeosciences 118(4):1732-1747

Mills GA (2005a) On the sub-synoptic scale meteorology of two extreme fire weather days during the Eastern Australian fires of January 2003. Australian Meteorological Magazine 54:265-290

Mills GA (2005b) A re-examination of the synoptic and mesoscale meteorology of Ash Wednesday 1983. Australian Meteorological Magazine 54:35-55

Mills GA (2008a) Abrupt surface drying and fire weather. Part 1: overview and case study of the South Australian fires of 11 January 2005. Australian Meteorological Magazine 57:299-309

Mills GA (2008b) Abrupt surface drying and fire weather. Part 2: a preliminary synoptic climatology in the forested areas of southern Australia. Australian Meteorological Magazine 57:311-28

Mills GA, McCaw L (2010) Atmospheric Stability Environments and Fire Weather in Australia - extending the Haines Index. CSIRO and Bureau of Meteorology, CAWCR Technical Report No. 20. Victoria

Mitchell RJ, Liu Y, O'Brien JJ, Elliot KJ, Starr G, Miniat CF, Hiers JK (2014) Future climate and fire interactions in the southeastern region of the United States. Forest Ecology and Management 327:316-326

Mölders N (2008) Suitability of the Weather Research and Forecasting (WRF) Model to Predict the June 2005 Fire Weather for Interior Alaska. Weather and Forecasting 23(5):953-973

Mölders N (2010) Comparison of Canadian Forest Fire Danger Rating System and National Fire Danger Rating System fire indices derived from Weather Research and Forecasting (WRF) model data for the June 2005 Interior Alaska wildfires. Atmospheric Research 95(2-3):290-306

Mooney SD, Harrison SP, Bartlein PJ, Daniau A-L, Stevenson J, Brownlie KC, Buckman S, Cupper M, Luly J, Black M, Colhoun E, D'Costa D, Dodson J, Haberle S, Hope GS, Kershaw P, Kenyon C, McKenzie M, Williams N (2011) Late Quaternary fire regimes of Australasia. Quaternary Science Reviews 30:28-46

Mori AS, Johnson EA (2013) Assessing possible shifts in wildfire regimes under a changing climate in mountainous landscapes. Forest Ecology and Management 310:875-886

Moritz MA, Parisien M-A, Batllori E, Krawchuk MA, Van Dorn J, Ganz DJ, Hayhoe K (2012) Climate change and disruptions to global fire activity. Ecosphere 3(6):49

Moritz MA, Batllori E, Bradstock RA, Gill AM, Handmer J, Hessburg PF, Leonard J, McCaffrey S, Odion DC, Schoennagel T, Syphard AD (2014) Learning to coexist with wildfire. Nature 515:58-66

Moss R, Edmonds J, Hibbard K, Manning M, Rose S, van Vuuren D, Carter T, Emori S, Kainuma M, Kram T, Meehl G, Mitchell J, Nakicenovic N, Riahi K, Smith S, Stouffer R, Thomson A, Weyant J, Wilbanks T (2010) The next generation of scenarios for climate change research and assessment, Nature 463:747-756

Murphy BF, Timbal B (2008) A review of recent climate variability and climate change in southeastern Australia. International Journal of Climatology 28:859-879

Murphy BP, Bradstock RA, Boer MM, Carter J, Cary GJ, Cochrane MA, Fensham RJ, Russell-Smith J, Williamson GJ, Bowman DMJS (2012) Fire regimes of Australia: a pyrogeographic model system. Journal of Biogeography 40:1048-1058

Nakicenovic N, Alcamo J, Davis G, de Vries B, Fenhann J, Gaffin S, Gregory K, Grübler A, Jung T-Y, Kram T, La Rovere EL, Michaelis L, Mori S, Morita T, Pepper W, Pitcher H, Price L, Riahi K, Roehrl A, Rogner HH, Sankovski A, Schlesinger M, Shukla P, Smith S, Swart R, van Rooijen S, Victor N, Dadi Z (2000) IPCC special report on emissions scenarios. Cambridge University Press, Cambridge, UK

NASA FIRMS (2014) MODIS hotspot/active fire detections. http:// earthdata.nasa.gov/firms. Accessed 26 January 2014

Nielsen-Pincus M, Moseley C, Gebert K (2014) Job growth and loss across sectors and time in the western US: The impact of large wildfires. Forest Policy and Economics 3:8199-206

Nitschke CR, Innes JL (2008) Climatic change and fire potential in south-central British Columbia, Canada. Global Change Biology 14:841-855

Noble IR, Barry GAV, Gill AM (1980) McArthur's fire danger meters expressed as equations. Australian Journal of Ecology 5:201-203

OEH (2012) Living with fire in National Parks - A strategy for managing bushfires in national parks and reserves 2012-2021. Office of Environment and Heritage, Sydney, Australia

Olson JS (1963) Energy storage and the balance of producers and decomposers in ecological systems. Ecology 44:322-331

Osborn TJ, Hulme M (1998) Evaluation of the European daily precipitation characteristics from the Atmospheric Model Intercomparison Project. International Journal of Climatology 18:505-522

Ott D, Rall BC, Brose U (2012) Climate change effects on macrofaunal litter decomposition: the interplay of temperature, body masses and stoichiometry. Philosophical Transactions of the Royal Society B 367:3025-3032

Papadopoulos A, Paschalidou AK, Kassomenos PA, McGregor G (2014) On the association between synoptic circulation and wildfires in the Eastern Mediterranean. Theoretical and Applied Climatology 115:483-501

Page SE, Siegert F, Rieley JO, Boehm HDV, Jaya A, Limin S (2002) The amount of carbon released from peat and forest fires in Indonesia during 1997. Nature 420:61-65

Papanikolaou N, Britton AJ, Helliwell RC, Johnson D (2010) Nitrogen deposition, vegetation burning and climate warming act independently on microbial community structure and enzyme activity associated with decomposing litter in low-alpine heath. Global Change Biology 16:3120-3132

Parkyn K, Yeo C, Bannister T (2010) Meteorological lessons learnt from Black Saturday. Proceedings of 2010 AFAC Conference, Darwin.

Pausas JG, Keeley JE (2009) A burning story: the role of fire in the history of life. Bioscience 59:593-601

Pausas JG, Keeley JE (2014) Abrupt climate-independent fire regime changes. Ecosystems 17:1109-1120

Peace M, McCaw L, Mills GA (2012) Meteorological dynamics in a fire environment; a case study of the Layman prescribed burn in Western Australia. Australian Meteorological and Oceanographic Journal 62:127- 142

Pechony O, Shindell DT (2009) Fire parameterization on a global scale, Journal of Geophysical Research 114:D16115

Pechony O, Shindell DT (2010) Driving forces of global wildfires over the past millennium and the forthcoming century. Proceedings of the National Academy of Sciences USA 107:19167-19170

Penman TD, Christie FJ, Andersen AN, Bradstock RA, Cary GJ, Henderson MK, Price O, Tran C, Wardle GM, Williams RJ, York A (2011) Prescribed burning: how can it work to conserve the things we value? Internatonal Journal of Wildland Fire 20:721-733

Penman TD, Bradstock RA, Price O (2013) Modelling the determinants of ignition in the Sydney Basin, Australia: implications for future management. International Journal of Wildland Fire 22:469-478

Perkins SE, Pitman AJ, Holbrook NJ, McAneney J (2007) Evaluation of the AR4 Climate Models' Simulated Daily Maximum Temperature, Minimum Temperature, and Precipitation Over Australia Using Probability Density Functions. Journal of Climate 20:4356-4376

Pielke RA, Cotton WR, Walko RL, Tremback CG, Lyons WA, Grasso LD, Nicholls ME, Moran MD, Wesley DA, Lee TJ, Copeland JH (1992) A comprehensive meteorological modeling system-RAMS. Meteorology and Atmospheric Physics 49:69-91

Piñol J, Terradas J, Lloret F (1998) Climate warming, wildfire hazard, and wildfire occurrence in coastal eastern Spain. Climatic Change 38:345-357

Pitman AJ, Narisma GT, McAneney J (2007) The Impact of Climate Change on the Risk of Forest and Grassland Fires in Australia. Climatic Change 84:383-401

Pitman AJ, Avila FB, Abramowitz G, Wang YP, Phipps SJ, de Noblet-Ducoudre N (2011) Importance of background climate in determining impact of land-cover change on regional climate. Nature Climate Change 1:472-475

Pitman AJ, Arneth A, Ganzeveld L (2012) Regionalizing global climate models. International Journal of Climatology 32:321-337

Poulter B, Frank D, Ciais P, Myneni RB, Andela N, Bi J, Broquet G, Canadell JG, Chevallier F, Liu YY, Running SW, Sitch S, van der Werf GR (2014) Contribution of semi-arid ecosystems to interannual variability of the global carbon cycle. Nature 509:600-603

Power SB, Casey T, Folland C, Colman A, Mehta V (1999) Interdecadal modulation of the impact of ENSO on Australia. Climate Dynamics 15:319-324

Preisler HK, Brillinger DR, Burgan RE, Benoit JW (2004) Probability-based models for estimation of wildfire risk. International Journal of Wildland Fire 13:33-142

Price C, Rind D (1994) Possible implications of global climate change on global lightning distributions and frequencies, Journal of Geophysical Research 99(D5):10823-10831

Price OF, Williamson GJ, Henderson SB, Johnston F, Bowman, DJMS (2012) The relationship between particulate pollution levels in Australian cities, meteorological variables, and landscape fire activity detected from MODIS hotspots. PLoS ONE 7:e47327

Price O, Bradstock R (2014) Countervailing effects of urbanization and vegetation extent on fire frequency on the Wildland Urban Interface: Disentangling fuel and ignition effects. Landscape and Urban Planning 130:81-88

Randall DA, Wood RA, Bony S, Colman R, Fichefet T, Fyfe J, Kattsov V, Pitman A, Shukla J, Srinivasan J, Stouffer RJ, Sumi A, Taylor KE (2007) Climate Models and Their Evaluation. In: Solomon S, Qin D, Manning M, Chen Z, Marquis M, Averyt K, Tignor M, Miller H (eds). Climate Change 2007: The Physical Science Basis. Contribution of Working Group I to the Fourth Assessment Report of the Intergovernmental Panel on Climate Change. Cambridge University Press, Cambridge, United Kingdom and New York, NY, USA, pp 589-662

Raupach MR (1994) Simplified expressions for vegetation roughness length and zero-plane displacement as functions of canopy height and area index. Boundary-Layer Meteorology 71:211-216

Raupach MR, Haverd V, Briggs PR (2013) Sensitivities of the Australian terrestrial water and carbon balances to climate change and variability. Agricultural and Forest Meteorology 182-183:277-291

Raymond CL, McKenzie D (2012) Carbon dynamics of forests in Washington, USA: 21st century projections based on climate-driven changes in fire regimes. Ecological Applications 22:1589-1611

Rienecker MM, Suarez MJ, Gelaro R, Todling R, Bacmeister J, Liu E, Bosilovich MG, Schubert SD, Takacs L, Kim G-K, Bloom S, Chen J, Collins D, Conaty A, da Silva A, Gu W, Joiner J, Koster RD, Lucchesi R, Molod A, Owens T, Pawson S, Pegion P, Redder CR, Reichle R, Robertson FR, Ruddick AG, Sienkiewicz M, Woollen J (2011)

MERRA - NASA's Modern-Era Retrospective Analysis for Research and Applications. Journal of Climate 24:3624-3648

Risbey JS, Pook MJ, McIntosh PC (2009) On the remote drivers of rainfall variability in Australia. Monthly Weather Review 137(10):3233-3253

Roberts G, Wooster MJ, Lagoudakis E (2008) Annual and diurnal African biomass burning temporl dynamics. Biogeosciences Discussions 5:3623-3663

Rockstrom J, Steffen W, Noone K, Persson A, Chapin FS, Lambin EF, Lenton TM, Scheffer M, Folke C, Schellnhuber HJ, Nykvist B, de Wit CA, Hughes T, van der Leeuw S, Rodhe H, Sorlin S, Snyder PK, Costanza R, Svedin U, Falkenmark M, Karlberg L, Corell R W, Fabry VJ, Hansen J, Walker B, Liverman D, Richardson K, Crutzen P, Foley JA (2009) A safe operating space for humanity. Nature 461:472-475

Rouifed S, Handa IT, David J-F, Hättenschwiler S (2010) The importance of biotic factors in predicting global change effects on decomposition of temperate forest leaf litter. Oecologia (2010) 163:247-256

Russell-Smith J, Yates CP, Whitehead PJ, Smith R, Craig R, Allan GE, Thackway R, Frakes I, Cridland S, Meyer MCP, Gill AM (2007) Bushfires ‘down under’: patterns and implications of contemporary Australian landscape burning. International Journal of Wildland Fire 16:361-377

Russell-Smith J, Murphy BP, Meyer CP, Cook GD, Maier S, Edwards AC, Schatz J, Brocklehurst P (2009) Improving estimates of savvanna burning emissions for greenhouse accounting in northern Australia: limitations, challenges, applications. International Journal of Wildland Fire 18:1-18

Saura-Mas S, Estiarte M, Peñuelas J, Lloret F (2012) Effects of climate change on leaf litter decomposition across post-fire plant regenerative groups. Environmental and Experimental Botany 77:274-282

Scheiter S, Higgins SI (2009) Impacts of climate change on the vegetation of Africa: an adaptive dynamic vegetation modelling approach, Global Change Biology 15:2224-2246

Scott AC, Glasspool IJ (2006) The diversification of paleozoic fire systems and fluctuations in atmospheric oxygen concentration. Proceedings of the National Academy of Sciences USA 103:10861-10865

Settele J, Scholes R, Betts R, Bunn S, Leadley P, Nepstad D, Overpeck JT, Taboada MA (2014) Terrestrial and inland water systems In: Field CB, Barros VR, Dokken DJ, Mach KJ, Mastrandrea MD, Bilir TE, Chatterjee M, Ebi KL, Estrada YO, Genova RC, Girma, Kissel ES, Levy AN, MacCracken S, Mastrandrea PR, White LL (eds). Climate Change 2014: Impacts, Adaptation, and Vulnerability Part A: Global and Sectoral Aspects Contribution of Working Group II to the Fifth Assessment Report of the Intergovernmental Panel on Climate Change. Cambridge University Press, Cambridge, United Kingdom and New York, NY, USA, pp 271-359

Sharples JJ, Mills GA, McRae RHD, Weber RO (2010) Foehn-like winds and elevated fire danger conditions in southeastern Australia. Journal of Applied Meteorology and Climatology 49:1067-95

Sharples JJ, McRae RHD (2013) A fire spread index for grassland fuels. 20th International Congress on Modelling and Simulation, Adelaide, Australia.

Skamarock WC, Klemp JB, Dudhia J, Gill DO, Barker DM, Duda MG, Huang X-Y, Wang W, Powers JG (2008) A Description of the Advanced Research WRF Version 3. NCAR, NCAR Technical Note, Boulder, CO, USA

Skinner WR, Flannigan MD, Stocks BJ, Martell DL, Wotton BM, Todd JB, Mason JA, Logan KA, Bosch EM (2002) A 500 hPa synoptic wildland fire climatology for large Canadian forest fires, 1959-1996. Theoretical and Applied Climatology 71:157-169

Stavros EN, Abatzoglou JT, McKenzie D, Larkin NK (2014) Regional projections of the likelihood of very large wildland fires under a changing climate in the contiguous Western United States. Climatic Change 126:455-468

Stern H, de Hoedt G, Ernst J (1999) Objective classification of Australian climates. Australian Meteorological Magazaine 49:87-96

Stocks BJ, Fosberg MA, Lynham TJ, Mearns L, Wotton BM, Yang Q, Jin J-Z, Lawrence K, Hartley GR, Mason JA, McKenney DW (1998) Climate change and forest fire potential in Russian and Canadian boreal forests. Climatic Change 38:1-13

Stone DA, Stott PA, Pall P, Min S-K, Nozawa T, Yukimoto S (2009) The detection and attribution of human influence on climate. Annual Reviews in Environmental Resources 34:1-16

Stott PA, Gillett NP, Hegerl GC, Karoly D, Stone D, Zhang X, Zwiers F (2010) Detection and attribution of climate achange: a regional perspective. WIREs Climate Change 1:192-211

Tang S, Dessai S (2012) Usable Science? The U.K. Climate Projections 2009 and Decision Support for Adaptation Planning. Weather, Climate and Society 4:300-313

Tarancón AA, Fulé PZ, Shive KL, Sieg CH, Meador AS, Strom B (2014) Simulating post-wildfire forest trajectories under alternative climate and management scenarios. Ecological Applications 24(7):1626-1637

Taylor C, McCarthy MA, Lindenmayer DB (2014) Non-linear effects of stand age on fire severity. Conservation Letters 7(4):355-370

Thomas PB, Watson PJ, Bradstock RA, Penman TD, Price OF (2014) Modelling surface fine fuel dynamics across climate gradients in eucalypt forests of south-eastern Australia. Ecography 37:1-11

Thonicke K, Spessa A, Prentice IC, Harrison SP, Dong L, Carmona-Moreno C (2010) The influence of vegetation, fire spread and fire behaviour on biomass burning and trace gas emissions: results from a process-based model. Biogeosciences 7(6):1991-2011

Timbal B, Arblaster JM, Power S (2006) Attribution of the late-twentieth-century rainfall decline in southwest Australia. Journal of Climate 19:2046-2062

Timbal B (2009) The continuing decline in southeast Australian rainfall: update to May 2009. CAWCR Research Letters Issue 5, CSIRO and Bureau of Meteorology, Victoria.

Toberman H, Chen C, Lewis T, Else JJ (2014) High-frequency fire alters C : N : P stoichiometry in forest litter. Global Change Biology 20:2321-2331

Turco M, Llasat M-C, von Hardenberg J, Provenzale A (2014) Climate change impacts on wildfires in a Mediterranean environment. Climatic Change 125:369-380

Turner A, Lewis M, Ostendorf B (2011) Spatial indicators of fire risk in the arid and semi-arid zone of Australia. Ecological Indicators 11:149-167

van der Linden P, Mitchell JFB (2009) (eds) ENSEMBLES: Climate change and its impacts - Summary of research and results from the ENSEMBLES project. Met Office Hadley Centre, Exeter, UK.

Van Wagner CE (1987) Development and Structure of the Canadian Forest Fire Weather Index System. Canadian Forestry Service, Technical Report 35, Ottawa, ON

Vázquez de la Cueva A, Quintana JR, Canellas I (2012) Fire activity projections in the SRES A2 and B2 climatic scenarios in peninsular Spain. International Journal of Wildland Fire 21(6):653-665

Venäläinen A, Korhonen N, Hyvärinen O, Koutsias N, Xystrakis F, Urbieta IR, Moreno JM (2014) Temporal variations and change in forest fire danger in Europe for 1960-2012. Natural Hazards and Earth System Sciences 14:1477-1490

Verdon DC, Kiem AS, Franks SW (2004) Multi-Decadal Variability of Forest Fire Risk - Eastern Australia. International Journal of Wildland Fire 13:165-171

Vivian LM, Doherty MD, Cary GJ (2010) Classifying the fire-response traits of plants: how reliable are species-level classifications? Austral Ecology 35:264-273

Wang Y-P, Leuning R (1998) A two-leaf model for canopy conductance, photosynthesis and partitioning of available energy I: Model description and comparison with a multi-layered model. Agricultural and Forest Meteorology 91:89-111

Wang YP, Law RM, Pak B (2010) A global model of carbon, nitrogen and phosphorus cycles for the terrestrial biosphere. Biogeosciences 7:2261-2282

Wang YP, Kowalczyk E, Leuning R, Abramowitz G, Raupach MR, Pak B, van Gorsel E, Luhar A (2011) Diagnosing errors in a land surface model (CABLE) in the time and frequency domains. Journal of Geophysical Research 116:G01034

Wastl C, Schunk C, Leuchner M, Pezzatti GB, Menzel A (2012) Recent climate change: long-term trends in meteorological forest fire danger in the Alps. Agricultural and Forest Meteorology 162-163:1-13

Wastl C, Schunk C, Lüpke M, Cocca G, Conedera M, Valese E, Menzel A (2013) Large-scale weather types, forest fire danger, and wildfire occurrence in the Alps. Agricultral and Forest Meteorology 168:15-25

Watson PJ (2009) Understanding Bushfire Fuels. Centre for the Environmental Risk Management of Bushfires. University of Wollongong, Wollongong, Australia

Watson PJ (2012) Fuel load dynamics in NSW vegetation. Part 1: forests and grassy woodlands. Centre for the Environmental Risk Management of Bushfires. University of Wollongong, Wollongong, Australia

Weaver CP, Lempert RJ, Brown C, Hall JA, Revell D, Sarewitz D (2013) Improving the contribution of climate model information to decision making: the value and demands of robust decision frameworks. WIREs Climate Change 4:39-60

Westerling AL, Hidalgo HG, Cayan DR, Swetnam TW (2006) Warming and earlier spring increase Western U.S. forest wildfire activity. Science 313:940-943

Wilby RL, Charles SP, Zorita E, Timbal B, Whetton P, Mearns LO (2004) Guidelines for use of climate scenarios developed from statistical downscaling methods. IPCC Data Distribution Centre, Switzerland

Willett KM, Gillett NP, Jones PD, Thorne PW (2007) Attribution of observed surface humidity changes to human influence. Nature 449:710-713

Williams AAJ, Karoly DJ (1999) Extreme fire weather in Australia and the impact of the El Niño-Southern Oscillation. Australian Meteorological Magazine 48:15-22

Williams AAJ, Karoly DJ, Tapper N (2001) The Sensitivity of Australian Fire Danger to Climate Change. Climatic Change 49:171-191

Williamson GJ, Prior LD, Grose MR, Harris RMB, Bowman DMJS (2014) Projecting canopy cover change in Tasmanian eucalypt forests using dynamically downscaled regional climate models. Regional Environmental Change 14:1373-1386

Woolford DG, Cao J, Dean CB, Martell DL (2010) Characterizing temporal changes in forest fire ignitions: looking for climate change signals in a region of the Canadian boreal forest. Environmetrics 21:789-800

Yue X, Mickley LJ, Logan JA, Kaplan JO (2013) Ensemble projections of wildfire activity and carbonaceous aerosol concentrations over the western United States in the mid-21st century. Atmospheric Environment 77:767-780

Zhang C, Hanqin T, Wang Y, Zeng T, Liu Y (2010) Predicting response of fuel load to future changes in climate and atmospheric composition in the Southern United States. Forest Ecology and Management 260:556-564

Zhang Q, Wang YP, Pitman AJ, Dai YJ (2011) Limitations of nitrogen and phosphorous on the terrestrial carbon uptake in the 20th century. Geophysical Research Letters 38:L22701

Zinck RD, Pascual M, Grimm V (2011) Understanding shifts in wildfire regimes as emergent threshold phenomena. American Naturalist 178:E149-E161

Zylstra P (2011) Forest Flammability - Modelling and Managing a Complex System. PhD thesis, University of New South Wales